

2008

# The reciprocating joule cycle engine for micro combined heat and power applications

Allen , Robert William

<http://hdl.handle.net/10026.1/759>

---

<http://dx.doi.org/10.24382/3270>

University of Plymouth

---

*All content in PEARL is protected by copyright law. Author manuscripts are made available in accordance with publisher policies. Please cite only the published version using the details provided on the item record or document. In the absence of an open licence (e.g. Creative Commons), permissions for further reuse of content should be sought from the publisher or author.*

**THE RECIPROCATING JOULE CYCLE ENGINE FOR MICRO  
COMBINED HEAT AND POWER APPLICATIONS**

**By**

**ROBERT WILLIAM ALLEN**

A thesis submitted to the University of Plymouth  
in partial fulfilment for the degree of

**DOCTOR OF PHILOSOPHY**

School of Engineering  
Faculty of Technology

**December 2008**

## **Copyright Statement**

This copy of the thesis has been supplied on condition that anyone who consults it is understood to recognise its copyright rests with its author and that no quotation from this thesis and no information derived from it may be published without the authors's prior consent.

# **Abstract**

**Robert William Allen**

## **The Reciprocating Joule Cycle (RJC) Engine for Micro Combined Heat and Power (CHP) Applications**

Micro CHP has been identified as a means of reducing the carbon dioxide emissions from household energy consumption. Large scale field trials undertaken in the UK, with systems internal to a single dwelling and based on Stirling engines, were disappointing because of the low thermal efficiencies of such engines. Alternative engines/devices with higher thermal efficiencies are currently being evaluated in Japan but such systems are external to the dwelling.

The reciprocating Joule cycle engine is proposed as an engine for a micro CHP system because of its potential to be more thermally efficient than a Stirling engine and at least as thermally efficient as an internal combustion engine. Such an engine has not previously been analysed in detail nor is there any information that such an engine has been built and operated, particularly at power output levels below 5 kW.

Mathematical modelling of the RJC engine is used to determine power outputs and efficiencies taking into account frictional, thermal and pressure losses. Such modelling indicated an engine with a maximum thermal efficiency of 33% making it suitable for micro CHP applications. When the individual models are combined to model a CHP system, and using the engine exhaust heat to preheat the combustion air, an overall maximum system efficiency of 79% was indicated.

## Abstract

The engine mathematical model was validated through the process of design, build, and testing of both a technology demonstration engine and a prototype engine. Also undertaken was the development and testing of a combustion chamber that achieved stable combustion in a pulsating pressurised air flow. The outcome from modelling and testing was a set of design parameters and constraints for the design of future engines.

It was concluded that a high efficiency micro CHP system, using a RJC engine, is achievable. However because of RJC engine's comparatively low power to volume ratio it is most likely that it could only be considered as a replacement for a single dwelling domestic boiler if positioned externally.

University of Plymouth Library
Item No 900857771X
Callmark STORE THESIS 629.25 ALL

# List of Contents

<b>Part 1. Introduction</b>	<b>1</b>
1.1 Current Status of Micro CHP	1
1.2 Requirements for Micro CHP	7
1.3 Aims of Research	7
<b>Part 2. The RJC Engine</b>	<b>9</b>
2.1 The RJC Engine	9
2.2 Thermodynamic Modelling	10
2.3 Application of the RJC Engine	14
2.4. Existing Patent Applications	15
2.5 Published Papers	18
<b>Part 3 Performance Modelling of The RJC Engine and CHP Systems</b>	<b>19</b>
3.1 Modelling	19
3.2 Basic RJC Engine Modelling	19
3.3 Findings from the Basic Model	
3.3.1 Effect of Clearance Volumes on Work Output	21
3.3.2 Effect of System Pressure	22
3.3.3 Effect of Inlet valve opening	23
3.4 Conclusions from Basic Modelling of the RJC Engine	25
3.5 Detailed Modelling	26
3.5.1 Friction Losses	26
3.5.2 Thermal Losses	26
3.5.3 Pressure Losses	27
3.6 Friction Modelling	28
3.6.1 Friction Reduction Methods	28

## List of Contents

3.6.2 Existing Friction Models	30
3.6.3 Modelling the RJC Engine	32
3.6.4 Friction Model	33
3.7 Thermal Loss Modelling	34
3.7.1 Existing Models	36
3.7.2 Modelling the RJC Engine	38
3.7.3 Thermal Model Evaluation	41
3.8 Pressure Loss Modelling	43
3.8.1 Modelling the RJC Engine	46
3.8.2 Exhaust Valve Modelling	50
3.8.3 Validation of Pressure Loss Modelling	51
3.8.4 Findings From Pressure Loss Modelling	54
3.8.5 Optimum Pressure Loss Modelling for a Specific RJC Engine.	56
3.8.6 Application of Valve Pressure Loss Modelling to Engine Design.	58
3.8.7 Limitations of Pressure Loss Modelling	59
3.9 Micro CHP System Modelling	60
3.9.1 Findings from Micro CHP System Modelling	65
3.9.2 Limitations Of Micro CHP Modelling	65
3.10 Overall Assessment of Modelling	66
<b>Part 4. Engine Development And Testing</b>	<b>68</b>
4.1 Test Engines	68
4.1.1 Description of the Technology Demonstration Engine	68
4.1.2. Expander Cylinder Head and the Inlet / exhaust valves	69
4.1.3. Compressor Head and Compressor Valves	71

## **List of Contents**

4.1.4 Combustion Chamber	72
4.1.5 First iteration on Engine Development	73
4.1.6 Second Iteration on Engine Development	78
4.1.7 Third Iteration on Engine Development	81
4.1.8 Fourth Iteration on Engine Development	83
4.1.9 Fifth Iteration on Engine Development	86
4.1.10 Sixth Iteration on Engine Development	87
4.1.11 Overview of the Development Iterations	90
4.2 Conclusions from the Development of the Technology Demonstration Engine	90
4.2.1 Combustion	90
4.2.2 Valves and Valve Gear	92
4.2.3 Compressor	93
4.2.4 Expander Pistons	93
4.2.5 Leakages and Pressure losses	93
4.2.5 Overall Conclusions on the Development of the Technology Demonstration Engine.	93
4.3 Development Programme and Funding	95
4.4 Design, Development and Testing of a RJC Prototype Engine for Micro CHP Applications	96
4.4.1 Use of Existing Components	96
4.4.2 Compressor Design / Selection	97
4.4.5 Prototype Engine Design.	98
4.4.4 Engine Modifications	99
4.4.5 Valve and Cam Box Design and Construction.	99
4.4.6 Compressor	100
4.4.7 Engine /System Design. Cam box Design and Settings.	100
4.4.8 Valves Used and Valve Seat Material	101



## **List of Contents**

4.4.9 Measuring Instrumentation.	102
4.4.10 Combustor Modifications	102
4.4.11 Compressor Type	103
4.4.12 Scroll Compressor Performance.	104
4.4 .13 Expander performance	105
4.4.14 Matching a Scroll Compressor to a Reciprocating Expander.	109
4.4.15 Effect of Clearance Volumes on Expander Performance	112
4.4.16 Suitability of a Scroll Compressor for the RJC Engine	113
4.4.17 Limitations	115
4.4.18 Summary	115
4.4.19 Lessons Carried Forward to Next Design Iteration	116
4.5 Test Engine Design, Construction and Performance	118
4.5.1 Cylinder Head Design.	118
4.5.2 Measuring instrumentation	121
4.6 Engine Operation	122
4.6.1 Expander Performance	122
4.6.2 Readings Taken	123
4.6.3 PV Indicator Diagrams	123
4.7 Interpretation of the Indicator Diagrams	124
4.7.1 Selected PV Diagrams	126
4.7.2 Polytropic Values for Expansion and Recompression	126
4.7.3 Friction	127
4.7.4 Understanding Friction	129
4.7.5 Engine Operation With Combustion	131
4.7.6 Further Understanding of Engine Friction	132
4.8 Reciprocating Compressor Performance	134

## **List of Contents**

4.9 Influence of Friction and Clearance Volumes on Expander Performance	135
4.10 Thermal Efficiency	136
4.11 Compressor Sizing and Exhaust Valve Control	139
4.11.1 Variable Valve Timing for Compressor Inlet Valve	141
4.11.2 Types of Variable Valve Timing Mechanisms	142
4.12 Conclusions From Engine Testing and Extrapolation of Data	143
4.12.1 Limits of Operation: Pressure and temperature.	143
4.12.2 Effect of Friction and Clearance Volumes	144
4.12.3 True Polytropic Values.	144
4.12.4 Apparent Valve Opening / Closing	145
4.12.5 Power and Size of Low BMEP Engines	145
4.12.6 Thermal efficiencies	145
<b>Part 5. Design of a RJC Engine</b>	<b>148</b>
5.1 Engine design	148
5.1.1 Cylinder dimensions	148
5.1.2 Piston Design	148
5.1.3 Valve and Cam Design (Expander)	151
5.1.4 Crankcase Design	152
5.1.5 Combustor Design	153
5.1.6 Rotary Valves	153
5.1.7 Hypocycloidal Drive	155

# List of Contents

## Part 6 Summary and Conclusions

6.1 Micro CHP Opportunities	157
6.2 The RJC Engine for Micro CHP Systems	157
6.3 Engine Design and Operation of Future Engines	157
6.3.1 Temperatures and pressures	158
6.3.2 Efficiencies	158
6.3.3 Compressor Requirements	159
6.3.4 Power Output, Speed, Cylinder Dimensions	159
6.3.5 Foot Print	160
6.3.6 Further Development	160
6.3.7 Overall Applicability and Viability	160

**Annex 1.**  
Spreadsheet

**Annex 2.**  
Spreadsheet  
Copy of Paper Ref 8

**Annex 3.**  
Spreadsheets

**Annex 4**  
Selection of Drawings  
Photographs  
Selection of Pressure vs Crank Angle Scope Outputs  
Selection of Spreadsheets  
Table 4.1

**References.**

# List of Figures, Tables, Photographs, drawings and Spreadsheets

## Part 1

- Fig 1.1 Theoretical Carbon Savings for Different Power to Heat Ratios
- Fig 1.2 Average Demand and Generation Profiles – Winter months
- Fig 1.3 Comparison of Carbon Saved Performance of CHP Systems

Table 1.1 Comparison of Proposed Micro CHP Devices/Engines

## Part 2

- Fig 2.1 Basic Schematic of an RJC Engine
- Fig 2.2 PV Diagrams for an RJC Engine
- Fig 2.3 Performance Mapping of the RJC Engine
- Fig 2.4 Efficiencies of a RJC Engine
- Fig 2.5 Patent Claim GB 23008864 Dated 1997
- Fig 2.6 Patent Claim EP 0810356 ABB Combustion Services 1998

Table 2.1 Definitions of Terms used in Fig 2.2

Table 2.2 Controlling Design Factors.

## Part 3

- Fig 3.1 Ideal PV Diagram for a RJC Engine
- Fig 3.2 Effect of Clearance Volume % on Achievable Work Output %
- Fig 3.3 Net Output J/cycle vs System Pressure bar g
- Fig 3.4 Thermal Efficiency Vs Inlet Valve Opening
- Fig 3.5 RJC Engine, Compressor and Net Work vs Inlet Valve Opening
- Fig 3.6 Frictional Force Over One Cycle
- Fig 3.7 Coefficient of Friction Over One Cycle
- Fig 3.8 Typical Characteristic of Ring Friction Force Over Cycle
- Fig 3.9 Comparison of Engine Friction Models
- Fig 3.10 Variation in Mechanical Efficiency Against IMEP for a Percentage Range of Ring Pack FMEP Contribution to Total FMEP.
- Fig 3.11 Relationship Between Re and Nu for RJC engines
- Fig 3.12 Pressure /Volume During Admission
- Fig 3.13 PV Diagram Showing Inlet Valve Pressure Losses TDC 60 degree Opening
- Fig 3.14 PV Diagram Showing Inlet Valve Pressure Losses TDC 80 degree opening
- Fig 3.15 PV Diagram Showing Inlet Valve Pressure Losses. 8 deg BTDC
- Fig 3.16 Exhaust Valve PV diagram
- Fig 3.17 Inlet Open at TDC
- Fig 3.18 Inlet Open 8 deg BTDC
- Fig 3.19 Inlet Cam Profiles
- Fig 3.20 PV Diagram With 'High Lift' Cam
- Fig 3.21 Valve Layout in Cylinder Head
- Fig 3.22 'High Lift' Cam Profile
- Fig 3.23 PV Diagram of a RJC Engine with 'High Lift' Cams
- Fig 3.24 PV Diagram For Full Expansion Stroke and Using 'High Lift' Cams
- Fig 3.25 PV Diagram for Recompression
- Fig 3.26 Micro CHP System Schematic
- Fig 3.27 Net Work Output vs Inlet Gas Temperature

## **List of Figures, Tables, Photographs, drawings and Spreadsheets**

- Fig 3.28 Thermal efficiency vs Inlet Gas Temperature**
- Fig 3.29 System Power and Heat Output vs Expander Inlet Temp C**
- Fig 3.30 Ratio Work /Heat Output for Varying Inlet Gas Temperatures**
- Fig 3.31 Overall System Thermal Efficiency Vs Expander Inlet Temperature**

- Table 3.1 Values Used in Basic RJC Modelling**
- Table 3.2 Model Values of FMEP (bar)**
- Table 3.3 Engine Dimensions and Parameters Used in Modelling**
- Table 3.4 Engine Dimensions and Operating Conditions**
- Table 3.4 Engine performance comparison with different inlet valve timing**
- Table 3.5 RJC Engine and Micro CHP Parameters used for Modelling**

### **Part 4**

- Fig 4.1a Diagrammatic Representation of Inlet Valve Gear**
- Fig 4.1b Valve Gear Details**
- Fig 4.1c Valve Gear Details**
- Fig 4.2a Compressor Valve Housing**
- Fig 4.2b Combined Compressor Inlet and Discharge Plate Valves**
- Fig 4.3 Compressor Air Receiver Vessel**
- Fig 4.4 Combustion Chamber Fitted to Existing Pipework.**
- Fig 4.5 Conventional Nozzle Assembly in Combustion Chamber**
- Fig 4.6 Compressor Suction and Delivery Valves.**
- Fig 4.7 Modified Burner Assembly**
- Fig 4.8 Combustor With Mixing Tube Assembly**
- Fig 4.9 Inlet Valve Opening Profiles**
- Fig 4.10 Modified Combustion Chamber**
- Fig 4.11 Physical Comparison of Combustion Chambers**
- Fig 4.12 Comparison of Combustors in Engine test Rig**
- Fig 4.13 New Combustion Chamber and Internal Fittings**
- Fig 4.14 Valve Timing**
- Fig 4.15 Air Volume Measuring Equipment**
- Fig 4.16 Cold Friction Characteristics of Technology Demonstration Engine**
- Fig 4.17 Performance of Positive Displacement Compressors**
- Fig 4.18 View of BMW Engine On Stand From Free End**
- Fig 4.19 Effect of Inlet Valve Timing on Pressure vs Crank Angle**
- Fig 4.20 Expander Power output With and Without Combustion**
- Fig 4.21 Net Power Outputs for Engine at Mass Flow Balance At Various Scroll Compressor Drive Ratios**
- Fig 4..22 Theoretical Assessment on The Influence of Clearance Volumes on Net Power Output.**
- Fig 4.23 Compressor Performance Comparisons.**
- Fig 4.24 Valve Configurations and Valve Movements**
- Fig 3.25 Schematic of Valve Actuation**
- Fig 4.26 a. PV Diagrams 700 RPM @ Increasing Torque**
- Fig 4.26 b. PV Diagrams 1000 RPM @ Increasing Torque & Supply Pressure**
- Fig 4.27 Differences Between Actual and Ideal Valve Openings**
- Fig 4.28 Zero Torque Friction Characteristic**
- Fig 4.29 Indicated power vs brake and frictional power**

## List of Figures, Tables, Photographs, drawings and Spreadsheets

- Fig 4.30 Supply pressure vs mechanical efficiency
- Fig 4.31 Engine operation on cold air and hot gas. (Various engine RPMs)
- Fig 4.32 Engine Cycle work vs Supply Pressure
- Fig 4.33 PV Diagrams for Portable Compressor
- Fig 4.34 Compressor Performance 7.5 Bar Supply
- Fig 4.35 Influence of System Efficiencies and Clearance Volume on Output
- Fig 4.36 Net output against gas inlet temperature
- Fig 4.37 Specific Fuel Consumption Vs Expander Inlet Temperature
- Fig 4.38 Thermal Efficiency Vs Expander inlet temperature Showing Combustor Inlet Temperatures From Regeneration
- Fig 4.39 Polytropic Index vs Swept Volume Ratio
- Fig 4.40 Variable Valve Timing Arrangement

- Table 4.1 Pressure Ratios vs. Inlet Valve Opening
- Table 4.2 Nozzle Plate Development
- Table 4.3 Scroll Compressor Characteristics
- Table 4.4 Scroll Compressor /Expander Matching Table
- Table 4.5 Data from PV Diagrams and Torque / Speed Measurements

### Part 5

- Fig. 5.1 Diagrammatic Representation of Taper Rotary Valve
- Fig. 5.2 Outline of Design of a Hypocycloidal Drive for an Opposed Piston RJC Engine

### Annex 1

- Spreadsheet 1.1 Carbon Saved Calculations

### Annex 2

- Paper. 'The Development of The reciprocating Joule Cycle engine for Micro CHP Applications' CIMAC Congress Kyoto 2004

### Annex 3

#### Selection of Spreadsheets

- Spreadsheet 3.1 Expander Model
- Spreadsheet 3.2 Prototype Joule Cycle Engine (fixed valve timing)
- Spreadsheet 3.3 Friction Modelling
- Spreadsheet 3.4 Thermal Modelling
- Spreadsheet 3.5 Engine Modelling Inlet Opens 8Deg BTDC
- Spreadsheet 3.6 Exhaust valve Modelling
- Spreadsheet 3.7 BMW Test Engine Modelling on Cold Air
- Spreadsheet 3.8 BMW Advanced Valve Timing and High lift Cam
- Spreadsheet 3.9 Valve Modelling and Influence of Advanced Valve timing
- Spreadsheet 3.10 CHP System Modelling

### Annex 4

#### Selection of Drawings

- Drawing 4.1 Compressor Valve Plate and Adaptor Ring
- Drawing 4.2 Head and cam-box assembly (Side Valve)
- Drawing 4.3 Exhaust Rocker Arm (Side Valves)

## **List of Figures, Tables, Photographs, drawings and Spreadsheets**

Drawing 4.4 Cylinder Head  
Drawing 4.5 Cylinder head Details  
Drawing 4.6 Exhaust Valve Details  
Drawing 4.7 Valve Seats  
Drawing 4.8 Cam Blanks  
Drawing 4.9 Rocker Arms  
Drawing 4.10 Cam set up

Photo 4.1 View of BMW Engine on Stand from Free End  
Photo 4.2 Right Hand Cylinder Head and Cam Box  
Photo 4.3 Cam Box, Cylinder Head and Cam box components  
Photo 4.4 Combustor Outer Tube with Modified Discharge Flange  
Photo 4.5 Can Box Rocker Arms and Rocker Shaft  
Photo 4.6 View of Valves from Inlet / Exhaust Cylinder Head Flange  
Photo 4.7 Dynamometer  
Photo 4.8 Dynamometer and Scroll Compressor Drive  
Photo 4.9 Combustion Chamber  
Photo 4.10 Hot gas Supply Pipe Work  
Photo 4.11 Burner Flame Test In Air  
Photo 4.12 Cylinder Head, Cam Box and Cam Box Components  
Photo 4.13 Cylinder Head Assembly  
Photo 4.14 Two Part Cylinder Head  
Photo 4.15 Cam Box  
Photo 4.16 Cam Box Mounted On Cylinder Head  
Photo 4.17 Cam Box Mechanisms  
Photo 4.19 Cylinder Head from Piston Side  
Photo 4.20 Portable Compressor and Pressure Sensing Modifications

### Selection of Pressure vs. Crank Angle Scope Outputs

Scope. Pressure vs. Crank Angle 700 RPM 29 N Torque  
Scope. Pressure vs. Crank Angle 1200 Rpm Zero Torque  
Scope. Pressure vs. Crank Angle Compressor 7.5 bar Discharge Pressure

### Selection of Spreadsheets

Spreadsheet 4.1 PV 800 Zero Torque  
Spreadsheet 4.2 PV 800 RPM 29 Nm Torque  
Spreadsheet 4.3 PV for 1000 RPM Zero Torque  
Spreadsheet 4.4 PV for 1000 RPM and 20 N.m. Torque  
Spreadsheet 4.5 Portable Compressor  
Spreadsheet 4.6 Compressor Modelling

Table 4.1 RJC Technology Demonstrator Engine Development

## **Acknowledgements**

The author acknowledges the support from Dr MA Bell for his support and guidance in the work undertaken.

The author wishes to thank the mechanical workshop staff of the School of Engineering for their assistance in the manufacture of components outside the skill of the author.

The project could not have been undertaken without the grant from the Proof of Concept Fund and the author acknowledges Dr S Boulton from the department of Research and Innovation for her support.



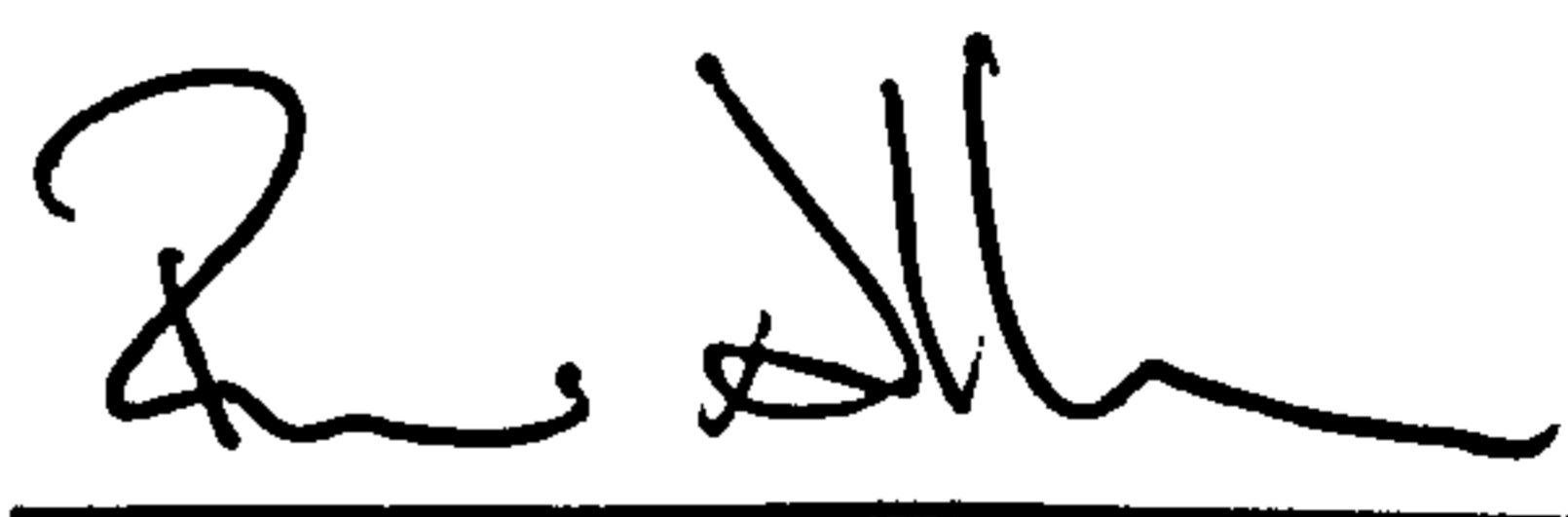
## Authors Declaration

At no time during the registration for the degree of Doctor of Philosophy has the author been registered for any other University award without prior agreement of the Graduate Committee.

Finance for the material aspects of this study was limited and came from the University of Plymouth Proof of Concept Fund, monies allocated to the author for academic supervision in KTP projects and small residues from previous departmental research. The work undertaken and reported is the sole effort of the candidate.

This is a unique area of work with only two major publications having been published both from the University of Plymouth. As a condition of the Proof of Concept funding, to protect intellectual property rights and potential patents, no detailed papers on the findings of the work undertaken have yet been written or published, nor have external contacts been made to disseminate or share in information.

Word count of the main body of the thesis: 28,855

Signed 

Date 12 Dec 2008

## Introduction

### **1.1 Current Status of Micro CHP**

The government target to cut 60% of CO<sub>2</sub> emissions by 2050 resulted from The Royal Commission on Environmental Pollution Ref 1. The Commission proposed four scenarios for meeting this target one of which involves up to 2.4 million gas fired Micro combined heat and power (CHP) units. This premise was based on the fact that Micro CHP is a highly fuel-efficient energy technology, which puts to use waste heat produced as a by-product of the electricity generation process. CHP can increase the overall efficiency of fuel utilisation to more than 75% Gross Calorific Value – compared with up to 40% achieved by fossil fuel electricity generation plants in operation today, and over 50% from modern Combined Cycle Gas Turbines – and has the potential to save substantially on energy bills.

It has been estimated that 700,000 units would cut the UK's CO<sub>2</sub> emissions by 5% by reducing the reliance on centrally generated electrical power produced at lower overall thermal efficiency. Ref 2 details the potential market for micro CHP in the UK.

The following definitions for micro CHP are accepted by Industry:

#### **1. General definition**

'A direct replacement for a boiler in a hydronic heating system, which simultaneously produces heat and electrical power'

#### **2. G 83/CEN Technical definition**

- Generator with an output < 16 A /phase -

#### **3. Domestic CHP functional definition- One unit per home -< 5kWe output.**

An essential component of a micro CHP plant is the engine/device that converts heat energy into electrical energy and the range of such engine/devices that have been suggested are:

1. Stirling engine
2. Spark ignition gas engine (Otto cycle)
3. Spark ignition gasoline engine (Otto cycle)
4. Diesel engine
5. Gas turbine (Joule Cycle)
6. Fuel Cell
7. Organic Rankine cycle

The Stirling engine is already being used in a micro CHP in domestic dwellings but its major drawback is that the amount of electrical power is small compared to its thermal input. A quoted output for one micro CHP system employing a Stirling engine is 1.0 kWe with 6 kWth (power to heat ratio 1:6) with a thermal efficiency estimated at less than 20%.

Small spark ignition gas engines and small diesel engines are currently used for multiple dwelling applications with gas ignition engines being preferred because fuel does not have to be stored on site. These plants are usually situated external to the multiple dwelling or in basement plant rooms. Some field trials are in progress in Japan using a single 160 cc single cylinder Honda gas engine (Ecowill) with an electrical output of 1 kW and again this is situated external to the building. Such engines would achieve a power to heat ratio of 1:3

Small gas turbines have been used but they suffer from low thermal efficiencies and there have not been any installations much below electrical powers outputs of 30kW. Such plants when used are situated outside buildings because of the size required for intakes and exhausts. As such they are discounted for Micro CHP.

Fuel Cell micro CHPs (Lifuel) are being field tested in Japan. Hydrogen for the fuel cell is generated from natural gas in a reformer to produce an electrical output of

## Part 1

1 kW and a claimed full load efficiency thermal efficiency of 35% (approximate power to heat ratio of 1:3). The efficiency of the reformation of gas to hydrogen is not known but could result in the release of unused gas (methane) in addition to CO<sub>2</sub> which will negate any savings in overall greenhouse gas emissions.

A comparison on a range of attributes for each type of devices/engines is made at Table 1.1 The basic requirement for any micro CHP plant is to reduce green house gas emissions by the efficient conversion of fuel into electrical power . It is assumed that waste heat can be effectively recovered from all engines/devices.

An addition to the prime movers listed in table 1.1 the Reciprocating Joule Cycle Engine (RJC) is to be added. This engine is described more fully in Part 2.

	Stirling Engine	Gas Engine	Diesel Engine	Gas Turbine	Fuel Cell
Fuel Type	Gas	Gas	Diesel / Veg Oil	Gas / Diesel Kerosine	Gas
Available	Yes	Yes	Yes	Yes	Yes
Output kWe	1.8	>1	>5	>20	1
Output kWth	8	>3	>5	>20	>3
Size (vol. occupied)	Med	Low	Low	Med	Low
Th. efficiency % Elec. power Output	<20	>25	>30	<20	35 max
Noise	Low	Med	High/Med	Med	Low
Cost	Med	Low	Low	High	High
Safety	High	Med	High	Med	Med
Potential Durability / life	Med/High	High	High	Med	Not known
Replacement for Internal domestic boiler single dwelling	Yes	External to Dwelling	External to dwelling	No	External to Dwelling
Overall Suitability	Limited by low electrical power output. Improvements unlikely	Has potential. More suitable for multiple dwellings	Has potential. Installation likely to be external to main dwelling	Low efficiency No small engines Not suitable	Has Potential. Greenhouse gas contribution from reformation not known

Table 1.1 Comparison of Proposed Micro CHP Devices/Engines

The Carbon Trust has undertaken a detail study of micro CHP performance including field trials, the vast majority being of the Stirling engine type. At Ref 3 they identified the theoretical relationship between the power to heat ratio, the overall plant efficiency and the percentage carbon savings and this is reproduced at Fig 1.1

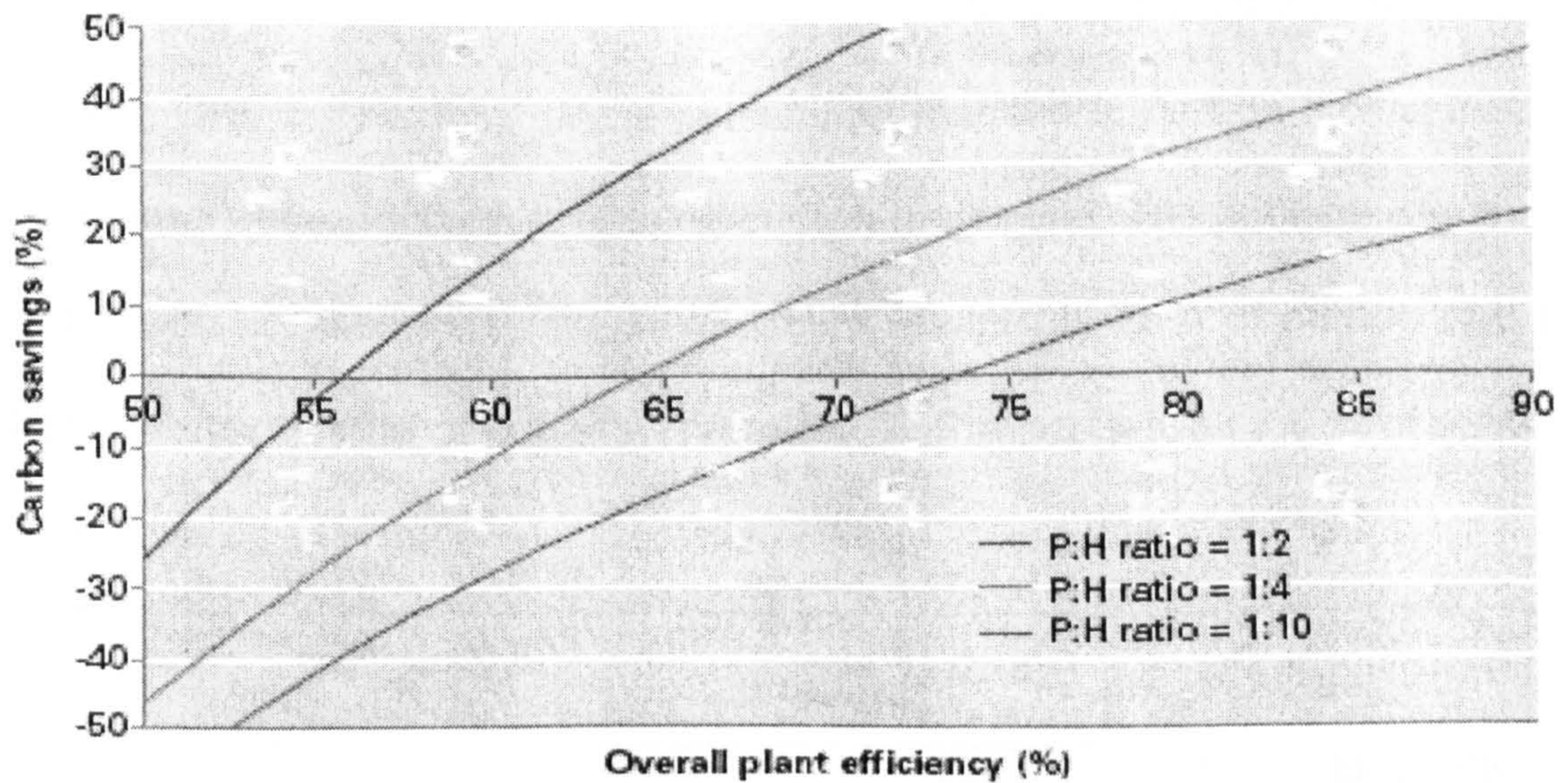


Fig 1.1 Theoretical Carbon Savings for Different Power to Heat Ratios

The theoretical mapping however does not take account of the variations in heat and power demand of a dwelling. Fig 1.2 from Ref 2 shows the average daily demand for heat and power over the winter months

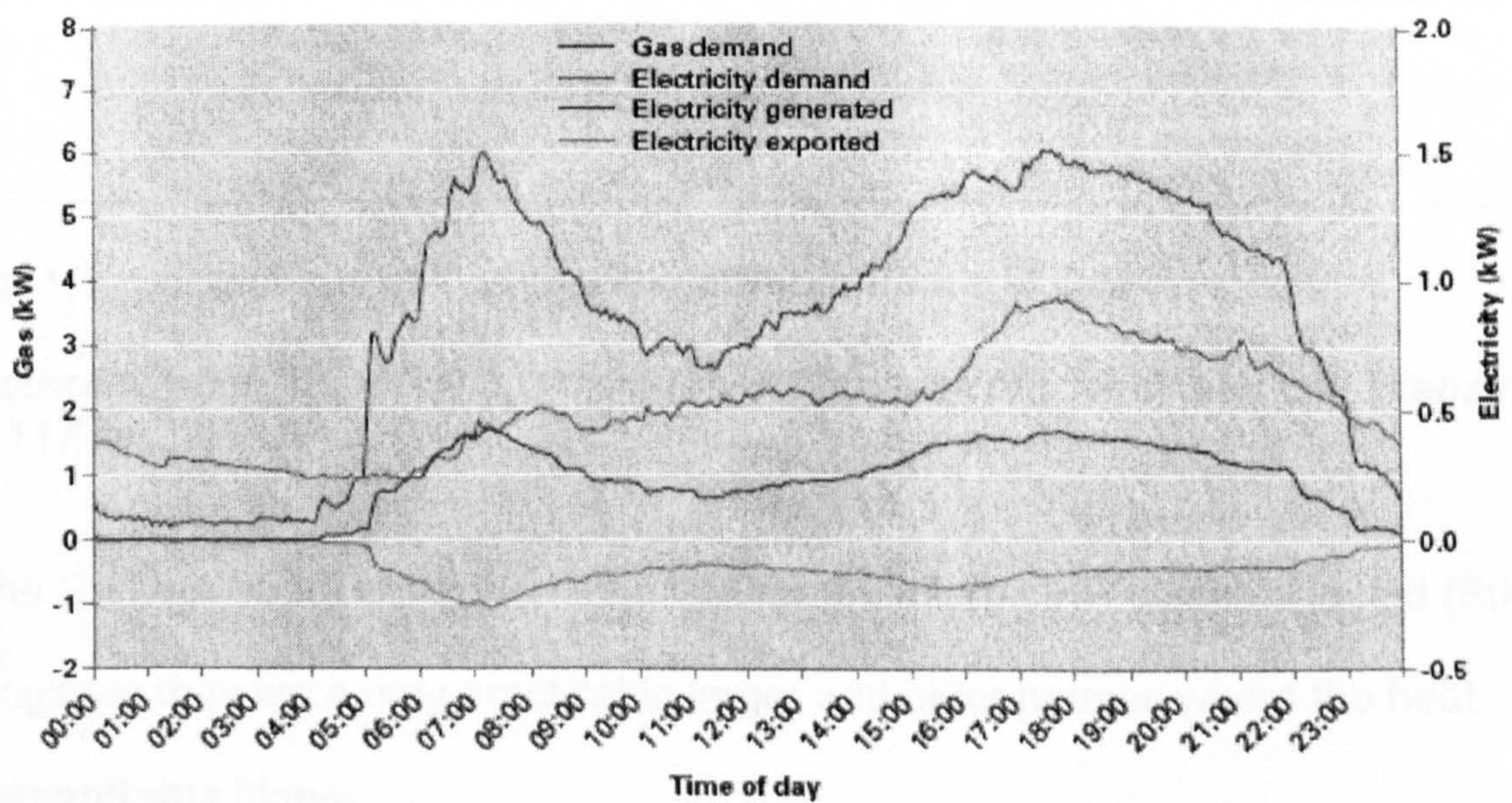


Fig 1.2 Average Demand and Generation Profiles – Winter Months

This daily variation has a significant impact on plant performance and thus reduction on CO<sub>2</sub> emissions. The findings from the carbon trust field trials was that for micro CHP only a third of those installed resulted in carbon savings with one third neutral and one third increasing carbon emissions. The findings are shown at Fig 1.3 with comparisons with Small CHPs (electricity 25% of output) and Large CHPs (electricity 50% of output). The micro CHP average was 7.5 % of output.

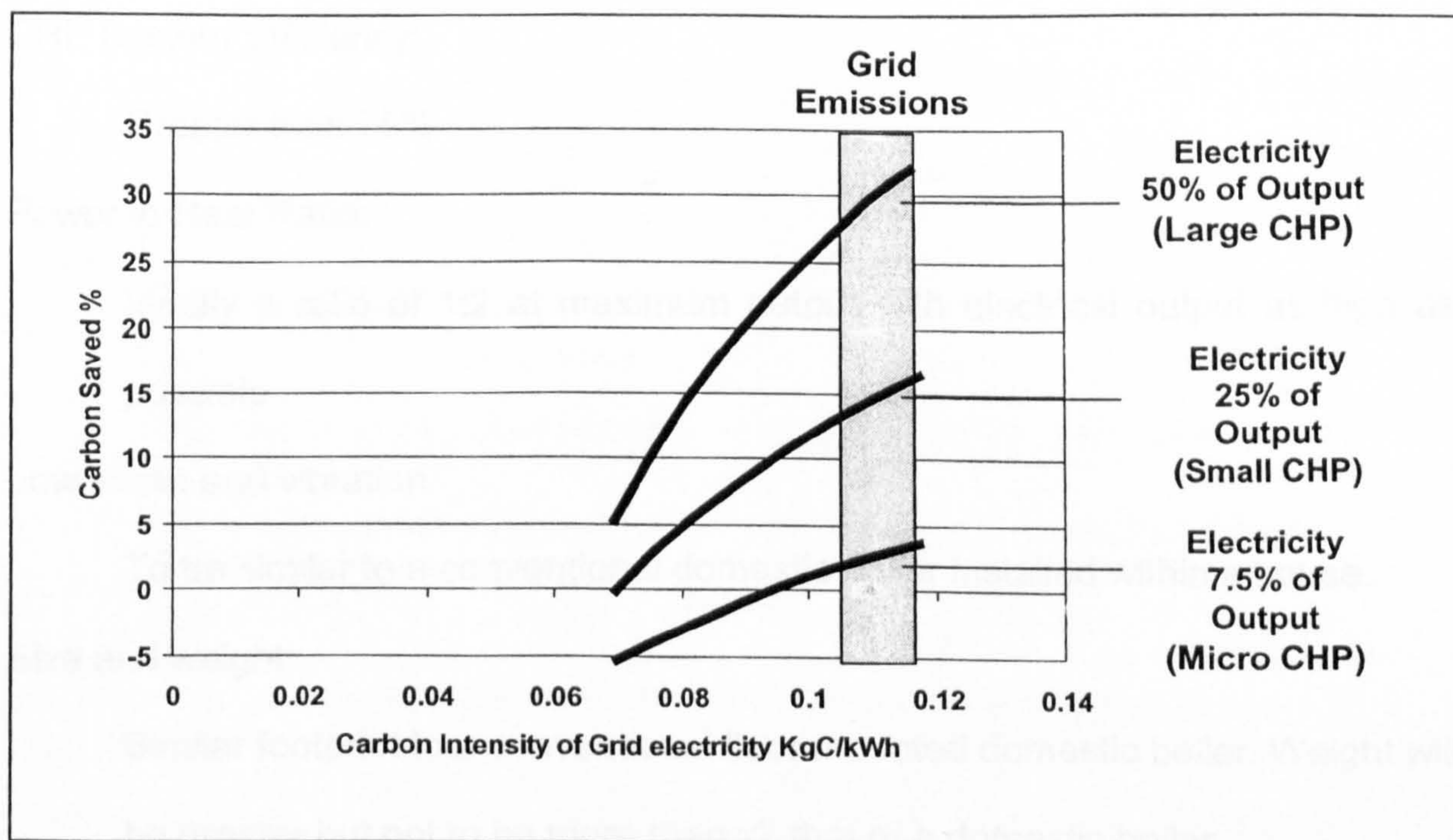


Fig 1.3 Comparison of Carbon Saved Performance of CHP systems

Source Carbon Trust Ref 3. Assumes 90% overall efficiency and grid intensity of 0.117 kgC/kWh)

The Carbon Trust further identified that for the micro CHP systems tested (Stirling Engines) they were only practical in larger and older houses where the heat demand was higher.

## 1.2 Requirements for Micro CHP

From table 1.1 and the findings from Ref 3 the ideal requirements for a micro CHP system are identified as:

Thermal efficiency of prime mover

Greater than a Stirling engine and ideally >25% (the same as a small CHP system)

CHP System Efficiency:

Greater than 75%

Power to Heat Ratio:

Ideally a ratio of 1:2 at maximum output with electrical output as high as possible

Low Noise and vibration

To be similar to a conventional domestic boiler installed within a house.

Size and weight

Similar footprint to a conventional floor mounted domestic boiler. Weight will be greater but not to be more than x2 that of a domestic boiler

Capital cost

Will be higher than a conventional boiler by up to x2

Service cost intervals

To be similar to servicing intervals on conventional domestic boilers. Costs may be higher due to the servicing of the prime mover.



**Running hours:**

Will need to operate for 12 months with an estimated average of 5 hours /day on an annual basis. (< 2000 hrs /year) Winter months will require more running hours and summer months

**1.3 Aims of Research**

The aims of the research were to identify the potential performance characteristics and design constraints of a RJC engine and a CHP system incorporating such an engine by:

1.
  - a. Detailed modeling of the RJC engine and a typical CHP system.
  - b. Building and testing RJC engines to evaluate both overall and component performance.
2. Proposing design requirements for future prototype RJC engines.

## 2.1 The RJC Engine

This type of engine employs the Joule (or Brayton) thermodynamic cycle, the same as a gas turbine. Its performance is determined by the characteristics of a positive displacement compressor and expander as opposed to rotodynamic. A positive displacement compressor is connected mechanically to a reciprocating expander, with energy added to the compressor air delivery in an external continuous combustion process, the whole to produce net power. Fig 2.1 illustrates the basic components of an RJC engine where both the expander and the compressor are of the conventional reciprocating piston type.

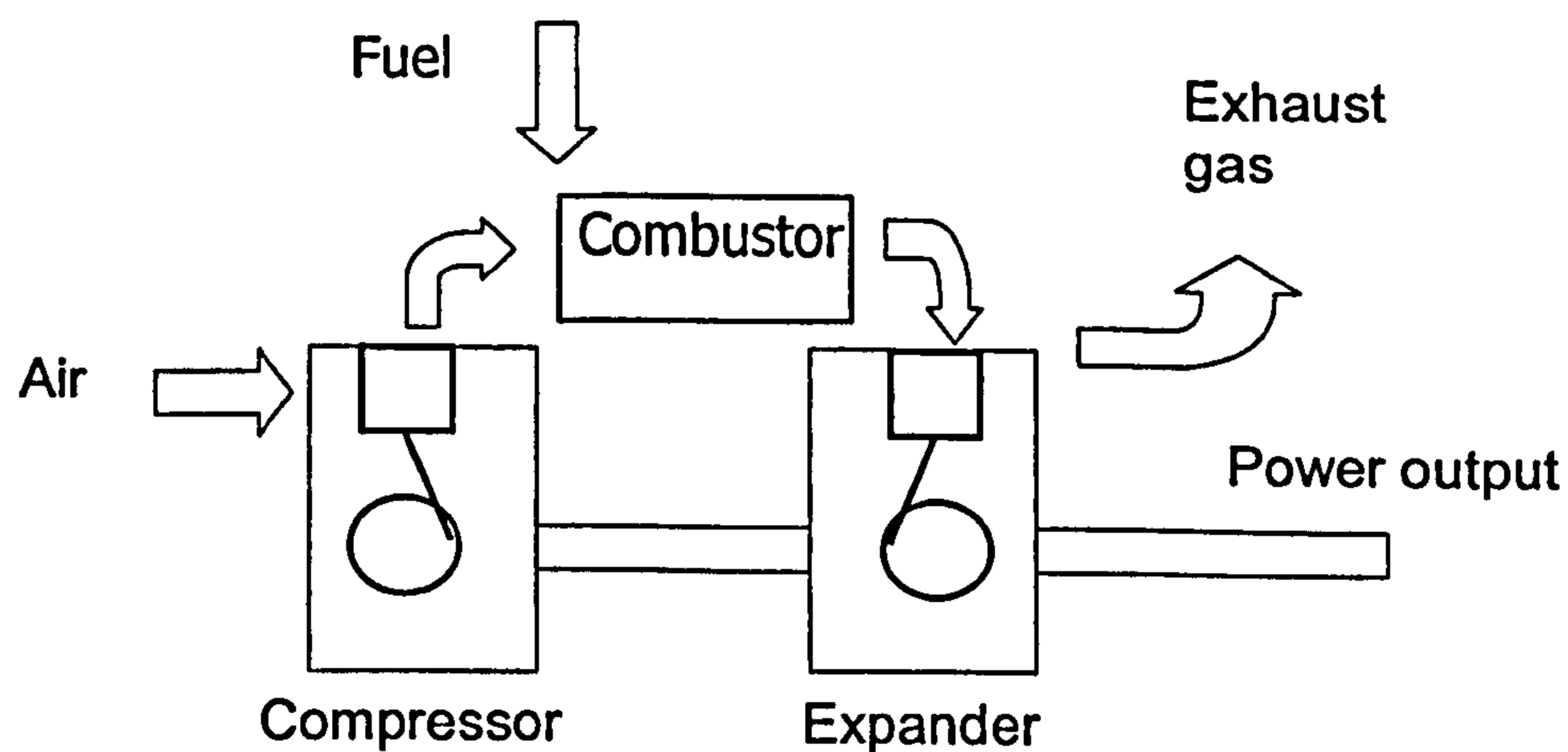


Fig 2.1 Basic Schematic of an RJC Engine

Although the concept of the RJC engine has been well understood for some time its development into a small practical prime mover has not been undertaken. One possible reason is that, like gas turbines, the response to power demands of the Joule cycle is inferior to that of internal combustion engine cycles and is therefore unsuitable for conventional automotive applications. The history of the RJC and proposals for engines are detailed

at Refs 5 and 6. Although the principle of the engine has been published there is no record in the public domain of an actual engine that has been built and operated.

## **2.2 Thermodynamic Modelling**

Previous research into the RJC engine at the University of Plymouth (UOP) using basic thermodynamic modelling had indicated that the RJC engine had the potential to be as thermally efficient as an internal combustion engine. The formulation of the basic thermodynamic model, and using air standard formulae, a first order assessment was made of performance Ref 7. The degree of refinement in the model allows for changes in gas properties, owing to combustion, leakages, pressure losses throughout the system, clearance volumes, and mechanical losses however they are only applied as percentages and not based on detailed analyses. The model does not allow for heat losses and the processes of compression and expansion are both assumed reversible and adiabatic. The manner in which the pressure drops and clearance volumes are incorporated into the model is illustrated by the respective pressure / volume charts Fig. 2.2 and defined in Chart 2.1

Part 2

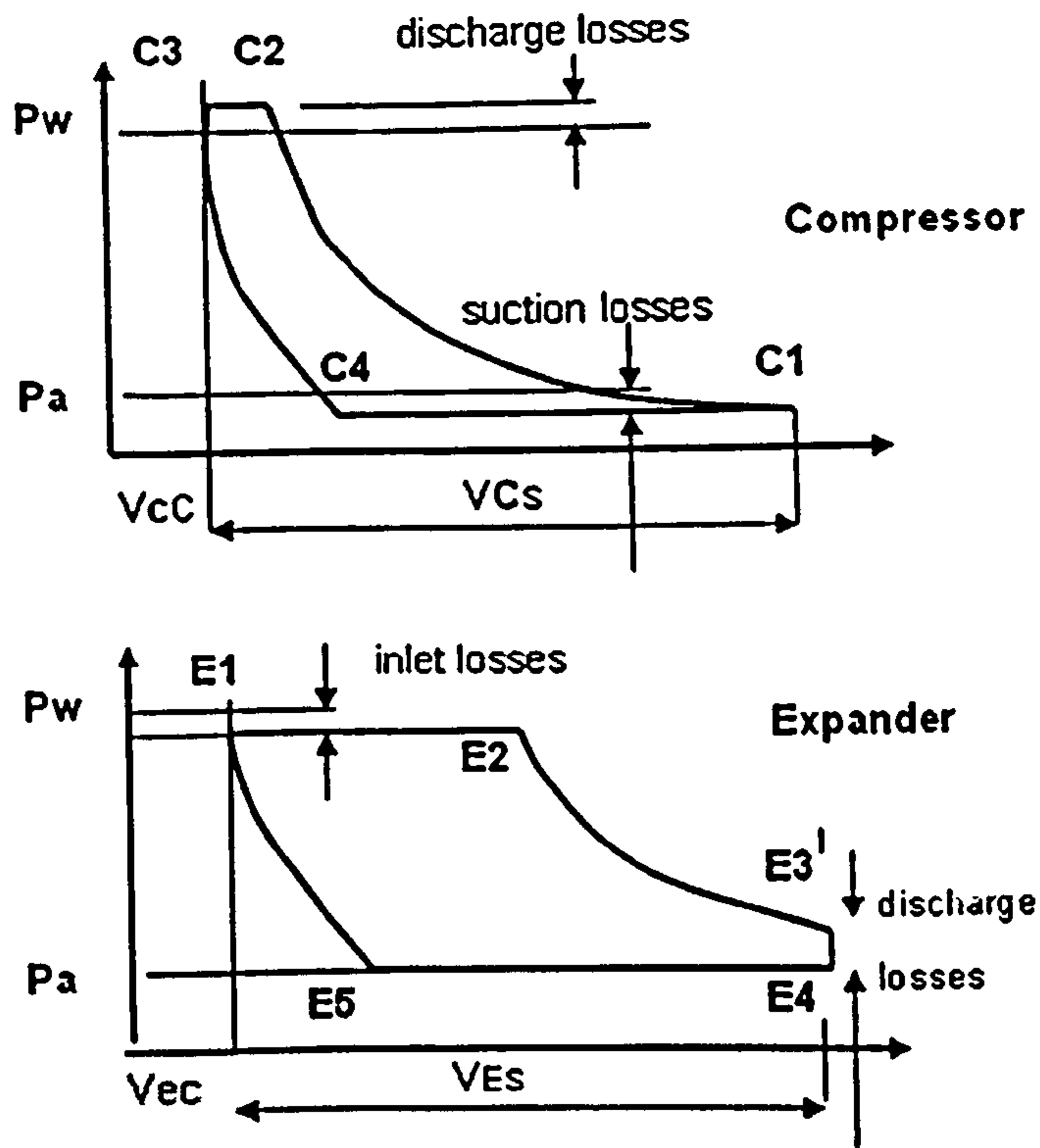


Fig 2.2 PV Diagrams for an RJC Engine

Pa	Atmospheric pressure
VcC	Compressor clearance volume
VcS	Compressor swept volume
Vec	Expander clearance volume
Ves	Expander swept volume
Compressor discharge losses	The compressor will compress air at a higher pressure than the system pressure resulting in additional work than the ideal
Compressor suction losses	The compressor suction will be below atmospheric pressure resulting in additional work than the ideal.
Expander inlet losses	A pressure drop across the expander inlet will result in lost expander work
Expander discharge losses	The expander will exhaust at above atmospheric pressure that will result in lost work.

Table 2.1 Definitions of Terms used in Fig 2.2

The controlling design factors of the engine established from the basic model are listed in Table 2.3

Operating pressure ratio	$r_p$
Maximum temperature controlled by air fuel ratio.	$T_{max}$
Compressor to expander swept volume ratio	$V_{Es} / V_{Cs}$
Clearance volumes	$V_{cc}$ and $V_{ec}$
Mechanical efficiencies	$\eta_m$
Pressure losses and Gas leakages.	$\Delta p$ See Fig 1.2

Table 2.2 Controlling Design Factors.

Combinations of the design factors in the basic model have been undertaken using spreadsheets an example copy of which is reproduced at Annex 2

The two most important design factors that influence the overall thermal efficiency and net specific work output are the pressure ratio and swept volume ratio. Using the values from Ref.7 for losses, clearances, valve timings and setting a maximum temperature of 1300 K a theoretical performance map is produced. This is shown Fig. 2.3

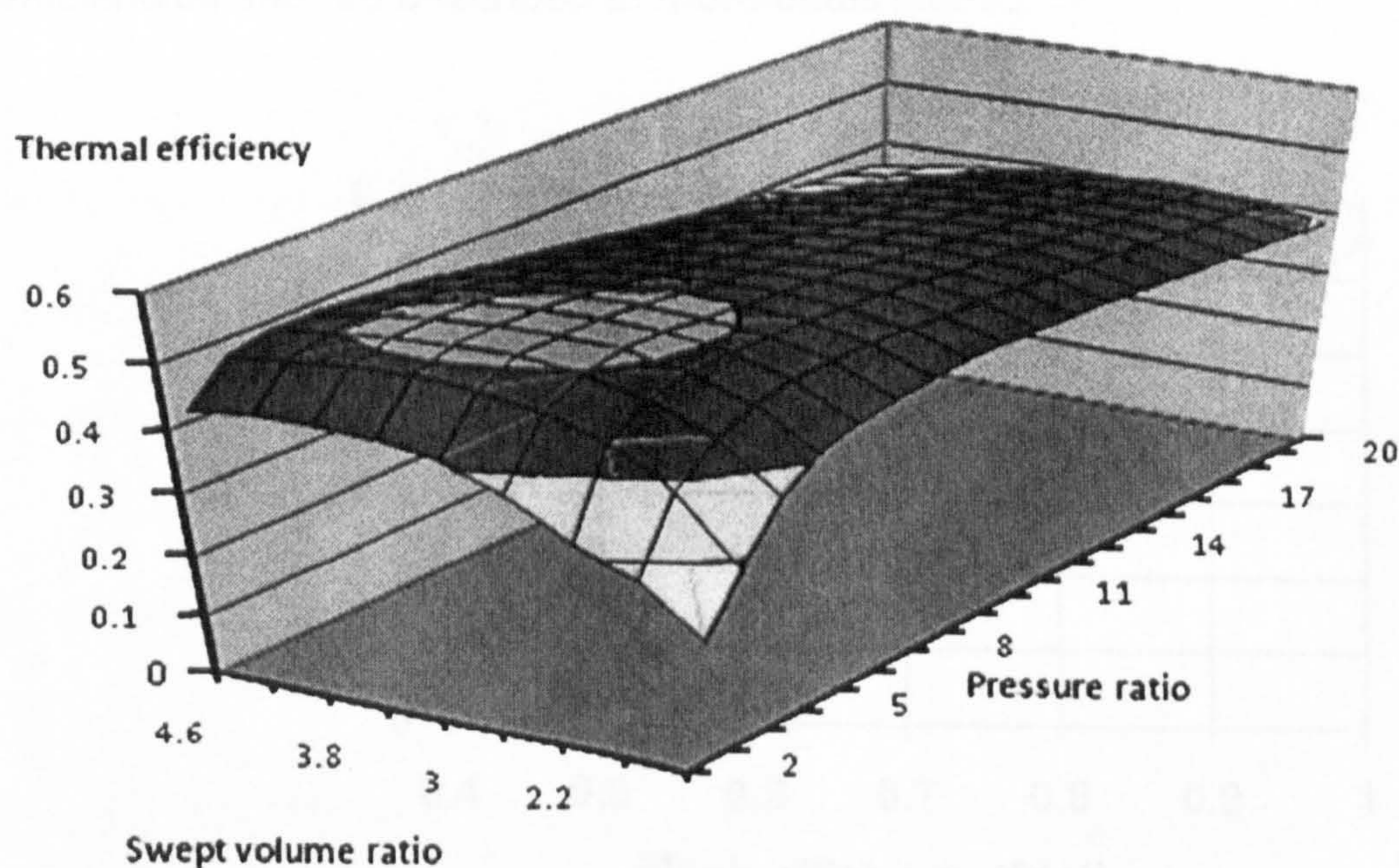


Fig 2.3 Performance Mapping of the RJC Engine

This performance map shows that high thermal efficiencies are theoretically possible with operating pressure ratios above 5 and swept volume ratios of around 2.5:1. This performance is based on the use of a recuperator that uses exhaust energy to pre-heat the combustion air (regeneration).

The basic model also shows that net work output is sensitive to frictional losses in the system (mechanical efficiency). Pressure losses also have a significant impact on the thermal efficiency. The greatest impact on net work output comes from the mechanical losses primarily in the form of friction between the lubricated surfaces. This is shown Fig 2.4 with the values determined via the thermodynamic model. The reason why friction has such a major impact is that with relatively lower pressures in the expanders, compared to internal combustion engines, high friction can represent a significant percentage of the expander work.

Pressure drops and leakage losses have a lesser effect on the thermal efficiencies and are described in more detail Ref 7.

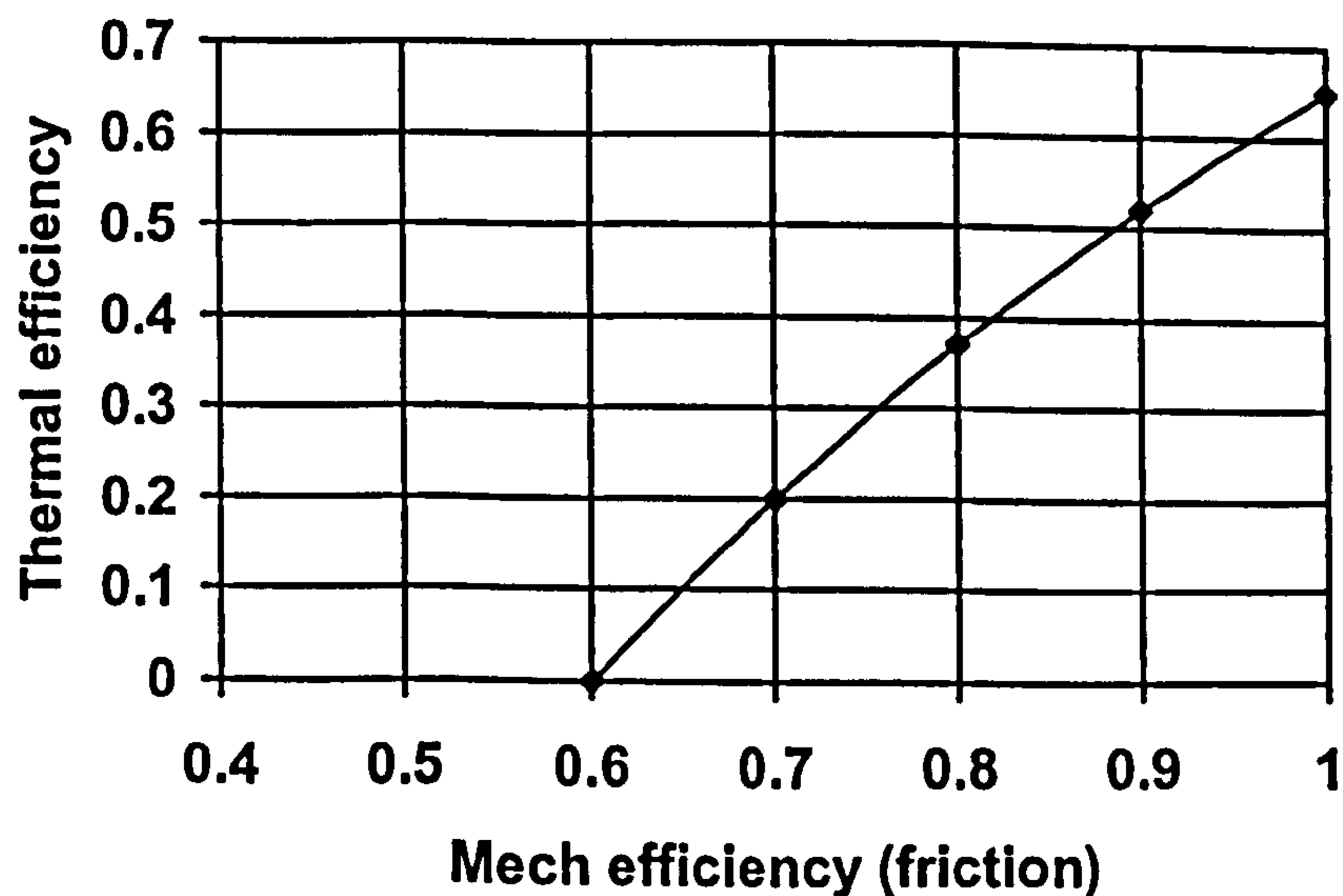


Fig. 2.4 Efficiencies of a RJC Engine

By varying the values of the design factors in Table 2.2 optimum values can be identified that result in high thermal efficiencies. The outcome from basic thermodynamic modelling is that the RJC engine has the potential to be as thermally efficient as the Otto or Diesel cycle engines and more thermally efficient than the Stirling cycle engine Ref 7.

### **2.3 Application of the RJC Engine**

The RJC engine lends itself best to steady operation with its output specified by its speed and power. It is also best suited to small power outputs (<30 kW) where it is theoretically as thermally efficient internal combustion engines. The RJC engine employed in a micro-CHP system has the potential to convert energy at over 80 % split between electrical power and usable heat, thereby reducing reliance on less thermally efficient centrally generated electricity which in turn will reduce overall CO<sub>2</sub> emissions. A conservative estimate of CO<sub>2</sub> emissions based on the electrical generation from a RJC micro-CHP system, utilising natural gas, is ~ 0.24 kgCO<sub>2</sub>/kWh, which is a major reduction when compared with the emission of 0.43 kgCO<sub>2</sub>/kWh from the electricity public supply network. Additionally, the external combustion process of the RJC engine has the potential to efficiently burn a wide range of gaseous and liquid fuels with low emissions of nitrous oxides and other exhaust contamination

The RJC engine has an application as the prime mover in micro CHP plant with sizes at the single dwelling/domestic level providing that the theoretical efficiencies can be realised.

## 2.4. Existing Patent Applications

For the RJC engine two patents were already registered (GB 2308864 and EP 0810356) and as such if a new engine patent was to be sought it would need to demonstrate that significant differences / improvements had been made over these existing patents. It is also noted that these two patents outlined at Figs 2.5 and 2.6 have both been deemed to have been withdrawn in 2000. From the experience gained from detailed modelling (Part 3) and engine testing (Part 4) and applying this to these two patents it is likely that neither would work satisfactorily

In patent GB 2308864, Fig 2.5, the system pressure is low at 1 bar and the temperature of the inlet gas is only 300 deg C. Modelling showed that zero thermal efficiency (self sustaining condition) was only achieved at 527 deg C and that at a system pressure of only 1 bar the frictional forces would result in mechanical efficiencies of less than 50%.



**UK Patent Application GB 2 308 864 A**

(43) Date of A Publication 09 07 1997

(11) Application No 9900033.6

(22) Date of Filing 09.01.1996

(71) Applicant

Service Services  
Abbots Meads, Back Lane, DRYBROOK,  
Gloucestershire, GL17 9DU, United Kingdom

Richard John Andrews  
2 Crescent Close, Bridgwood, STYCHOUSE,  
Gloucestershire, GL10 2AP, United Kingdom

(72) Inventor(s)

Service Services  
Richard John Andrews

(74) Agent and/or Address for Service

Service Services  
Abbots Meads, Back Lane, DRYBROOK,  
Gloucestershire, GL17 9DU, United Kingdom

(31) INT CL<sup>8</sup>  
F02B 23/00 23/16

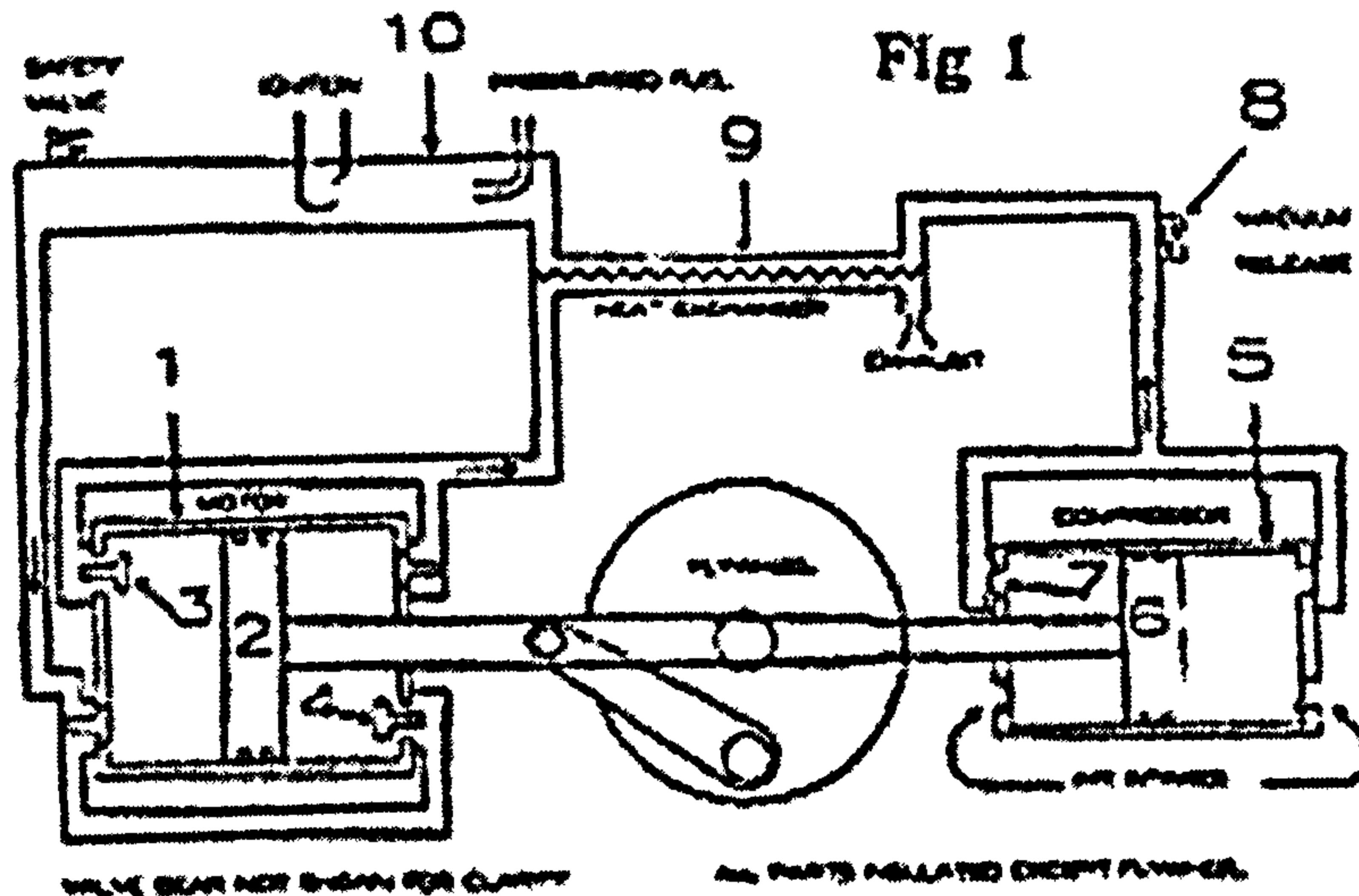
(52) UK CL (Section O)  
F1E 8/1A1 8/1A2

(58) Documents Cited  
GB 1160246 A GB 6528391 A US 4476821 A  
US 4325434 A

(54) Field of Search  
UK CL (Section O) F1E  
INT CL<sup>8</sup> F02B 23/00 23/16 23/18 23/19

(54) Mechanically coupled heat engine and compressor arrangement

(57) The piston 6 of the compressor 5 is mechanically coupled to the piston 2 of the engine 1. The output from the compressor 5 passes through a heat exchanger 9, where the gas is heated by the engine exhaust gases, before reaching the heat input section 10 where fuel, no methanol/water or surfactant or is burnt. The heat exchanger 8 tends to keep heat recirculating within the engine until it is output as mechanical energy. Four cylinders may be used, in a 90 degree layout. Vane-type or turbine compressors and motors may be used instead. A diaphragm engine using a low grade heat source is disclosed.



GB 2 308 864

Fig 2.5 Patent Claim GB 23008864 Dated 1997

For patent EP0810356 (ABB Combustion Systems), Fig 2.6, whilst the system pressure is above 5 bar and inlet gas temperature is >800C the use of an inlet side valve results in a potentially large clearance volume and thus

a reduction in specific work output. Additionally valve sizes and cylinder dimensions i.e. bore to stroke ratios were not defined.



**United States Patent** [19]  
**Hufton**

[11] **Patent Number:** 6,012,280  
 [45] **Date of Patent:** Jan. 11, 2000

[34] **RECIPROCATING ENGINE**

[70] **Inventor:** Peter F Hufton, 79 Beilfeld Road,  
 Epsom, Surrey, United Kingdom,  
 TW20 4RL

[21] **App. No.:** 08/966,153

[22] **Filed:** May 30, 1997

[30] **Foreign Application Priority Data**

Jan. 1, 1996 [GB] United Kingdom 9614981

[51] **Int. Cl. 7** F02C 3/03

[52] **U.S. Cl.** 60/39.63; 60/762; 92/133;  
 92/063; 2

[56] **Field of Search** 60/39.63, 39.63,  
 60/762, 92/133, 92/2

[96] **References Cited**

**U.S. PATENT DOCUMENTS**

1,036,079 04/12/1909 FORD  
 1,321,962 12/29/19 FORD

3,826,081 7/27/74 Van Auweraete  
 4,166,574 2/19/77 Ekin  
 4,179,879 12/23/78 Kimmel

**FOREIGN PATENT DOCUMENTS**

70778 03/979 U.S.S.R. 92196; 2  
 80949 11/991 U.S.S.R. 92196; 2

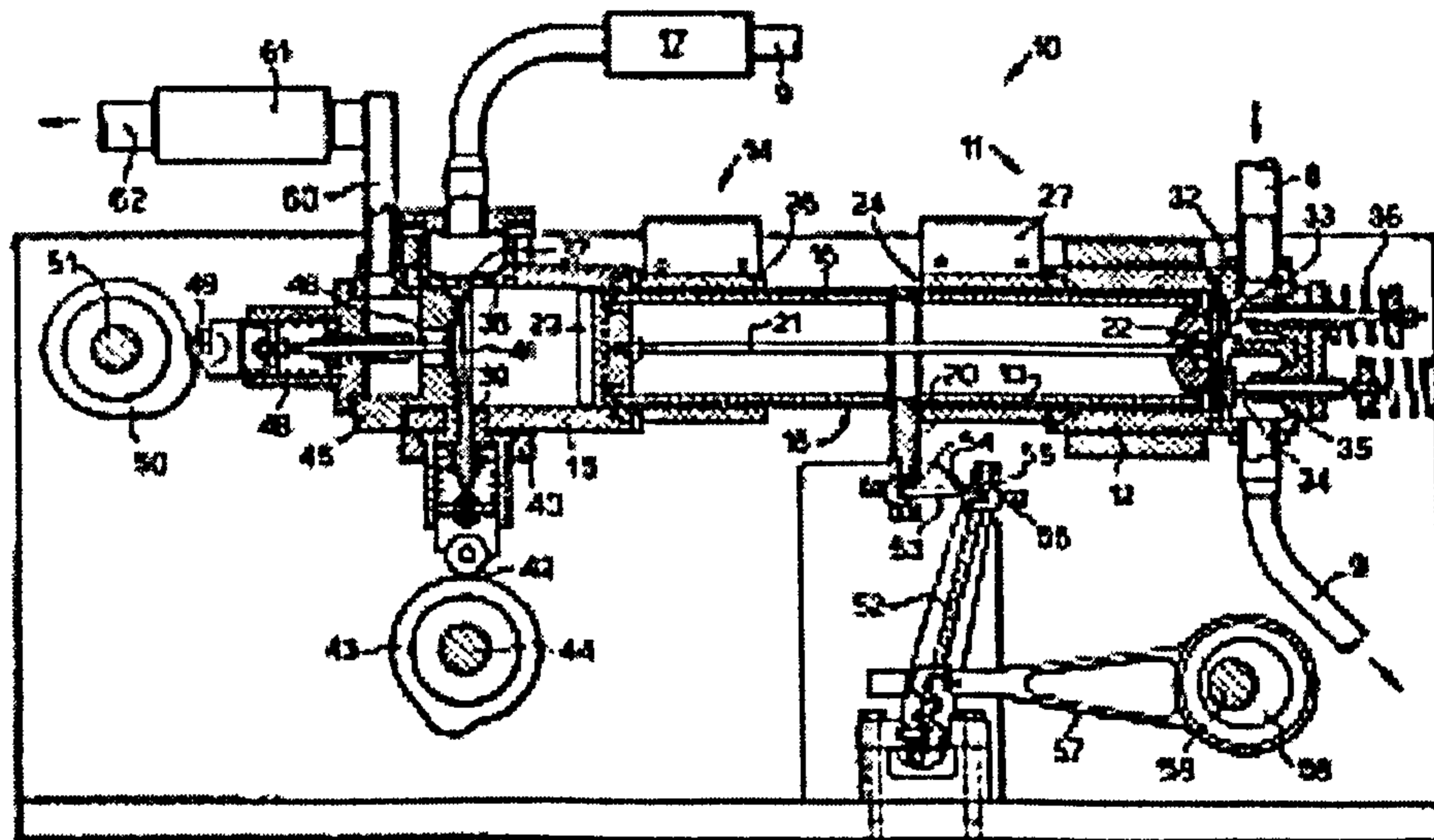
**Primary Examiner—Michael Kuznetz**

**Attorney, Agent, or Firm—W. Warren Talbot, Parkes & Mansell PLLC**

[57] **ABSTRACT**

A reciprocating engine (10) comprises separate cylinders (12 and 13) for air compression and expansion with heating of the compressed air taking place in a heat exchanger (17) or combustor (14) located between the cylinders (12 and 13). The flow of gas into the expander cylinder (13) is controlled by an admission valve (37). The stem (41) of the admission valve (37) extends transversely across the expander cylinder (13) and is cooled by the flow of exhaust gases out of the expander cylinder (13).

13 Claims, 4 Drawing Sheets



Application Deemed to be Withdrawn 21/8/2000

Fig 2.6 Patent Claim EP 0810356 ABB Combustion Services 1998

In both patents there was little detail was given on the combustor and the compressor both of which have been determined to be critical for a RJC engine to produce net power. The conclusion drawn is that a RJC engine designed based on the findings in this work can be patented as it would

incorporate novel and unique aspects and be a demonstrable improvement on previous patent applications.

## **2.5 Published Papers**

One of the conditions for patent application is that the information has not previously been published or made known to others. Although a general paper on the general modelling and the findings from Part 4 (Annex 2) has been published Ref.8 no further papers has been written until the intellectual property rights have been resolved.

## **Performance Modelling of the RJC Engine and CHP Systems**

### **3.1 Modelling**

The objective of detailed modelling is to simulate an actual process and to allow variations in the parameters that will enable predictions of performance e.g. thermal efficiency and specific work output. The optimised parameters such as valve diameters and valve lift can then be taken forward into detail physical designs

Modelling is undertaken in three stages these being

1. Basic engine modelling to determine likely performance
2. More detailed modelling to determine specific losses and thus refine the basic engine model
3. Applying the detailed engine model to determine CHP system performance

### **3.2 Basic RJC Engine Modelling**

Modelling was conducted on an opposed piston engine detailed at Part 4.4, with one piston as an expander and one piston as a compressor and using air standard equation Ref 9. The operating conditions initially chosen were for a system pressure of 7.5 bar g and a maximum gas inlet temperature of 850 C. The pressure of 7.5 bar g represents that which can be reasonably achieved in a single stage compressor whilst the gas inlet temperature of 850 C represents a safe maximum for the expander piston.

The expander model considers the ideal PV diagram Fig 3.1 to determine the ideal work per cycle

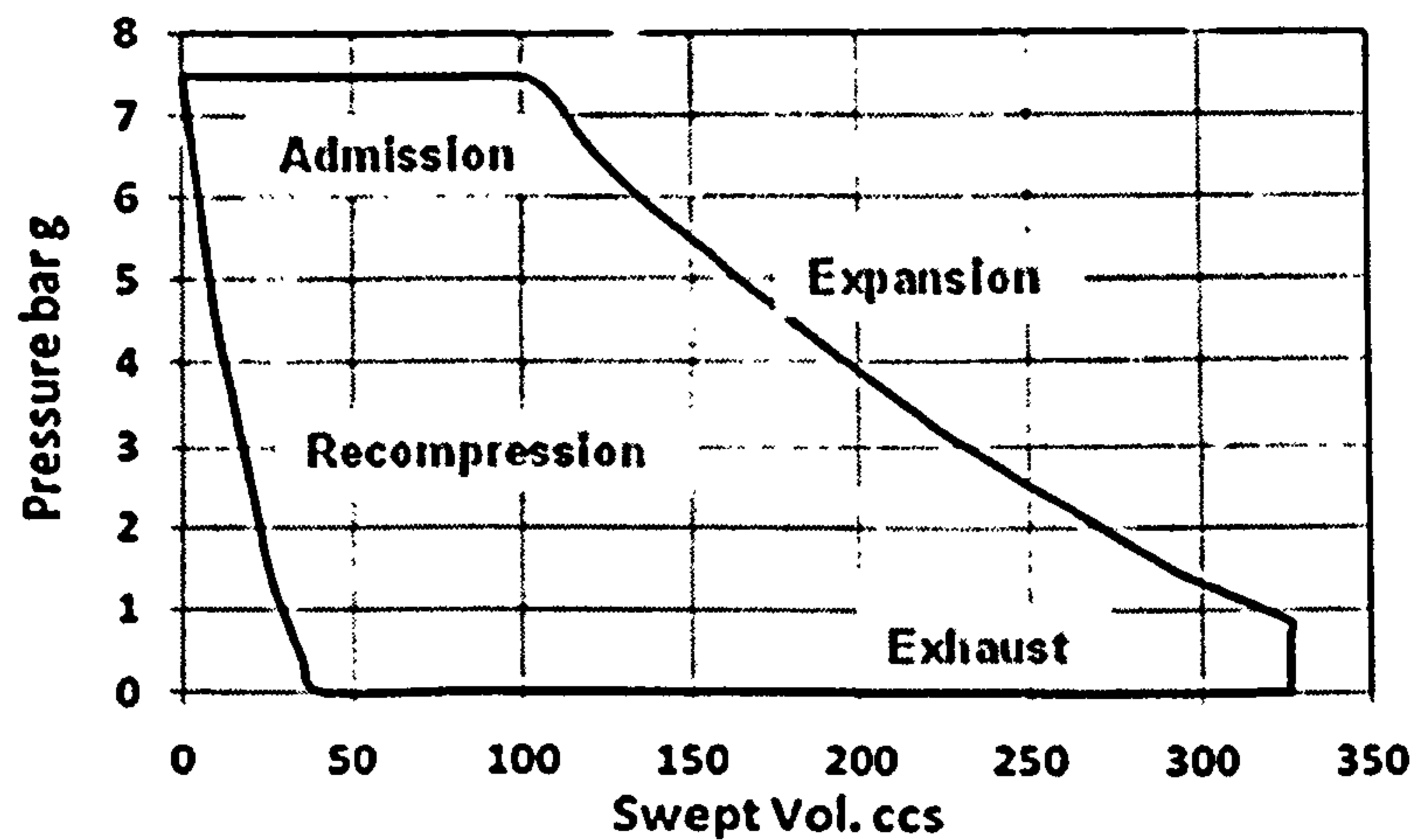


Fig. 3.1 Ideal PV Diagram for a RJC Engine.

The compressor performance was modelled on a performance evaluation carried out on a single cylinder compressor detailed at Part 4.8. The compressor performance evaluation compared the actual PV diagrams against an ideal PV diagrams which realised a 15% difference. This means that for the calculation for ideal work required by the compressor a correction has to be made to obtain the actual work required. Mechanical efficiencies of 0.9 were assumed for both the expander and compressor. The values used in the modelling are detailed at Table 3.1 and the spreadsheet for the model is at Annex 3.

Expander		Compressor	
Bore mm	82	PV efficiency	0.85
Stroke mm	61.5	Mechanical efficiency	0.9
Swept Vol. ccs	325	Mass flow rate Kg/sec	Matched to expander requirement
Clearance vol. ccs	Variable 1-16% of swept volume	Discharge temperature deg C	50
Inlet opening, degrees	Variable 50~100	Polytropic index of compression. See <i>Part 4.1</i>	1.2
Mechanical efficiency	0.9		
RPM	1500		
System pressure Bar g	Variable 2~9		
Hot gas inlet temperature deg C	850		
Polytropic index of expansion	1.37		
Polytropic index for recompression	1.2		
Expansion pressure loss	5% of work		
Recompression pressure loss	5% of work		

Table 3.1 Values Used in Basic RJC Modelling

Gas inlet opening and closing i.e. inlet valve opening/closing as well as exhaust valve opening/closing are assumed to be instantaneous. This is obviously not the case so to compensate a first estimate of pressure losses with fixed values of 5% are given for expansion and recompression. Detail pressure loss modelling is undertaken Part 3.8

### 3.3 Findings from the Basic model.

#### 3.3.1 Effect of Clearance Volumes on Work Output

Clearance volumes have a significant effect on the available power produced by the expander. For the conditions of 7.5 bar g system pressure, gas inlet

temperature of 850 C and a gas inlet valve opening of 70 degrees of the stroke the results is shown in Fig 3.2

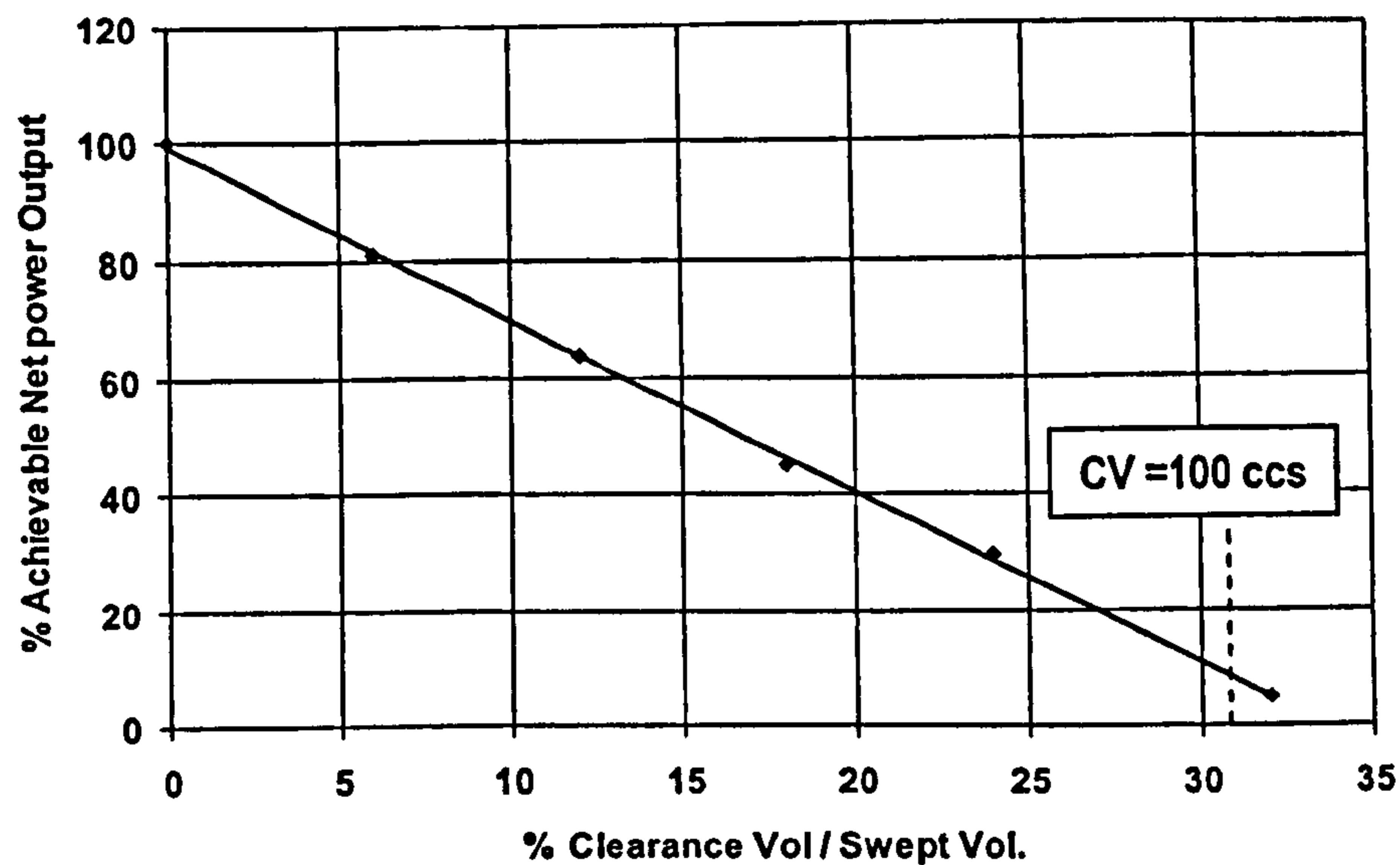


Fig. 3.2 Effect of Clearance Volume % on Achievable Work Output %

The higher the clearance volume the greater the amount of recompression work required and thus reduced work output. Some clearance volume is required to accommodate downward movement of valves but ideally should be no more than 3%

### 3.3.2 Effect of System Pressure

With a fixed clearance volume of 3%, an inlet gas temperature of 850 C and inlet valve opening of 70 degrees the system pressure was varied from 2 to 9 bar g. The results are shown in Fig 3.3 where there is an increasing net power output with system pressure

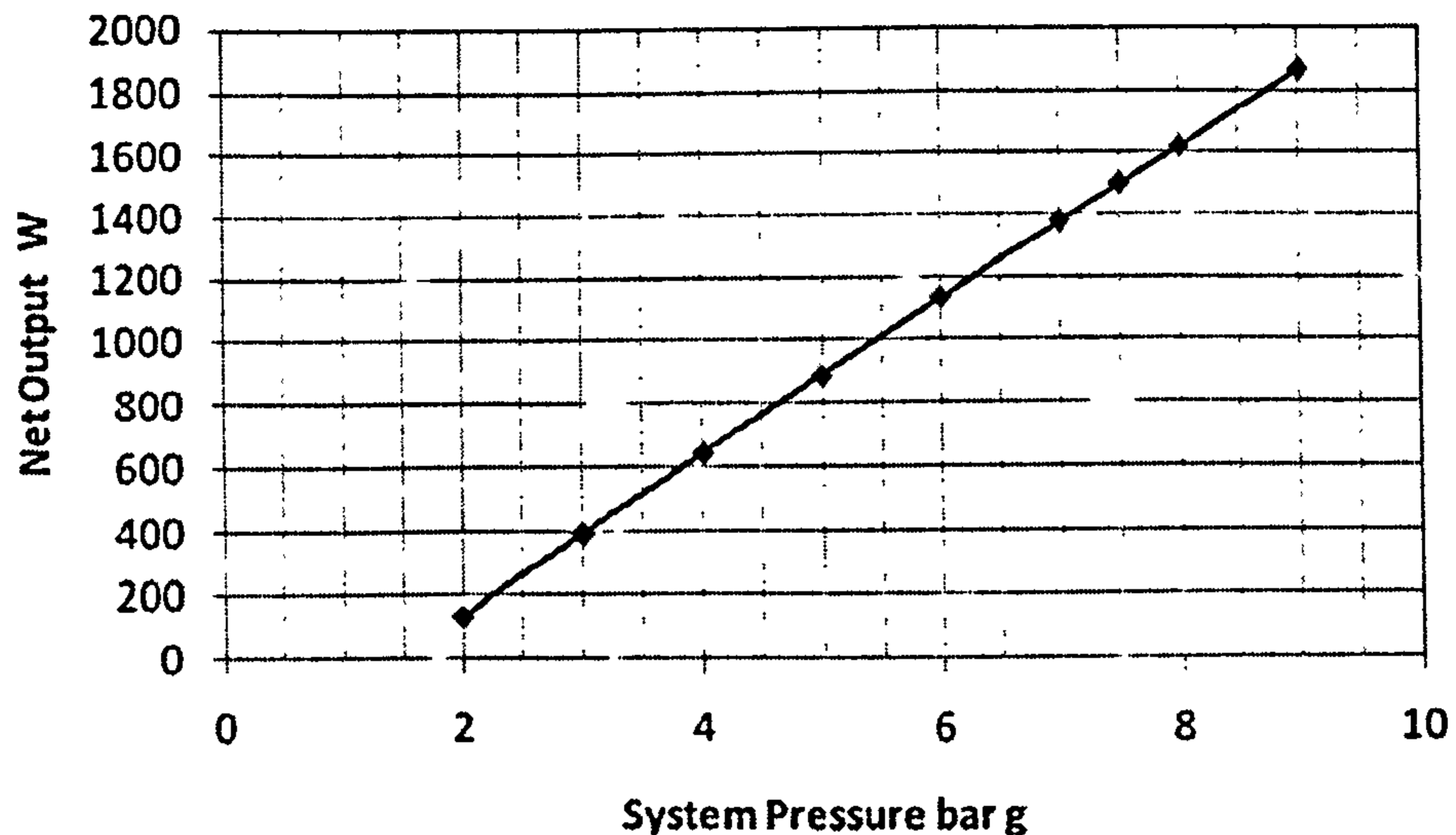


Fig 3.3 Net Output J/cycle vs. System Pressure bar g

However the compressor model does not take into effect that in single stage compression to high pressures there is an increase in compressed gas temperature and thus a reduced mass flow. In reality single stage compression is often limited to no more than 8 bar g. For further modelling a maximum system pressure of 7.5 g is used.

### 3.3.3 Effect of Inlet Valve Opening

The basic model uses a valve that has instantaneous opening and closing. Where such a profile is used then the maximum thermal efficiency of 24% occurs at 60 degrees, Fig 3.4. If regeneration is employed i.e. hot engine exhaust gas is used to preheat the air prior to combustion then there is an improvement in thermal efficiency. For preheated combustion at 300 C the thermal efficiency increases to 33%. A valve opening greater than 60 degrees results in lower thermal efficiencies because the mass flow is greater and thus more energy is required to heat the compressed air to 850 C



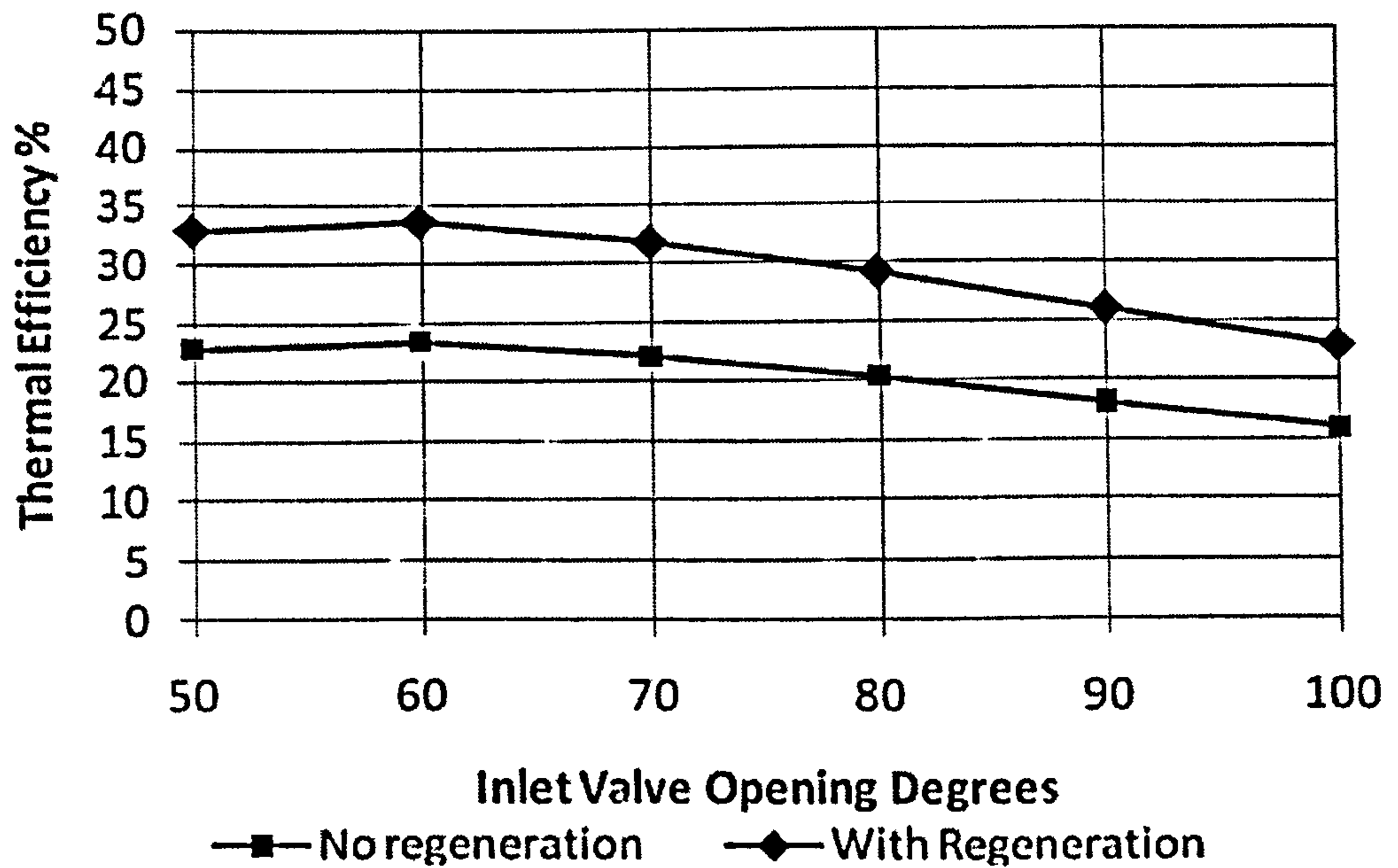


Fig 3.4 Thermal Efficiency Vs Inlet Valve Opening

This is further demonstrated in Fig 3.5 where the RJC engine work and compressor work and the difference (net work) plotted against inlet valve opening. In practice the inlet valve will open to its maximum lift over a period, remain at its maximum lift for a further period and then close over another period. This implies that in practice the opening angle will be greater than 60 degrees to allow the flow through of hot gas to be equivalent. This is investigated in the detailed modelling of pressure losses in Part 3.8. and is termed apparent valve opening.

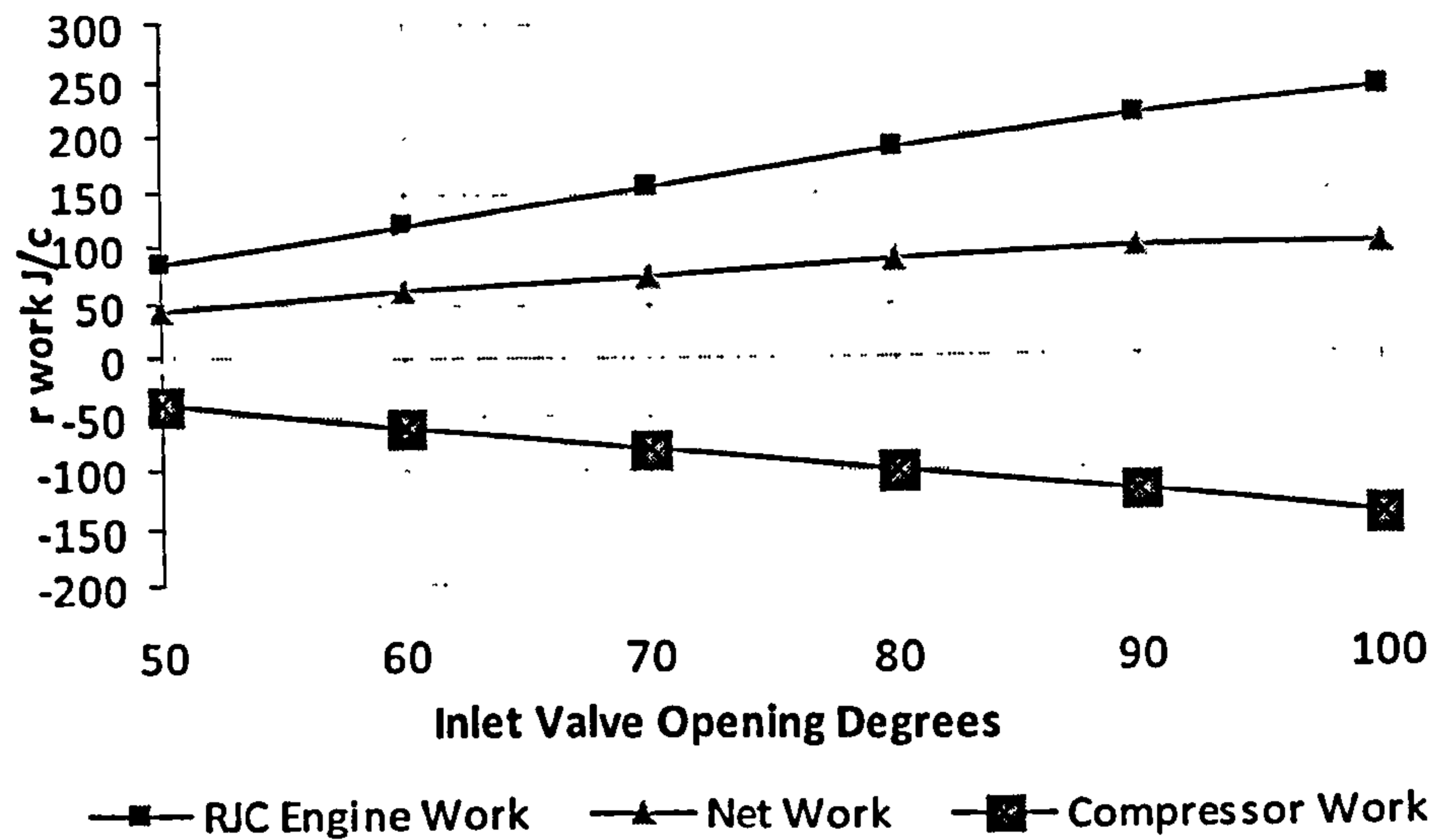


Figure 3.5 RJC Engine, Compressor and Net Work vs. Inlet Valve Opening

### 3.4 Conclusions from Basic Modelling of RJC Engine

- Thermal efficiencies of up to 33% are achievable with regeneration to 300 C. Without regeneration maximum thermal efficiency is 24%.
- Improving the mechanical efficiency of both the expander and compressor from 0.9 to 0.95 improves the thermal efficiency by 2.2%.
- Maximum thermal efficiency occurs at an inlet valve opening around 60 degrees. This is for an instantaneous opening and closing inlet valve.
- Net output at the condition of maximum thermal efficiency is 1200 W. The power output of 3 kW identified at Part 2 will require an engine with a displacement of around 1000 ccs. The detail modelling will investigate the performance of engines of this displacement.

### 3.5 Detailed Modelling

Detail modelling replaces the estimated values for friction, indices for expansion and compression and pressure losses (used in basic modelling) with more accurate values. When these values are applied a better indication of efficiencies and performance for both the RJC engine and micro CHP system can be derived.

The basic expression that connects all of the losses to the RJC engine output is defined as

$$\text{Actual work} = \text{Indicated work} - (\text{Friction losses} + \text{Thermal losses} + \text{Pressure losses})$$

Where indicated work is that measured from a PV diagram

The three loss terms are defined as:

#### 3.5.1 Friction Loss

The frictional losses in any engine is the work required to overcome friction in bearings, ring and liner interface, cam box mechanisms and oil pump drive etc.

The total of all this frictional work is the difference between measured indicated work and measured brake work and can be expressed as energy loss per cycle, frictional power loss or frictional mean effective pressure (FMEP)

#### 3.5.2 Thermal Loss

The hot gas admitted to the engine will reduce in temperature during the expansion process. This process is not adiabatic but polytropic and as such heat is released by the gas by convection and radiation to the cylinder walls, piston crown and cylinder head. The heat released is the process of thermal loss and it is by determination of this loss that the temperature at the end of expansion, and thus pressure, which will determine the indicated work done and final gas temperature.

### 3.5.3 Pressure Loss

Pressure losses reduce the amount of work available from expansion and increase the amount of work in recompression. Pressure loss modelling, validated by measurements of a PV diagram of an experimental engine, allow variations to be made in valve size, valve lift, stroke to bore ratios and 'cam profiles/timing' to minimise these losses.

### **3.6 Friction Modelling**

The friction in a reciprocating engine is the sum of the frictional energy losses generated from the following:

1. Ring pack and liner interface
2. Crank and cam shaft drive bearings
3. Crankcase oil seals
4. Crankcase pressurisation from blow-by gasses
5. Cam-box drive
6. Cam-box mechanisms
7. Inlet and exhaust valve stem friction in valve guides
8. Output drive couplings.
9. Oil pump
10. Water pump (if fitted)

For a given engine RPM the frictional work being the difference between indicated and brake work remains sensibly constant but at higher pressures represents a reducing percentage of indicated power. This is in line with the test data at Part 4 in that the maximum mechanical efficiency attained was at 7.5 bar air supply pressure.

Ring pack friction can account from between 40% – 80% of the total engine friction

Refs 10 and 11

### 3.6.1 Friction Reduction Methods

Noting that up to 80% of friction is generated between the rings and the cylinder over a cycle then if this can be reduced it would significantly improve the overall mechanical friction. Ref 12 also investigated the effect of using a single piston ring and found that even though peak frictional forces increase the overall effect was to reduce the frictional force by up to 50%. This is illustrated in Fig 3.6 which shows an idealised characteristic.

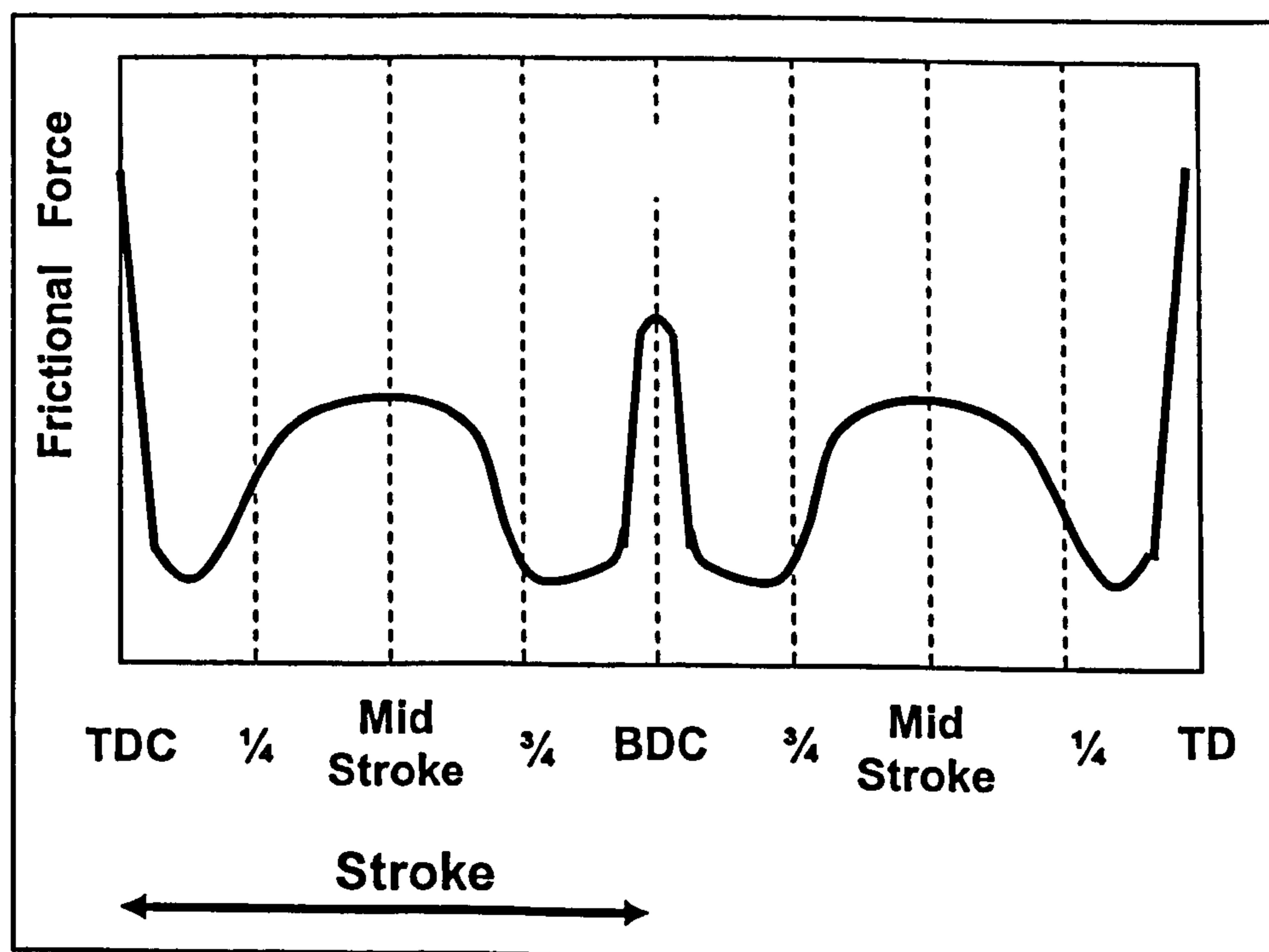


Fig 3.6 Frictional Force Over One Cycle

Ref. 13 however does go some way to explain ring pack friction and how it varies over the stroke. It describes tests on a single cylinder four stroke diesel test engine

that had a floating cylinder where piston ring frictional forces could be measured from the forces induced on the cylinder. A typical plot of friction force over a single cycle is reproduced at Fig 3.8 which shows high frictional peaks at TDC and BDC.

This can be further explained by examination of a typical Stribeck curve Fig 3.7 that relates the coefficient of friction to the instantaneous velocity of the piston during a cycle. The x axis for the Stribeck curve has the value of:

**Dynamic Viscosity ( $\mu$ ) x Sliding Speed (V) / Pressure Between Sliding Surfaces (P)**

Hence if the supply pressure increases the Stribeck plot is moved to the left. This would result in higher peak pressures at TDC but lower pressures at mid stroke.

Ref.13 also showed that overall frictional force reduced as pressure was increased.

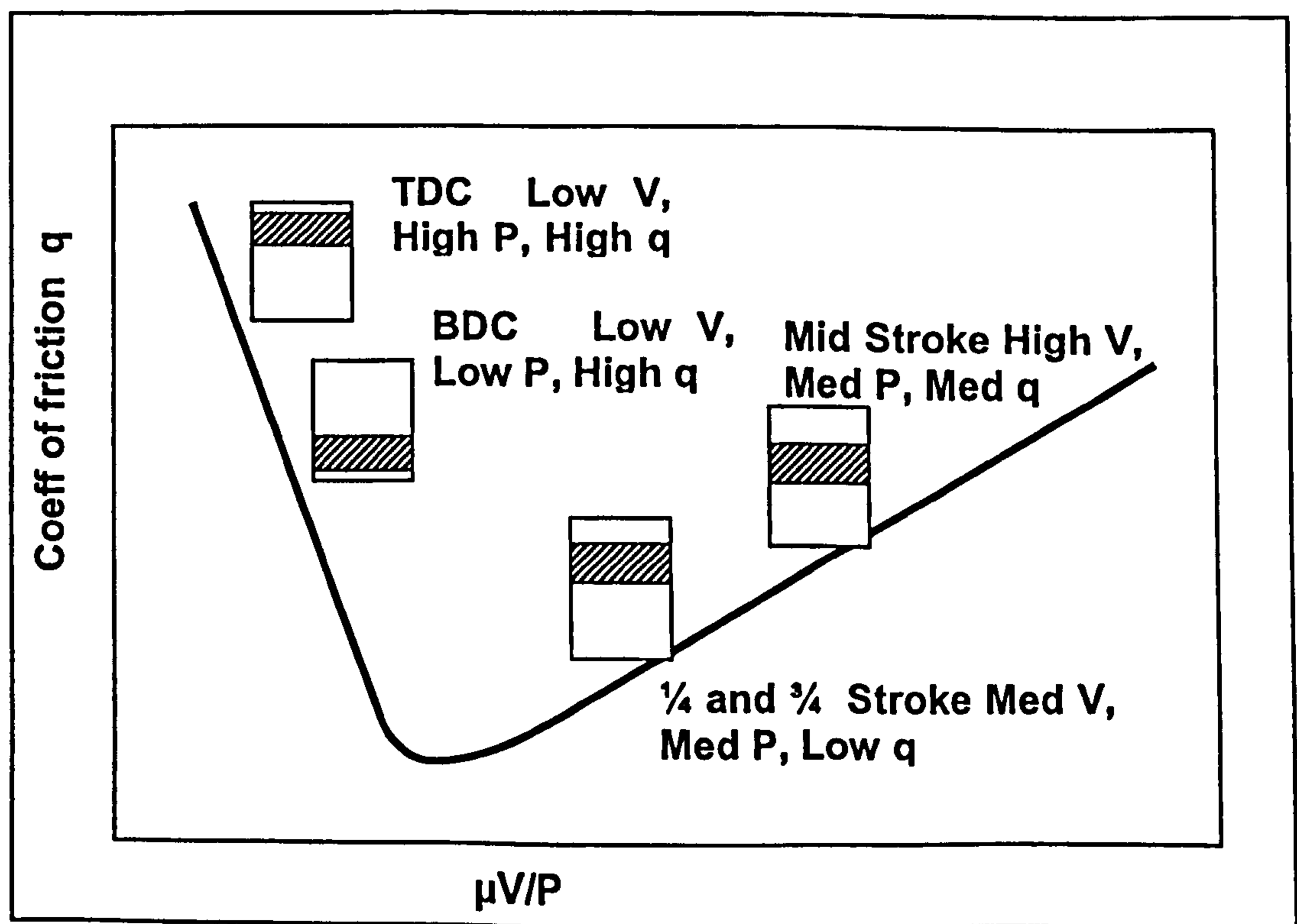
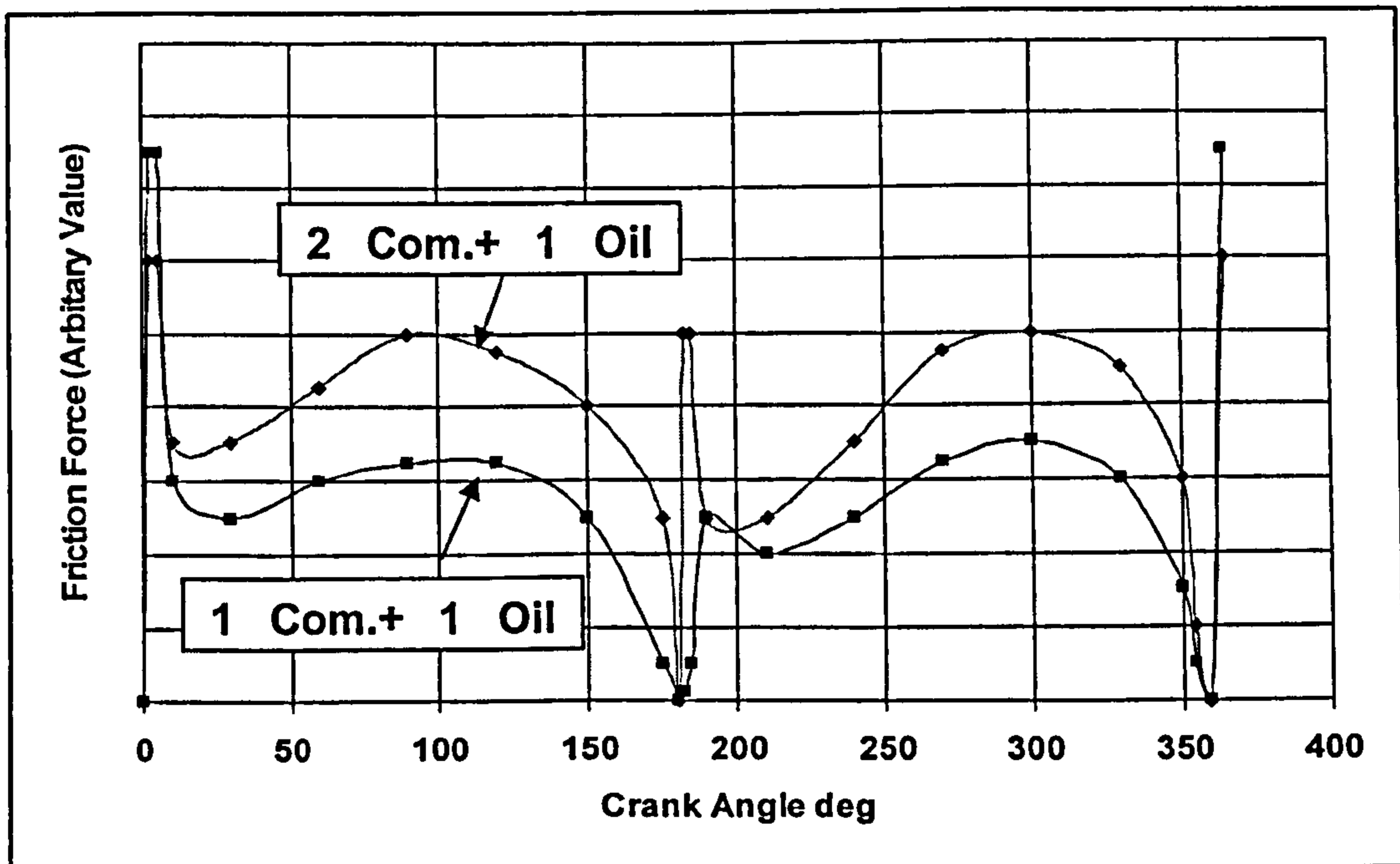


Fig 3.8 Coefficient of Friction Over One Cycle



**Mean friction Force = ~70% Maximum**

Fig 3.8 Typical Characteristic of Ring Friction Force Over Cycle

### 3.6.2 Existing Friction Models

More recent work on ring pack /piston/cylinder friction reduction has been reported at Ref.14. This work investigated oil control ring and piston ring design, cylinder honing patterns, piston skirt profiles and the influence of lubricant viscosity. The work comprised of tests on a 6 cylinder Waukesha gas engine, having a BMEP of 14 Bar, and theoretical modelling. By the optimisation of each of all the aspects of piston friction a 50% reduction was anticipated.

The overall conclusion from these two references is that a 50 % reduction in piston friction is achievable. Additionally if an engine was designed with antifriction bearings then there would be further reductions in frictional work

Almost all friction modelling that has been reported is based on experimental data.

There is no universal relationship that covers all engines and the empirical data

reported in each case relates to specific engine types and sizes. Typical of the relationships reported are:

For large four stroke automotive engines Winterbourne Ref 15 gives the expression:

$$\text{FMEP (bar)} = 0.137 + P_{\text{max}}/200 + 0.162.mps$$

where mps is the mean piston speed in m/s and P<sub>max</sub> is in bar g

And for similar engines Chen and Flynn Ref 16 gives the expression

$$\text{FMEP (bar)} = 0.061 + P_{\text{max}}/60 + 0.294.N/1000$$

where N is the engine speed in revs /min and P<sub>max</sub> is in bar g

Blair Ref 17 derived two separate relationships one for a small four stroke automotive engines:

$$\text{FMEP} = 25000 + 125LstN$$

And one for high speed two stroke engines with rolling element bearings

$$\text{FMEP (bar)} = 150 . Lst . N$$

where Lst is the length of stroke and N is the engine speed in revs/minute.

When the above models are applied to an inlet pressure of 7.5 bar g, there is considerable variation in FMEP Table 4.1.

Model	1500 RPM	3000 RPM
Winterbourne	0.627	1.163
Chen and Flynn	0.6725	1.068
Blair Auto	0.365	0.481
Blair	0.137	0.274

Table 3.2 Model Values of FMEP (bar)



### 3.6.3 Modelling the RJC Engine

The wide variation in Table 3.2 means that existing models cannot be used with confidence for a RJC engine and as such a different approach has to be taken.

The primary reasons for deriving a friction model for an RJC engine are to:

- Generate a value of ring pack friction that can be used in thermal modelling.
- Generate a value of FMEP for any RJC engine such that the net work output and mechanical efficiency can be determined from a model of the IMEP (which takes into effect pressure losses).

The heat generated from the ring pack friction, within the cylinder, will add to the heat transfer from the cylinder and from published data on motoring trials of various engines this can vary from 40% to 80% of the total FMEP. At Ref 14 piston ring pack FMEP was measured accurately, using a six cylinder gas engine running at 1800 RPM with each cylinder having a displacement of 3 litres. Values measured ranged from 13 to 19 kPa dependent upon the viscosity of the oil used and for a SAE 40 grade the value was 17 kPa. Ref 14 also states that ring pack friction contributed 40% of the total engine friction. Comparison of this single value with other friction models Fig 3.9 shows that it lies on the same characteristic as the Blair two stroke correlation. It is then assumed that the ring pack friction characteristic increases with increasing RPM and follows the Blair correlation. It is this characteristic that is then used for piston ring friction in thermal modelling for the RJC engine.

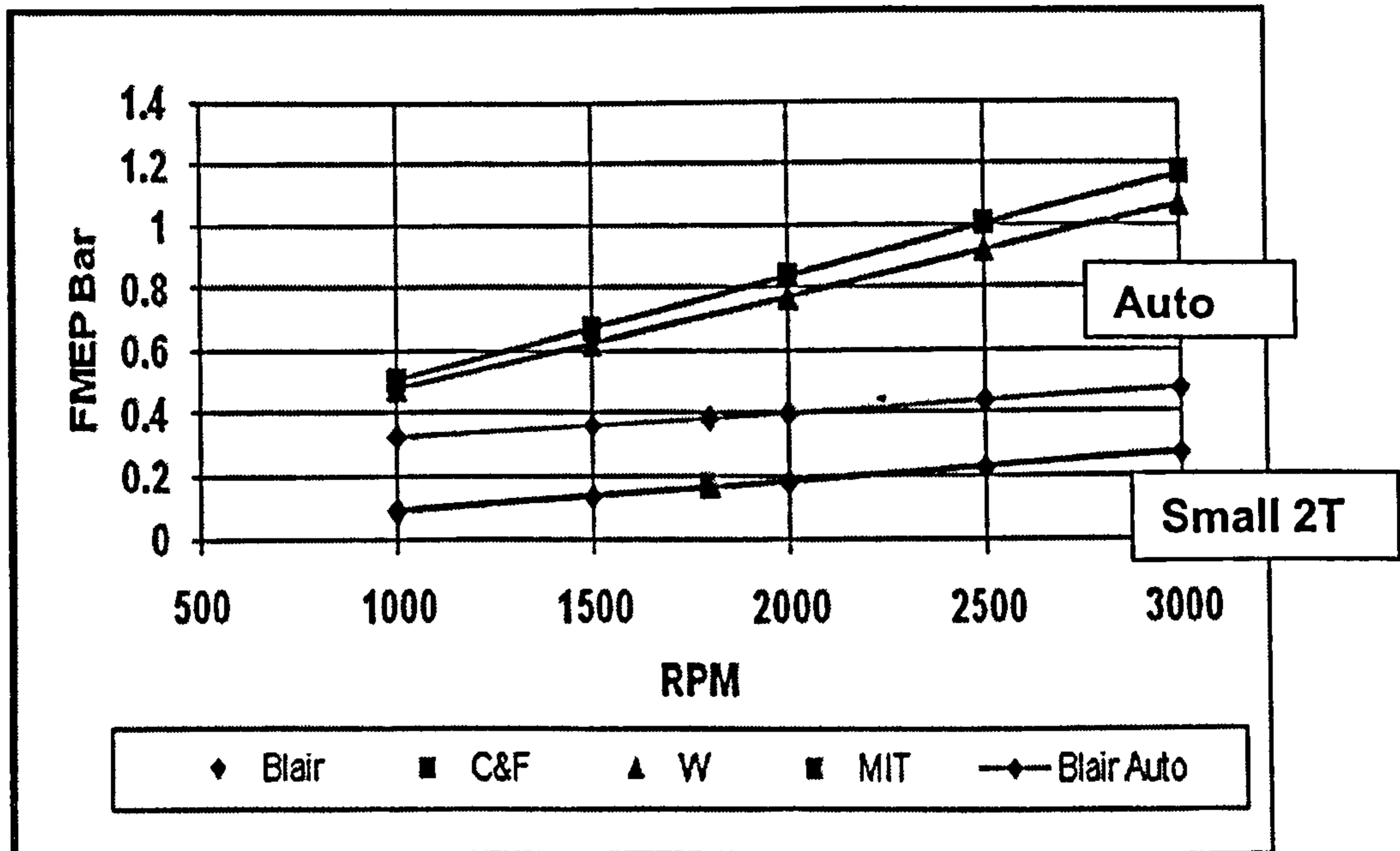


Fig 3.9 Comparison of Engine Friction Models

Overall engine friction is dependent upon engine design and several assumptions have to be made to determine an overall FMEP. These assumptions are

- The engine IMEP is 3.865 bar g (taken from Fig 4.26a)
- Ring pack friction is 40% of total engine friction
- The Blair correlation is used for ring pack friction

Applying these assumptions to a ring pack FMEP at 1500 RPM (0.137 bar, Table 3.2) results in a total FMEP of 0.3425 bar. Hence the mechanical efficiency at this speed and inlet conditions would be 91%

#### 3.6.4 Friction Model

Using the expression for ring pack FMEP (bar) =  $150 \cdot \text{Lst} \cdot N \cdot \text{Ref}15$  based on the single value reported at Ref 14 gives a reasonable first estimate. The ring pack friction derived in this manner is then used in thermal modelling. Determining the overall FMEP relies on the assumption of percentage contribution from ring pack

FMEP. Fig 3.10 shows the variation in mechanical efficiency for a range of IMEPs and the percentage contribution to overall FMEP from the ring pack FMEP

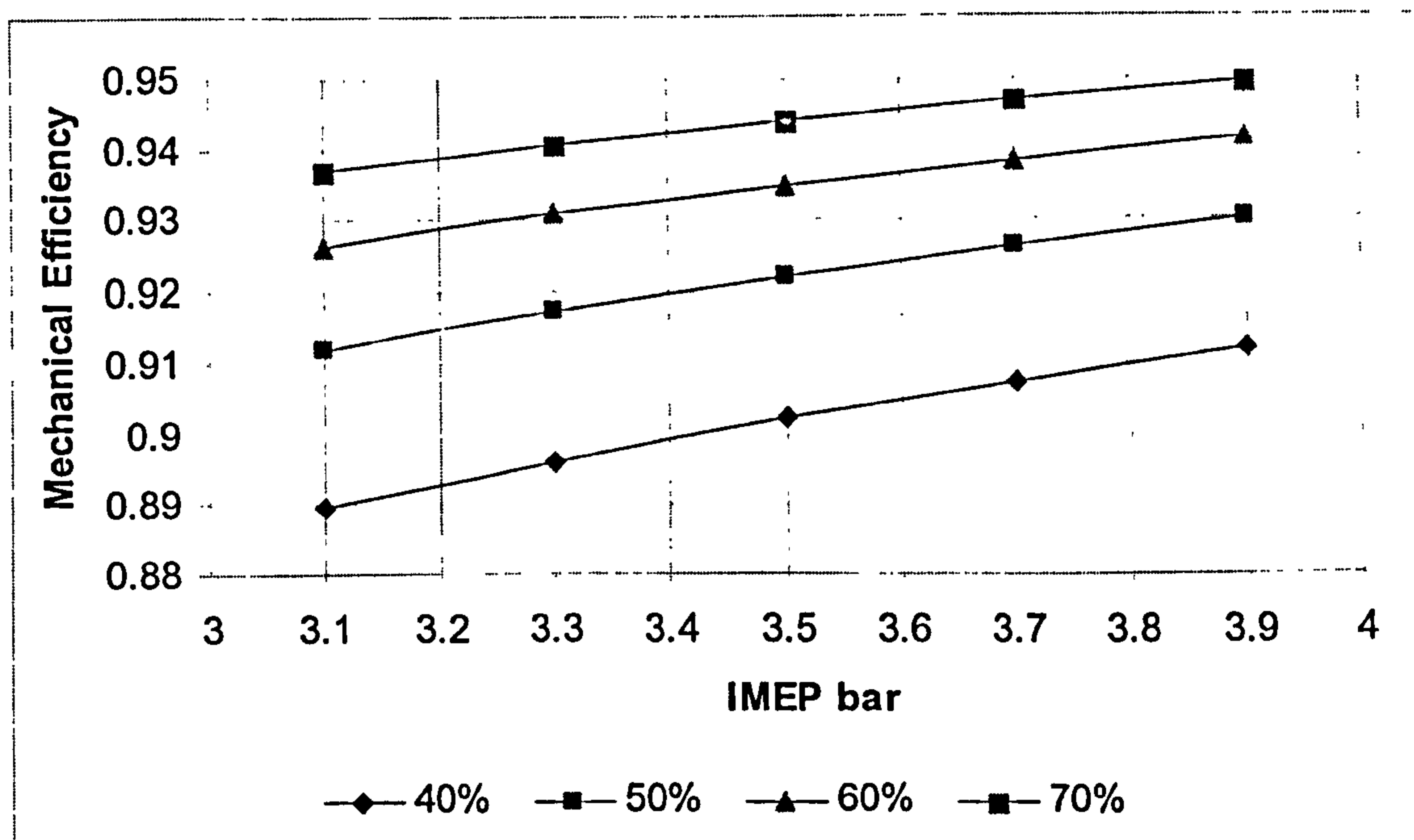


Fig 3.10 Variation in Mechanical Efficiency Against IMEP for a Percentage Range of Ring Pack FMEP Contribution to Total FMEP.

Fig 3.10 shows that the mechanical efficiency is likely to be within the range of 89% to 95%. A conservative value of 90% is carried forward into subsequent engine and Micro CHP modelling.

### 3.7 Thermal Loss Modelling

Hot gas contained in a cylinder will lose heat to the surroundings the amount dependent upon the temperature of the gas, the thermal resistance of the cylinder walls and time. In a reciprocating engine, assuming isentropic expansion, the temperature at the end of expansion will be lower than the initial temperature. In an actual engine the expansion is not isentropic but is better represented by a polytropic process and this process takes into account the heat loss to the

surroundings. The objective of modelling this process is to determine a relationship that relates an engine's physical and operating parameters i.e., stroke, bore, RPM, to gas inlet conditions (i.e. temperature and pressure) such that the expansion work and final gas conditions can be determined.

Additionally the sliding of the piston rings against the cylinder liner will generate frictional and a proportion of this heat energy will add to the heat energy of the gas.

For a gas flowing through a cylinder with heat transfer through the cylinder walls a general expression that relates the Nusselt number to the Reynolds number and Prandtl number can be used.

$$\text{Nu} = C'.\text{Re}^x. \text{Pr}^n \quad (4.1)$$

For gas temperatures ranging between 400 and 900 C the Prandtl number remains sensibly constant hence the above expression can be written as:

$$\text{Nu} = C.\text{Re}^x \quad (4.2)$$

Where

$$\text{Nu} = \frac{h.b}{k}$$

And where:  $h$  is the overall surface heat transfer coefficient in  $\text{W}/\text{m}^2 \text{K}$

$b$  is a significant dimension, normally taken as the bore of the cylinder, in m.

$k$  is the thermal conductivity of the gas in  $\text{W}/\text{m K}$

and where  $\text{Re}$  the Reynolds number is a non dimensional function of the mass flow of the gas, a significant dimension and the dynamic viscosity of the hot gas.

3.7.1 Existing Models

Several heat transfer correlations for in cylinder heat transfer have been published the most comprehensive being that by Taylor Ref 19 and Annand Ref 21

Taylor derived the expression:

$$\text{Nu} = 10.4.\text{Re}^{0.75} \quad (4.3)$$

using test data from a range of engines varying in size from large marine two stroke diesel engines to small high speed automotive petrol engines.

In this relationship he defined the Reynolds number as:

$$\text{Re} = \frac{\dot{m}.d}{A.\mu}$$

Where;

$\dot{m}$  = mass flow                      in kg /sec

$d$  = piston diameter                in m

$A$  = piston area                      in  $\text{m}^2$

$\mu$  = dynamic viscosity            in kg/s.m (at mean gas temperature)

For the Nusselt number Taylor derived the measure of  $h$  from:

$$Q = h.A.(T_g - T_c) \quad (4.4)$$

Where:

$Q$  is the heat transferred from the hot gas

$T_g$  is the mean gas temperature K

$T_c$  is the coolant temperature in K

$A$  is the cylinder wall area

Taylor derived his correlation by measurements of  $Q$  from the mass flow rate and temperature rise in the coolant plus an estimate for the heat generated by mechanical friction.

An alternative correlation derived by Annand Ref 21 was for small two stroke air cooled engines which related the Nusselt number to the Reynolds number by the relationship

$$\text{Nu} = 0.26.\text{Re}^{0.7} \quad (4.5)$$

In this relationship he defined Reynolds number as

$$\text{Re} = \frac{\rho.v.d}{\mu}$$

Where

$\rho$  = mean density of the hot gas in  $\text{kg/m}^3$

$v$  = mean piston speed in  $\text{m/s}$

$d$  = piston diameter in  $\text{m}$

$\mu$  = dynamic viscosity in  $\text{kg/s.m}$  (at mean gas temperature)

The value of  $h$  is derived from:

$$Q = \sum h.A (T_w - T_c) \quad (4.6)$$

Where  $A.T_w$  is the sum of:

area of cylinder x cylinder wall temperature

area of cylinder head x cylinder head temperature

area of piston crown x piston crown temperature.

And  $T_c$  is the temperature of the surrounding air.

These two models, both based on experimental data, vary in that for a typical RJC engine of bore 100mm and stroke 120 mm with inlet gas conditions of 7.5 bar g at 850 C and running at 1500 RPM the Reynolds number from the Taylor model is 4340 and for the Annand model is 29200 with Nusselt numbers of 5614 and 347 respectively.

### 3.7.3 Modelling the RJC Engine

These two correlations require that a value of  $Q$  to be derived or measured. For the RJC engine, which has a smaller air mass flow than IC engines of similar displacement, it is necessary to derive an expression for the expansion heat loss and frictional heat generated. If it is assumed that during hot gas admission no heat transfer takes place then using standard air formulas the expression for the heat loss during a polytropic expansion is:

$$\dot{m} \left( \frac{(\gamma-n)}{(n-1)} \right) \frac{R}{(\gamma-1)} (T_1 - T_2) = \dot{Q}_{\text{loss}}$$

Where

$\gamma = C_p/C_v$  is the adiabatic index at the mean gas temperature

$n$  = index of polytropic expansion

$\dot{m}$  = mass flow rate

$T_1$  = the initial gas temperature deg K

$T_2$  = the final gas temperature deg K

And where  $T_2 = T_1 / (V_1/V_2)^{n-1}$

With  $V_1$  the volume at the start of expansion

And  $V_2$  the volume at the end of expansion

Ref. 11 and Ref 17 state that heat transfer to the coolant during the exhaust stroke of an engine is approximately equal to the heat transfer during the expansion stroke. In addition a value for frictional heat,  $Q_f$ , (derived from friction modelling) has to be added such that for the expansion stroke

$$\dot{Q}/2 = \dot{m} \left( \frac{(\gamma-n)}{(n-1)} \right) \frac{R}{(\gamma-1)} (T_2 - T_1) + \dot{Q}_f/2 \quad (4.7)$$

and that for a full cycle, assuming no heat loss during hot gas admission, and that the heat transfer during the exhaust stroke is equal to the heat transfer during the expansion stroke then:

$$h.A(T_w - T_c) = 2\dot{m} \left( \frac{\gamma - n}{n - 1} \right) \frac{R}{\gamma - 1} (T_2 - T_1) + \dot{Q}_l \quad (4.8)$$

gives a relationship between the overall heat transfer coefficient  $h$  and the polytropic index of expansion.

To determine this relationship then an estimate has to be made for values of  $T_w$  for cylinder wall, cylinder head, and piston crown for a given gas inlet temperature. (in actual engine testing it would be possible to measure these values).

The assumptions made for surface temperatures were:

1. Cylinder wall 230C – this is a sensible upper limit for a lubricant in the boundary close to the surface. Although cooling could be used in an actual engine to reduce the cylinder side surface temperature this was not applied in the modelling conducted.
2. Piston crown 350 C – piston undercrowns, and cooled by the lubricant, rarely exceed values of 250C hence a temperature difference across the crown of 100 C is not unreasonable
3. Cylinder head 50 C below the mean gas temperature. The heat transfer across a cylinder head is limited by the greater thickness of the cylinder head (needed to accommodate valves and valve guides).
4. The coolant temperature is taken as 15 C for air cooled engines.

The above values are based on the author's past experience with IC engines



There are two methods to solve equation 4.8. The first is to assume a value of the index of polytropic expansion ( $n$ ). For a simple joule cycle engine Ref 22 the polytropic efficiency is given as:

$$\text{Polytropic Efficiency} = \frac{\frac{\gamma-1}{\gamma}}{\frac{n-1}{n}} \quad (4.9)$$

and for small Joule cycle engines a value of 90% is typical.

Hence for a given gas inlet temperature the value of  $\gamma$  is known and using the expression for polytropic efficiency at a value of 90% the value of  $n$  can be determined and thus  $h$ .

The second method is to use the Annand model and for a given set of engine parameters and conditions derive a value for  $h$  and thus solve for  $n$ . Ref 22 states that polytropic efficiencies for Joule cycle engines are no higher than 93% nor much lower than 85%.

Two thermal models were generated one based on using the piston area only (Taylor) and a mean gas temperature and one based on the full area (Annand) of the cylinder (head, cylinder wall and piston crown areas) with assumptions made for the mean surface temperatures of each of the three areas. In both models the Reynolds number was based on the Annand correlation as this model incorporated the mean piston speed (piston stroke), mean gas density (mean gas temperature) and that the correlation was derived from testing small two stroke engines, these being more in common with a RJC engine.

### 3.7.3 Thermal Model Evaluation

To assess both thermal models six conditions were used with engines having the dimensions given at Table 3.3 all with a hot gas supply at 7.5 bar g.

Engine	Bore mm	Stroke mm	Inlet Gas C	RPM
1 (BMW)	82	61.5	600	1500
2 (BMW)	82	61.5	600	3000
3 (BMW)	82	61.5	850	1500
4 (BMW)	82	61.5	850	3000
5	100	100	850	1500
6	110	110	600	3000

Table 3.3 Engine Dimensions and Parameters Used in Modelling

Engines 5 and 6 are representative of those likely to be employed for a typical micro CHP whilst conditions 1-4 represent the experimental BMW engine reported at Part 4

The mean gas temperature is found by averaging the cylinder gas temperature over the full expansion stroke based on a theoretical expansion model and using the polytropic index of expansion  $n$  (90% polytropic efficiency) with the value of  $\gamma$  being taken at the inlet gas temperature.

The theoretical model had an instantaneous inlet valve closure (closing) such that the volume of gas at inlet valve closure was 27.7 % of the swept volume. This was based on equal work from the admission and the expansion of the gas over the

expansion stroke and was derived from simple work modelling of an ideal engine and proved during cold operation of the BMW test engine.

Using the above assumptions and solving equation (4.8) for a range of  $n$  values (derived over a range of polytropic efficiencies) give values of  $h$  (the overall heat transfer coefficient) and thus a relationship between  $Re$  and  $Nu$ . Fig 3.11 shows the relationship between  $Re$  and  $Nu$  for a polytropic value of 87%. The spreadsheets from which the values in Fig 3.12 were derived are at Annex 3.

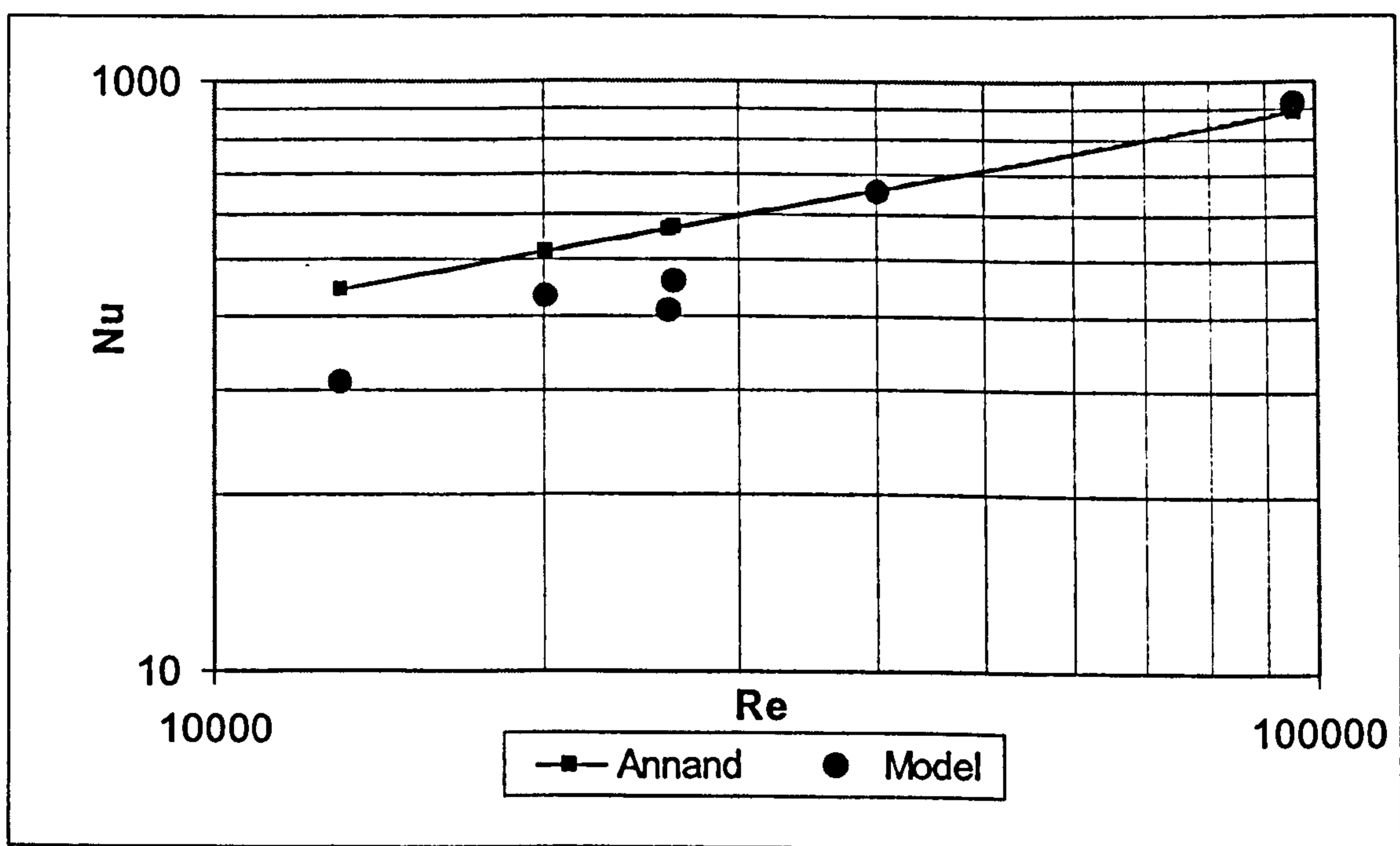


Fig. 3.11 Relationship Between  $Re$  and  $Nu$  for RJC engines

The limitations of the models shown in Fig 3.11 are:

- Assumes surface temperatures for cylinder wall, piston crown and cylinder head. These are maximum values and Ref 11 reports a measured cylinder wall temperature of 220 C as against an assumed temperature of 230C
- Uses an ideal cycle with pressure losses not taken into account.
- All piston ring frictional heat is added to the gas.

- The Annand model was derived from small IC two stroke engines running at higher RPMs than the RJC engine

Notwithstanding the limitations the thermal model of the RJC engine shows that it correlates with the Annand model with the greatest divergence at low Re numbers. Until physical measurements can be taken from an actual RJC engine the Annand model be used in the determination of the overall heat transfer coefficient.

### **3.8 Pressure Loss Modelling**

Pressure losses that occur across the inlet and exhaust valves reduce the indicated work. To determine the pressure losses the valves can be viewed as either variable nozzles or variable orifices. Because conditions in the cylinder (pressure and volume) vary over the cycle then an iterative approach has to be employed. For the admission stage a two step approach can be used. The first step is an expansion of the gas in the cylinder as the piston moves away from TDC thus reducing the pressure, followed by admission of hot gas at supply pressure to increase the pressure in the cylinder. This process is illustrated in Fig 3.12

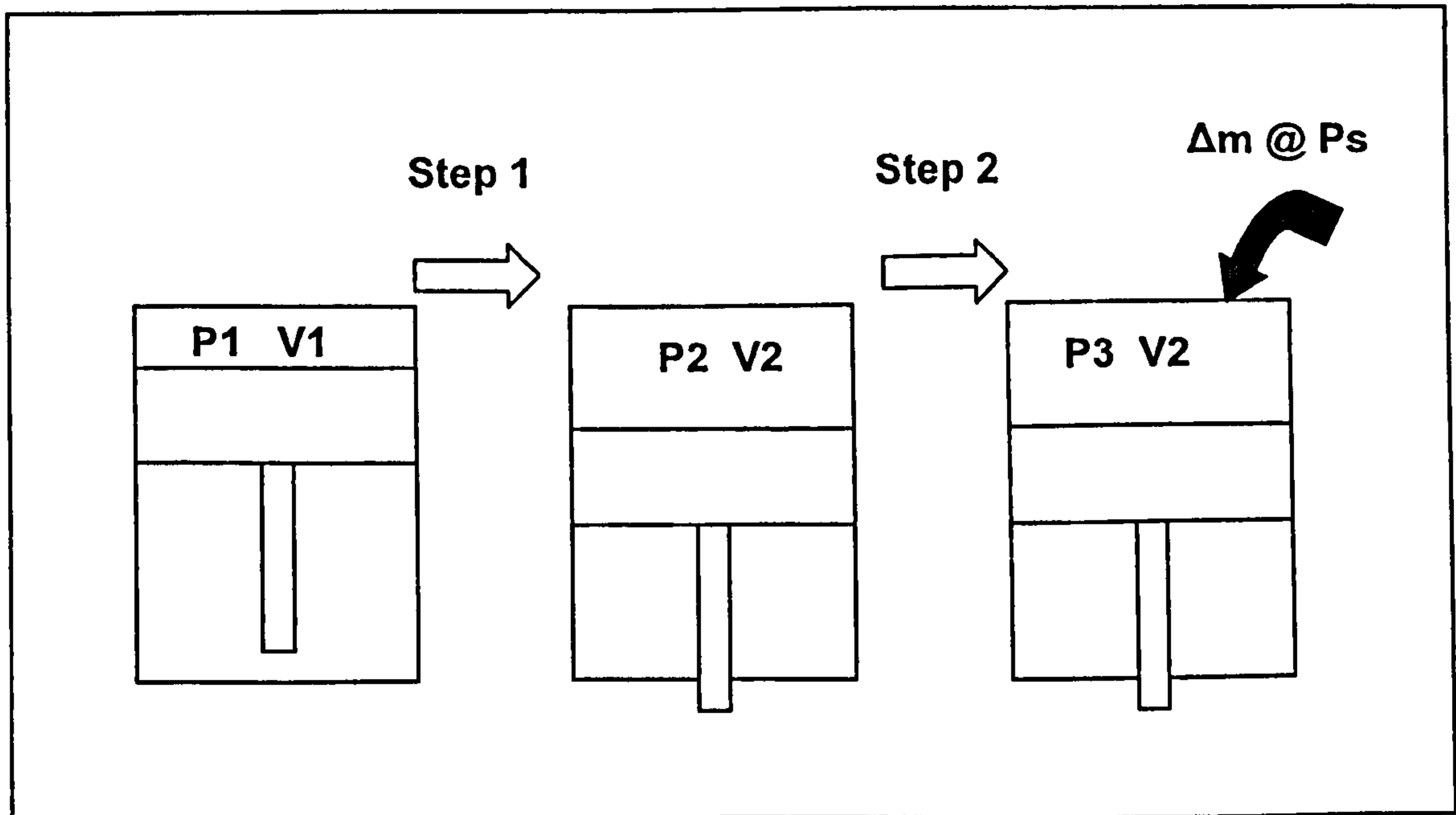


Fig. 3.12 Pressure /Volume During Admission

Step 1 is the expansion of hot gas is defined by the relationship

$$\frac{P_1}{P_2} = \left(\frac{V_2}{V_1}\right)^n \quad (4.10)$$

Step 2 the admission of hot gas at supply pressure  $P_s$  and temperature  $T_s$  is defined by the relationship

$$P_3.V_2 - P_2.V_2 = \Delta m.R.T_s \quad (4.11)$$

and assumes a constant inlet gas temperature

Assuming incompressible flow and the inlet valve behaving as an orifice then the mass flow rate through the inlet valve at step is given by:

$$\Delta m = \rho .\Delta t . A_v . C_d . \sqrt{2\Delta P/\rho} \quad (4.12)$$

Where the flow rate across an orifice is  $\dot{V}$  and

$$\dot{V} = A_v.C_d . \sqrt{\frac{2\Delta P}{\rho}}$$

and where

$$\Delta V = \Delta m / \rho \quad \text{in time } \Delta t \quad \text{and}$$

$\rho = P_s/RT_s$  assuming constant gas temperature

thus

$$P_3 = \frac{P_1}{\left(\frac{V_2}{V_1}\right)^n} + \left(\frac{1}{V_2}\right) \cdot P_s \cdot \Delta t \cdot A_v \cdot C_d \cdot \sqrt{\frac{2\Delta P}{\rho}} \quad (4.13)$$

over the time interval  $\Delta t$  and where

$A_v$  is the average valve opening area over time  $\Delta t$

$C_d$  is the valve discharge coefficient

$\Delta P = P_s - P_2$

$n$  = the polytropic index of expansion taken at the gas inlet temperature and 87% polytropic efficiency.

Thus:

$$P_3 = \frac{P_1}{\left(\frac{V_2}{V_1}\right)^n} + \left(\frac{1}{V_2}\right) \cdot P_s \cdot \Delta t \cdot A_v \cdot C_d \cdot \sqrt{2R \cdot T_s} \cdot \sqrt{1 - \frac{P_1}{\left(\left(\frac{V_2}{V_1}\right)^n \cdot P_s\right)}} \quad (4.14)$$

The above expression is considered valid for small values of  $\Delta t$  and employing an iterative process such that  $P_3$  becomes  $P_1$  for the next period of  $\Delta t$ .

For simplification the iteration was conducted at intervals of swept volume which meant that the time intervals  $\Delta t$  were not constant.

### 3.8.1 Modelling the RJC Engine

The solution to equation (4.14) was undertaken on spreadsheets using variations in cylinder physical characteristics ie bore, stroke, valve diameter, valve lift and lift profile as well as engine speed and gas inlet conditions.

The simulated cylinder pressure can be compared with the cylinder pressure of an ideal engine on a PV diagram and the pressure losses and resulting lost work can be determined.

The model can be applied to either poppet or ported rotary valves the only difference being in the value of Cd used. For poppet valves a representative value of Cd has used and this was taken from Refs 10 and 11 where the value of Cd was compared against the non dimensional valve lift ( VL/ VD). For typical valve diameters and valve lifts likely to be experienced in an RJC engine gave a mean value of Cd = 0.75 (Cd varies from 0.65 to 0.85 over the range of VL/VD of 0 to 0.3) and this was used in the modelling.

The first comparison was made with an engine with the physical characteristics and operating conditions given in Table 3.4. In this table valve diameters and lift were varied to generate a PV diagram that had minimum losses compared to the ideal Fig 3.13

Bore mm	100	Valve dia. VD mm	2 x 35
Stroke mm	120	Max valve lift VL mm	10
Swept vol cc	942	Valve profile	sinusoidal
Clearance vol cc	30	Cam angle deg	60 and 80
RPM	1500	Inlet Valve opens at	TDC
Ps abs bar	8.5	Ideal cam opening	70 deg
Ts deg C	850		

Table 3.4 Engine Dimensions and Operating Conditions

Fig 3.13 and Fig 3.14 show the PV characteristic generated and ideal as well as the pressure drop across the valve modelled as an orifice for a 60 and 80 degree inlet valve opening.

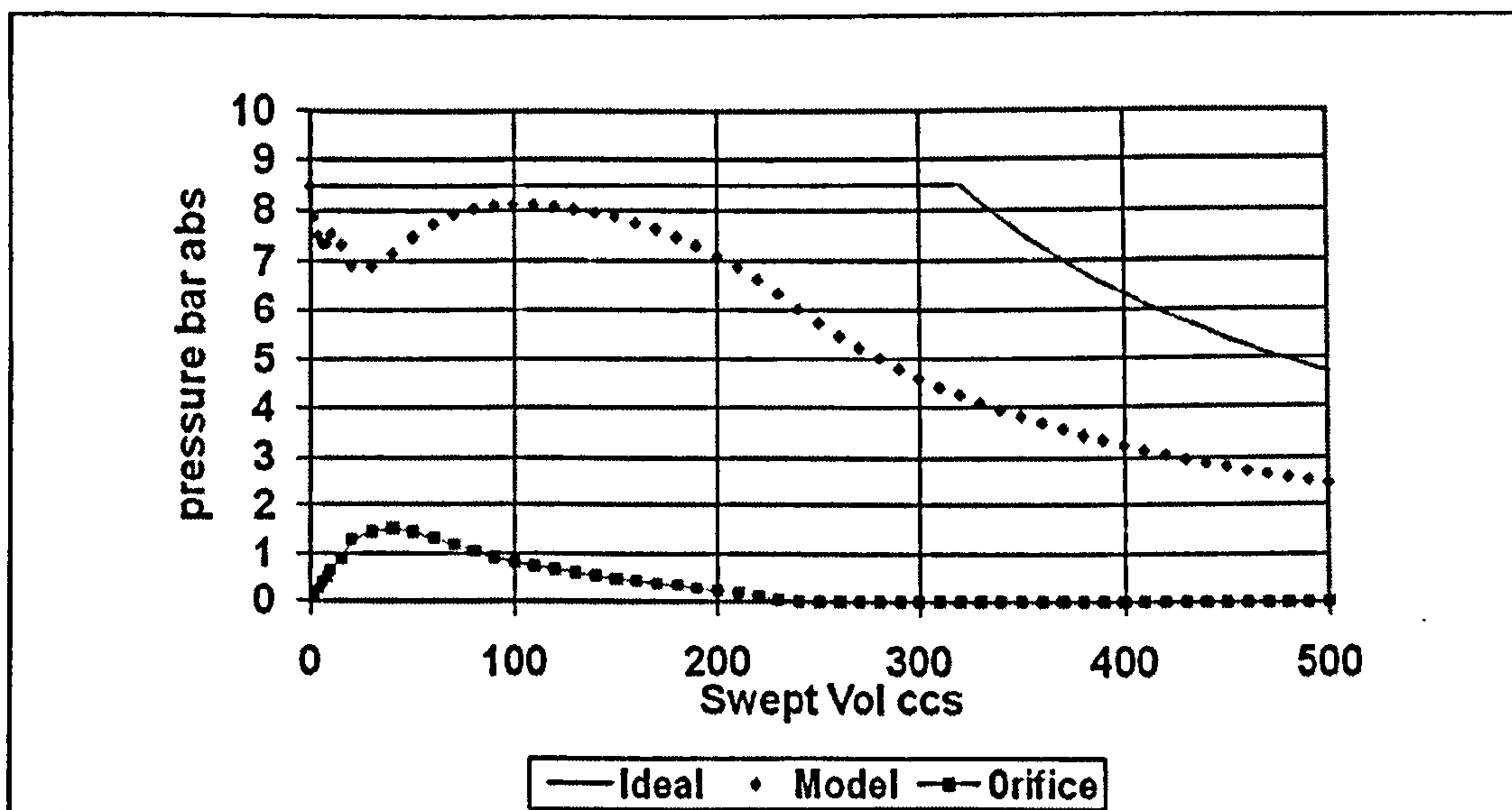


Fig 3.13 PV Diagram Showing Inlet Valve Pressure Losses TDC 60 degree opening

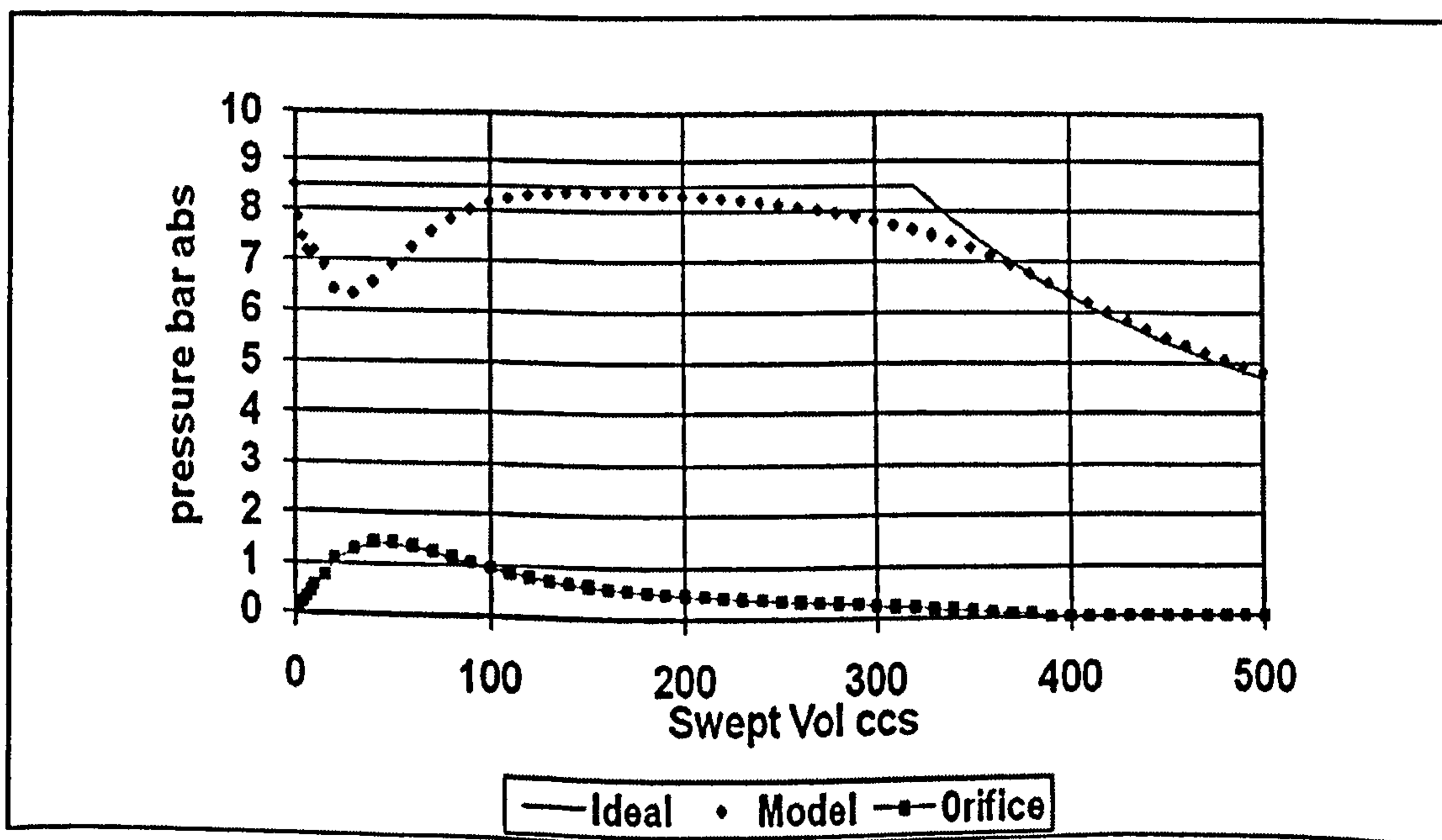


Fig 3.14 PV Diagram Showing Inlet Valve Pressure Losses TDC 80 degree opening



The most notable aspects of these PV diagrams is the pressure drop as the inlet valve begins to open at TDC and the pressure drop as the valve closes. When compared with an ideal valve opening of 70 degrees the pressure drop on closing is more pronounced for the 60 degree opening but is partially compensated by the 80 degree opening. For both conditions it indicates that the valve opening is insufficient to allow the supply gas to compensate for the pressure drop due to the increasing volume. Similar pressure drops were observed in the testing of the BMW engine and also in the earlier technology demonstrator engine (Part 4). It was considerably reduced by advancing the inlet valve timing allowing the inlet valve to open earlier before TDC

The model was adjusted to advance the timing such that the inlet valve opened at 8 deg BTDC. This had the effect of reducing the initial pressure drop but the pressure drop on valve closing remained. Whilst advancing the inlet valve timing reduces the initial pressure drop the valve has now to open over 88 degrees and this results in a greater air mass and hence an increase in compressor work.

The PV diagram for an inlet valve opening at 8 deg BTDC is shown in Fig 3.15

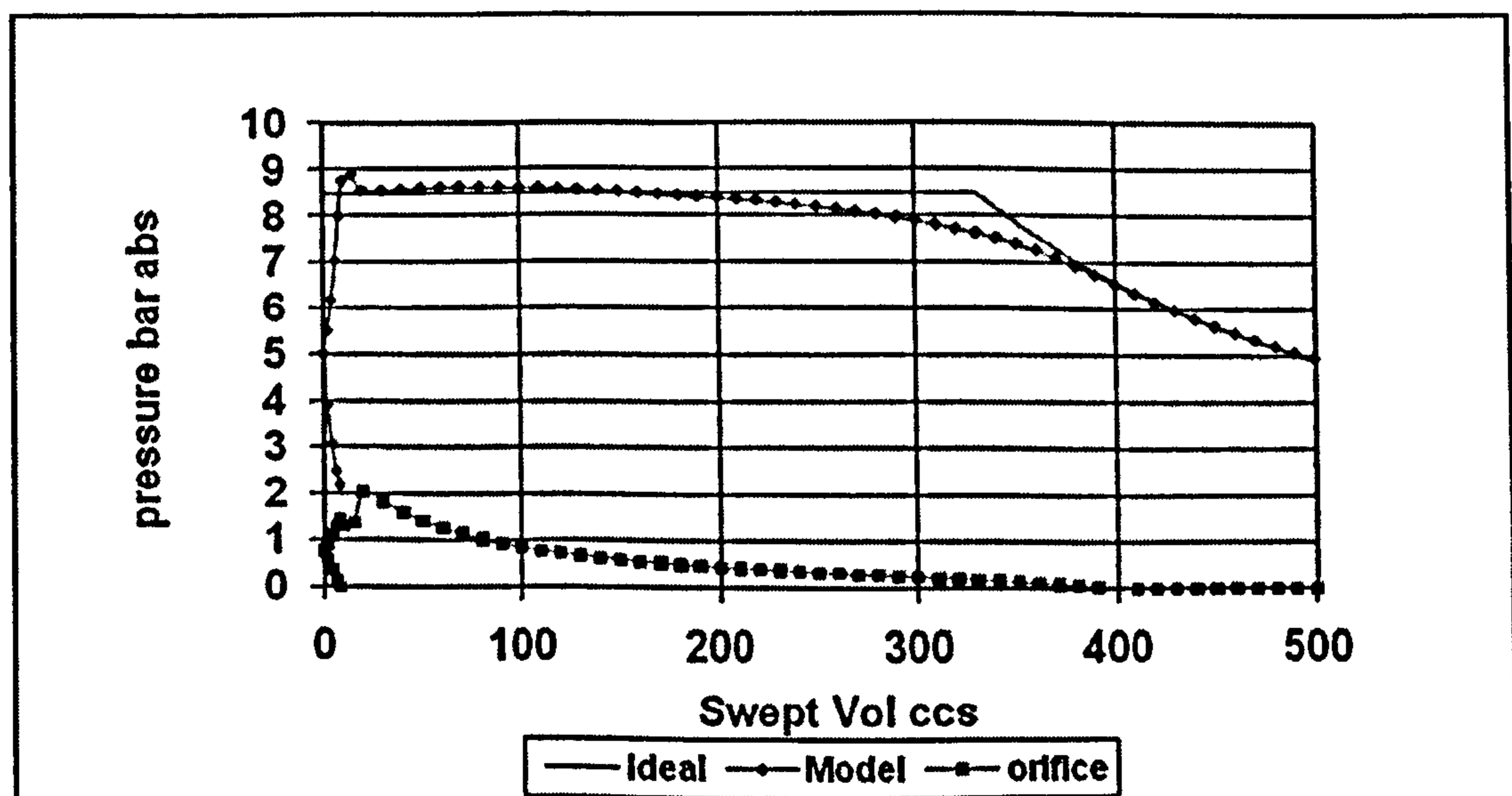


Fig. 3.15 PV Diagram Showing Inlet Valve Pressure Losses. 8 deg BTDC

### Part 3

A comparison of performance was conducted between the above two models and is tabulated at in Table 3.5

	Inlet opens at TDC	Inlet opens 8 deg BTDC
Stroke mm	120	120
Bore mm	100	100
Displacement ccs	942	942
Clearance volume ccs	30	30
Supply pressure bar g	7.5	7.5
Supply temp deg K	850	850
RPM	1500	1500
Inlet valve dia mm	70	70
Inlet valve lift mm	10	10
Exhaust valve dia mm	70	70
Exhaust valve lift mm	12	12
Ideal inlet valve opening deg	70	70
Ideal exhaust valve opening deg	145	145
Model inlet valve opening deg	80	88
Model Exhaust valve opening deg	156	160
Model indicated work expansion J/cycle	470.4	522.4
Model indicated work recompression	123	112.8
Model Net work J/cycle	347.4	409.6
Ideal work expansion	533.3	533.3
Ideal work recompression	114.2	114.2
Ideal Net work/cycle J/cycle	419.1	419.1
Mass flow ideal kg/sec	0.0227	0.0227
Mass flow model kg/sec	0.0208	0.0254
Indicated Power ideal Watts	10477.5	10477.5
Indicated Power model Watts	8685	10240
Brake Power (at 90% mech eff)	7825	9216
Ideal compressor power	4608.6	5627.9
Net Compressor power (at 90% efficiency)	6023	7355
(At 85% cycle efficiency)		
Ideal power output Watts	1802	1861
<b>Net power ouput Watts</b>	<b>2543.5</b>	<b>2758.5</b>

Table 3.5 Engine performance comparison with different inlet valve timing

Table 3.5 shows that a small adjustment to the valve timing, whilst increasing the amount of work from the compressor, results in a 3.3 % improvement in net power output. Further improvements will be obtained with increases in the mechanical efficiency of both the expander and compressor and typically for 95% mechanical efficiencies for both expander and compressor the improvement is 8.5%. Such a strategy of defining the inlet valve timing should therefore be considered in the design of RJC engines.

### 3.8.2 Exhaust Valve Modelling

A similar approach was used to model the exhaust valve and this is detailed in the spreadsheets at Annex 3 and uses the same physical and operating characteristics as employed in the inlet valve modelling. It was found that to ensure the final pressure at recompression did not exceed supply pressure the exhaust valve had to remain open longer than that of an ideal valve. In the ideal cycle for the engine at Table 3.5 the exhaust valve would need to close at 35 deg BTDC whilst to achieve the same final recompression pressure the model exhaust valve had to close at 23 deg BTDC. ie 12 degrees later. As the flow area of the exhaust valves reduced during closing it throttles the gas and a pressure is built up in the cylinder. This increased pressure results in additional work required with a reduction in net power output. Again large flow area valves need to be employed to minimise these pressure losses. To achieve the results shown in Fig 3.16 two exhaust valves of 35mm dia. and a maximum lift of 10 mm were used.

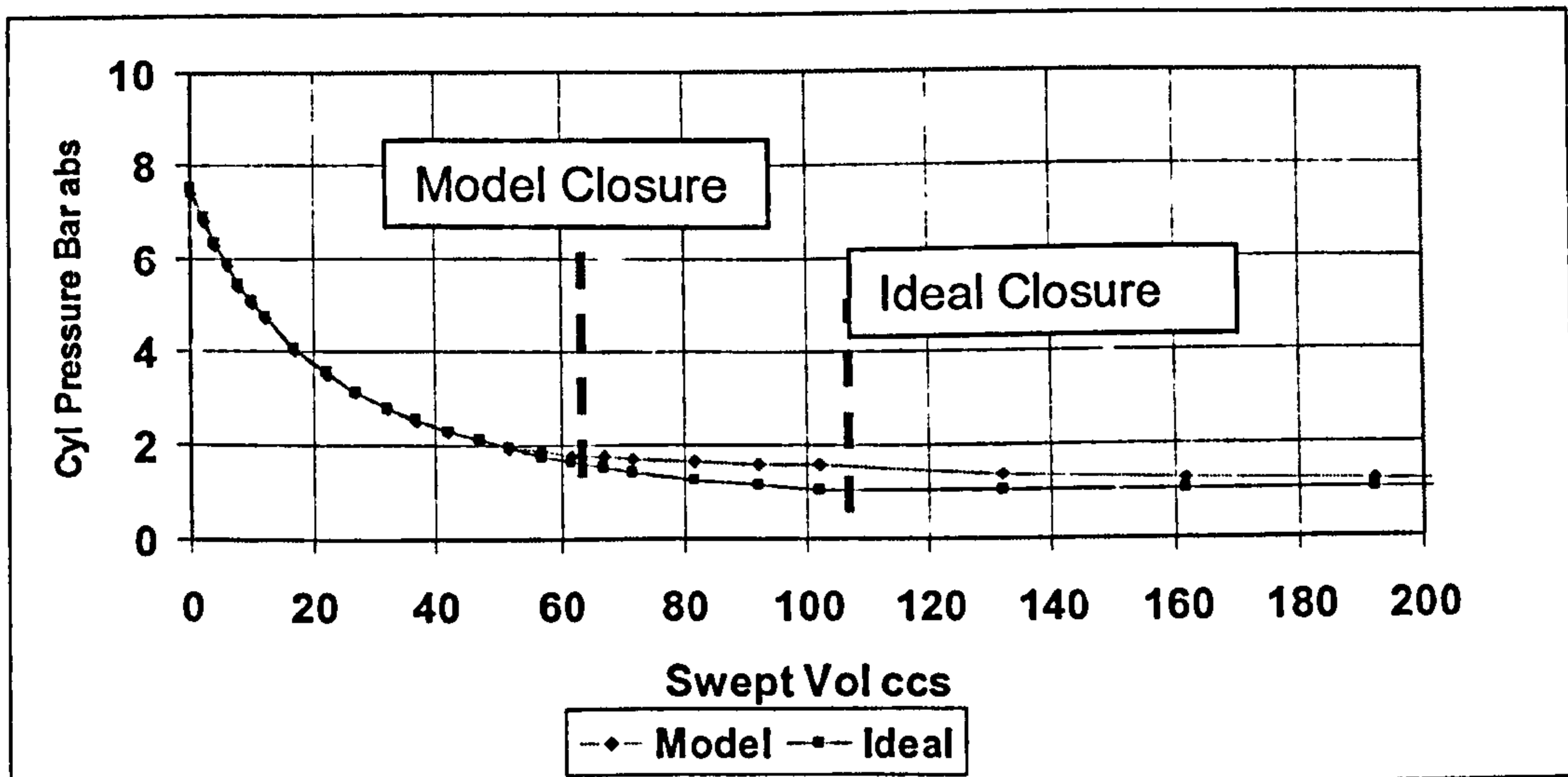


Fig 3.16 Exhaust Valve PV diagram

### 3.8.3 Validation of Pressure Loss Modelling

Using the same modelling approach the BMW test engine was analysed and compared with test data generated in the cold condition. The first PV diagram generated, shown at Fig 3.17, is with the inlet valve opening at TDC. The cylinder pressure shows a decrease just after TDC where the volume of inflowing air is restricted by the valve opening and is insufficient to maintain the cylinder pressure at the supply pressure compared to the ideal. Also shown in Fig 3.17 is the PV diagram from the test engine

Varying the inlet valve timing in the model such that opening occurred before TDC had the effect of reducing the initial pressure drop. Most of the test data from the BMW engine was derived with the inlet valve being advanced to 10 deg BTDC although clearances between cam and valve actuating mechanism effectively reduced this to about 8 degs. The effect of advanced valve timing is shown at Fig 3.19

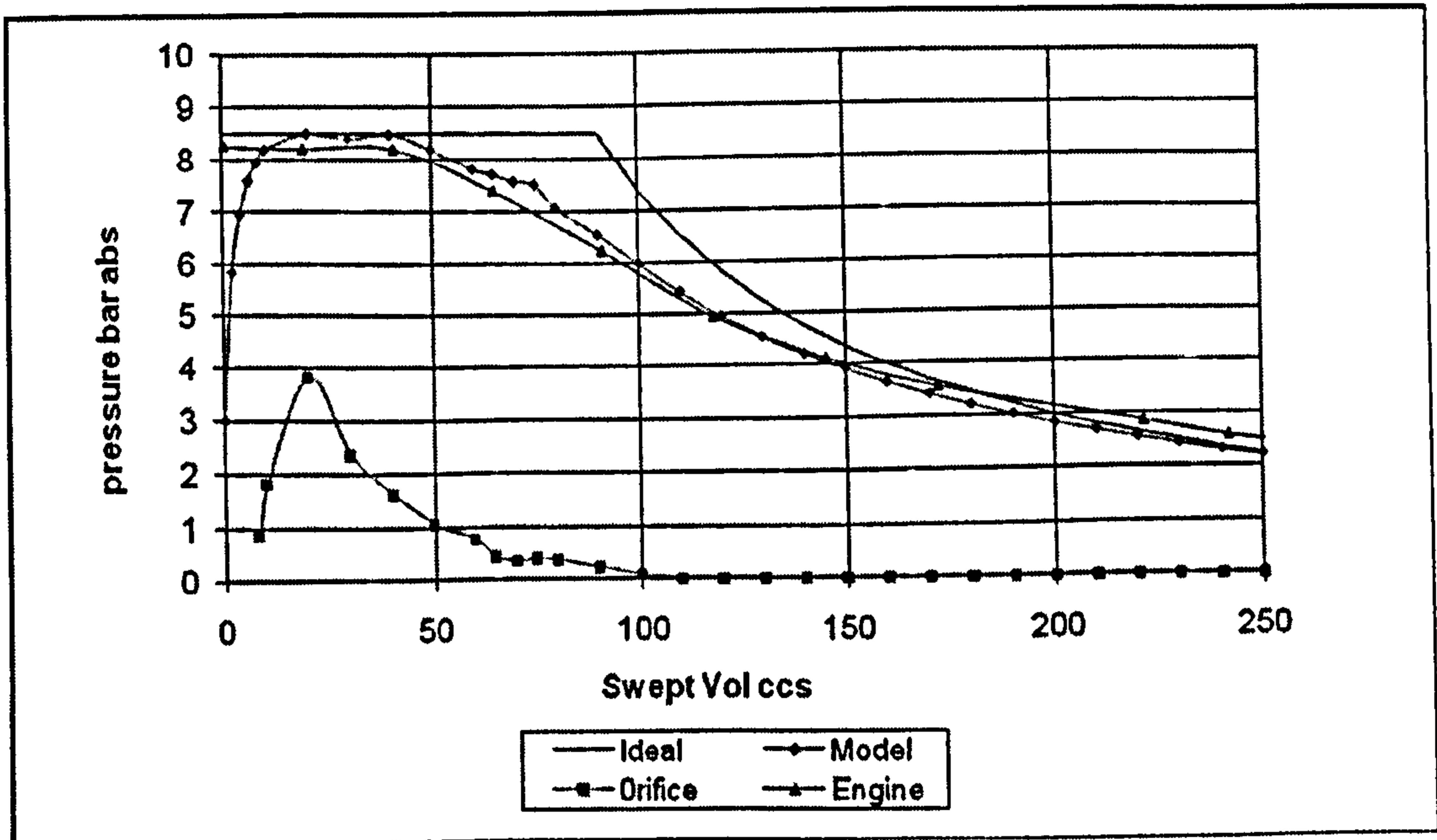


Fig 3.17 Inlet Open at TDC

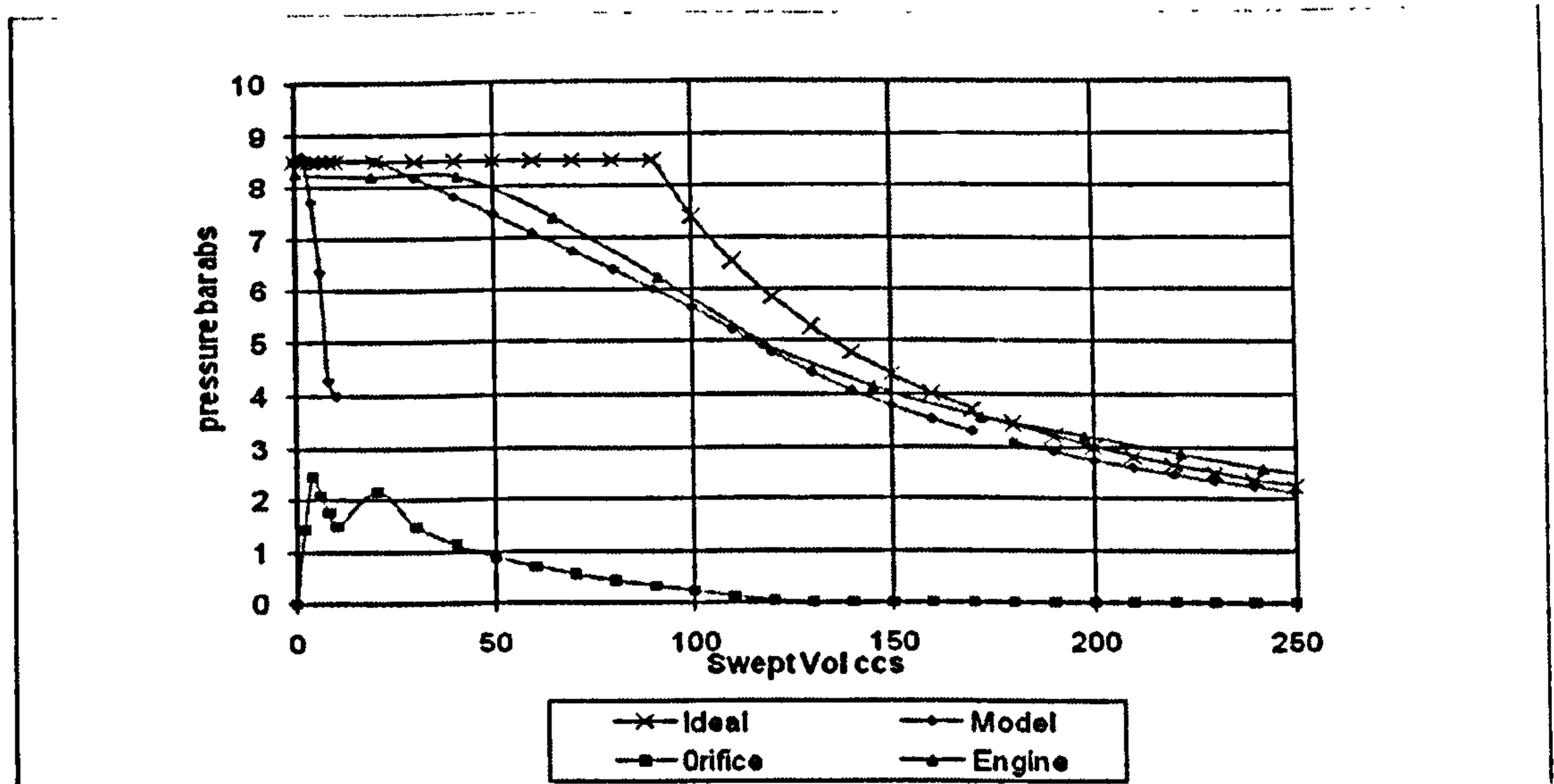


Fig 3.18 Inlet Open 8 deg BTDC

For the inlet valve opening at TDC the cam angle was 70 deg whilst for the inlet valve opening at 10 deg BTDC the model cam angle was set at 90 deg the same as the BMW test engine.

There is good correlation between the model and test data for both cases even though with advanced valve timing the model demonstrates some instability

around TDC. Further refinements of the model could be made in this area of operation to reduce this instability.

An alternative approach to altering the valve timing was investigated and this looked at the concept of 'high lift' or 'sport' cams. Such cams do not increase the maximum valve lift but alter the cam profile such that the value  $\sum Av.\Delta t$  is increased. A cam with such characteristics was investigated with the cam profile as shown in Fig 3.19

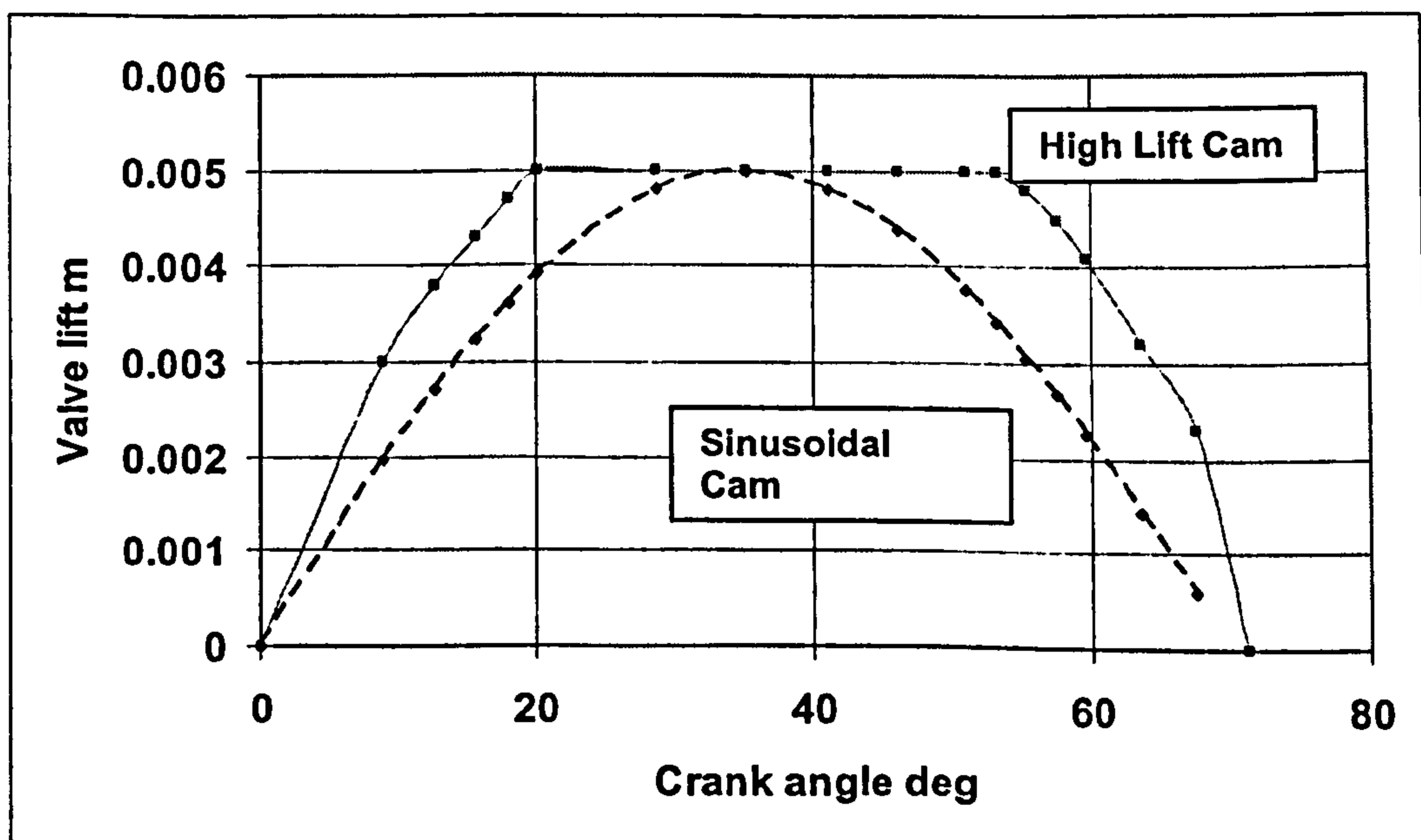


Fig 3.19 Inlet Cam Profiles

Applying this 'high lift' cam profile to the model results in the PV diagram at Fig 3.20 and demonstrates that a 'high lift' cam profile can reduce the initial pressure drop and with a reduced loss at valve closing. It should be noted that the cam angle is 70 deg and that opening occurs at TDC. Additionally the 'high lift cam' results in a PV characteristic close to the ideal and thus pressure losses are minimised.

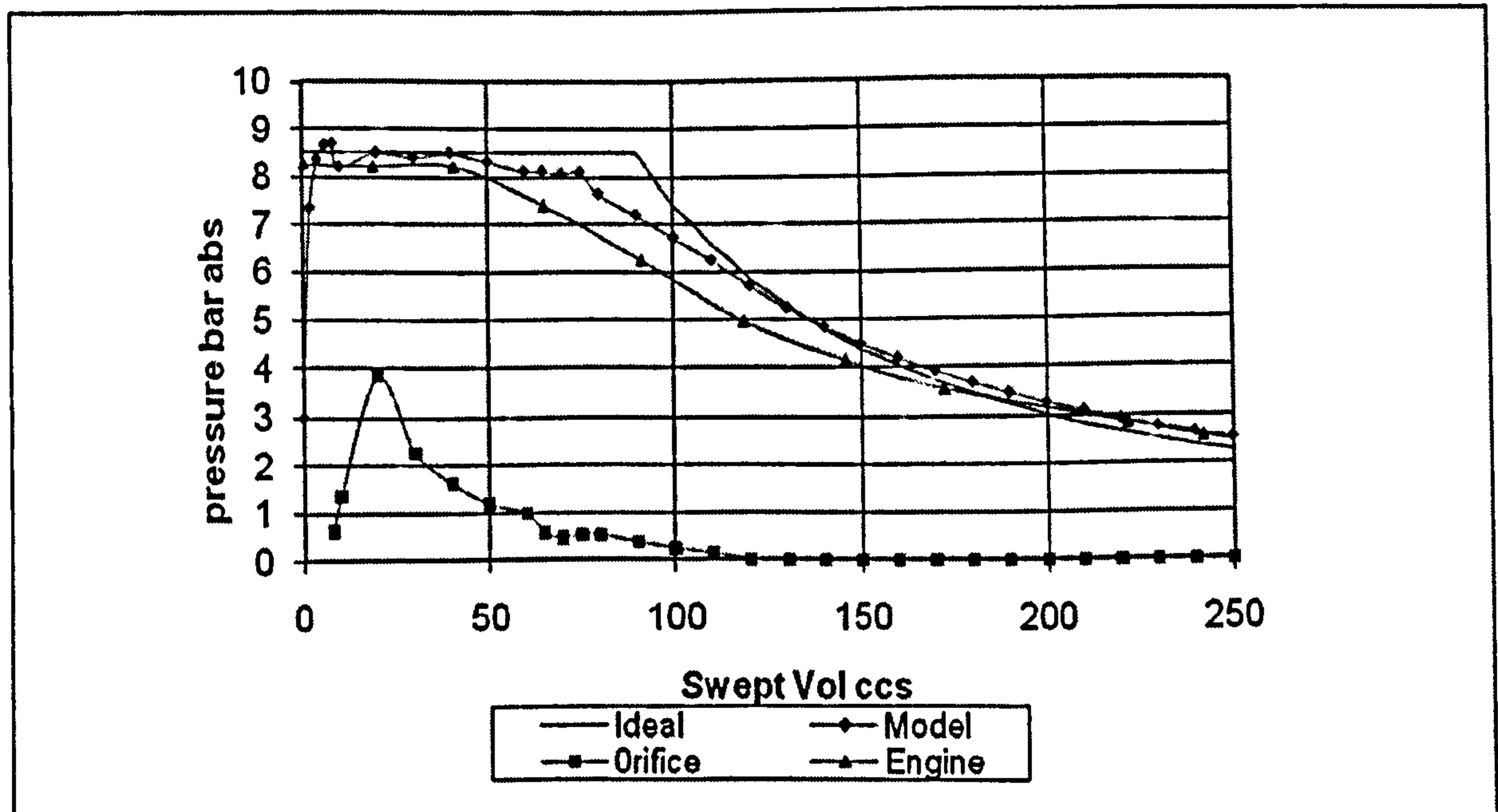


Fig 3.20 PV Diagram With 'High Lift' Cam

#### 3.8.4 Findings From Pressure Loss Modelling

The most significant outcome from pressure loss modelling is the relatively large valve flow area needed to minimise the losses. This is not seen in the 'cold' operation of the BMW test engine where the as fitted single inlet valve of 25 mm dia. and 5 mm lift running at only 700 RPM was adequate, but is seen in the model (inlet temp 850 deg C) for an engine of 100 mm bore and 120 mm stroke and operating at 1500 RPM. For this condition and to minimise pressure losses the valve area is provided by two inlet valves each of 35 mm dia. and 10 mm lift.

These valve sizes and lift needed for the exhaust were 35 mm diameter and 12 mm lift so that for this displacement of engine (942 ccs) the cylinder head must be able to accommodate all four valves. Ref 11 states that for a four valve compression ignition engine with a flat cylinder head 'each inlet valve diameter could be up to 39 % of the bore diameter and each exhaust valve could be 35% of the bore diameter. With diameters of 35 mm for all four valves this is close to the

maximum size possible in an engine of 100 mm bore. However valve seats have also to be accommodated which increases the diameter needed for each valve and if the valve seat maximum diameter is taken as 45 mm it is not possible to fit all four valves within a cylinder head of engine bore 100 mm

The implications of the above are that

***An RJC engine with a capacity of 1000 ccs must have a bore greater than the stroke ie 'over square'.***

Fig 3.21 shows the valve positioning, with a maximum contained diameter of 45 mm of all four valves in an engine of 120 mm bore and 100 mm stroke with a capacity of 1130 ccs.

For engines of different displacement a bore to stroke ratio of 1.2:1 will have to be employed.

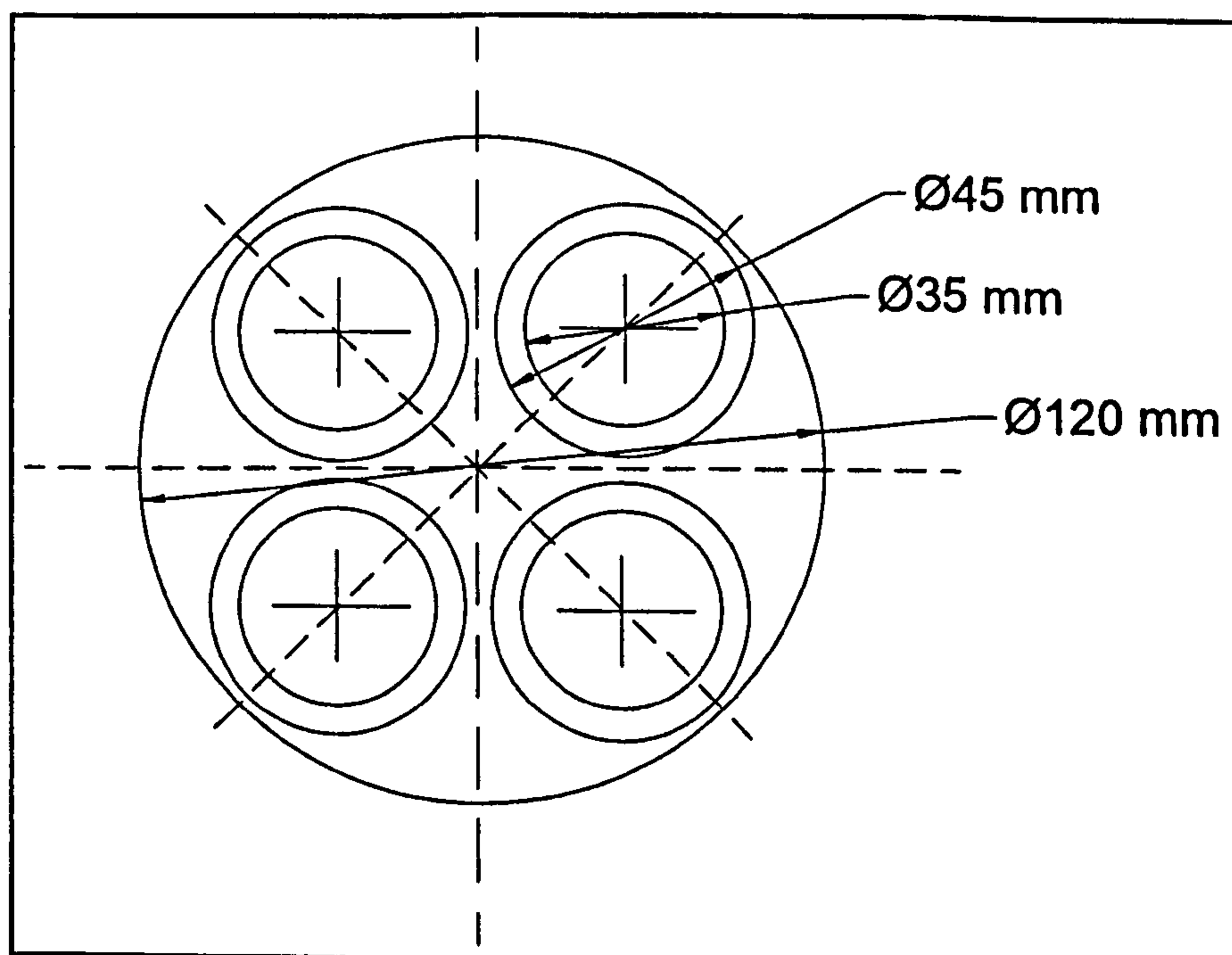


Fig 3.21 Valve Layout in Cylinder Head



3.8.5 Optimum Pressure Loss Modelling for a Specific RJC Engine

The RJC specifications for the model are: a bore of 120 mm, a stroke of 100 mm operating at 1500 RPM with inlet gas conditions of 7.5 bar g and 850 deg C. The valve lift profile was 'high lift' with a maximum lift of 10 mm. The lift profile is shown at Fig 3.22

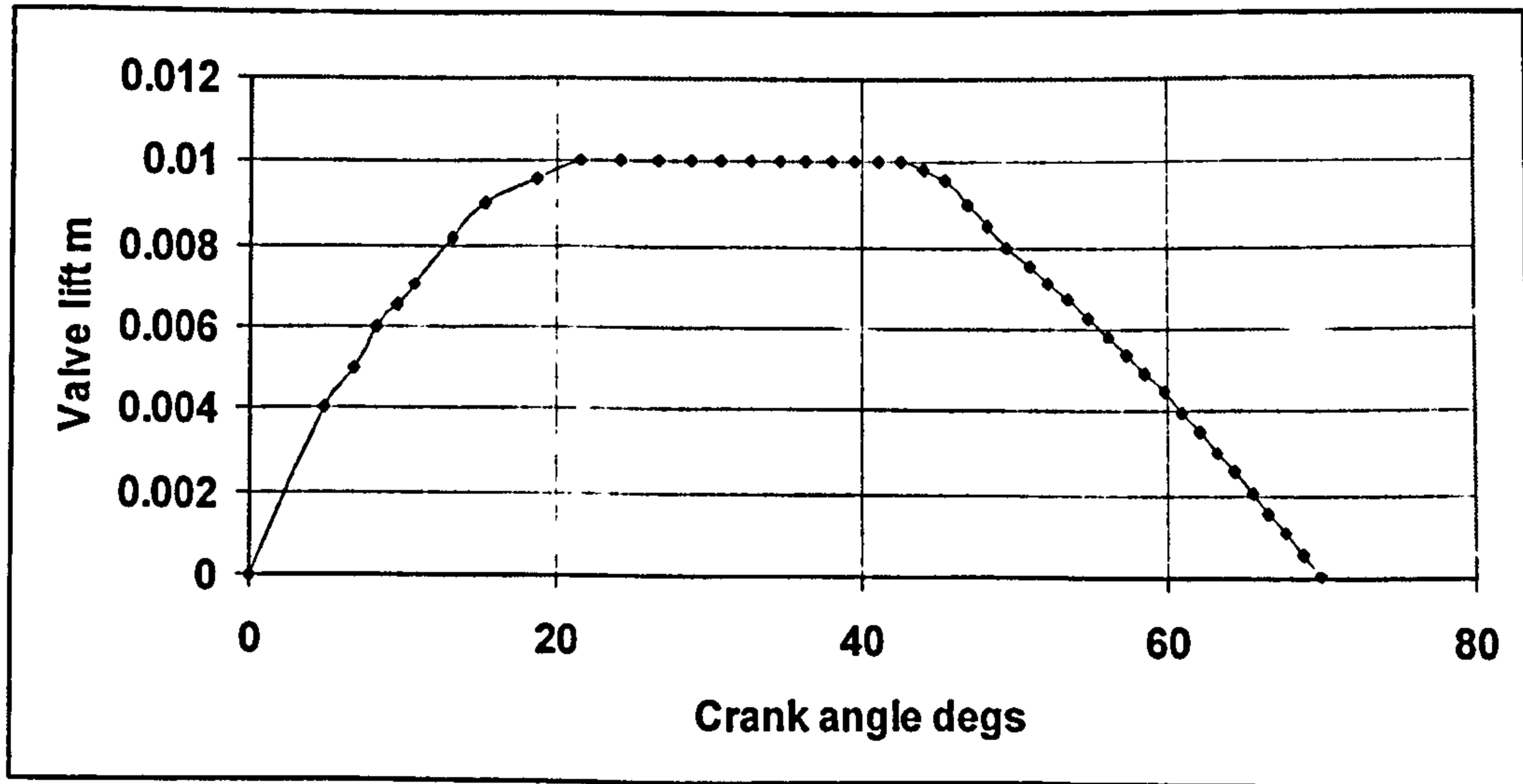


Fig 3.22 'High Lift' Cam Profile

Applying these values results in the PV diagram shown at Fig 2.23

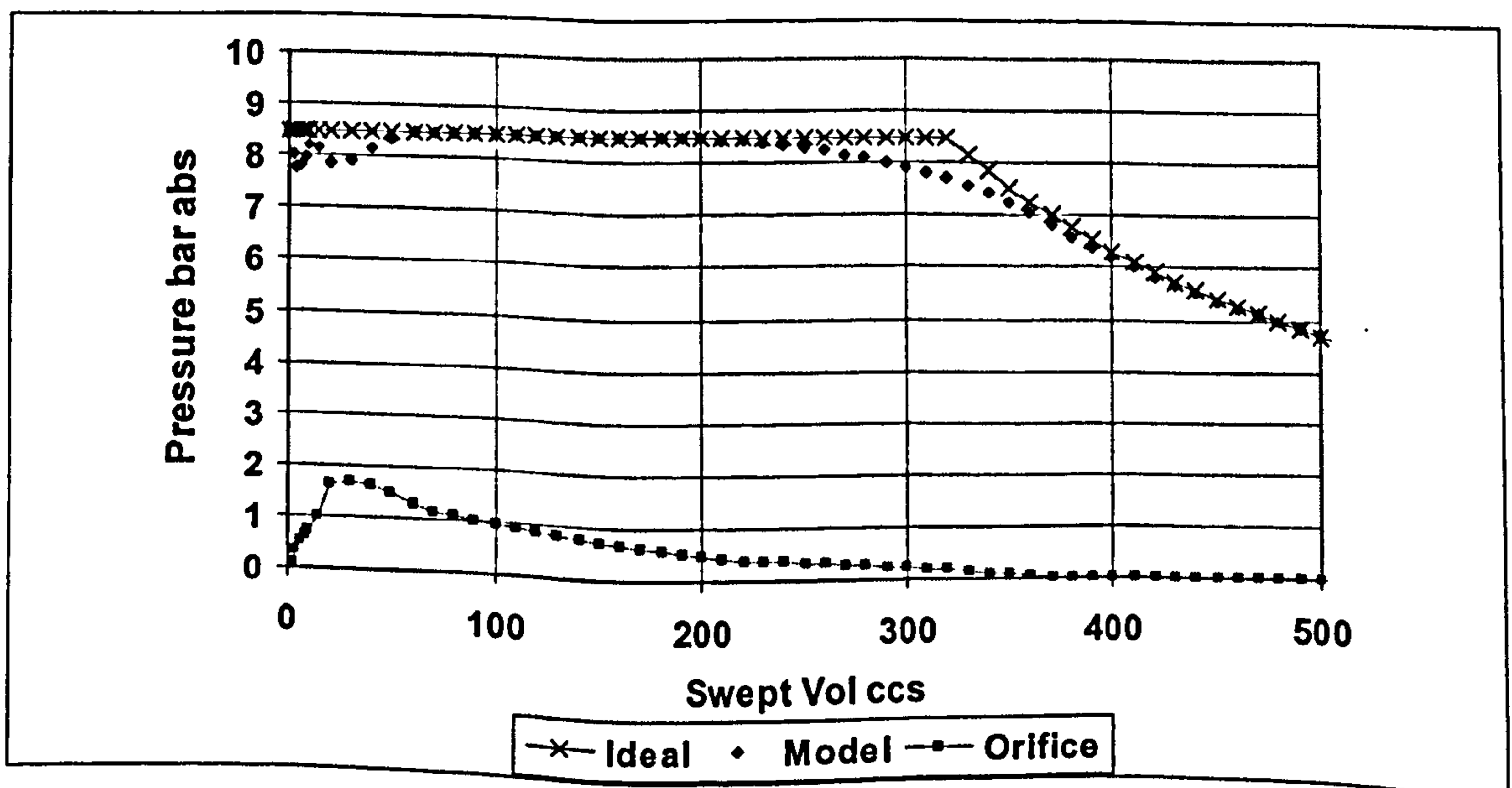


Fig 3.23 PV Diagram of a RJC Engine with 'High Lift' Cams

And for the full expansion the PV diagram is shown at Fig 3.24

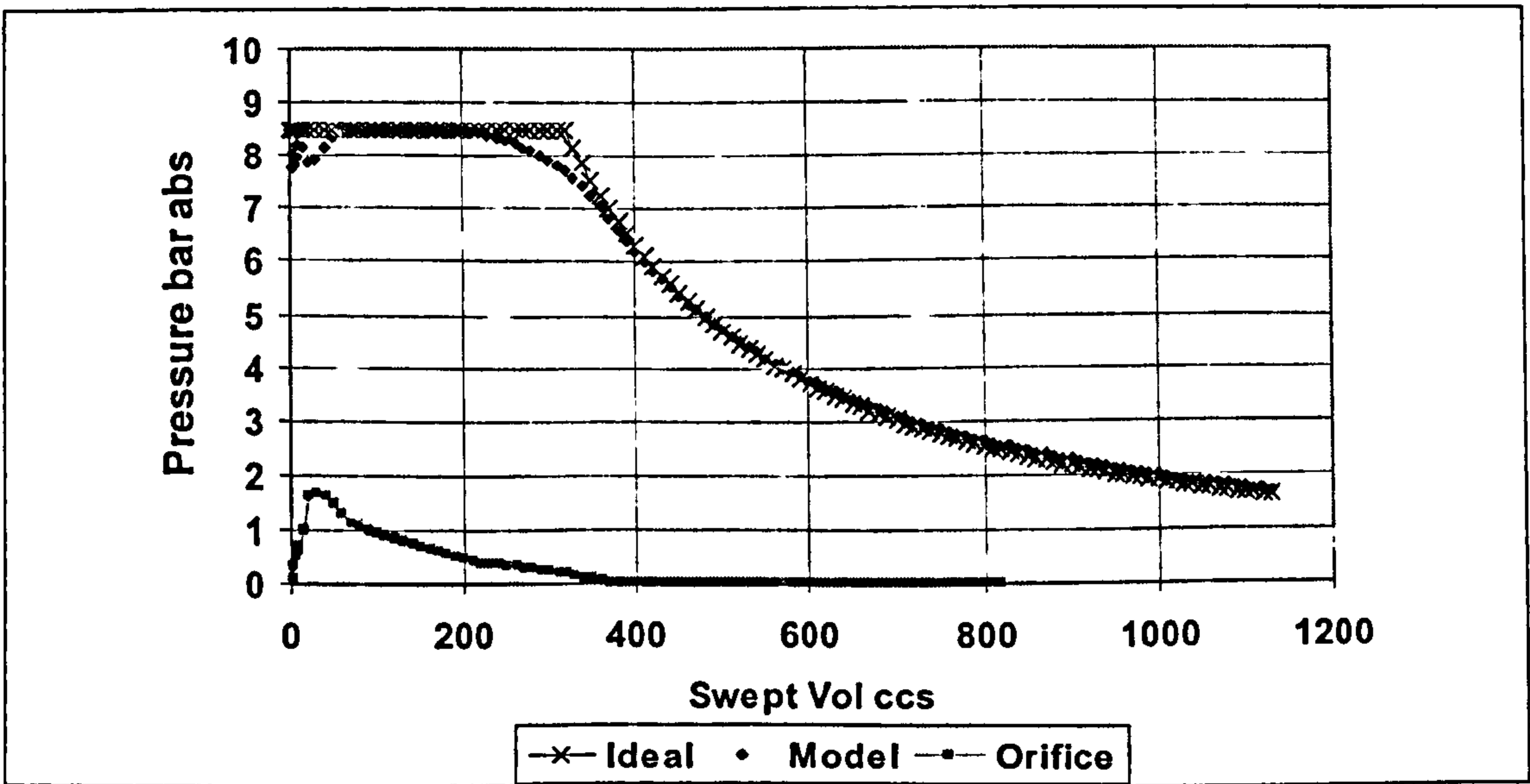


Fig 3.24 PV Diagram For Full Expansion Stroke and Using 'High Lift' Cams

The difference in gross work per cycle in Joules for the expansion is:

Model	Ideal	Difference	% Difference
433.5	437.25	3.75	0.86

For recompression during the exhaust stroke the PV diagram is shown at Fig 3.25

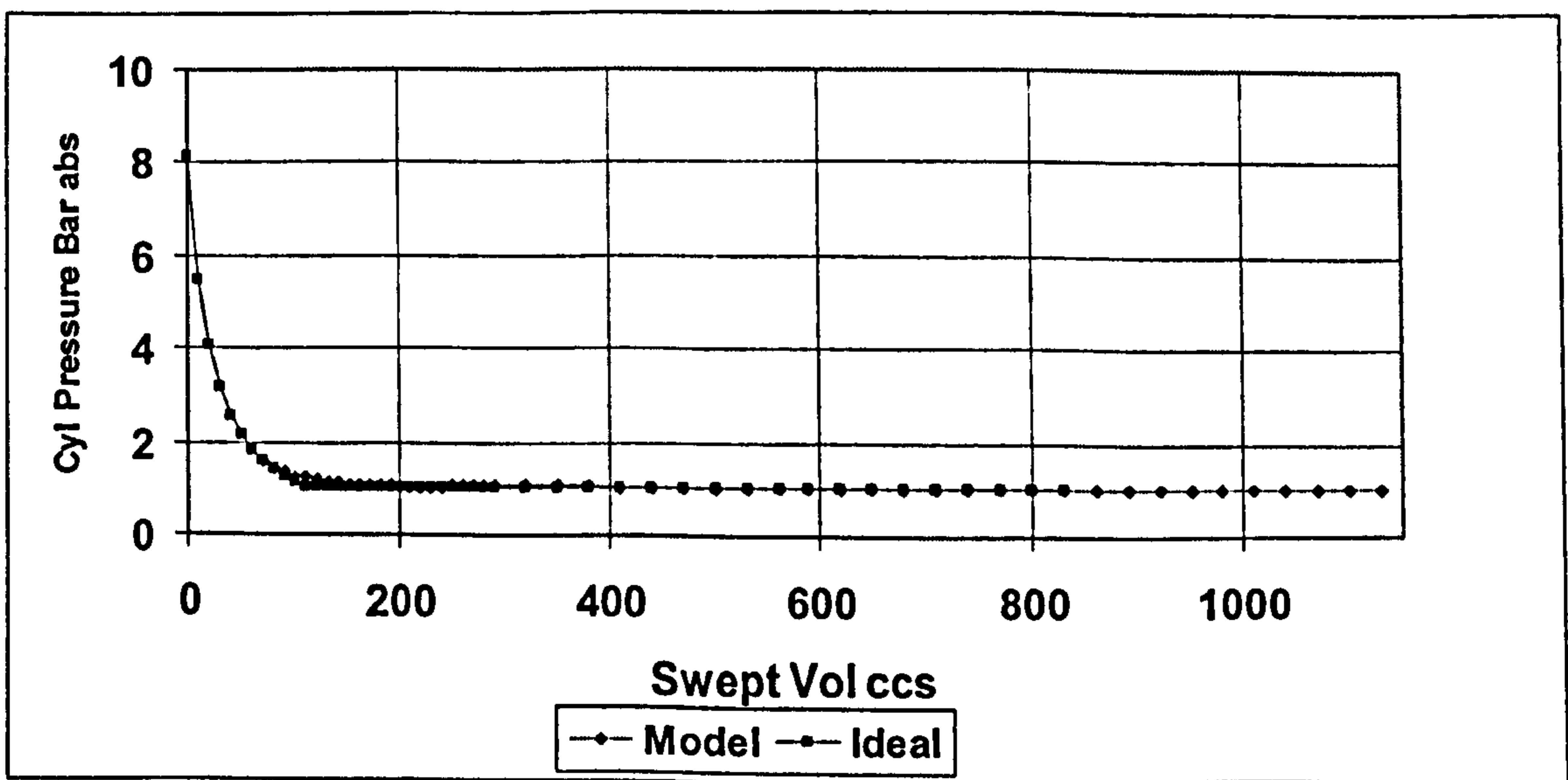


Fig 3 25 PV Diagram for Recompression

The difference in gross work per cycle in Joules for the exhaust stroke is:

Model	Ideal	Difference	% Difference
24	21.7	2.3	10.6

Summing the expansion stroke and exhaust stroke over the whole cycle:

	Ideal	Model
Expansion	437.25	433.5
Exhaust	-21.7	-24
Net Joules /cycle	415.55	409.5

And the overall difference is 1.45 %

### 3.8.6 Application of Valve Pressure Loss Modelling to Engine Design

The modelling of pressure losses have the following implications:

- Large valve flow areas are required to minimise pressure losses. Limiting valve lift to 10 mm thus requires large valve diameters which can only be accommodated in larger bore engines. For a given engine displacement this results in  

***' a minimum stroke to bore ratios of 1:1.2'***
- 'High lift' cam profiles can reduce pressure losses .The model has demonstrated that these pressure losses can be reduced to obtain 98.5% of the ideal cycle work. A slight improvement on this value could be attained with minor adjustments to valve timing.
- The modelling was conducted using poppet valves but the model is also applicable to rotary valves where the value of Cd would be in the order of

0.9 as against 0.75 for poppet valves Ref 11. This represents a 20% increase indicating that the valve flow area for a rotary valve could be 20% lower than an equivalent poppet valve.

- Engine speed has a major impact on pressure losses. For a 120mm bore, 100 mm stroke engine at 1500 RPM the lost work during the expansion stroke is 0.86% of the ideal. At 3000 RPM this loss increases to 20%. This implies that in order to reduce this loss even larger bore engines (having the same displacement) are required. This is not a practical solution and thus implies that

***'there is a limiting RPM for RJC engines without experiencing a significant loss in net power output owing to pressure losses'.***

### 3.8.7 Limitations of Pressure Loss Modelling

The finite differenced derived model will be more accurate as the steps get smaller and may reduce the instability experienced around TDC with advanced valve timing.

Compressibility effects have been ignored because each step represents only a small pressure change.

The coefficient of discharge  $C_d$  is taken as a constant but Ref 11 shows it varying as the ratio of valve lift to diameter ( $L/V_d$ ) varies. In the model the  $C_d$  value is taken as a mean between the maximum and minimum valve lift ratio. At low values of lift the actual  $C_d$  value would be lower than the average value used and thus at valve opening and closing the model in cylinder pressure will be lower. Varying values of  $C_d$  could be incorporated into future models.

### 3.9 Micro CHP System Modelling

By combining all the above models an overall prediction can be made of the performance of a micro CHP system that incorporates a RJC engine. The system schematic is shown at Fig 3.26 in which calculated values have been attributed to the micro CHP system temperatures. The RJC engine and micro CHP parameters are given in Table 3.5

RPM	Supply pres	Eng Size	B/S mm	Heat Exchanger Effectiveness
Fixed	Fixed			
1500	7.5 bar g	1130 cc	120/100	0.7

Expander Mechanical Efficiency	Compressor Mechanical Efficiency
90%	90%

Table 3.5 RJC Engine and Micro CHP Parameters used for Modelling

This modelling was conducted on an engine with inlet gas conditions at a constant 7.5 bar g. and temperatures from 550 C to 850 C and constant RPMs of 1500 and 3000 with details in spreadsheet form in Annex 3

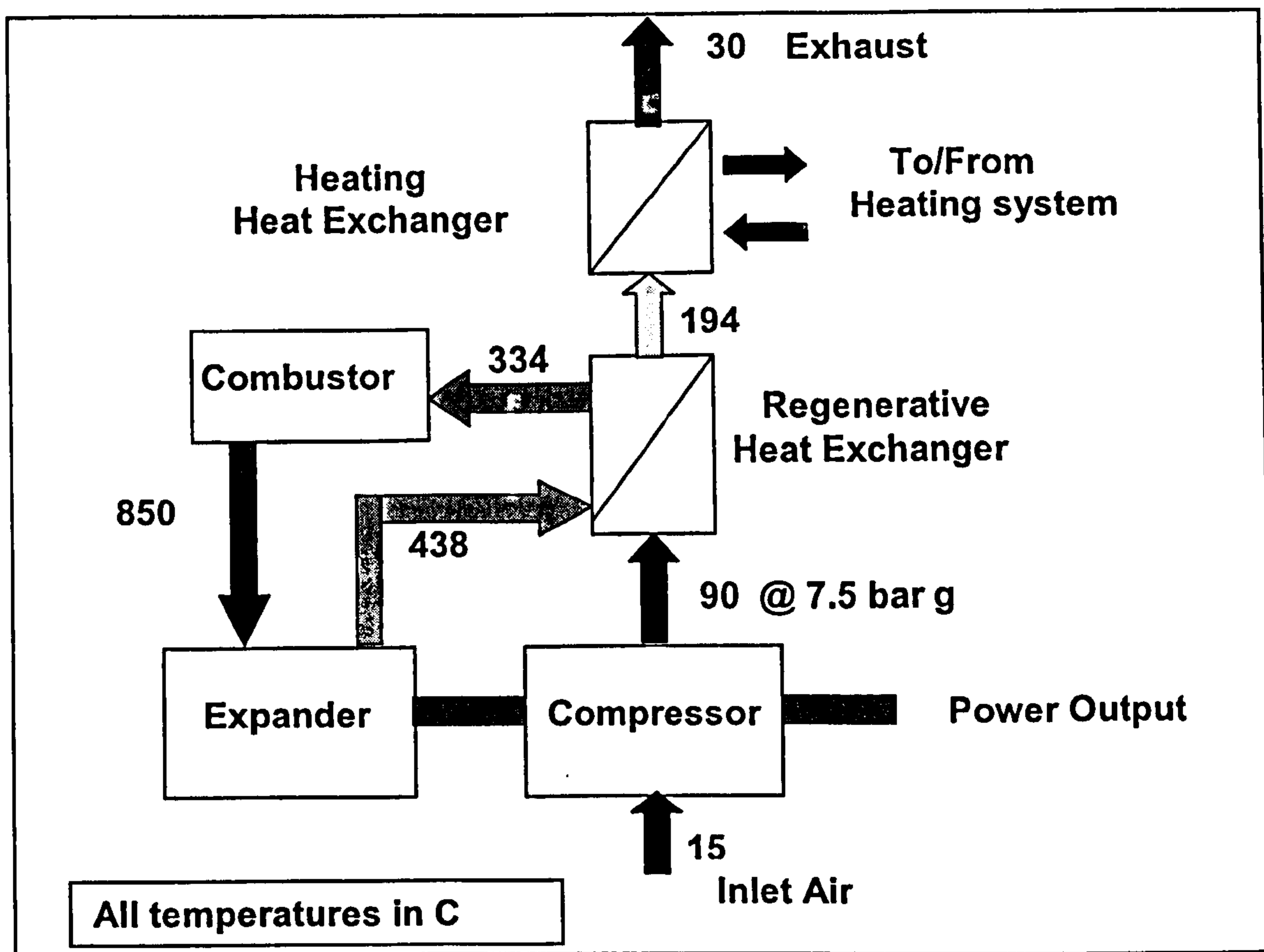


Fig. 3.26 Micro CHP System Schematic

The micro CHP system in Fig 3.26 assumes an expander gas inlet temperature of 850C and utilises exhaust gas regeneration to preheat the air from the compressor prior to combustion. For lower expander gas inlet temperatures the expander exhaust gas temperature will be lower and the regenerative inlet temperature will also will be lower. If the expander RPM and compressor discharge pressure are to be kept constant (see part 4.11.1 compressor variable inlet valve timing) then for lower expander inlet temperatures the compressor has to deliver a greater mass flow and thus absorbs more of the expander work reducing the net power output. Regeneration heats the air prior to combustion thus and reduces the amount of heat required by combustion. The regenerator has been modelled as a heat exchanger using an assumed value of effectiveness from Table 3.5 and equation (4.15)

$$\epsilon = \frac{(T_{hin} - T_{hout}) C_c}{(T_{hin} - T_{cin}) C_{min}} \quad (4.15)$$

Where  $C_{min}$  is the smaller of  $\dot{m}hC_{ph}$  and  $\dot{m}cC_{pc}$

and  $C_c = C_{pc}$

The details of the model results are at Annex 3 and the significant performance values of net work output and thermal efficiency are shown at Figs 3.27 and 3.28.

The temperatures calculated in the model for heat exchanger inputs and outputs and expander inlet temperature of 850 deg C at 1500 RPM are included in Fig 3.27

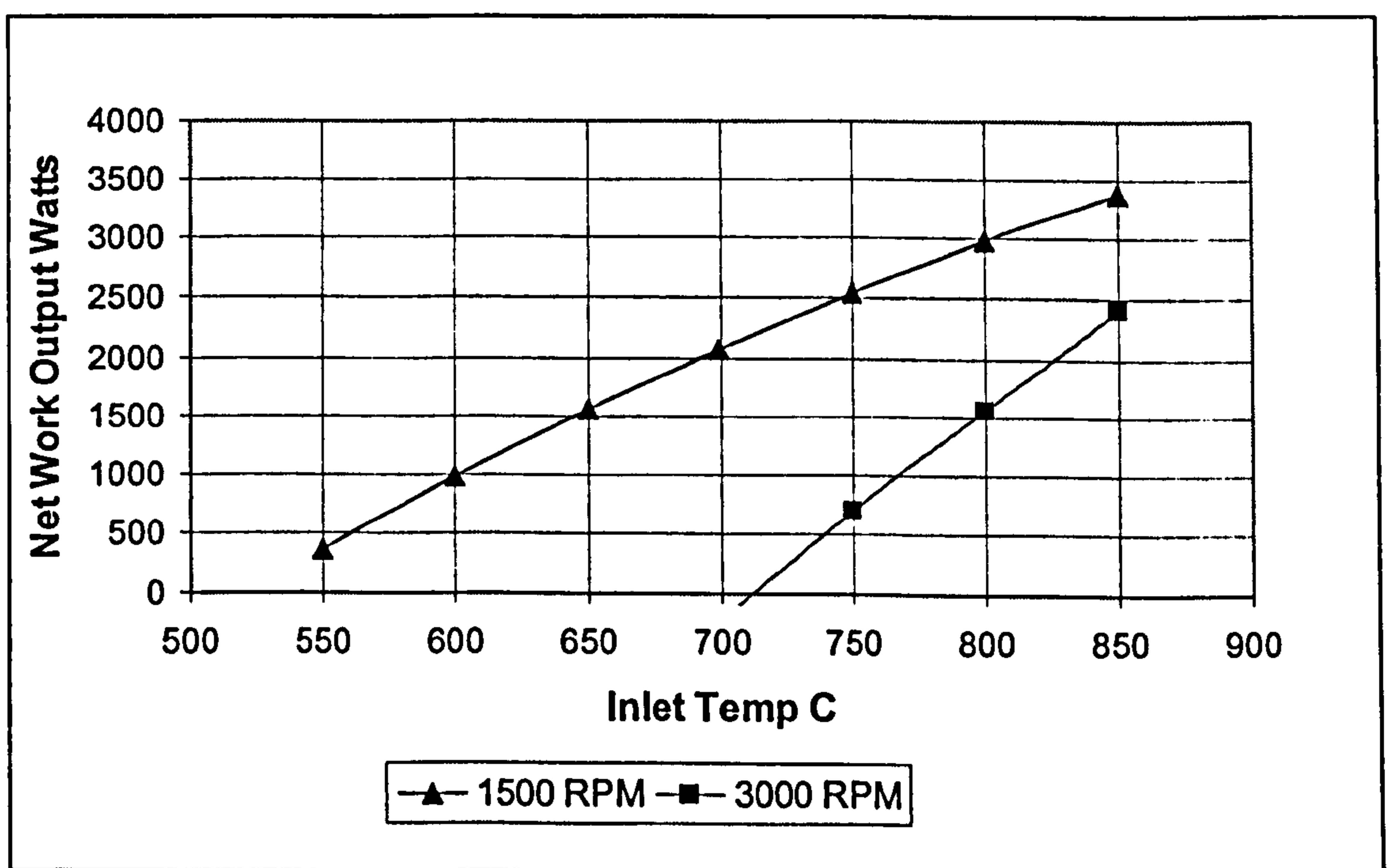


Fig 3.27 Net Work Output vs Inlet Gas Temperature

The engine thermal efficiency is defined as:

**Power Output / Heat Supplied By Combustion**

and is calculated from modelling as a maximum of 27% at a gas inlet temperature of 850C (Fig. 3.27). Only small improvements are likely on this value of thermal efficiency and can only come from a reduction in the engine and compressor

friction. If the expander and compressor individual mechanical efficiencies of 95% are used instead of 90% the RJC engine thermal efficiency would be increased to 33%

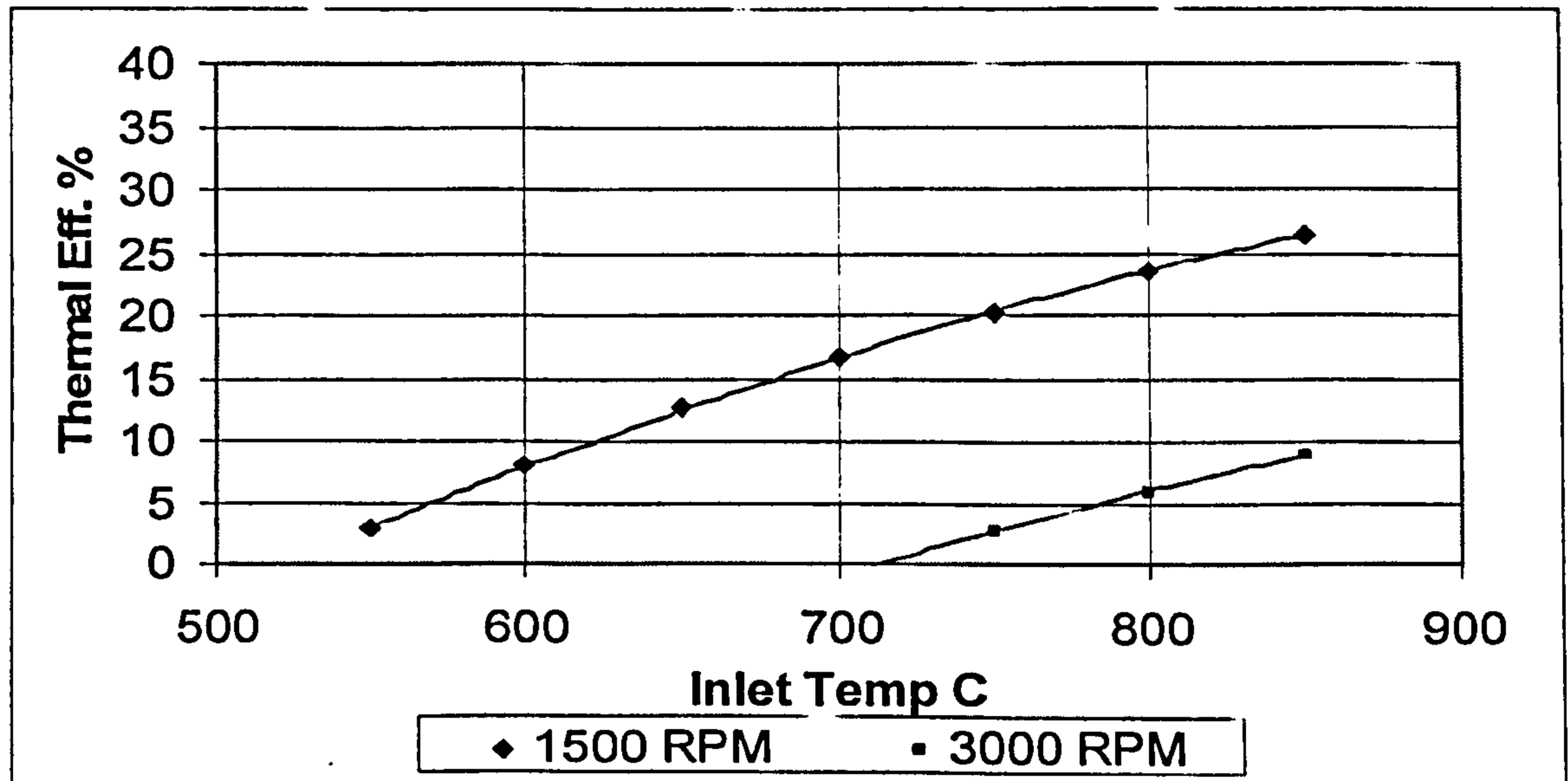


Fig 3,28 Thermal efficiency vs Inlet Gas Temperature

Both the above figures demonstrate the significance of the pressure losses that occur if the engine is run at 3000 RPM rather than at 1500 RPM. The cycle IMEP at 1500 RPM is 3.86 bar whilst at 3000 RPM with the same size valves is 3.18 bar. The net power output at an inlet gas temperature of 850 C was found to be 3387 Watts for a displacement of 1130 ccs thus:

*For comparative purposes with other reciprocating engines a ratio of net power output in Watts to swept volume in ccs can be used. The value of this ratio for a RJC engine, from the model, is 3 Watts per cc'*

For the range of inlet gas temperatures examined only an engine speed of 1500 was developed further . The power output and the heat available to the heating system for a range of expander inlet temperatures is shown at Fig 3.29



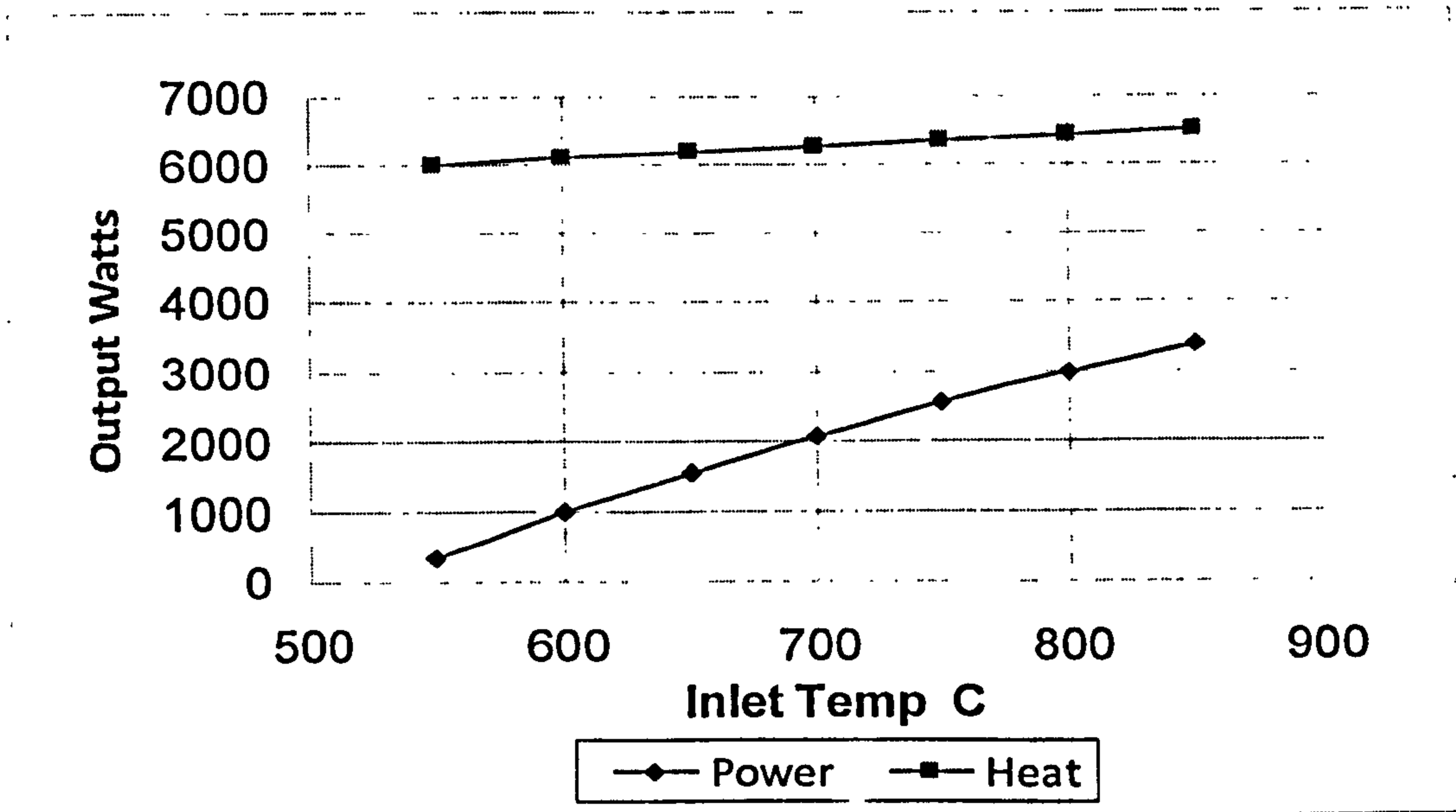


Fig 3.29 System Power and Heat Output vs Expander Inlet Temp C

The ratio of net work output to the system heat is shown at Fig 3.30 This ratio is of importance in CHP applications because it defines the usable energy outputs for a range of system maximum temperatures (expander inlet temperatures).

The ideal heat transfer from the Annand model (at 1500 RPM) would be 3800 Watts (Annex3). As a conservative estimate 3000 Watts for jacket and oil cooling is assumed and this value is added to the system heat

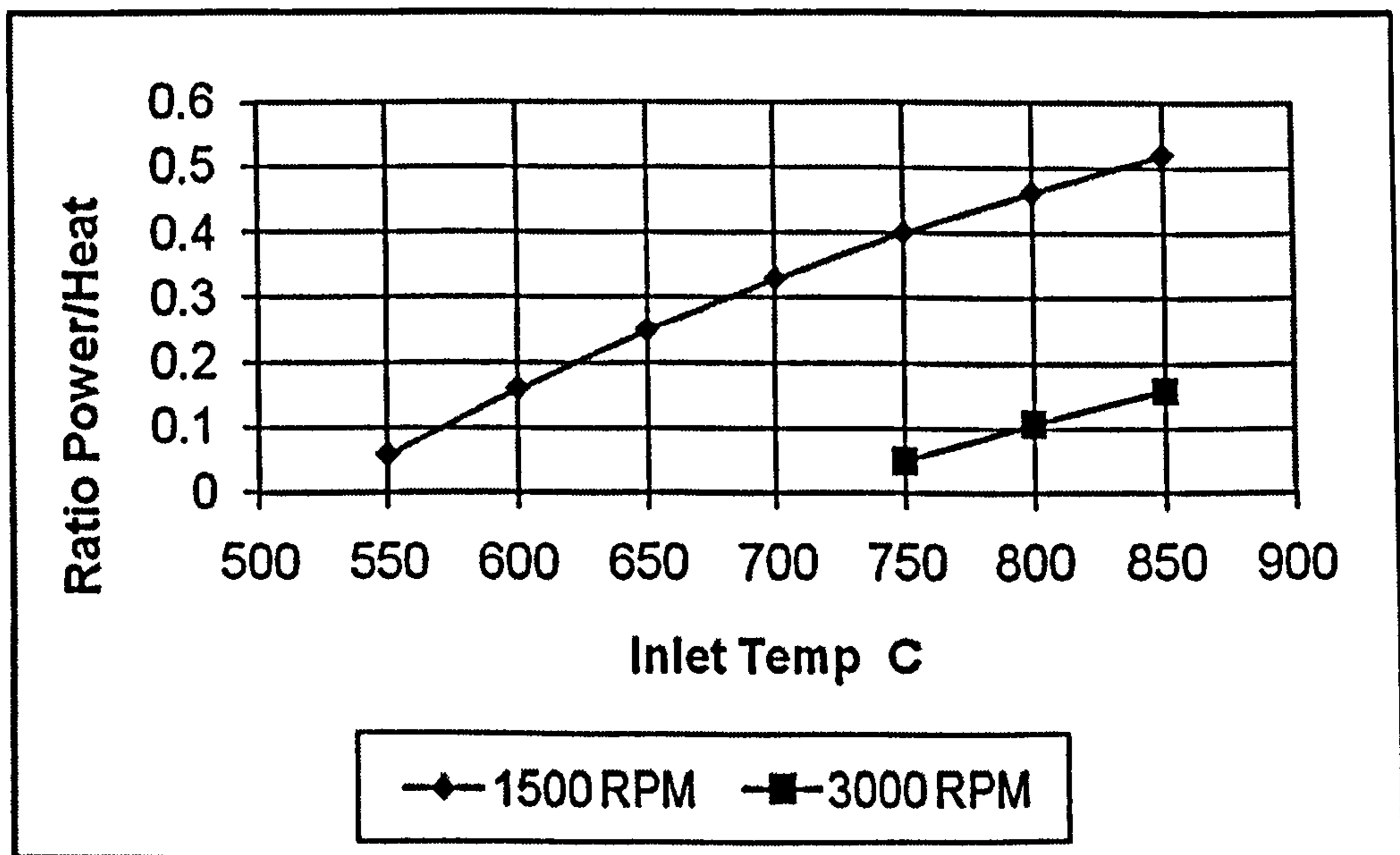


Fig 3.30 Ratio Work /Heat Output for Varying Inlet Gas Temperatures

The overall system thermal efficiency is defined as:

**(Power Output + Heat to System) / Heat Supplied By Combustion**

and is shown in Fig. 3.31

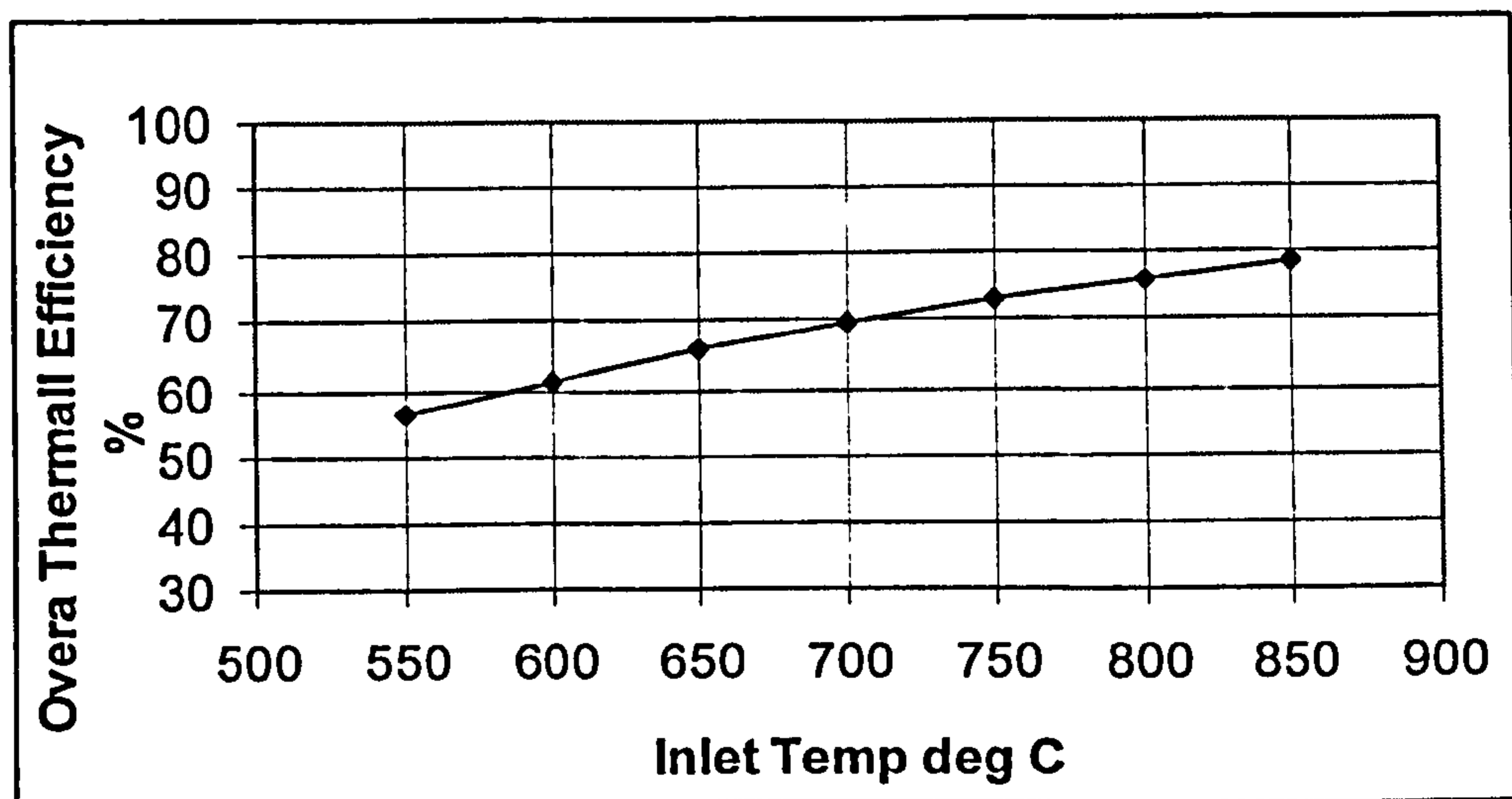


Fig. 3.31 Overall System Thermal Efficiency Vs Expander Inlet Temperature

The overall thermal efficiency at a gas inlet temperature of 850C is 79%

### 3.9.1 Findings from Micro CHP System Modelling

- Thermal efficiencies of 33% are achievable with maximum regeneration. Higher thermal efficiencies can be attained with increases in mechanical efficiencies.
- Power to heat ratios vary from 1:2 at 850C expander inlet temperature to 1:6 at 600C expander inlet temperature.
- An overall thermal efficiency of 79% is attainable at an expander inlet temperature of 850C. This is a conservative percentage and is based on expander cooling jacket and hot oil heat recovery of 3000 W.

### 3.9.2 Limitations of Micro CHP Modelling

- The modelling of the Micro CHP system does not take into account heat losses to the surroundings by radiation, even from insulated components,

and any such losses will reduce the engine thermal efficiency and overall thermal efficiency.

- The heat exchanger effectiveness for both regeneration and heat to the system are assigned values of 0.7. These are considered conservative and actual values of effectiveness will depend upon specific design of heat exchanger
- Jacket cooling of the expander cylinder and oil cooling was an estimation and based on thermal modelling. The thermal modelling would need to be refined, and be based on an actual physical engine design, to obtain a more accurate value for jacket and oil heat recovery.
- Combustion efficiency is assumed to be 100%

### **3.10 Overall Assessment of Modelling**

- Friction modelling is the least precise and had to rely on existing empirical models and, specific data from reliable sources. However the models carried forward to thermal and whole engine modelling are considered to be representative.
- Thermal modelling required that a value of the polytropic index of expansion be determined. Using the expression for polytropic efficiency at a value of 87% provided the polytropic index. This in turn allowed cylinder gas temperatures to be derived as well as a relationship between the Reynolds and Nusselt Number. Whilst small variations in the polytropic index make little difference to the net work output lower temperatures at the end of expansion will reduce the amount of heat energy for regeneration and thus the overall thermal efficiency. Thermal modelling can be improved by replacing some of the assumed temperatures of 'in cylinder' components

with measured values. The thermal model generated compared well with the Annand correlation. Additionally thermal modelling demonstrated the significant effect ring pack friction has on the overall heat transfer and thus the need for accurate frictional modelling of piston ring / liner interaction.

- Pressure loss modelling revealed the significant effect of valve flow area and engine speed on pressure losses and thus indicated work. The model correlated well with test data from the BMW engine on cold air giving confidence that the model was representative of in cylinder pressures. Knowing the in cylinder pressure over the whole cycle allowed indicated power to be derived the net power output from an engine of known displacement.
- Micro CHP system modelling required that assumptions be made of the temperatures at several positions in the system. It is considered that such assumptions are reasonably accurate although they do not take into account radiation heat losses even from well insulated surfaces and includes only an estimate for heat recovered from jacket cooling and the engine lubricating oil. Overall system modelling generates thermal and system efficiencies and as well as a ratio of power to heat.

## **Engine Development and Testing**

### **4.1 Test Engines**

Two separate engines and systems were developed and tested. The first being termed a technology demonstration engine based on a conventional 4-cyl in line automotive block and which also involved the design, build and testing of combustion chambers. The second engine was based on a BMW R 650 air cooled motor horizontally opposed piston engine for which two separate designs of cylinder heads and valve gear were built and tested. The process of engine development and the design and testing of unique components for both engines is described.

#### **4.1.1 Description of the Technology Demonstration Engine.**

A conventional four cylinder diesel engine had been modified to form the basis of the RJC technology demonstration engine. Whilst this type of engine does not represent an engine suitable for micro CHP application it represented a convenient method to allow investigation into component development and performance. Lessons learnt from the development work on this engine were carried forward into the design of a prototype RJC engine that would meet the defined requirements for a micro CHP system

The engine used is a Ford 2.5 litre with a bore of 93.67 mm and a stroke of 90.54 mm giving a swept volume of 2496 cc. The engine was configured such that two cylinders were used for expansion, one cylinder for the compressor and the remaining cylinder left in situ to provide overall engine balance. Compressed air could be supplied to the engine and with the use of the existing started motor arrangement the engine could be started and then motored on compressed air. The major modifications to the engine at the start of this project are described.

#### 4.1.2. Expander Cylinder Head and the Inlet / exhaust valves.

The original four cylinder head was cut in half to form a platform for the expander cylinders inlet and exhaust valves and their actuating gear. An overhead camshaft in anti friction bearings was fitted to the cylinder head to actuate the two inlet and two exhaust valves. The exhaust valves were directly operated from the camshaft but in the case of the inlet valves where the system pressure was acting on the stem side of the valve a different configuration was employed.

The inlet valve actuation gear is diagrammatically shown at Figure 4.1a with details visible in Figures 4.1b and 4.1c.

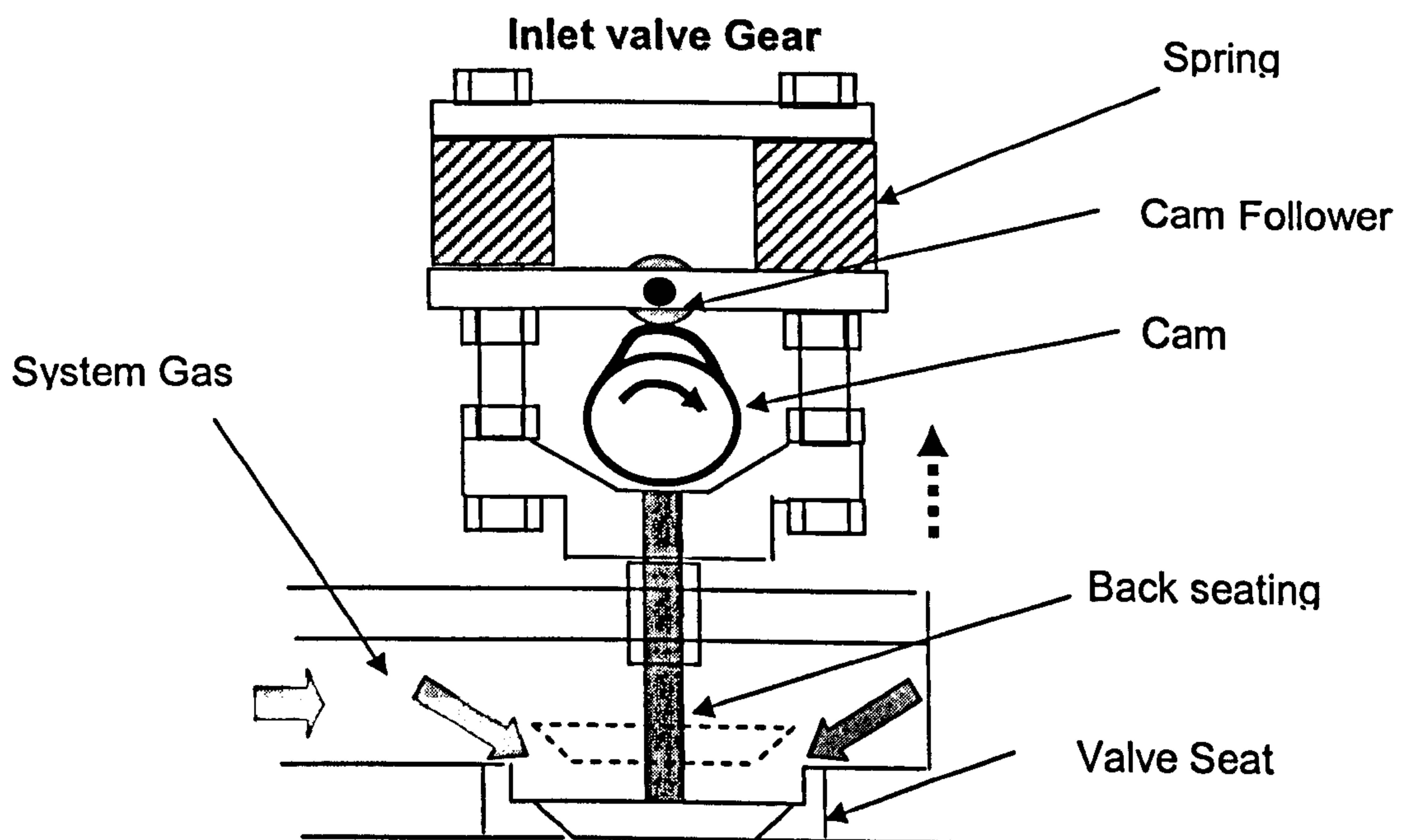
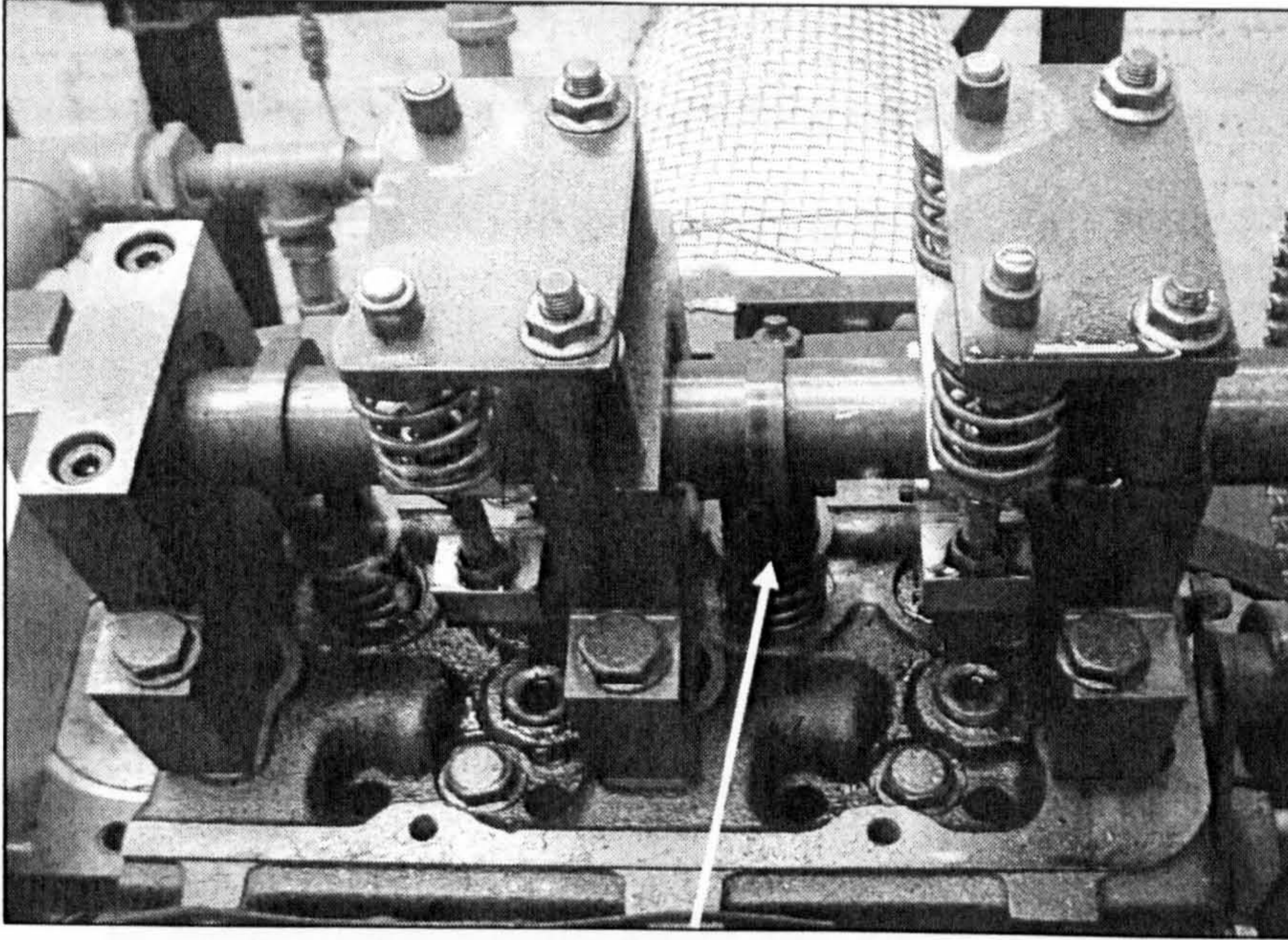


Fig 4.1a Diagrammatic Representation of Inlet Valve Gear



Direct OHC Operated Exhaust Valve

Fig 4.1b Valve Gear Details

Fig 4.1a Compressor Valve Housing

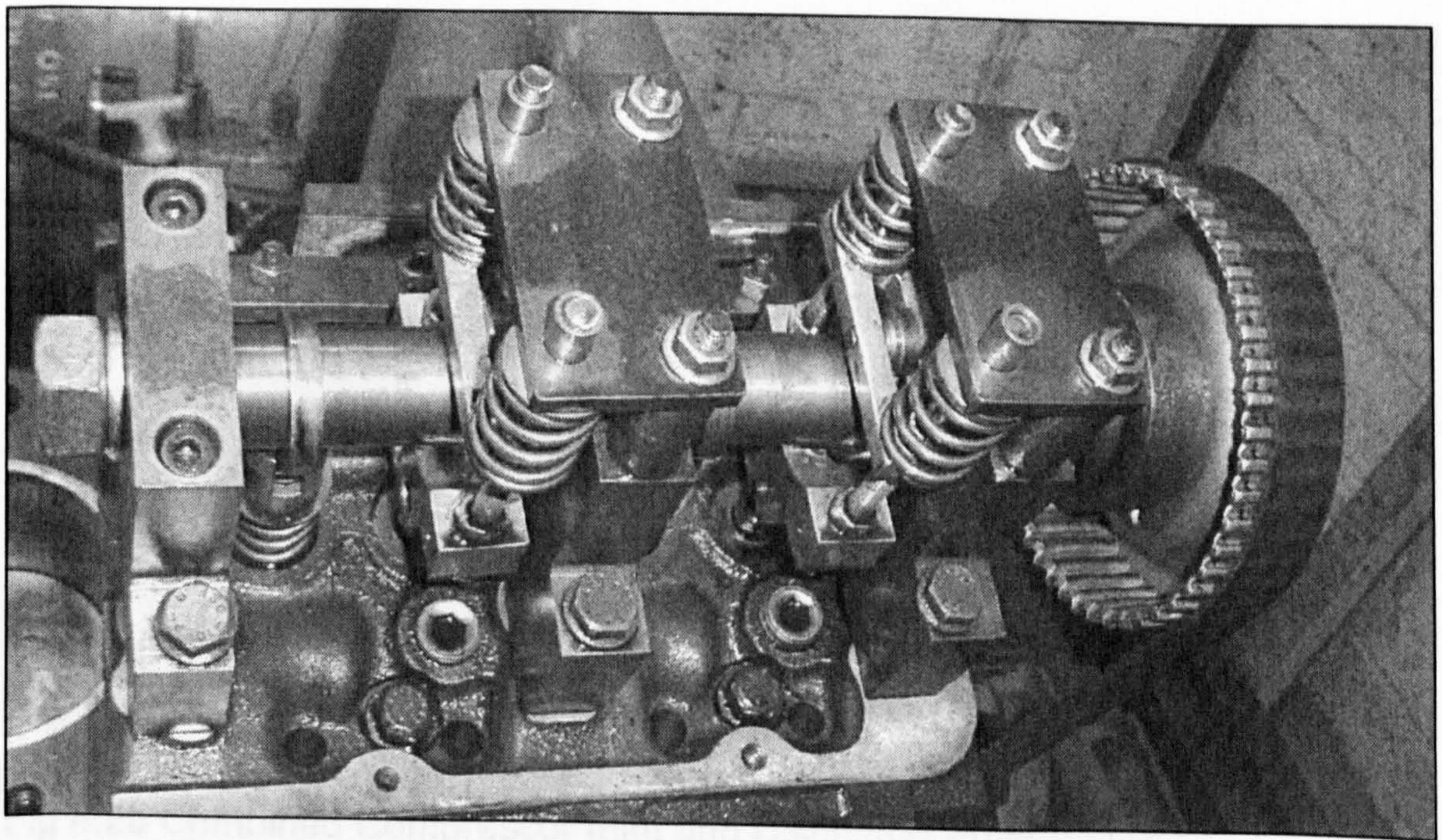


Fig 4.1c Valve Gear Details

4.1.3. Compressor Head and Compressor Valves.

A compressor head had been manufactured to house a combined inlet and exhaust valve assembly shown at Figs 4.2a and 4.2b

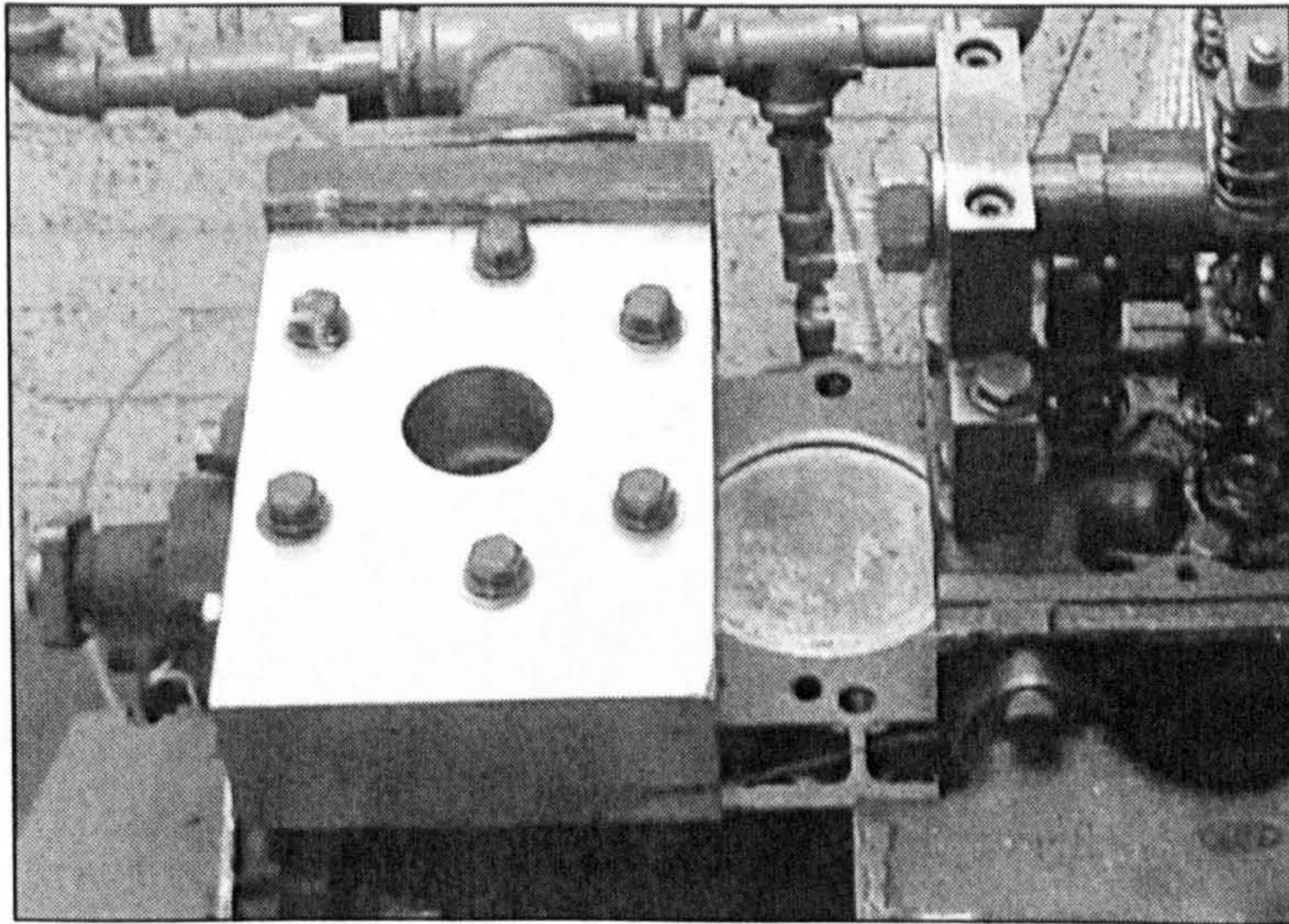


Fig 4.2a Compressor Valve Housing

**Compressor Plate Valves**

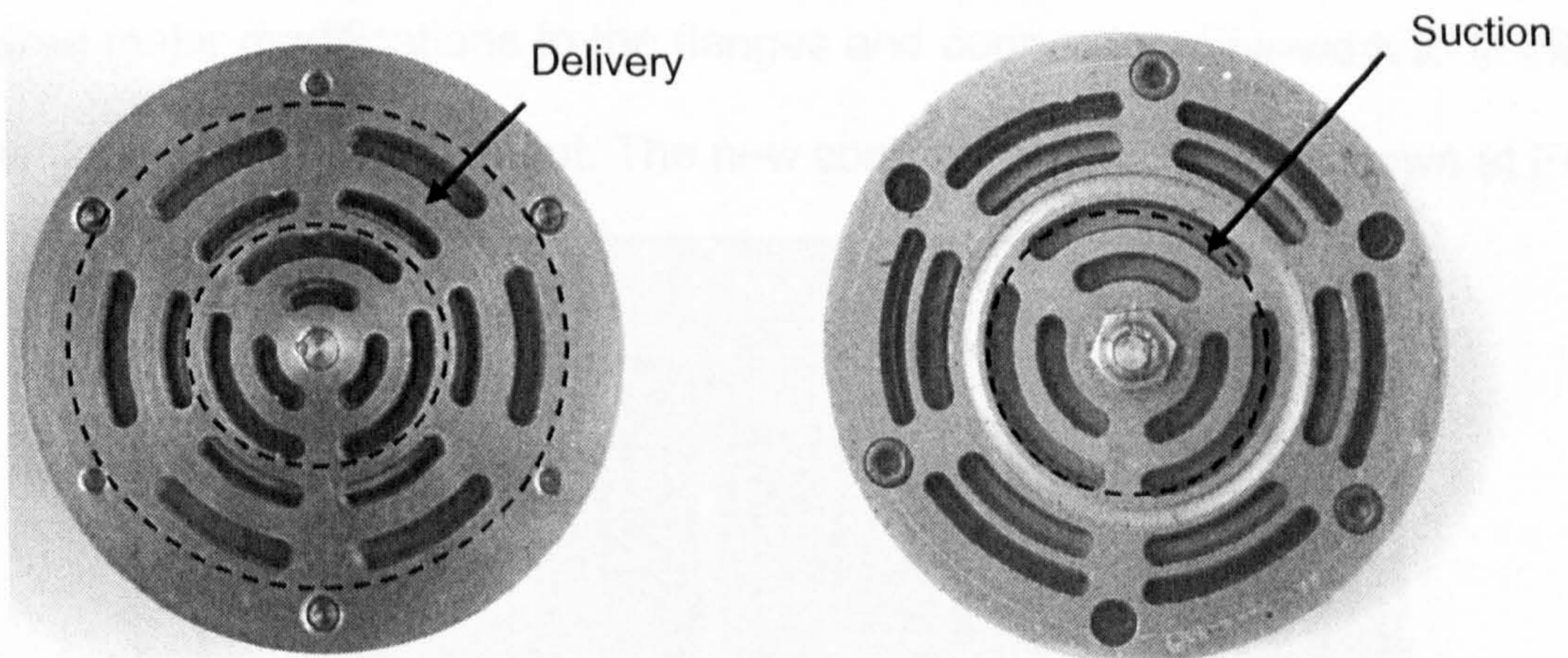


Fig 4.2b Combined Compressor Inlet and Discharge Plate Valves



The compressor discharge was fed to an air receiver vessel Fig 4.3 and then to the combustion chamber.



Fig 4.3 Compressor Air Receiver Vessel

#### 4.1.4 Combustion Chamber

The existing combustion chamber reported Ref.5 was still fitted. This combustion chamber was reported to give poor ignition and unstable combustion. A new combustion chamber had been manufactured but at the start of the project required major modifications to the flanges and connecting pipe-work to fit into the existing pipe-work arrangement. The new combustion chamber is shown at Fig 4.4

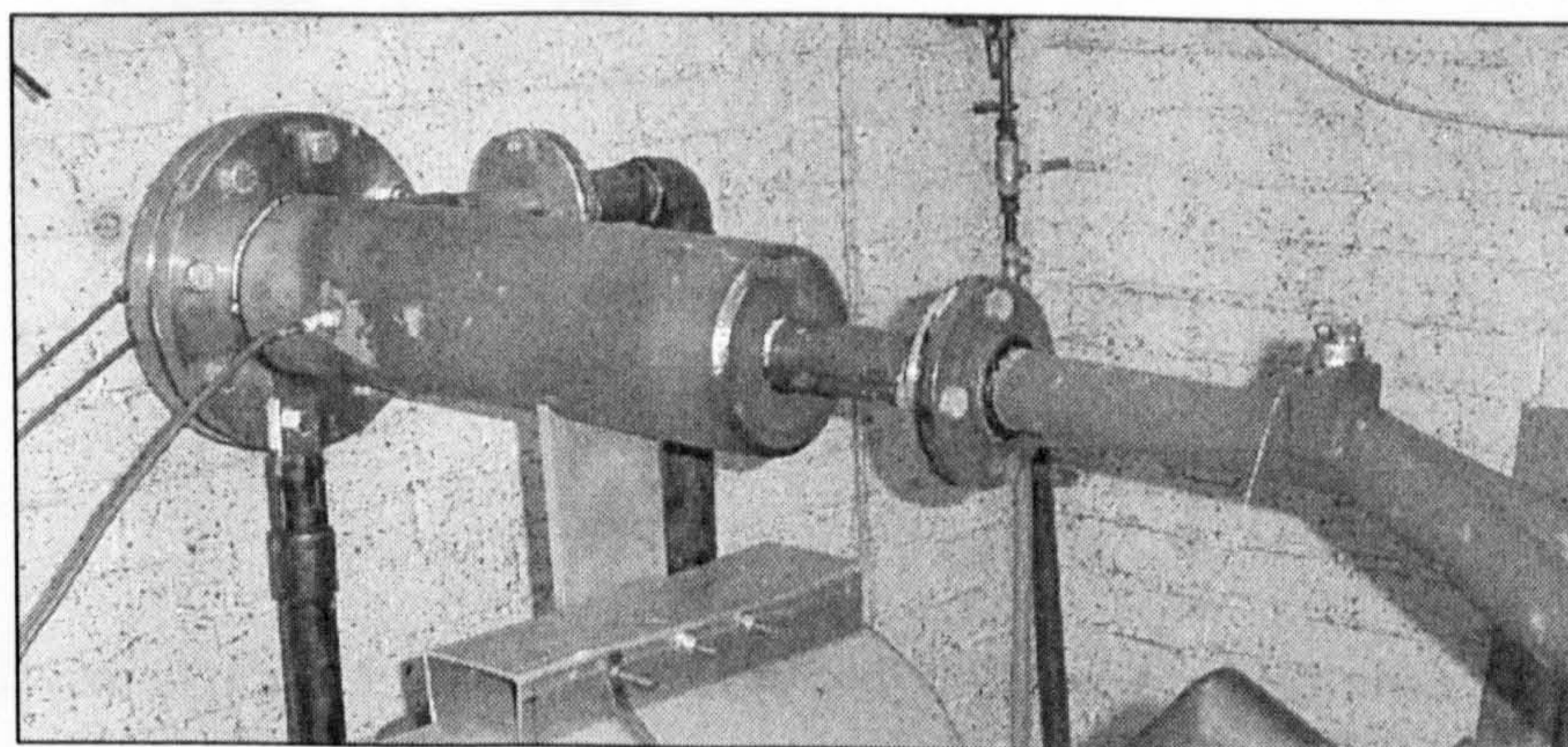


Fig 4.4 Combustion Chamber Fitted to Existing Pipework.

The combustion chamber was already fitted with a spark plug holder but the back flange was blank and therefore required modifications to mount a gas burner assembly.

#### 4.1.5 First iteration on Engine Development

The objective of the first iteration was to achieve stable ignition and combustion. The combustion chamber and gas nozzle tested prior to the start of this project used the principle of injecting natural gas at pressures up to 10bar via a nozzle and inducing some of the air supplied via a cone shaped swirl plate. Prior to the start of the project a conventional burner assembly had been obtained which comprised of a nozzle holder surrounded by induced air passages and a shroud for the flame area. This is diagrammatically shown at Fig 4.5.

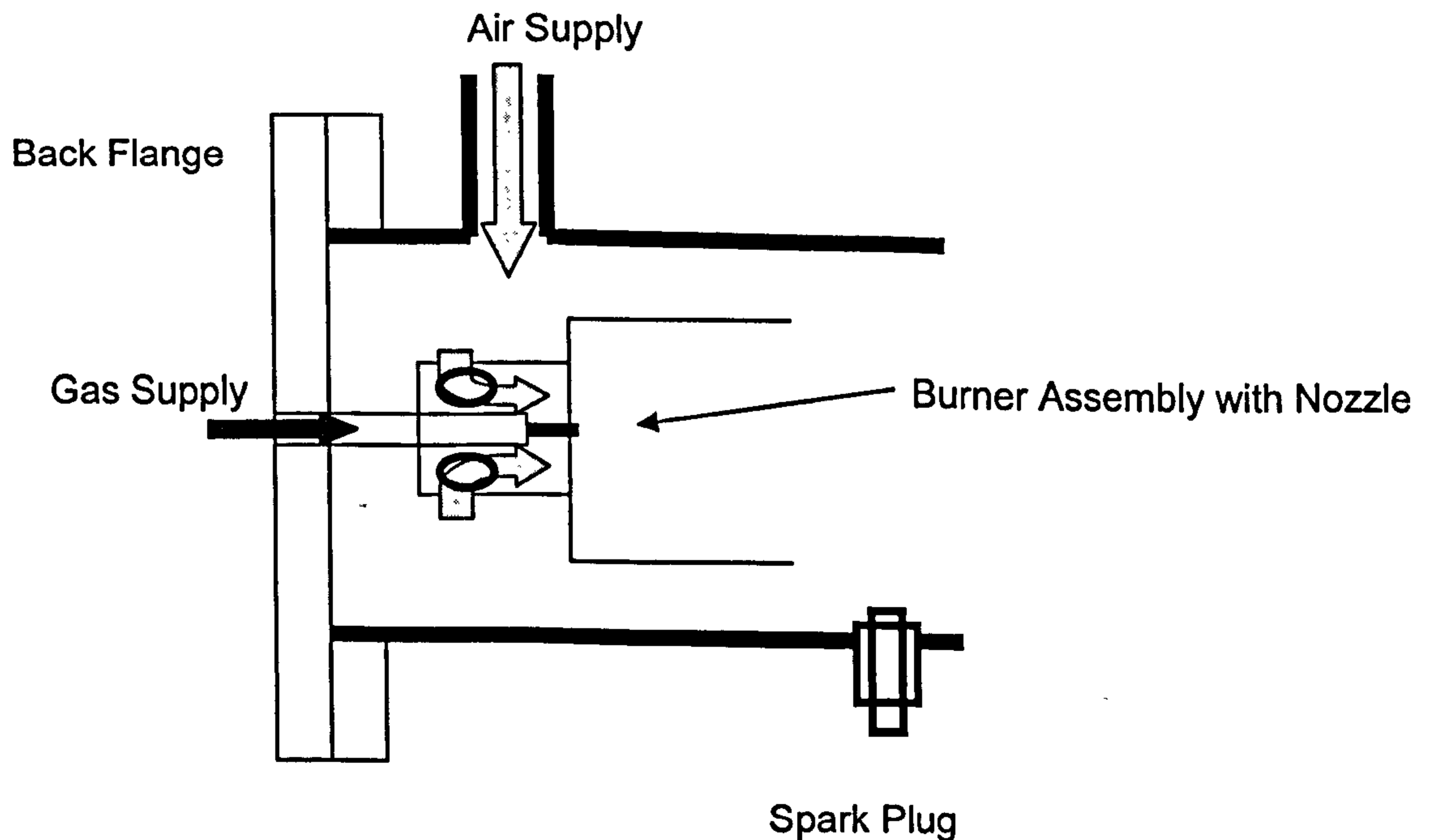


Fig 4.5 Conventional Nozzle Assembly in Combustion Chamber

The burner assembly was mounted on the back flange and a gas supply was provided. In addition a pressure tapping was made in the back flange and pipe-work led to a pressure gauge.

With this configuration the engine was motored on air and gas induced into the combustion chamber. A series of explosive ignitions was experienced with erratic combustion indicating the mixture in the combustion chamber varied from stoichiometric at the point of ignition to a weak mixture as the gas is burnt. This is then repeated as the amount of unburnt gas builds up and reaches a level of flammability. Under these conditions an engine gas inlet temperature of 400C was achieved. Additionally several major mechanical deficiencies on the engine were found and required rectification work. The deficiencies and the work undertaken included:

1. Major blow-by from the expanders. The original configuration had not been fitted with piston rings in a view to minimising friction. All pistons were fitted with the correct rings.
2. Damage to valve gear. The cams fitted had too sharp a profile that lead to bending of the exhaust valve spindles and valve guide breakages, and inlet valve cam follower breakages. New valves and guides were fitted and cam profiles modified to give a 'softer' operation. The inlet valve cam followers, originally small ball races, were replaced with a brass in steel bearing assembly.
3. New inlet valve seats were manufactured and ground in to reduce leakages

A larger gas nozzle (0.64mm) was manufactured and fitted for the next operation of the engine. A small improvement in ignition and combustion was experienced.

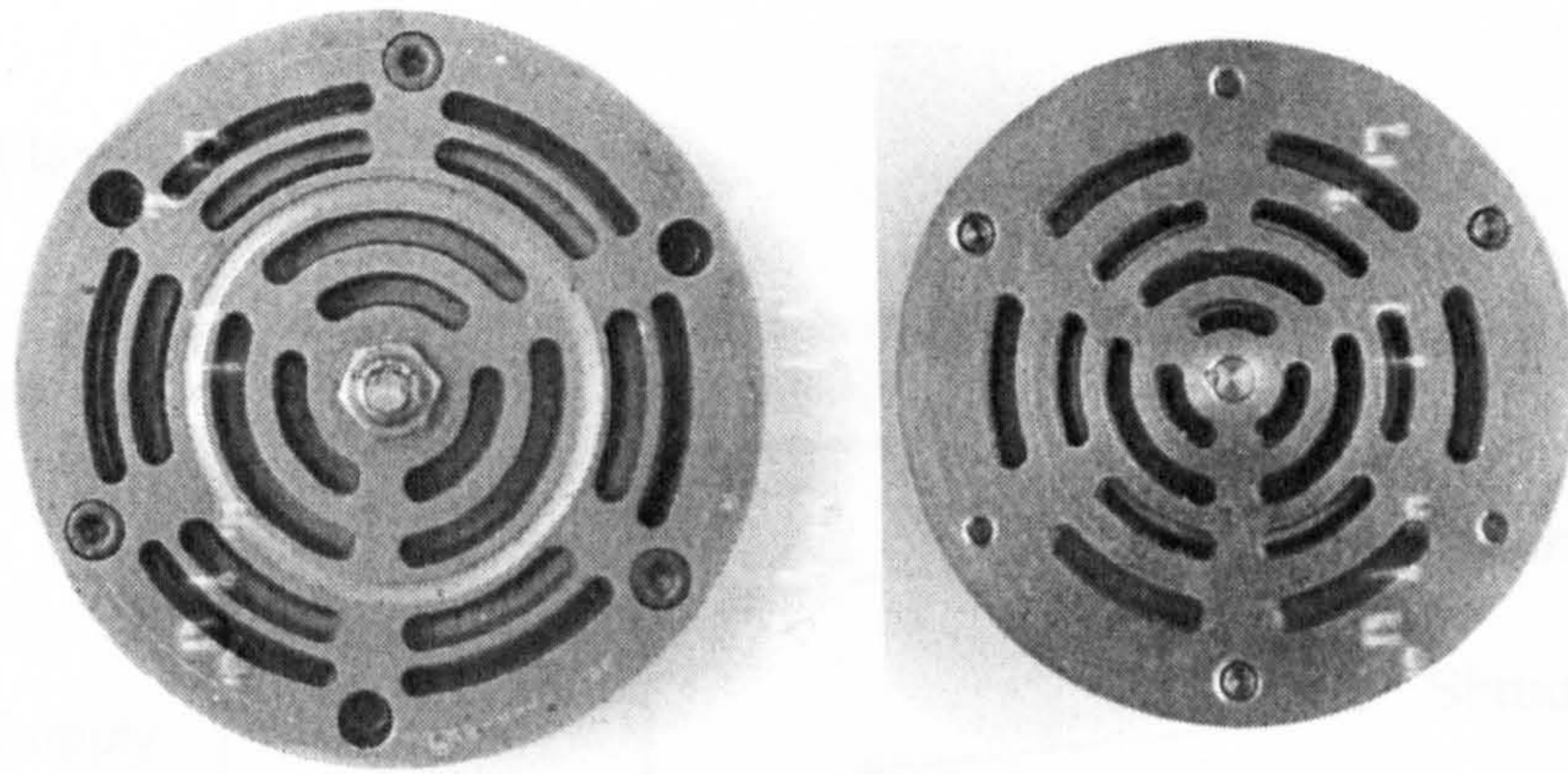
## Part 4

Further increases in gas nozzle size from 0.8 to 1.0 mm gave some improvements on ignition and once the temperature in the combustion chamber had risen stable combustion then existed with temperatures reaching 600 C.

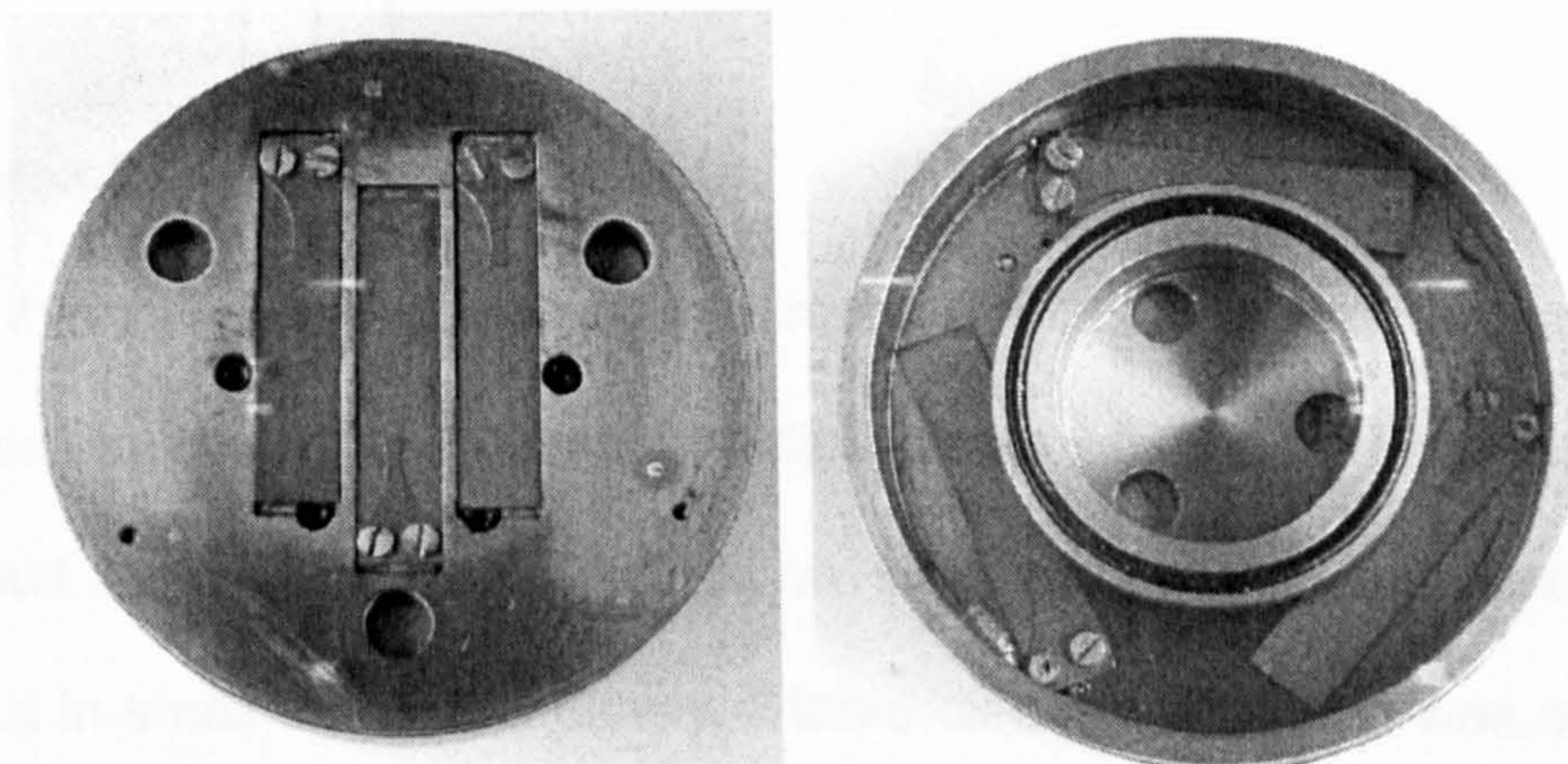
Under these conditions the commercial burner suffered heat damage and a new burner assembly of similar design was manufactured from steel. Further additional work was undertaken to modify the rig and included:

1. The spark plug holder was modified to move the tip of the spark plug nearer to the edge of the burner assembly shroud.
2. A sight glass was fitted into the back flange of the combustor to observe combustion conditions.
3. The performance of the compressor combined inlet/discharge valve was measured and it was found to require an inlet depression of 0.2 bar before the inlet plate opened and that the volumetric efficiency was ~70%. A new design of compressor head was manufactured incorporating three reed valves for both suction and discharge. The performance of this new design gave a volumetric efficiency of 75%. The new suction and delivery valves are shown at Fig 4.6 and detail drawings are at Annex 4

Plate Valves



Reed Valves



Suction

Deliver

Fig 4.6 Compressor Suction and Delivery Valves.

4. A circular baffle plate was fitted to the burner shroud in an attempt to provide more air to gas/air mixing zone within the shroud.

The modified burner assembly is shown at Fig 4.7

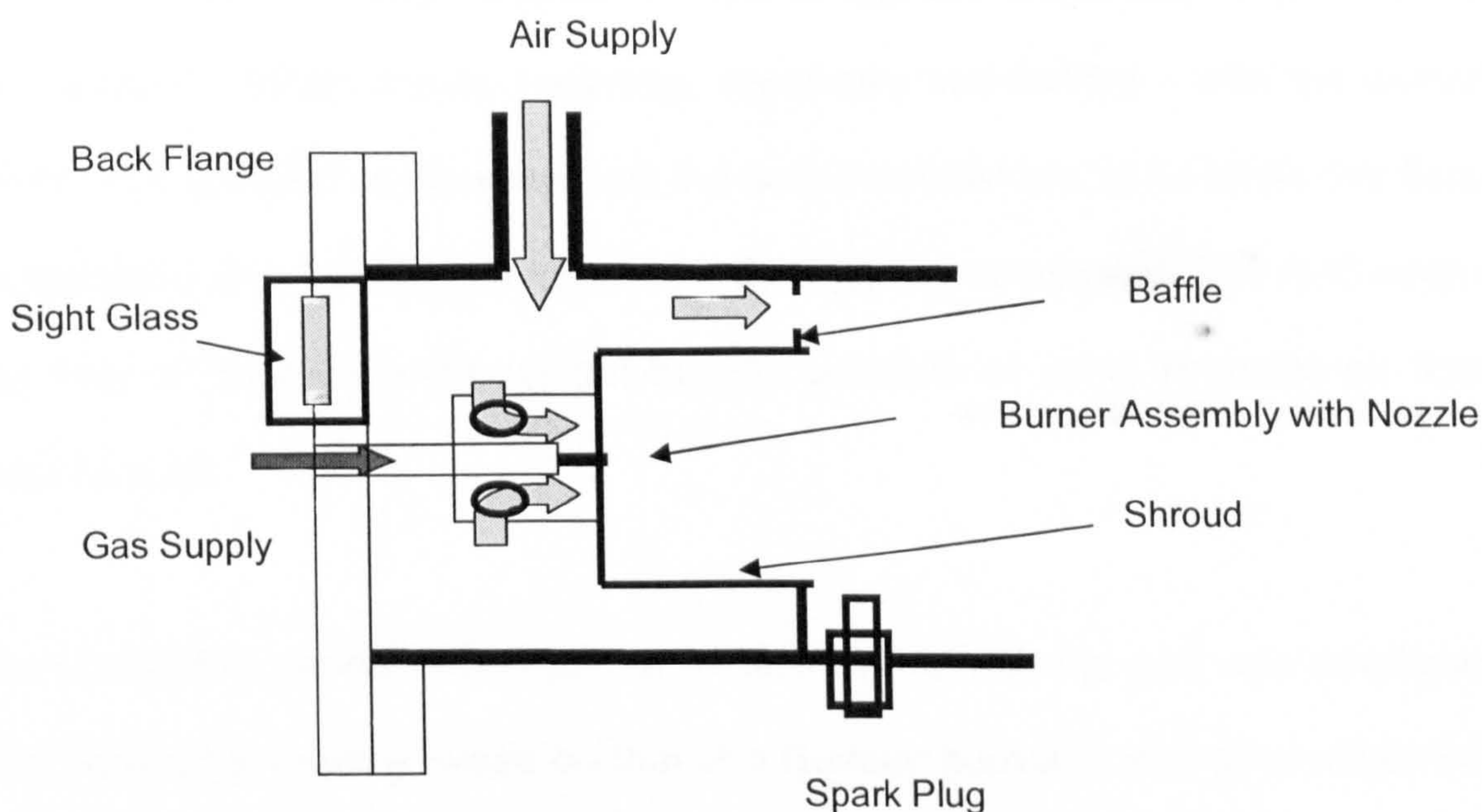


Fig 4.7 Modified Burner Assembly

Although this arrangement gave some improvements in ignition and combustion it was difficult to control in that minor adjustments of gas or external air supplied could result in extinguishing combustion such that any adjustments had to be carried out in small steps and slowly. Stable clean combustion was observed and a maximum temperature of 600 C was achieved at 600 RPM and a hot gas inlet pressure of 4 bar g

It was considered that the development of this type of burner assembly could not be taken much further in that there was still a fundamental weakness in achieving stable ignition and controllable combustion.

#### 4.1.6 Second Iteration on Engine Development

The objectives of the second iteration was to achieve more stable conditions for ignition and combustion and investigate the effect of the valve timing by use of different profiled cams.

The amounts of air and fuel theoretically required result in air fuel ratios greater than stoichiometric conditions i.e. weak mixtures where the range is approximately

from 60:1 to stoichiometric. Gas turbine technology use combustion chambers with air supplied in three phases – primary, secondary and tertiary – with the primary air for stoichiometric combustion and the secondary/tertiary air to dilute the flame temperature and heat the air mass flow through the combustor. The RJC engine has less air mass flow throughput but the principle of using separate air flows remains valid.

The concept of providing a separate air flow to mix with the gas was developed. This concept is broadly based on that of a Bunsen burner in that air is mixed with gas in a tube to ensure adequate mixing before ignition at the tube outlet or nozzle plate. Because the combustion chamber operates at system pressure the air supplied to the gas for combustion has to be supplied separately from the diluting air. The design developed and manufactured consisted of an air gas mixing chamber, a mixing tube with a bore to length ratio of at least 10:1 and a nozzle plate to decelerate the mixture and thus reduce the velocity of the gas air mixture below that of the flame velocity. The basic concept is shown in fig 4.8 with detail drawings at Annex 4

Prior to final design and manufacture the concept was tested outside the combustion chamber to determine the best position for the spark plug to ensure stable ignition. The outcome of this work was that a pilot hole was incorporated into the nozzle plate angled at 45 deg such that the jet of mixture impinged on the spark gap. In air, such an arrangement gave instant ignition every time.

The air supply pipe work to the combustion chamber was modified to give two separate supplies each controlled by a valve.

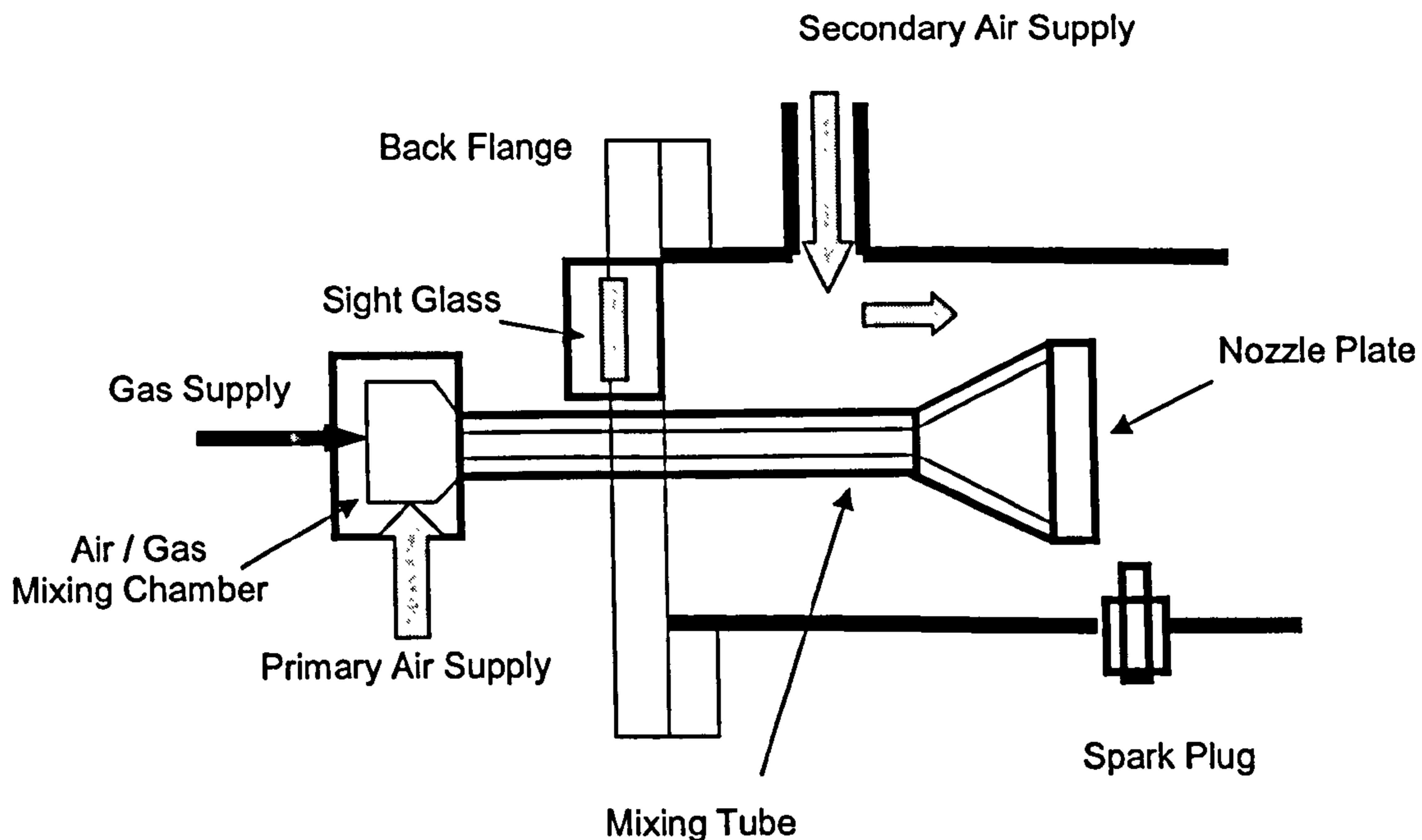


Fig 4.8 Combustor with Mixing Tube Assembly

New valve cams were designed and manufactured to give a 175 degree opening 6 mm lift for the exhaust and 80 degree opening and 6 mm lift for the inlets. A second set of inlet valves of 100 degree opening and 6 mm lift were also manufactured and tested. The effect of inlet valve opening on system pressure ration is shown in Table 4.1

Inlet cam opening	Measured pressure ratio $r_p$	Predicted pressure ratio $r_p$
70 deg	3.52	4
80 deg	3.00	3.4
100 deg	2.34	2.8

Table 4.1 Pressure Ratios vs. Inlet Valve Opening



The difference between predicted and measured pressure ratios can be explained by the fact that the predicted pressure ratio assumes a square shaped opening and closing profile with no pressure losses during opening and closing Fig 4.9

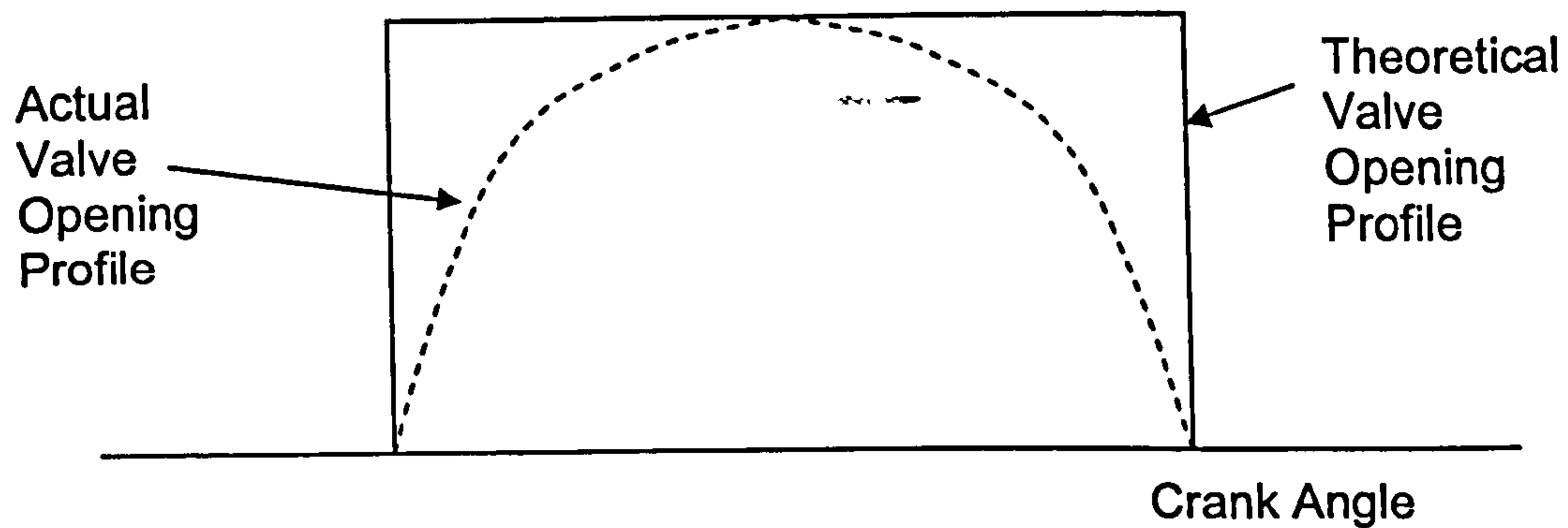


Fig 4.9 Inlet Valve Opening Profiles

Operation of the engine produced a gas temperature of 700 C stable ignition and stable and controllable combustion conditions. Self sustaining conditions however could not be achieved. The combustor chamber and discharge pipe-work glowed a bright red validating the measured gas temperature and observed stable combustion conditions. The flow rates of the primary and secondary air were adjusted but the primary air always needed to be fully open whilst the secondary air could be partially but never completely closed. This indicated that with this burner / combustor arrangement clean and stable combustion could be achieved .

#### 4.1.7 Third Iteration on Engine Development

The objective of the third iteration was to further improve combustion conditions to raise the gas temperature, and achieve self sustaining conditions. From visual observation of the combustion chamber it was clear that significant heat losses were being incurred. This was addressed by:

## Part 4

1. Altering the secondary air inlet to the gas exit end of the combustion chamber and fitting an inner flame tube. This is shown in Fig 4.10

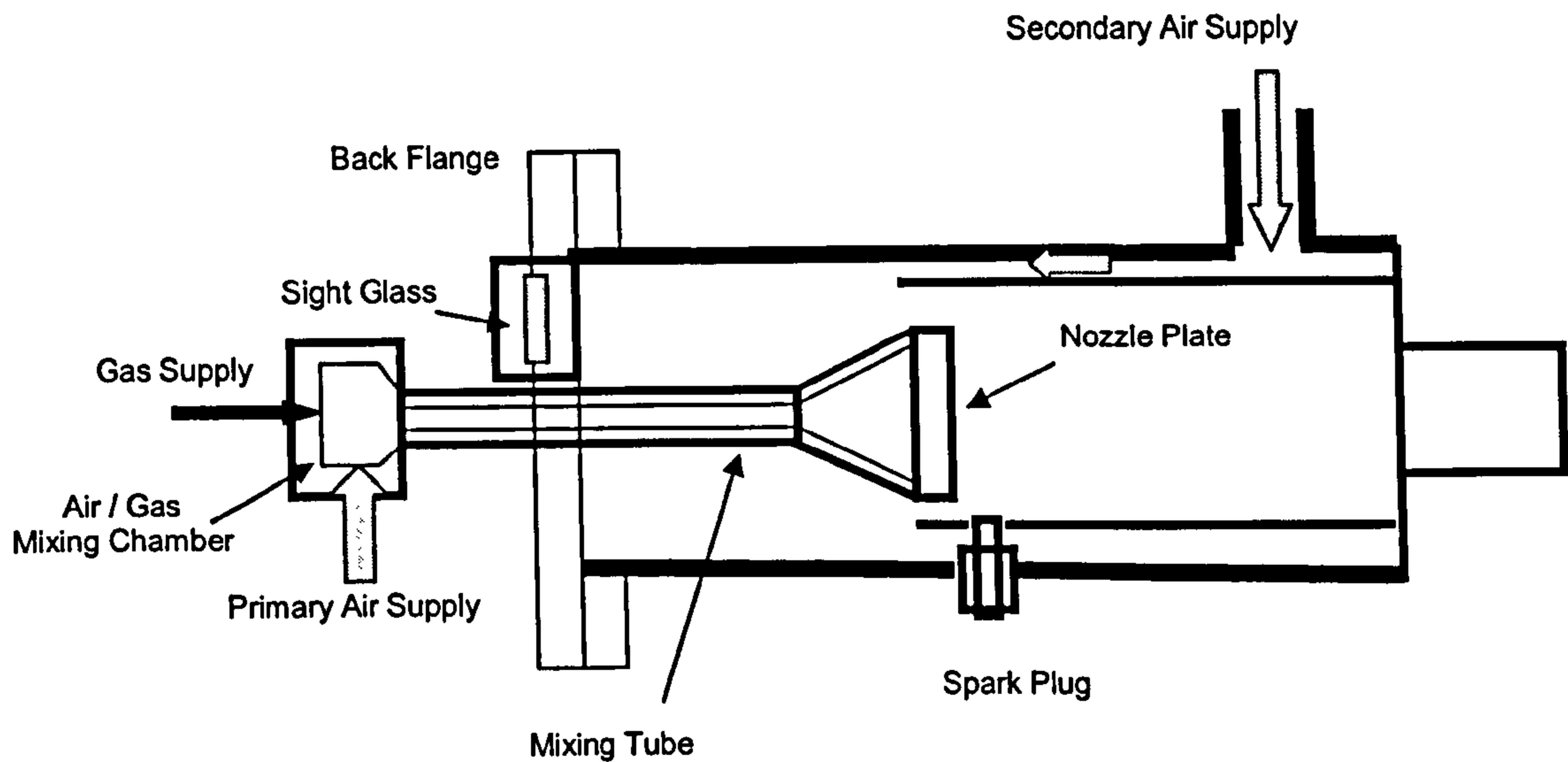


Fig 4.10 Modified Combustion Chamber

2. Insulating the combustion chamber and engine gas inlet pipe work
3. The air receiver bottle was removed from the system because it was felt it was no longer necessary and would help maintain the temperature of the compressed air from the compressor.

The insulation had a significant effect on the temperature of the expander inlet gas which reached 750 C. In addition if the engine was allowed to run until sufficient heat had been built up in the engine block and the lubricating oil then self sustaining conditions were achieved. However this was only under conditions of a rich mixture and is explained by the higher gas flow rate adding to the overall mass flow rate.

A new nozzle plate with larger nozzle holes (to allow more primary air flow) was installed and the system converted from compressed natural gas to run on propane with an inlet supply pressure of >4 bar

The engine self sustained at 750C with clean combustion and a minimal supply of gas controlled by a needle valve. The system pressure was 2.8 bar.

#### 4.1.8 Fourth Iteration on Engine Development

The objectives of the fourth iteration were to further improve the combustion conditions and maximise the work output from the expanders by accurate valve timing. It was realised that the existing combustion chamber could not be modified much further so a new chamber was designed and built. The opportunity existed of converting an existing stainless steel flanged tube to a smaller more compact combustion chamber. The overall volume reduction was from 15.25 litres to 4.5 litres and the physical comparison is shown at Fig 4.11

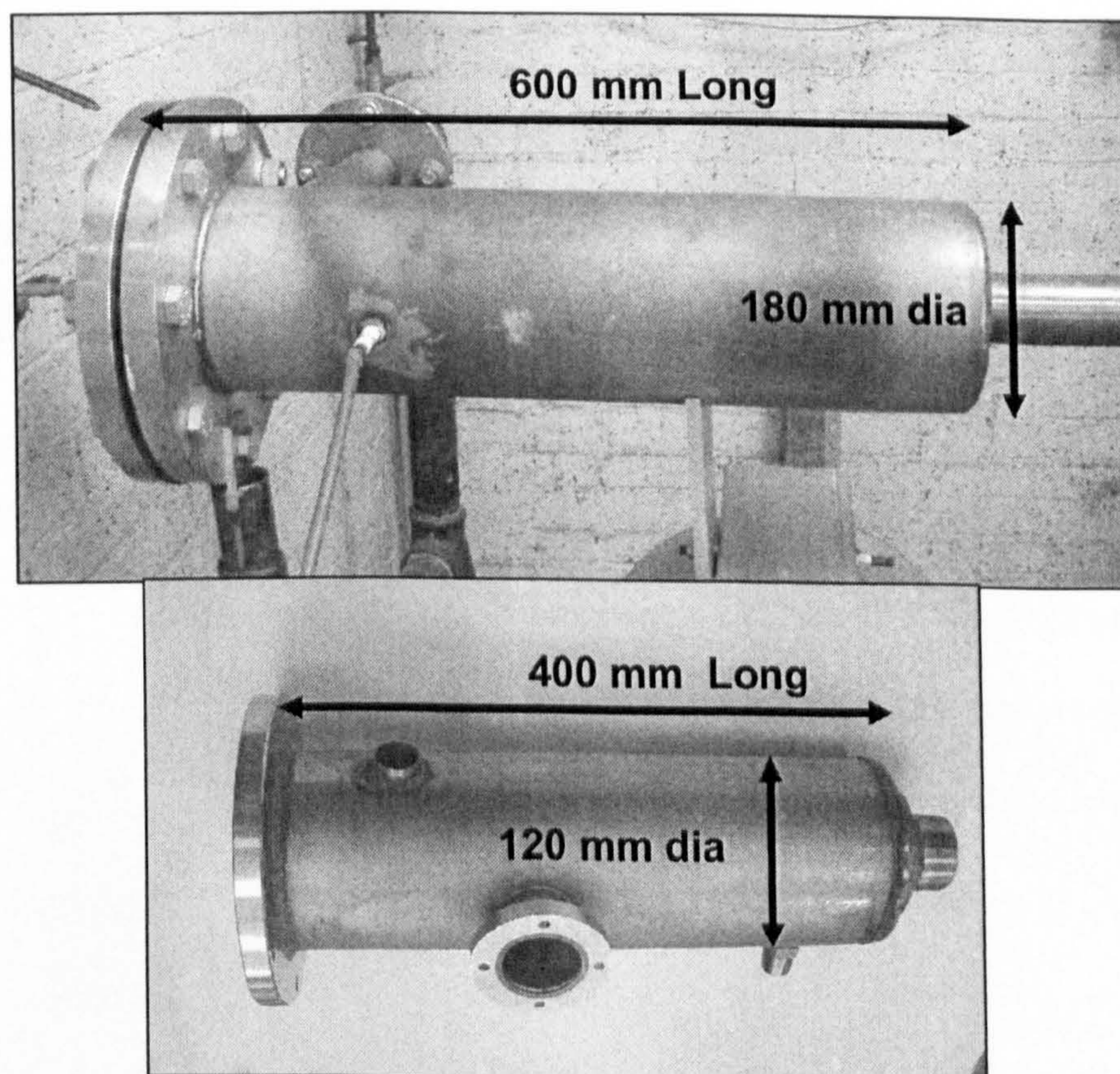


### Fig 4.11 Physical Comparison of Combustion Chambers

The position in the test rig of the combustors is shown in Fig 4.12 which also shows the new air pipe work arrangement.

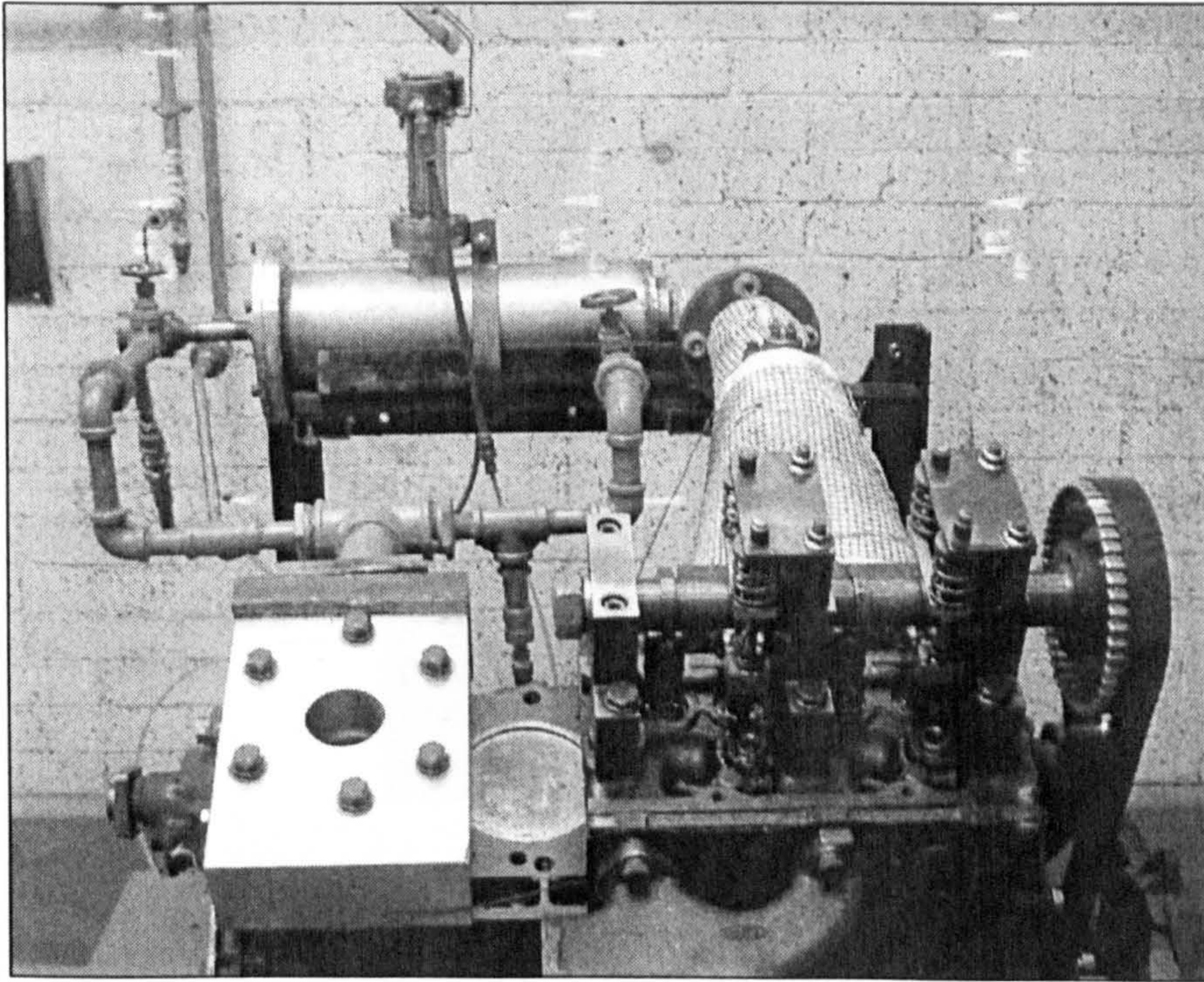


Fig 4.12 Comparison of Combustors in Engine test Rig

The lessons learnt from the first combustion chamber were built into the new design. New mixing tubes/nozzles, inner combustion tube, sight glass and spark plug holder were designed and manufactured. These are shown at Fig. 4.13

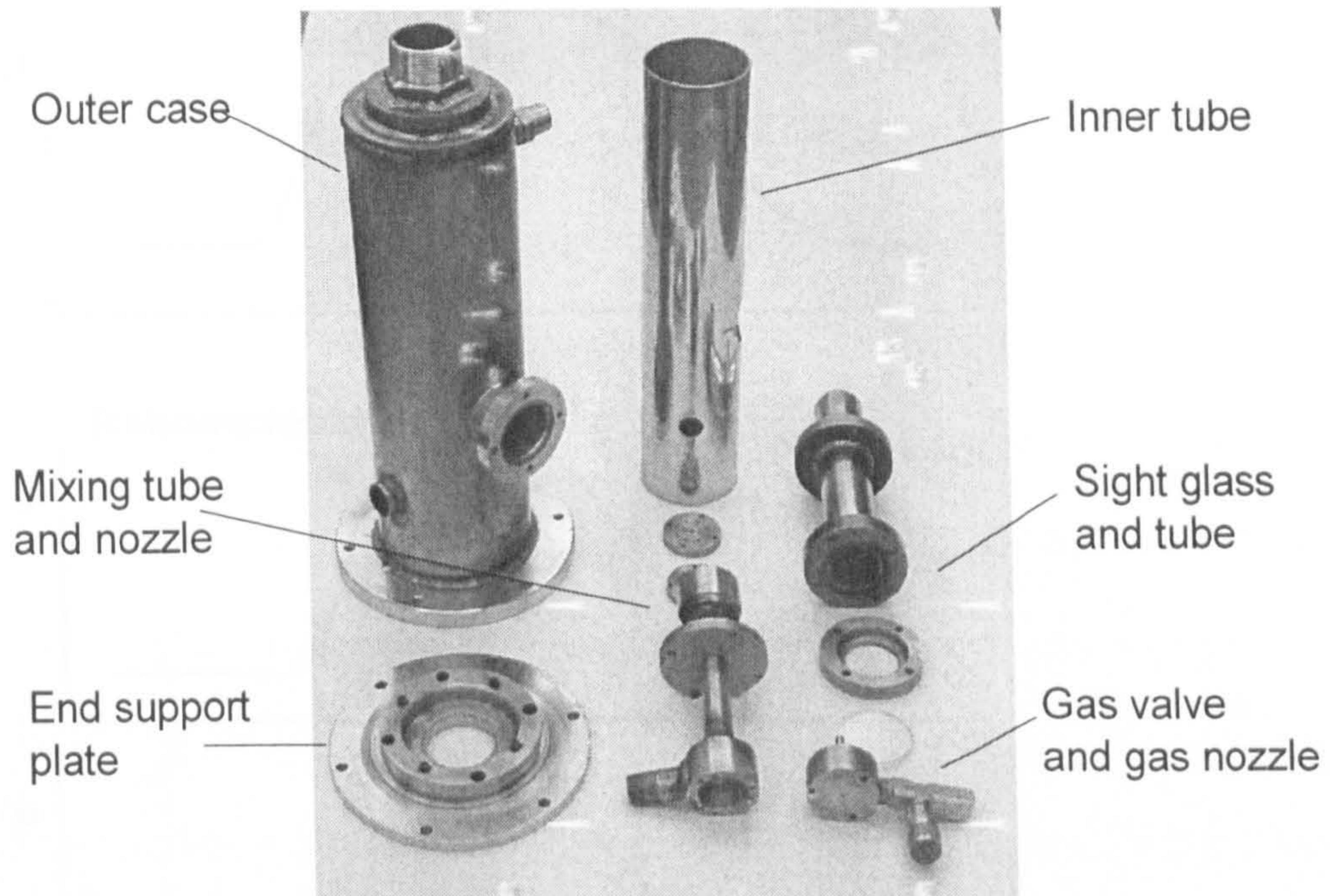


Fig 4.13 New Combustion Chamber and Internal Fittings

Valve timing had a direct influence on system pressure. A pressure transducer was purchased and fitted to the engine through the original injector mounting holes such that cylinder pressure could be measured. The transducer was only suitable for low temperatures so the engine was motored on compressed air only. If the timing was set for the inlet to open at TDC Fig 4.14—a. a pressure drop occurred during the initial valve opening. When the valve was sufficiently opened, allowing higher gas flows, the cylinder pressure rose to match the supply pressure. If the timing was advanced Fig 4.14—b then the initial pressure drop could be reduced and further advances resulted in the ideal Fig 4.14—c. Running the engine with combustion, with the valve timing set to the ideal position (10 deg BTDC) gave self sustained operation with clean combustion

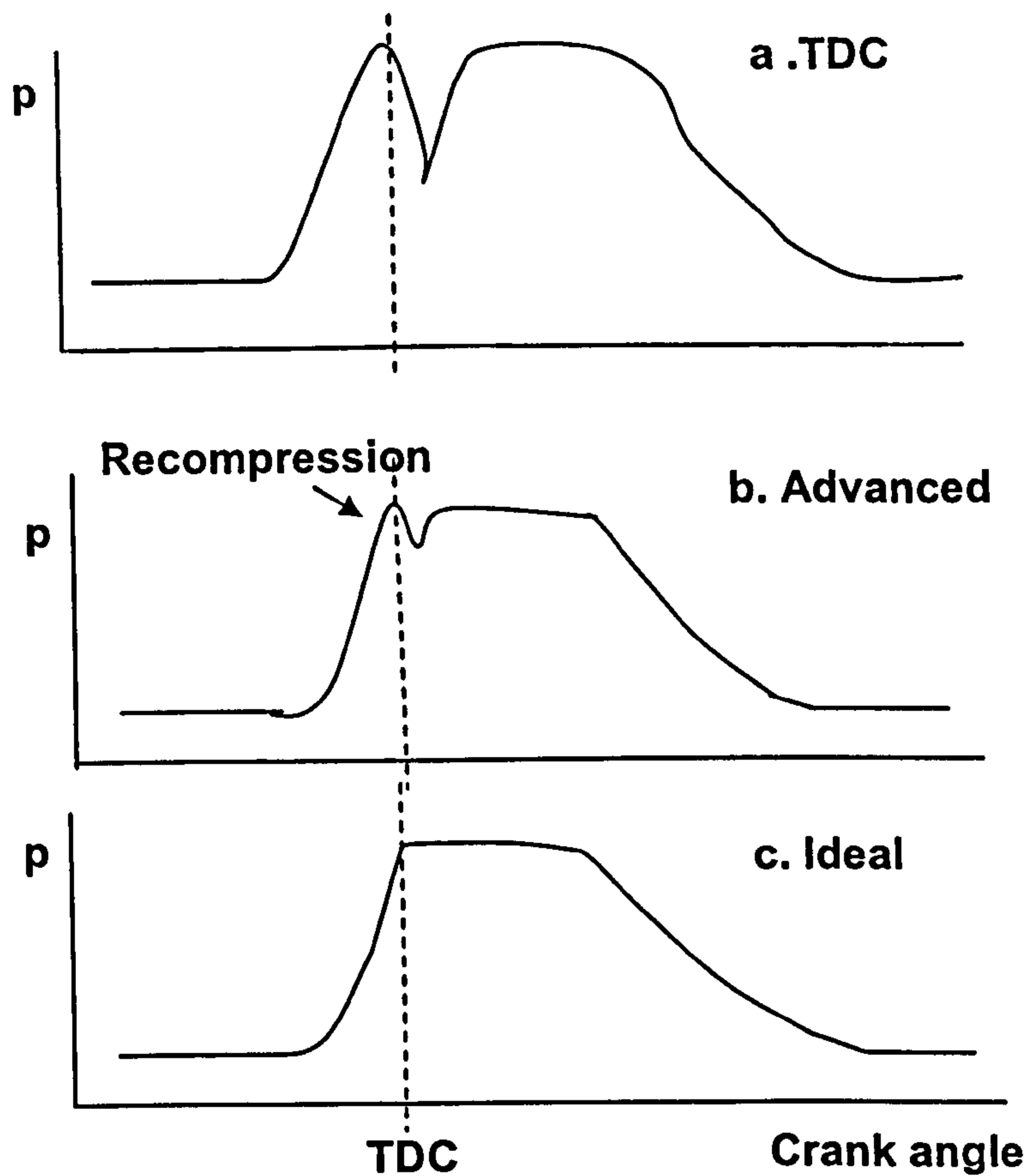


Fig 4.14 Valve Timing

The new combustor and accurate valve timing resulted in self sustained operation with expander gas inlet temperatures of 780 C. Modification to the secondary air supply by enlarging the holes in the combustor inner tube further improved the combustion resulting in a gas inlet temperature of 820 C.

All these operations were conducted with inlet valve cams of 100 degree opening and a measured system pressure of 2.8 bar. Operation of the engine at increased pressure would theoretically result in higher thermal efficiency so the inlet valve cams were changed to those with an 80 degree opening and 6 mm lift which gave a measured system pressure of 4 bar. Some improvement to engine operation at

self sustained conditions was achieved with a gas inlet temperature of 870 and an engine RPM of 850.

This appeared to be a limitation as it was not possible to increase the engine RPM. by increasing the gas supply.

#### 4.1.9 Fifth Iteration on Engine Development

The objective of the fifth iteration was to increase the engine RPM and develop a net power output. The existing system had a swept volume ratio of 2:1 and from the theoretical model improved thermal efficiency would be achieved with a swept volume ratio of 2.5:1. The rationale is that with the reduced compressor swept volume the mass flow is reduced and hence the work absorbed will be less. This results in an increase of net work output which will be realised by a higher engine RPM. To alter the swept volume ratio required major modifications to the compressor in that a smaller diameter piston had to be employed. The modifications undertaken included

1. The manufacture of a sleeved liner to fit in the existing bore. This had to be machined from solid and then honed on the internal diameter.
2. The use of a piston from a Ford 1.8 diesel engine
3. Modifications on the piston to fit a manufactured flat crown such that the top of the crown was at the top of the bore at TDC. In addition the size of the new piston crown manufactured from steel was such as to be the same mass as the original piston connecting rod assembly.
4. Modifications to the new piston gudgeon pin to fit the connecting rod from the 2.5 litre engine
5. Machining of the original connecting rod end to fit into the new piston.

Operation of the engine resulted in slightly poorer performance. Observation of combustion conditions showed an orange flame indicating that the compressor now supplied insufficient air. The engine would only self sustain with an increased gas supply where it significantly added to the total mass flow. Replacing the 80 degree inlet valves to those with 70 degrees and a 4 mm lift to limit the amount of gas used by the expanders and reducing all leakages in the system to a minimum resulted in only a marginal improvement in combustion conditions. It was determined at this stage that further engine development would not improve performance because of the work required to overcome friction. The theoretical model had shown that the performance of the engine was significantly degraded by low mechanical efficiency.

### 4.1.10 Sixth Iteration on Engine Development

The objective of the sixth iteration was to determine the power needed to overcome friction in the engine. To estimate the power absorbed by the engine due to friction the total energy of the compressed air needed to motor the engine was determined. It was recognised that this would only give an estimate of frictional power. The method employed to measure total energy supplied is diagrammatically shown in Fig 4.15.



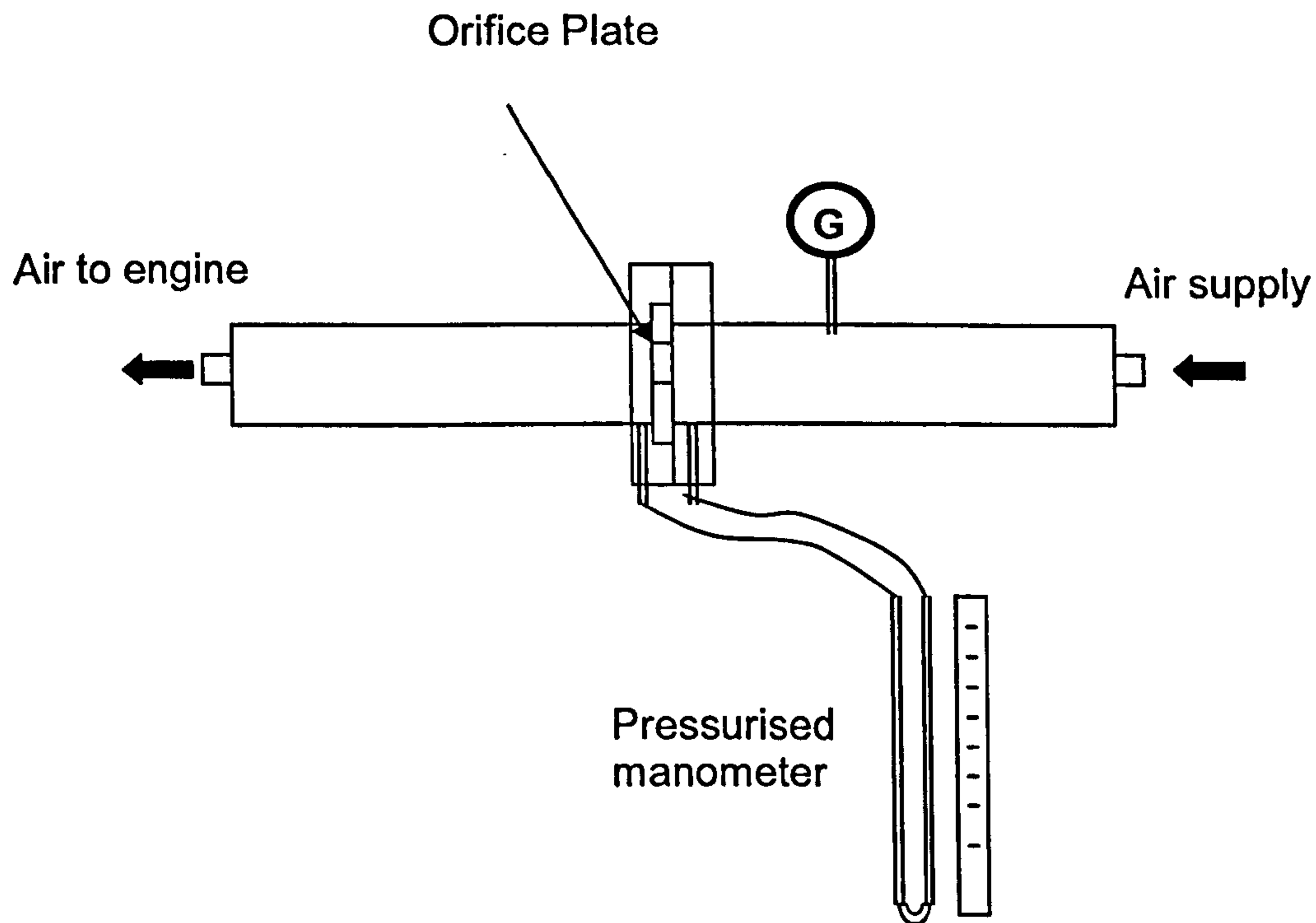


Fig 4.15 Air Volume Measuring Equipment

In addition the compressor cylinder head was removed to ensure that the external compressed air work input only overcame the frictional resistance of the engine. The engine was motored at varying inlet pressures and speeds and the work supplied was calculated from the volume flow and the supply pressure. The work required was also determined from empirical formulae at Ref 9. The results and extrapolation are shown at Fig 4.16

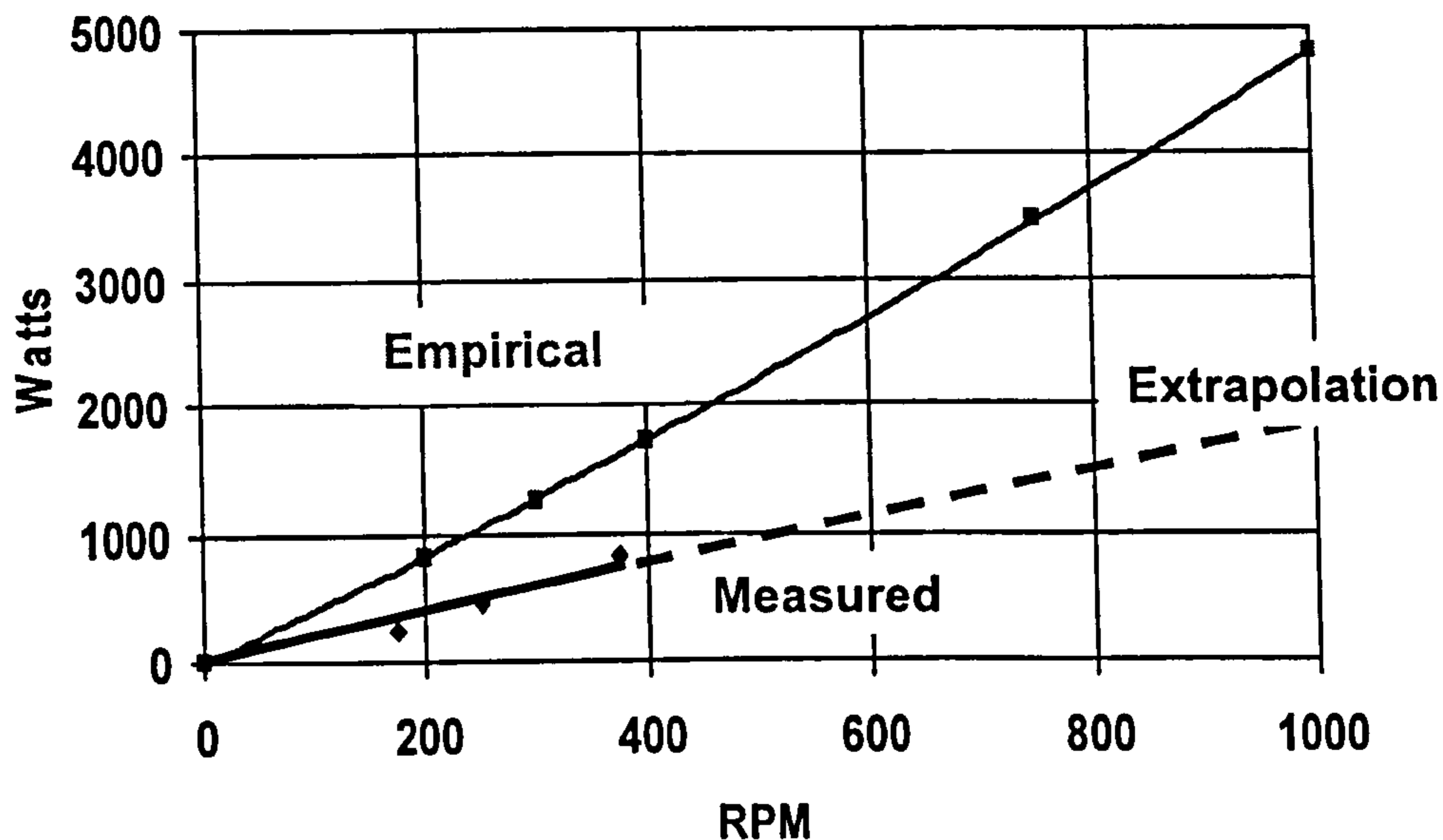


Fig 4.16 Cold Friction Characteristics of Technology Demonstration Engine

The overall assessment was that at 600 RPM the engine, when cold, absorbed 1.2 kW. Using an overall mechanical efficiency of 0.5 for both the compressor and expanders in the basic theoretical model the engine net work output was almost zero. With the overall mechanical efficiency then taken as 100% the model predicted a net power output of ~0.75 kW. Differences between the measured and calculated values of friction can be partially explained by the fact that:

- Friction loading was measuring at cold conditions whereas self sustaining conditions were only achieved with the engine hot
- The method used to determine the friction characteristics and the extrapolation of the results will only give an estimate.

This gave a partial explanation why the technology demonstration engine would only self sustain and not produce net positive work. However the values of friction obtained do give a good indication of the relatively large amount of work needed to overcome friction in a RJC engine. No further development activities were

undertaken on the engine as it was considered little would be gained and all future work would be directed at designing a full prototype engine.

#### 4.1.11 Overview of the Development Iterations

Table 4.2 at Annex 4 gives an overview of the development activities and the timescale

### **4.2 Conclusions from the Development of the Technology Demonstration Engine.**

#### 4.2.1 Combustion

Achieving stable ignition and clean stable combustion under pulsating pressurised conditions and at relatively low air flow rates represented the biggest challenge and approximately 70% of the overall development activity. No published data applicable for the design conditions was found so the development process had to proceed by trial and modification but based broadly on known technology e.g. gas turbine combustors and industrial burners. The most significant development was the use of an enclosed mixing tube in which the gas and some of the compressor discharge air were mixed to stoichiometric conditions. Stable ignition was achieved by taking a small amount of this mixture via a small pilot hole in the nozzle plate and directing it at the spark plug gap.

Nozzle plate design was based on achieving a sufficient mixture velocity via the multiple holes to provide a stable flame velocity. Various combinations of the number and diameter of the nozzle holes were tried and for a mixing tube bore of 15 mm the best results were found with 9 holes of 2 mm diameter. This

combination gave the highest expander gas inlet temperature at the completion of the fourth iteration.

Table 4.2 shows the development of nozzle plate design and the expander inlet temperatures achieved.

Hole size mm	No of holes	Total area mm <sup>2</sup>	Ratio of total nozzle area to mixing tube cross sectional area (15mm dia)	Max Expander inlet temperature deg C
4	24	301.5	1.7 :1	650
2.5	12	58.8	1:3	750
2.5	9	44.2	1:4	780
2	9	28.26	1:6.26	870

Table 4.2 Nozzle Plate Development.

Secondary air supply was via the holes in the combustor inner tube and to some extent by leakages around the spark plug holder and the sight glass tube both of which penetrated the inner tube into the combustion zone. The leakage area was fixed by the design and manufacture but by trial and error the size and number of secondary air holes in the inner tube were progressively increased such that at the end of the fourth development iteration there were eight holes of 3 mm dia. The position of the holes was such to provide a flow of air over the outside of the inner tube and thus some insulation between the combustion zone and the outer combustor walls. Further development of the combustor for higher flow rates of gas and air could not be undertaken because under self sustaining conditions the engine speed could not be increased above 850 RPM

The basic design of the combustor had proved to be acceptable but further refinements in geometry would need to be undertaken requiring the design of a purpose built combustor

#### 4.2.2 Valves and Valve Gear

The existing valve gear was retained but new seat inserts were manufactured for the back seating inlet poppet valves. The original seats were manufactured from a heat resistant stainless steel and could not be ground in by conventional means to provide adequate sealing. The new seats were manufactured from mild steel and ground in to give good sealing. Although not an ideal material for long term use they proved adequate for the period of development and testing of the engine.

Most of the work on the valve actuating mechanism involved testing of different cam profiles and cam lift. Profiles on the direct acting exhaust valves cams were made 'softer' after initial problems of valve stem bending and guide breakages. The final design was for cams of 175 deg and 6 mm lift and these proved adequate. Five different inlet cam profiles were tested with the best engine performance being achieved with an inlet profile of 80 deg and 6 mm lift.

An engine speed limit was set on the inlet valve actuating mechanism of 1000 RPM as it was felt that component failure was likely to occur at higher speeds.

The lesson learnt from this design is that a different valve actuating design concept will have to be used for future engines and that can:

1. Operate at speeds up to 3000 rpm
2. Operate at temperatures of up to 900C for extended periods
3. Have low height
4. Have low friction characteristics

### 4.2.3 Compressor

The use of an automotive engine block with one cylinder adapted to act as a reciprocating compressor was a logical starting point. A new compressor head was designed and manufactured incorporating reed valves. Whilst this gave an improvement in volumetric efficiency, and was one factor in achieving self sustained operation, it is recognised that the power required by the compressor, both for air delivery and in overcoming friction was high.

Modifications to the compressor cylinder to give a swept volume ratio of 2.5:1 from the original 2:1 resulted in poorer engine performance in that self sustained operation could only be achieved with a rich mixture. This degraded performance is due to reduced mass flow with insufficient air being supplied to allow complete and efficient combustion. The conclusions drawn from this is that even though the theoretical model shows that a physical swept volume ratio of 2.5:1 should give a higher overall thermal efficiency in reality the volumetric efficiency of the compressor at 80% results in insufficient air being supplied for combustion.

In the next stage of the project the problem of improving compressor performance has to be addressed. This would need to be a balance between the total power absorbed by the compressor, the mass flow and volumetric efficiency. As such all types of positive displacement compressors for the compression of air for the RJC engine needed to be examined.

### 4.2.4 Expander Pistons

With expander inlet temperatures of 870 C there was some concern that the existing aluminium pistons from the original engine block would suffer damage and or distortion. Examination of the pistons at the end of development testing showed

them to be in good condition. It was concluded that for a prototype engine aluminium pistons would be adequate as long as they were provided with cooling from the lubricating oil.

### 4.2.5 Leakages and Pressure losses

Internal and external leakages were always present especially on the inlet valve arrangement. Such accumulated leakages from all sources could impair the performance of the engine and it was only possible to reduce this overall leakage to an estimated 5% of the compressor delivery. The major leakage was from inlet valve guides and in the latter stages of the development programme a pressurised oil seal arrangement was designed and tested.

One pressure loss was measured, this being the difference in pressure from compressor discharge to that measured in the combustion chamber. The value was 0.2 bar which was considered acceptable for this stage of the project. Future designs would aim to reduce this value.

### 4.2.5 Overall Conclusions on the Development of the Technology Demonstration Engine.

The major conclusion from the development is that an RJC engine can be made to work but that any future design must concentrate on reducing friction.

The objectives of the project to date in both the deliverables and timescale were met in that:

1. The main achievement through progressive development iterations was the self-sustained operation of the 'technology demonstration engine'

2. Component development, where proven successful, to be carried through to the design and development of the prototype engine and in particular the combustion chamber.

#### **4.3 Development Programme and Funding**

An application for funding was made to the Carbon Trust in September 2003 which required details of the proposed development programme and costings for each activity of development. This application reached the last 25% of submissions but failed to make final selection indicating that the concept of the RJC engine for micro CHP applications had technical merit and was potentially commercially viable. The total funding requested was £120,000.

An alternative low cost programme was developed which aimed to build a pre-prototype engine using components from a small horizontally opposed piston engine with other components manufactured in house. This low cost approach reduced the scope of the originally proposed project in that the development of an engine rather than the development of a micro CHP system would be undertaken.



## **4.4 Design, Development and Testing of a RJC Prototype Engine for Micro CHP Applications**

Lessons learnt from the development of the technology demonstration engine confirmed the conclusions from Ref. 7 that low friction engine was necessary requirement. The ideal engine should have the following basic design requirements:

- Nominal output of 3 kWe at ~35% thermal efficiency for the RJC engine.
- 3000 rpm max with minimal noise and vibration
- Minimal size and weight – footprint the same as a domestic boiler (600 mm x 600 mm)
- Reliable and durable.

The value of 3 kWe was chosen as it represented a target to be achieved in that it was high enough to provide most of the needs of a domestic dwelling during peak requirements and at least equal to the best claimed by alternative technologies.

### **4.4.1 Use of Existing Components**

Cost, time and resources prevented design and manufacture of some key components from scratch. In particular conventional automotive engine pistons would be employed with some modifications undertaken, and where possible other readily available automotive components would be used.

For the first prototype design the combustion chamber from the technology demonstration engine would be used.

#### 4.4.2 Compressor Design / Selection

A review was undertaken on all types of positive displacement compressors used for the compression of air with a discharge capability of > 4 bar. The range included:

1. Reciprocating piston
2. Screw – oil lubricated
3. Vane – oil lubricated
4. Scroll

An assessment was made of each type of compressor based on

1. Volume delivered / Power consumed
2. Noise and vibration
3. Size / weight / volume
4. Ancillary requirements – additional volume
5. Initial Cost and Maintenance Cost

Fig 4.17 shows a comparison of the performance of commercially available compressors. The comparison looks at the volume delivered / power consumed for varying discharge pressures.

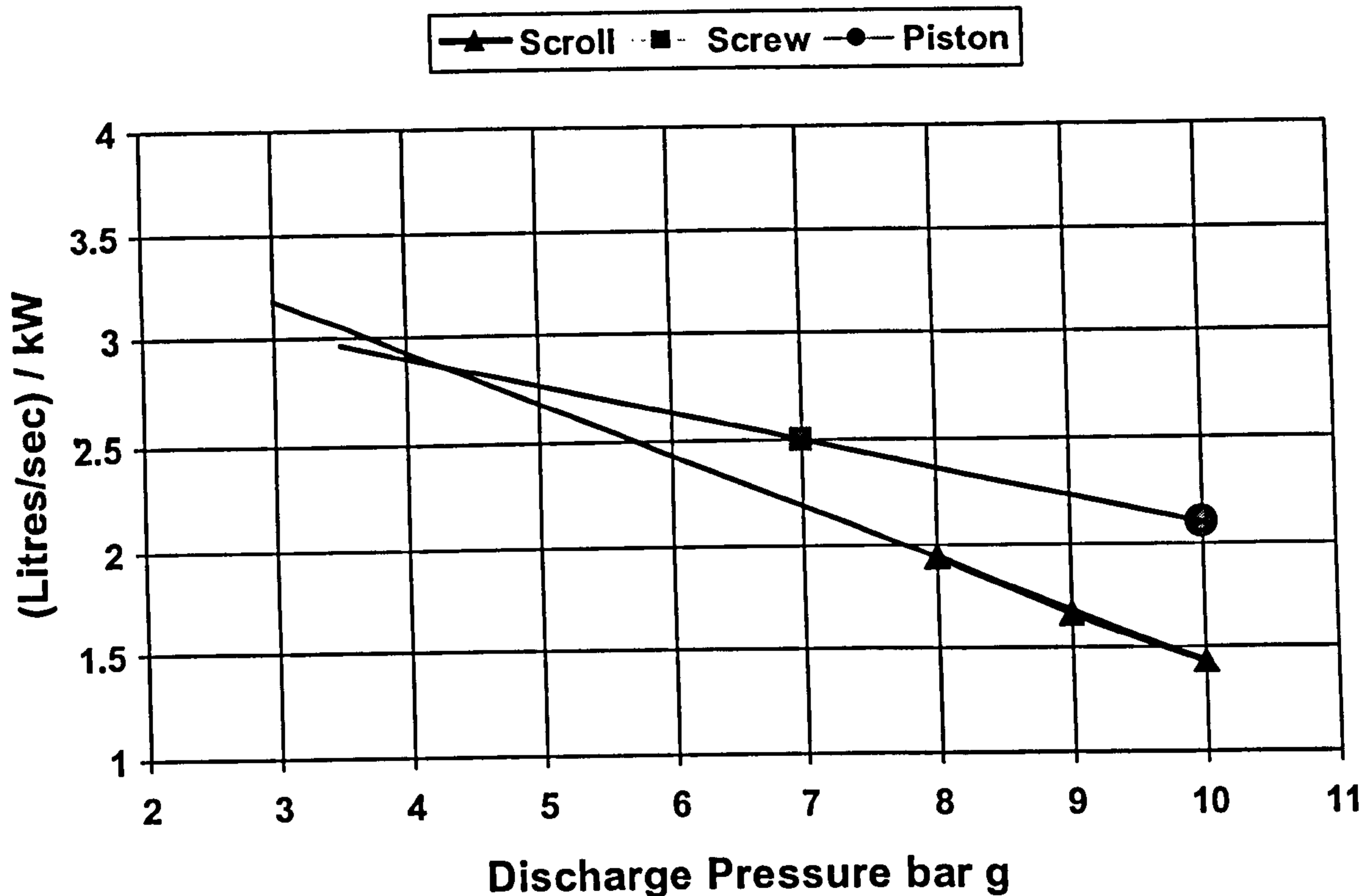


Fig 4.17 Performance of Positive Displacement Compressors.

This comparison shows that at discharge pressure below 5 bar the scroll compressor has a performance equivalent to that of the screw or piston type.

In addition the scroll compressor has the advantage of being low noise, < 60 dB(A), low vibration, long periods between maintenance and low overall size and volume. Such compressors are now the compressor of choice in small scale air conditioning systems and railroad brake systems.

#### 4.4.3 Prototype Engine Design.

A review of the detail design requirements from Part 4.4 was undertaken but with the constraints of designing and building a RJC engine within a limited time scale and budget. Whilst the use of hypocycloidal drives and rotary valves were considered (described in Part 5) these would require extensive development. A compromise was to employ an existing internal combustion engine of compact

design and modify it to a RJC engine and use poppet valves. The engine selected was an air cooled BMW R650 motor bike engine which had opposed horizontal pistons with a stroke of 61.5 mm and a bore of 82 mm.

#### 4.4.6 Engine Modifications

The following major engine modifications were identified

1. New cylinder heads
2. New cam boxes and valve actuating gear
3. New oil supplies and oil returns to the cam boxes
4. New flywheel and drive shaft to be mounted on the original clutch drive ring for RH head cam box drive
5. New drive shaft to fit the existing taper shaft for power output to the dynamometer and to drive the LH cam box
6. Engine stand to fit to the dynamometer bed plate
7. Cam box toothed drive belt tensioners.
8. Retain the existing pistons. With this configuration the clearance volume was determined by calculation and liquid measurement at 100 cc. Although this was much higher than ideal it was considered acceptable but its impact would be determined by engine trials

#### 4.4.5 Valve and Cam Box Design and Construction.

Several problems were encountered with the valve actuating mechanism on the technology demonstrator design, the most serious being valve stem side forces. To overcome these problems it was decided to employ a design incorporating rocker arms.

Additionally there were concerns that slippage of the cam belt drive pulley could occur with the valves then making contact with the cylinder head so a side valve design was adopted. This concept gave the following advantages:

1. Positive action of valves, and reduced side forces on valve stems.
2. No possibility of valves hitting the piston due to cam belt slippage
3. Compact and Minimum size width to fit within a 600 mm width envelope
4. Cam box under cylinder barrel to give compactness.
5. Belt driven from crankshaft at both ends of the engine that allowed valve timing of each cylinder

### 4.4.6 Compressor

A separate compressor was to be utilised driven from the engine output shaft via a 'V' belt. Such a configuration allowed for the compressor RPM to be altered by changing the pulley drive ratio.

### 4.4.7 Engine /System Design. Cam box Design and Settings.

The Engine was mounted on a fabricated stand to align with an eddy current dynamometer on a common bedplate. Each cylinder had a separate head and cam box with separate oil supplies. Drawings and photographs of major components are at Annex 4. All major components were fabricated and machined at the University the vast majority by the author. The design and build programme took 9 months.

The Cam box consisted of a fabricated aluminium housing containing two camshafts mounted in rolling element bearings and a common rocker shaft mounted in oilite bushes One camshaft is driven via a belt drive from the crankshaft and the other camshaft gear driven from the drive camshaft. This

allowed the timing of the exhaust and inlet cams to be adjusted independently to find the best setting. The exhaust cam angle was set at 140 degrees and inlet at 70 degrees. These openings were calculated to give a recompression to 5.2 bar g and expansion to a low pressure. The valves were operated by separate rocker arms with the inlet valve being pushed off its seat and the exhaust being pulled off its seat. This configuration meant that positive pressure together with the valve springs held the inlet valve on its seat. Valve lift for both inlet and exhaust was 7mm. Fig 4.18 shows the engine mounted on its stand viewed from the free end.

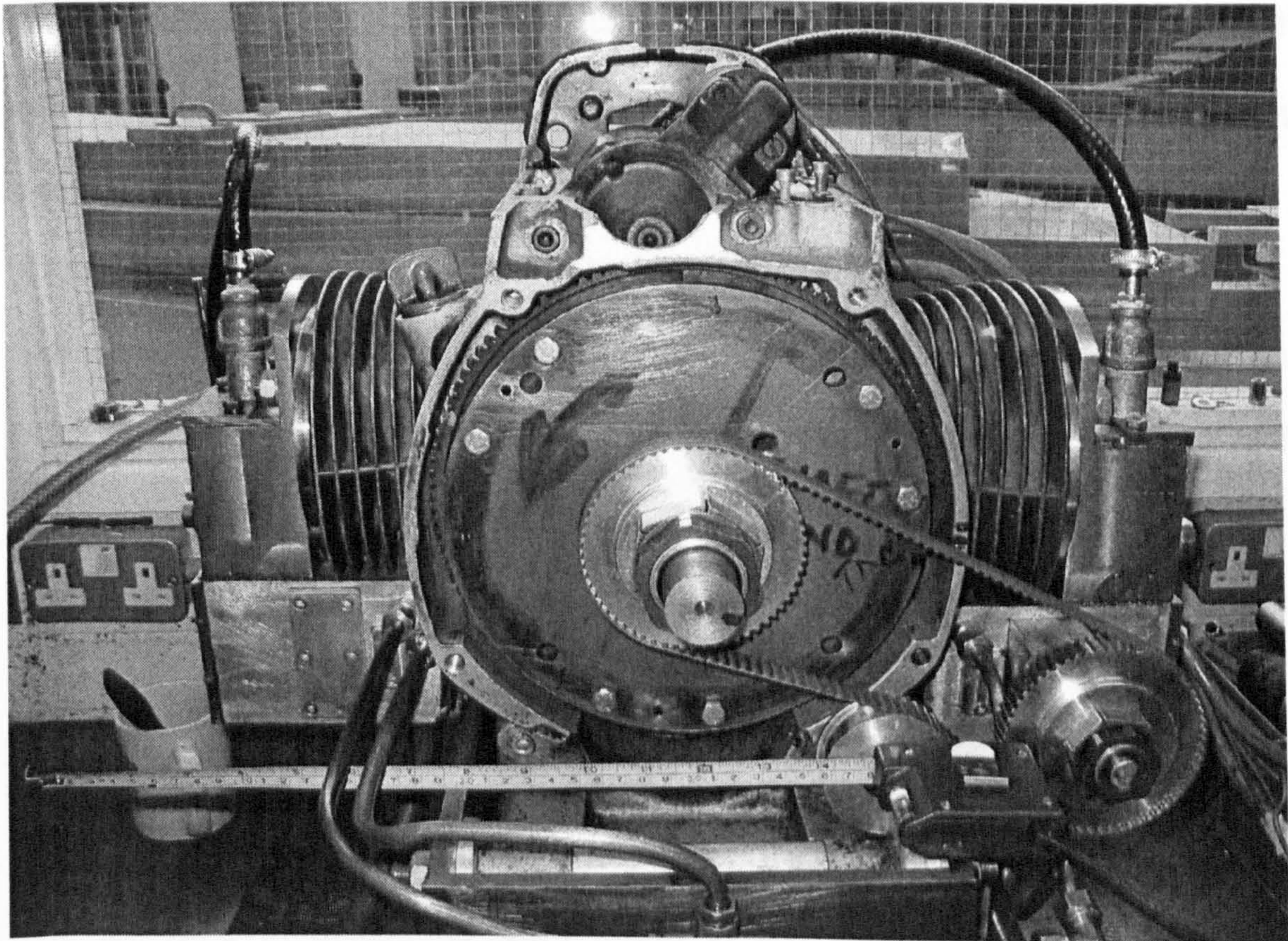


Fig 4.18 View of BMW Engine on Stand from Free End

#### 4.4.8 Valves Used and Valve Seat Material

The valves used in the technology demonstration engine (Ford 2.5 L DI engine) were again employed but with their sealing surface profile modified to a 45 degree angle. Valve seats were manufactured from grey cast iron for ease of grinding in.

#### 4.4.9 Measuring Instrumentation.

An existing dynamometer was connected to the engine using a drive shaft that incorporated two universal joints. The dynamometer was a Schenck FA 100 eddy current dynamometer Series 2000C by which torque could be applied and measured along with engine speed. It was recalibrated for the ranges of 0-50 Nm and 0-2000 RPM

The thermocouple from the technology demonstrator was utilised to measure gas temperatures up to 1000C

A small analogue piezo-resistive silicon diaphragm pressure transducer was fitted into the left hand head but was only suitable for air motoring operation not hot gas (i.e.>600C) operation.

The same orifice plate/U tube manometer was used to measure inlet air flows.

Standard 50 mm 0-10 bar pressure gauges were fitted to the combustion chamber (with extended pipe work to isolate from the high temperatures) and to the air flow measuring orifice pipe work.

Visual indication of flame colour in combustion chamber could be observed via the sight tube.

#### 4.4.10 Combustor Modifications

The following modifications were made to the combustion chamber from that employed on the first test engine:

1. New hot gas discharge flange
2. New gas and air mixing tube and combustion plate
3. New internal combustion tube

4. New hot gas discharge pipe work to the cylinders fabricated from stainless steel.

Modifications were also undertaken to improve flame stability. This took the form of evaluating different nozzle plates in free air using compressed air and compressed gas in the mixing tube. It was found that reducing the gas velocity at the nozzle plate improved stability over a range of compressed gas and air supplies. The nozzle plate that gave the best performance comprised of a perforated plate of 45 mm effective diameter with 1.5 mm holes pitched at 2.5 mm centres. With a gas air mixing tube internal diameter of 15 mm then the area of the nozzle plate hole area was 255% larger. The design of the combustion chamber and photographs of the improved nozzle plate are at Annex 4

#### 4.4.11 Compressor Type

It was initially estimated that the engine would operate at a 5 bar g system pressure because the modelling at Ref 3 indicated that this would give an adequate thermal efficiency without the requirement of high pressure components and was within the known performance of the combustion chamber. Two types of positive displacement compressors were considered these being a reciprocating compressor and a scroll compressor. The scroll compressor was chosen because:

1. Constant and non cyclic air delivery for a given speed
2. At 5 bar discharge pressure it had a similar power requirement to a reciprocating compressor for the same air delivery. Part1. Fig 4.17
3. Low friction and low noise needed for micro CHP in a domestic application.



The scroll compressor chosen was an Atlas Copco type ATSL -165C rated at 6.8 litres/sec FAD at 3150 RPM and 8 bar discharge pressure absorbing 3.7 kW. In addition the discharge air was oil free.

#### 4.4.12 Scroll Compressor Performance.

A separate test rig was designed and built to assess the performance over various speeds and discharge pressures. Measurements of torque, speed, inlet air flow, discharge pressures and discharge temperatures were taken and mapped. The table of outputs is at Table 4.3 and graphical representation is at Annex 4

Drive RPM	Comp RPM	Pressure	Torque	Man mm H2O	Dis Temp deg C	Power kW	FAD l/s ave.
1920	3135	6.67	18.2	60	152	3.66	6.9
		5.69	16.5	60	142	3.32	
		4.7	15.1	60	130	3.04	
		3.72	13.5	60.5	102	2.71	
		2.94	12	60.5	96	2.41	
1670	2727	6.67	17.8	44	140	3.11	5.94
		5.69	16.2	44	135	2.83	
		4.7	14.6	44.1	122	2.55	
		3.72	13	44.6	106	2.73	
		2.94	11.2	44.8	92	1.96	
1530	2500	6.67	18	35.5	138	2.88	5.37
		5.69	16.3	36	130	2.61	
		4.7	14.4	36.2	120	2.31	
		3.72	12.6	36.6	105	2.02	
		2.94	11	37	90	1.76	
1380	2253	6.67	18	30	122	2.6	4.87
		5.69	16	30	120	2.31	
		4.7	14.1	30	115	2.04	
		3.72	12.3	30	106	1.78	
		2.94	10.6	30	90	1.53	
1230	2009	6.67	18.5	23	115	2.38	4.27
		5.69	15.9	23	112	2.05	
		4.7	14.1	23	110	1.82	
		3.72	12.1	23	103	1.56	
		2.94	10.2	23	83	1.31	

Table 4.3 Scroll Compressor Characteristics

The RJC engine arrangement allowed for the compressor to be V belt driven from the engine crankshaft at the dynamometer end with the ability to change the drive ratio by the use of different diameter drive pulleys. This gave a fixed mass flow rate for a given speed requiring exact matching to the expander mass flow requirements at a given temperature. This matching would then be determined from the separate expander and compressor performance characteristics

### 4.4.13 Expander Performance

The engine was initially operated against the dynamometer on an external air supply without combustion and the compressor disconnected to determine the power/speed relationships. The first aspect noted was the high exhaust noise which indicated a high pressure at the end of the expansion.

The simple piezo pressure transducer was mounted to the cylinder head of one piston and connected to an oscilloscope to investigate the pressure characteristics during a cycle. It was observed that there was a delay between achieving maximum recompression and inlet valve opening. Adjustments to the timing from inlet opening at TDC to 10 deg BTDC reduced the time from full recompression to inlet valve opening and there was a marked improvement in the expander power output and a reduction in the amount of air consumed. This timing adjustment had no significant effect on the pressure in the cylinders at exhaust valve opening at BDC and the high exhaust noise was still present. Reproductions of the typical traces observed and the effect of altering the valve timing are show at Fig. 4.19

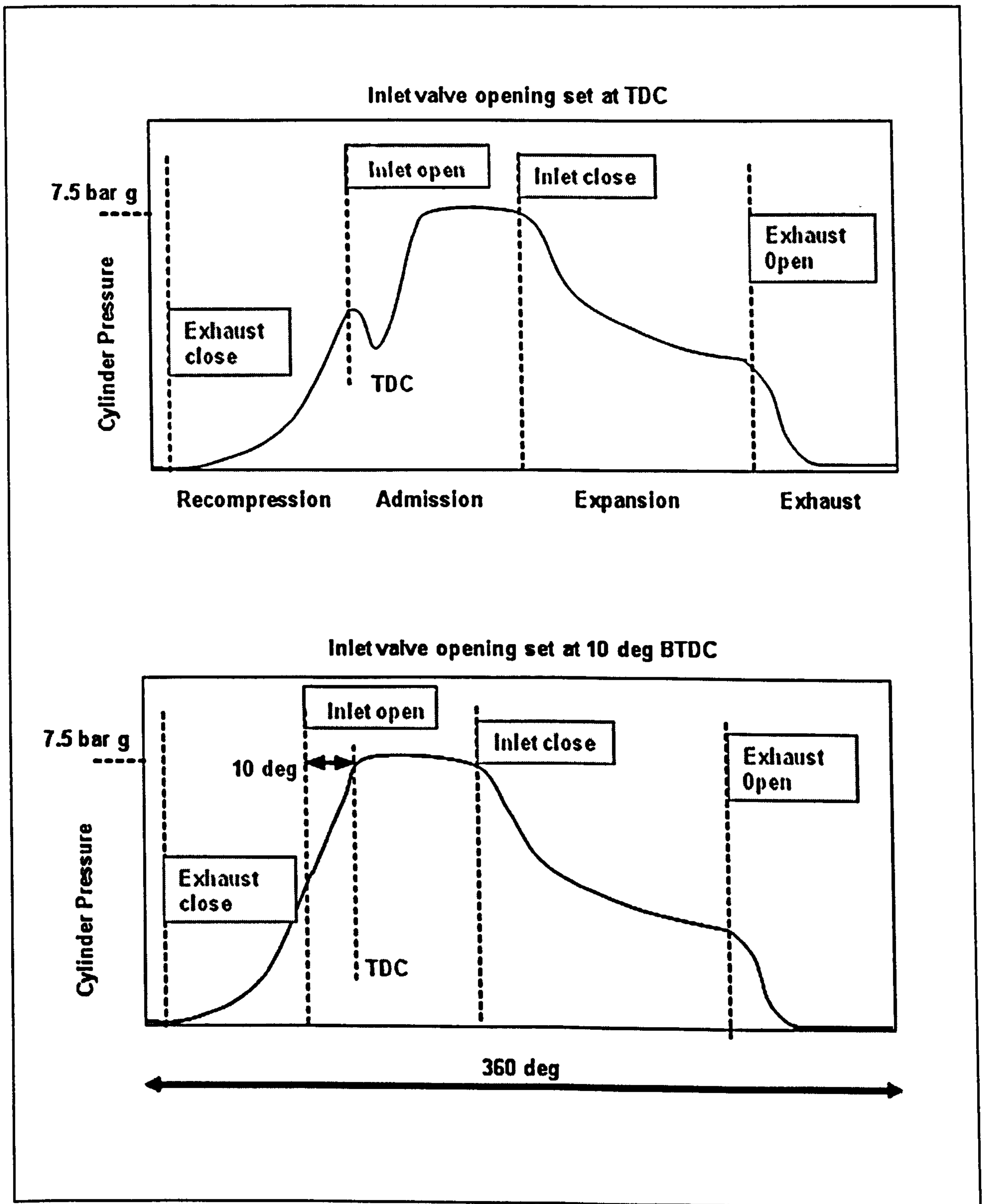


Fig 4.19 Effect of Inlet Valve Timing on Pressure vs. Crank Angle

The engine was run with combustion to determine the power speed characteristics. The objective was to attain stable combustion and operation with a gas inlet temperature to the cylinders of 850C. Again this was with an external air supply and with the compressor disconnected and 10 deg BTDC Fig 4.20 shows the output (inlet valve opening 10 deg BTDC) when operated with and without combustion.

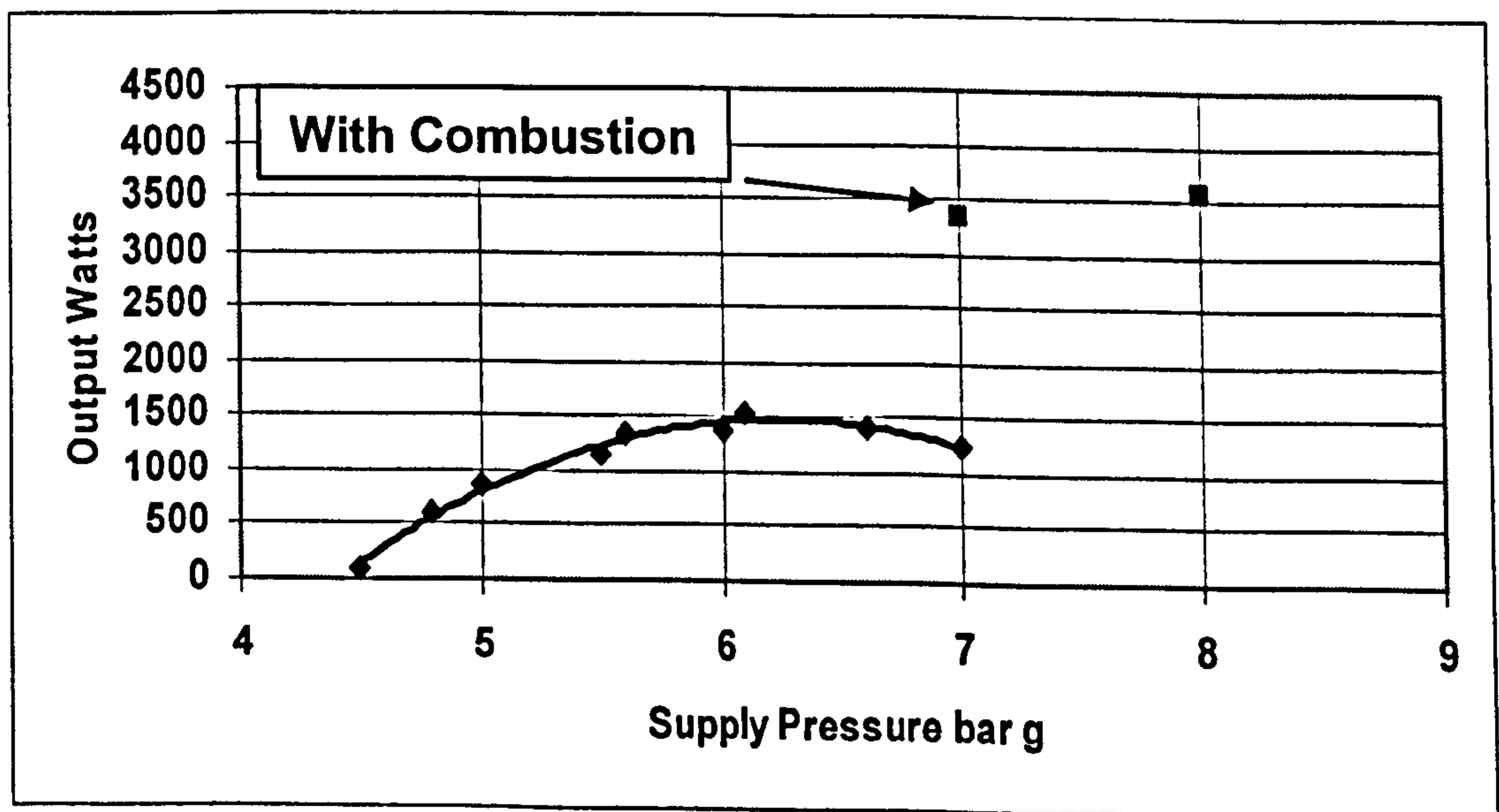
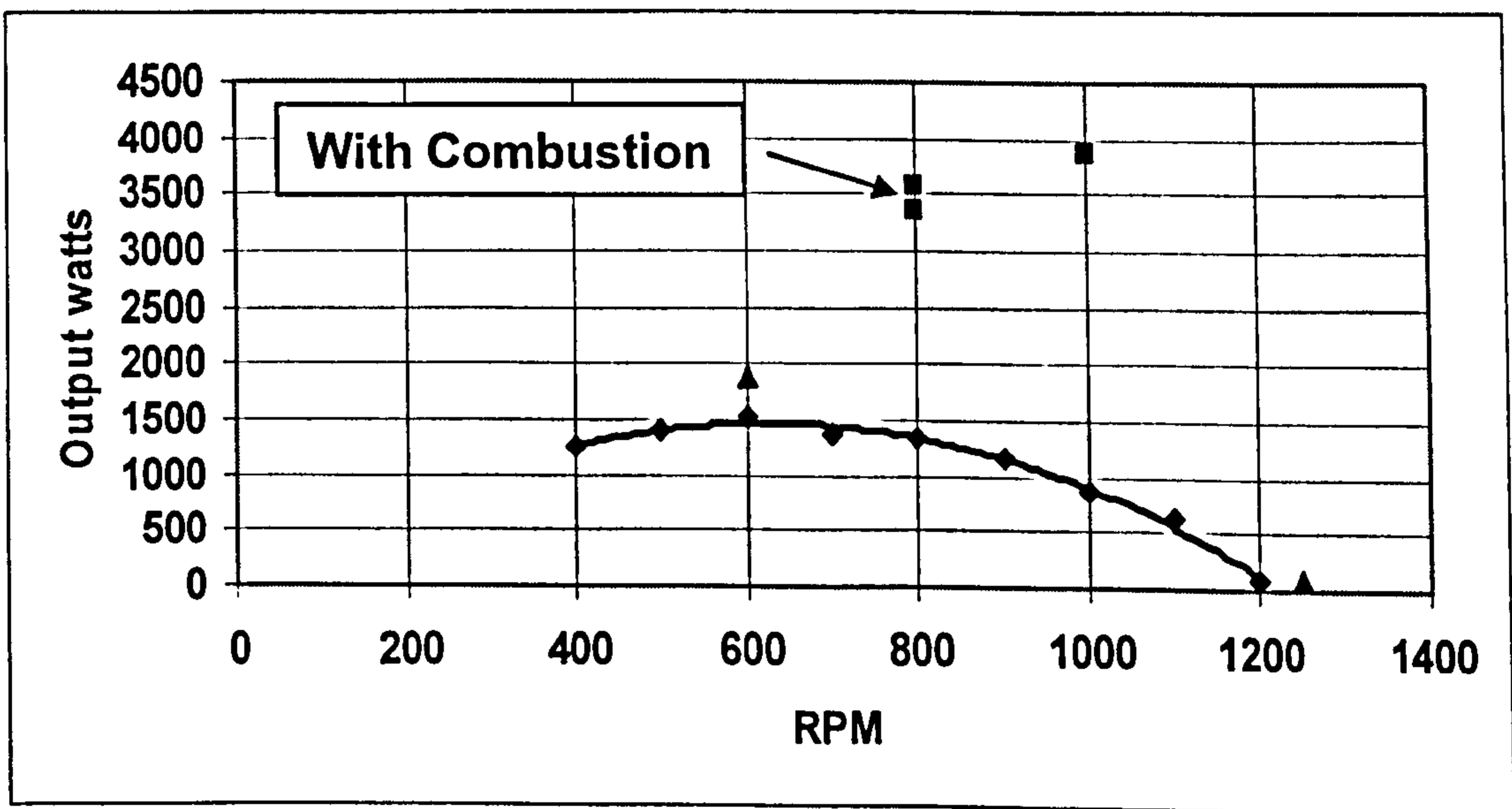


Fig 4.20 Expander Power output With and Without Combustion

The scroll compressor was then connected using a drive ratio of 2:1. The aim was to run the engine at 1000 RPM and at 6 bar supply pressure, with combustion, but the engine would not self sustain even at 900C gas inlet temperature. By examination of the compressor performance curves it was determined that the compressor could not deliver the required mass flow of air. The drive pulleys were changed to a drive ratio 2.2:1. to increase the mass flow, resulting in higher power requirement. Again the engine would not self sustain although less external air was required to maintain operation.

A review of the data was conducted including an examination of the pressure crank angle characteristics and the effect of altering the inlet valve timing. The following information was considered:

1. Recompression is to a low value and by calculation using an assumed value of  $n=1.3$  was to 4.5 bar g.
2. Exhaust valve opening occurred at 2 bar g
3. Flow rate through the poppet valves was low at initial and final valve opening resulting in a delay in pressure build up during admission.
4. The high clearance volume necessitated that additional air was required to compensate for the low recompression pressure. Also with a large clearance volume the total volume for expansion was thus increased and with a fixed volume for expansion resulted in a high exhaust pressure.

Using standard air equations, and noting that the scroll compressor will deliver 4.875 litres /sec FAD at 2250 RPM and 7 bar g, the air requirement for the two expander cylinders at an inlet temperature of 850C and 1000 RPM is 5.6 litres/s. even though the potential power output of the expanders at 3500 W is higher than

the compressor requirements of 2600 W. Hence there is no matching of the flows between the compressor and the expanders. Only by significantly increasing the inlet temperature or increasing the compressor speed (drive pulley ratio  $> 2:2.1$ ) would mass flow matching be achieved.

#### 4.4.14 Matching a Scroll Compressor to a Reciprocating Expander.

The mass flow from a scroll compressor is proportional to speed and for a set speed is constant irrespective of the discharge pressure.

The mass flow through a reciprocating expander is determined by the volume admitted (determined by inlet valve opening) system pressure (cylinder pressure when gas is admitted at TDC) RPM and temperature. For a fixed inlet pressure and fixed RPM then a reduced mass flow through the expander can only be achieved by increasing the temperature of the gas admitted or reducing the volume admitted

Matching calculations for six conditions were undertaken and these are outlined in Table 4.4

	Condition 1	Condition 2	Condition 3	Condition 4	Condition 5	Condition 6
Drive ratio	2.7:1	2.7:1	2.2:1	2.2:1	2.0:1	2.0:1
Expander RPM	1000	1000	1000	1000	1000	1000
Compressor RPM	2700	2700	2200	2200	2000	2000
Recompression to bar g	7	5	7	5	7	5
Hot Gas Flow Litres /sec	3	3	3	3	3	3
Compressor power requirements W	3112	2550	2610	2073	2380	1816
Compressor delivery kg /sec	0.0072	0.0072	0.0059	0.0059	0.0052	0.0052
Hot gas temp to achieve mass balance deg C	921	623	1184	790	1335	933
Expander output W	3140	1675	3140	1675	3140	1675
Net output W	28	--876	539	--398	760	--141

Table 4.4 Scroll Compressor /Expander Matching

For condition 1 at 7 bar, balance on mass flow and power output is achieved at a gas temperature of ~ 921C. For condition 2 at 5 bar the expander power output reduces by ~50% but scroll compressor power consumption only reduces by 18% then a mass balance can only be achieved at a lower temp (623 C) and a negative net power.

Altering the drive ratio from 2.7:1 to 2.2:1 and to achieve a mass balance at 7 bar g the gas temperature has to be increased to 1184 C with a net output of 529 Watts. Reducing the pressure to 5 bar g and a mass balance results in a gas temperature of 790 C but a negative net output of 398 Watts

Altering the drive ratio from 2.7:1 to 2.0:1 and to achieve a mass balance at 7 bar g the gas temperature has to be increased to 1335 C with a net output of 760 Watts. Reducing the pressure to 5 bar g and a mass balance results in a gas temperature of 733 C but a negative net output of -141 Watts.

Conditions 1-6 are shown graphically at Fig. 4.21

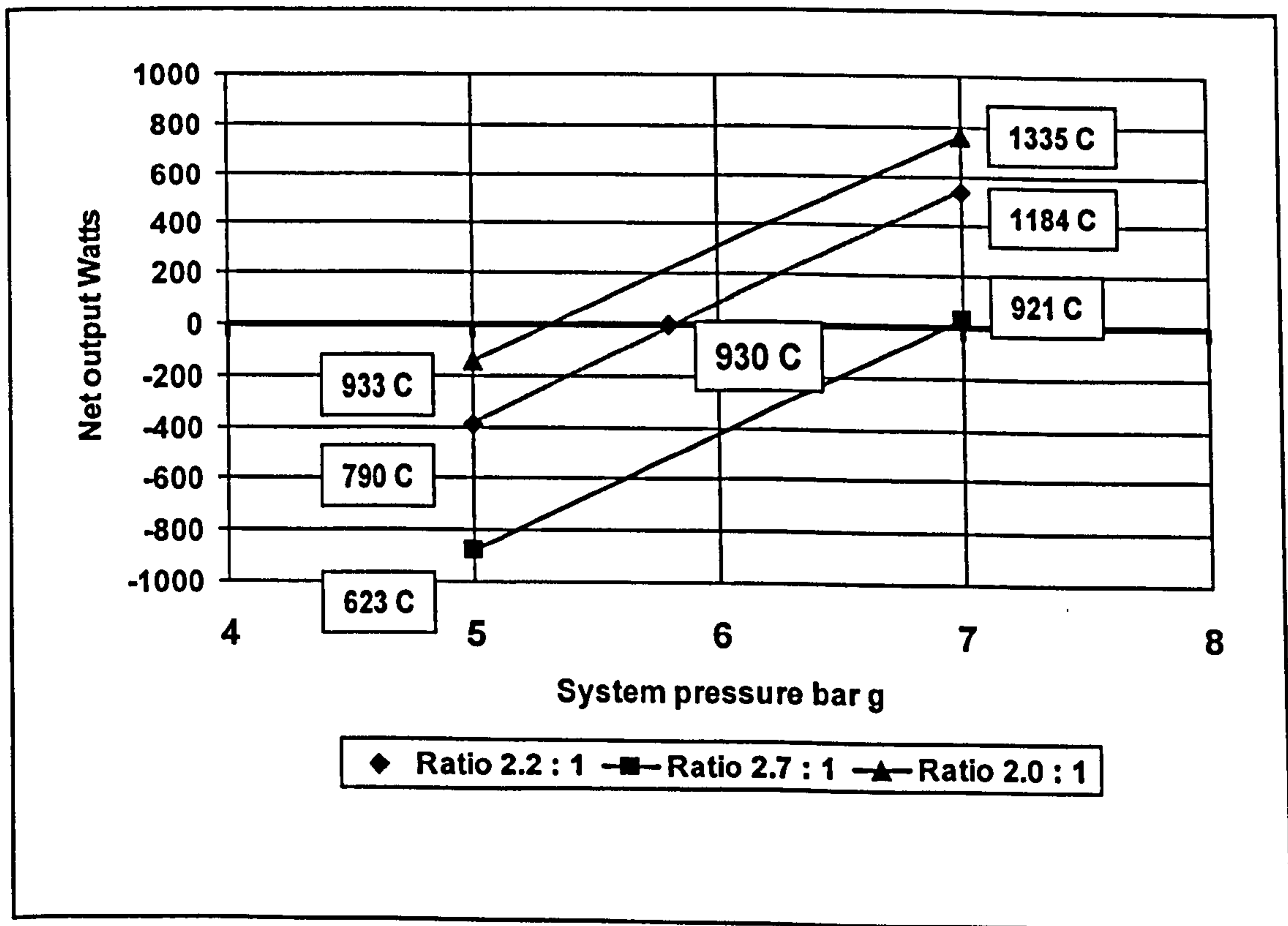


Fig 4.21 Net Power Outputs for Engine at Mass Flow Balance At Various Scroll Compressor Drive Ratios



Overall with a max input temperature limited to 850 C for metallurgical and safety reasons it is not possible to achieve a self sustaining condition.

#### 4.4.15 Effect of Clearance Volumes on Expander Performance

For a fixed swept volume the clearance volume has a major influence on net power output. The larger the clearance volume the greater the required recompression work. This is only partially offset by the increase in expander work output from the expansion of a larger volume of gas. In addition with a large clearance volume the exhaust pressure is higher representing wasted energy.

The effect of clearance volume was calculated using the following assumptions.

For Expander:

System Pressure 7.5 bar g

Gas inlet temp 850 C

RPM 1000

Mech eff 0.8

Recompression to 7.5 bar g

Inlet Valve closes at 90 cc of swept volume

Polytropic index of expansion  $n=1.3$

For Compressor:

Reciprocating type;

Mech Eff 0.8;  $n=1.3$ ; Discharge temp 90C and matched mass flow rate.

The results are shown graphically in Fig 4.22

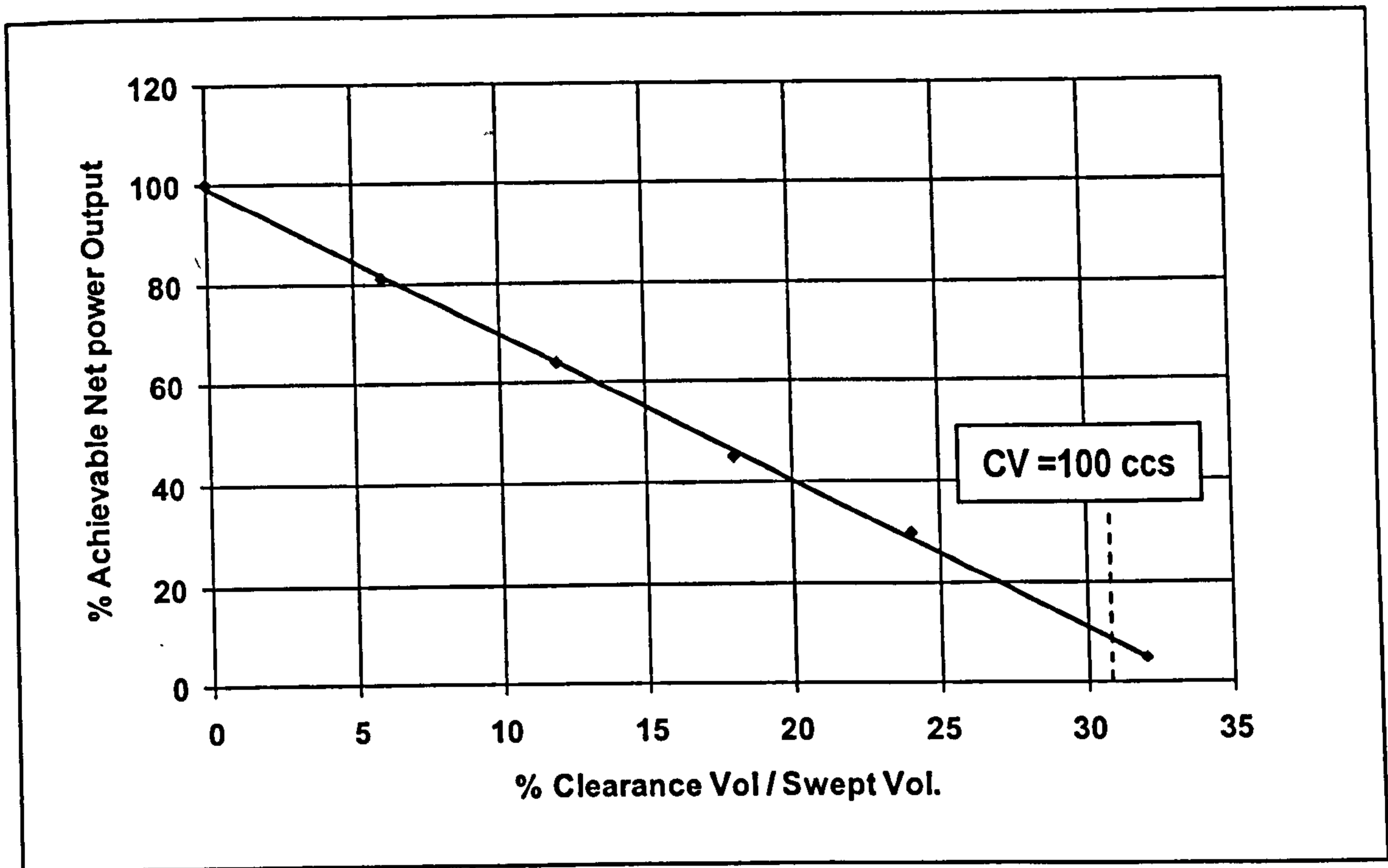


Fig 4.22 Theoretical Assessment on The Influence of Clearance Volumes on Net Power Output.

Fig 4.22 also shows the clearance volume of the engine (100 ccs for a swept volume of 325 ccs) indicating less than 5% achievable net power output. By comparison a clearance volume of 3% of swept volume results in a 90% achievable net power.

From Fig 4.22 and the conditions examined it can be stated that: ***'For every 1% of expander clearance volume net power reduces by 3%'***

#### 4.4.16 Suitability of a Scroll Compressor for the RJC Engine

A scroll type air compressor delivers air at up to 150 deg C which is up to 60 deg C higher than a typical reciprocating compressor. For an equivalent mass delivery it therefore consumes more power than a reciprocating compressor. The additional power consumed is calculated at 580 watts at 3135 RPM and 7 bar g., for the scroll compressor used, when compared to a reciprocating compressor delivering

the same mass flow rate and operating at 80% mechanical efficiency. The output of the scroll compressor and comparison to a reciprocating compressor is shown at Figs 4.23

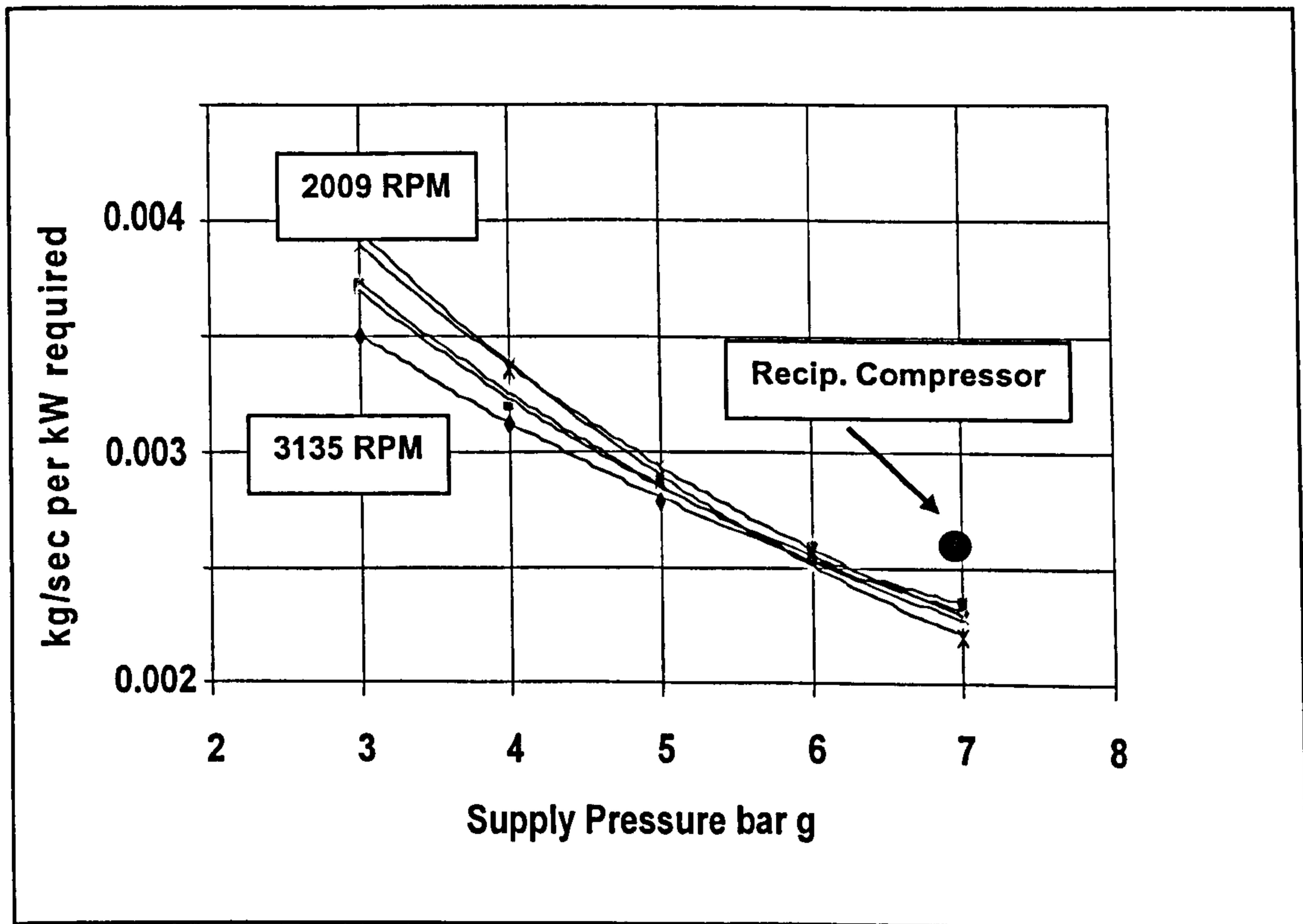


Fig 4.23 Compressor Performance Comparisons.

The implication is that more of the expander work is required to drive the scroll compressor detracting from the net power output. On the other hand the higher discharge temperature of the scroll compressor will require less fuel to be used, to raise the temperature to say 850 C, the net result being similar thermal efficiencies for an engine with the same expander but using the two different compressors.

Because it is important to maximise the net power output, and not exceed 850 deg C inlet gas temperatures, a reciprocating compressor is better suited for use as part of a RJC engine.

#### 4.4.17 Limitations

The engine designed, built and tested did not perform as expected and the following limitations on testing were identified.

- Accurately measuring the cylinder pressure in the cylinder over a cycle meant that indicator diagrams could not be constructed and thus engine friction could not be measured.
- Valve timing had a significant influence on net power output. With the fixed valve timing arrangement between inlet and exhaust the maximum net output was achieved by advancing to 10 deg btdc. This increased the recompression pressure resulting in less air needed to be introduced into the cylinder at each rev and thus a higher cylinder pressure
- Limitations on air supply for motoring tests and the extra air required to fill the clearance volume due to lower than required recompression meant that motoring could only be conducted at engine speeds up to 800 RPM

#### 4.4.18 Summary

The lessons learnt from the side valve design engine were:

1. Clearance volumes have a major effect on:
  - a. Recompression work to system pressure.
  - b. Low clearance volumes are required to maximise net power output.
2. More accurate pressure vs. crank angle characteristic are required to:
  - a. Construct accurate PV diagrams to determine indicated work and frictional work.

- b. Determine the effect of throttling on the poppet valves and adjust opening times and cam angles to compensate.

3. Scroll compressor performance:

The characteristics of a scroll compressor is that it is a constant Mass (FAD) machine for a given speed. The specific performance of the scroll compressors in terms of Kg/sec per kW required at 7 bar discharge pressure is a calculated 10% lower than an equivalent reciprocating compressor. This additional work input is seen in higher discharge temperatures of some 50 deg C. On this basis the scroll compressor detracts from the potential net power output of the whole engine, and when maximising the net power output is the aim, a scroll compressor is unsuitable for an RJC engine.

#### 4.4.19 Lessons Carried Forward to Next Design Iteration

The following lessons were carried forward to the next design and operation in that:

1. The clearance volume would need to be reduced to achieve a net power output for a temperature limit of 850C As no problems were experienced with the cam belt drives the earlier concerns were not realised. This meant that an overhead valve rather than a side valve configuration could be used
2. The external compressed air supply needed to be improved to increase the range of engine operation under motoring conditions.
3. The accurate measurement of cylinder conditions over a cycle would need to be obtained to generate indicator diagrams and thus values of engine friction and valve losses. From this an accurate expander performance map could be constructed

4. The design of the cam box and valve operating mechanism needed to be simplified to facilitate the use of different cam profiles and valve timing to obtain optimum power outputs.

5 Investigations into the use of an engine driven reciprocating compressor would need to be undertaken. For this type of compressor typical indicator diagrams would need to be generated from which an accurate performance map could be constructed.

The major design modification carried through to next design iteration was to reduce clearance volumes and this could only be practically achieved by an overhead valve configuration necessitating the design and fabrication of new cylinder heads, cam boxes and valve actuating gear.

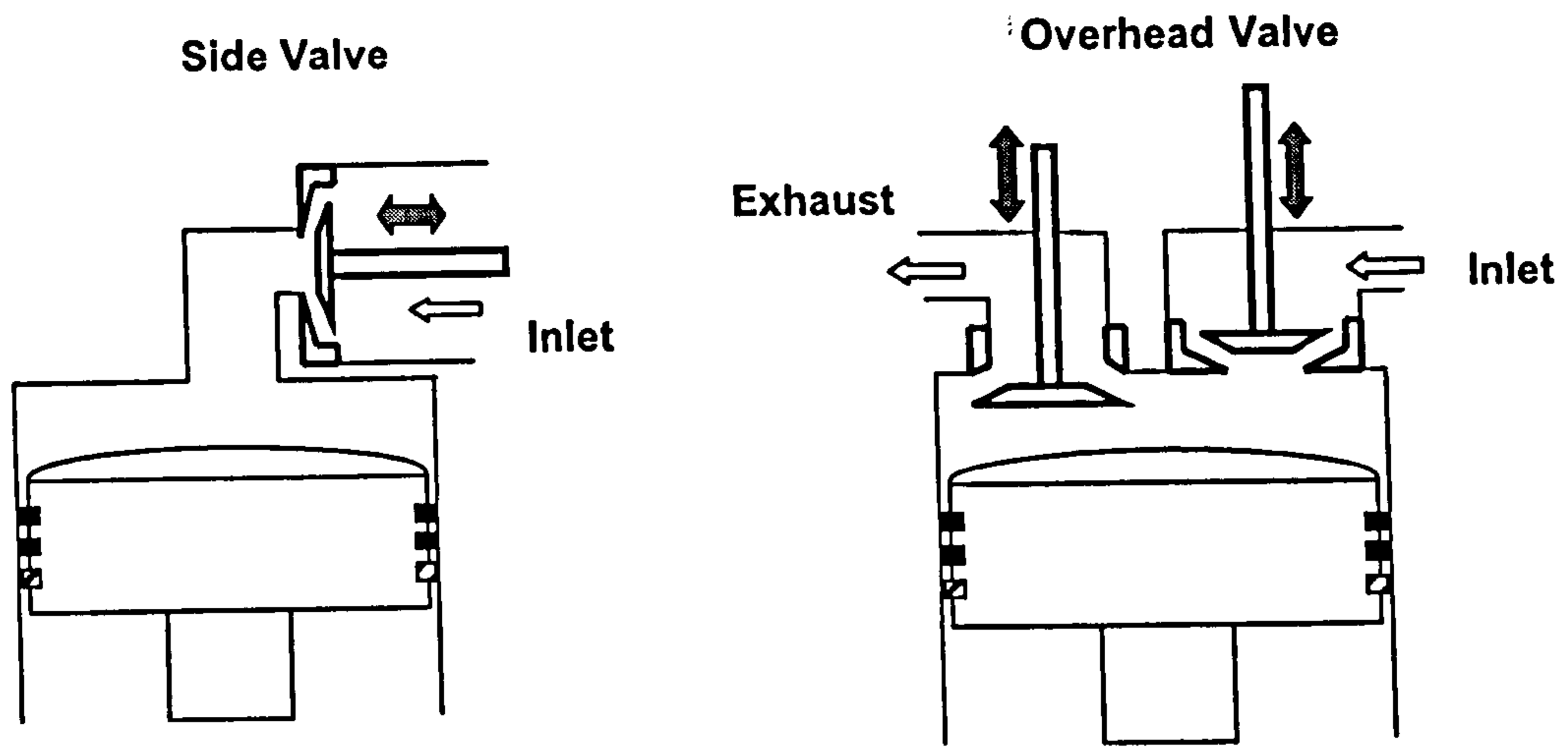
## 4.5 Test Engine Design, Construction and Performance

### 4.5.1 Cylinder Head Design.

The starting point for the new cylinder heads and cam boxes was to determine the operation of the inlet and exhaust valves, in an overhead valve configuration, and the maximum diameter of valve seats that could be physically accommodated within the cylinder head

The Inlet valve had to seat against the inlet pressure and hence had to move upwards into the head. The exhaust valve was to be of conventional design and move downwards into the cylinder. It was decided that the cam box would be of a single camshaft configuration with a direct acting cam actuated exhaust valve via a 'bucket' type cam follower to reduce side forces on the valve spindle. The inlet valve was to be driven by a cam actuated rocker arm from the same cam shaft that lifted the inlet valve off its seat.

The arrangement for the inlet valve required a spring to force the valve on to its seat and the rocker arm to act against a valve collet holder. This ensured positive movement of the valve. Both inlet and exhaust employed compression springs of a much lower rate than in internal combustion engines. Fig. 4.24 shows a schematic arrangement of the valve movement and the difference in clearance volumes whilst Fig. 4.25 shows a schematic arrangement of valve actuation.



Clearance volume 100 ccs

Clearance volume 30 ccs

Fig 4.24 Valve Configurations and Valve Movements

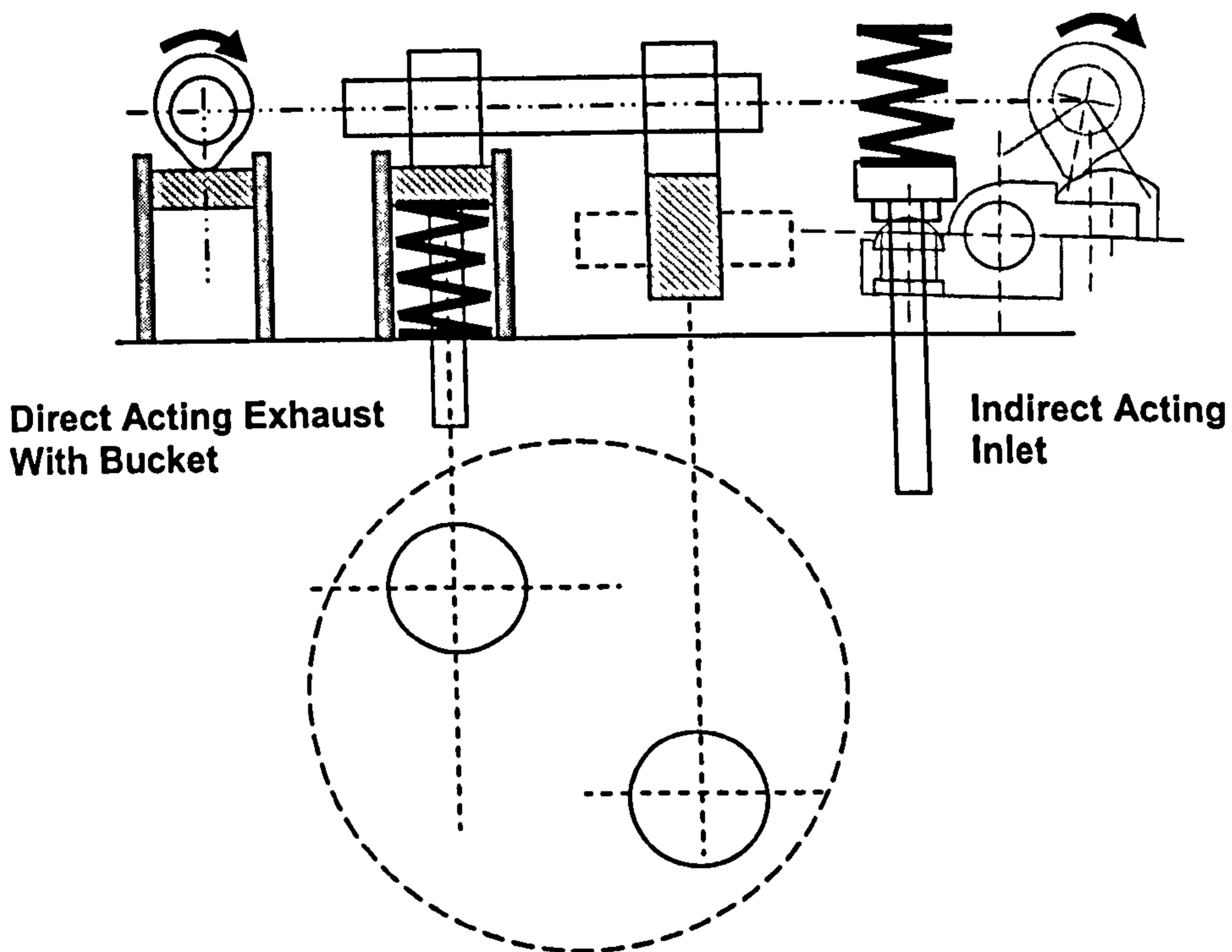


Fig 3.25 Schematic of Valve Actuation

A handed cylinder head and cam box was required for each of the cylinders  
 The original pistons from the R650 engine were retained. Consideration was given to modifying the pistons from the dome type crown to a flat crown by machining away the dome and mechanically fitting a new flat crown. This was not



undertaken because of the limited metal thickness in the piston walls to accommodate tapped holes to retain a flat crown. Consequently the clearance volume could not be reduced to an ideal minimum of less than 3 % but had to remain at the calculated value of 30 cc representing a 9.2 % of the swept volume. This compared with 30% in the side valve configuration

The valves used for the design were from a 2.0 litre Honda VTEC engine for the exhaust and from a 2.5 litre Ford diesel engine for the inlet. The inlet valve was machined to 30 mm dia. from 35 mm dia. and to a 45 degree angle. This more robust inlet valve was chosen to accommodate any side forces on the valve stem. Conventional valve guides for both valves were used and lubricated from the cam box without valve stem seals. The valve diameters were a maximum that could be accommodated into the cylinder head.

The first set of cams were designed for 80 deg inlet and 120 degree exhaust. The exhaust valve opening of 120 deg would give a theoretical recompression of 4.5 bar g using an n value of 1.3 if no throttling during closure occurred. The effect of valve throttling could not be determined at this stage of the design and hence the actual amount of recompression would have to be determined from the test results. The inlet valve cam opening of 80 deg was an increase of 10 deg to that employed in Part 4.4. The lower clearance volume and higher recompression pressure meant that less gas would be admitted to the expander without incurring high exhaust pressures. This would result in an increase in expander work

The oil supply to the cam boxes was taken from the engine oil pressure warning switch tapping and returned to the sump via pipe work that connected to the

crankcase openings for the original engine pushrods. Oil flow control was regulated by an inline valve to ensure the cam boxes did not flood at higher RPMs. New valve seats were manufactured from grey cast iron being a material that could be more easily machined and ground. The cylinder head was designed and manufactured in two pieces to allow positive fitting and location of the valve seats. The mating surfaces of the valve faces and valve seats were ground in to a leak free fit using compressed air to determine when this was achieved. Drawings and photographs of key components are at Annex 4.

### 4.5.2 Measuring instrumentation

Torque and engine speed were measured using the existing dynamometer which was recalibrated for the anticipated speed/load range. The dynamometer was driven from the engine by a shaft with universal joints at both ends this shaft being a standard component from a VW Golf.

A new pressure transducer of high accuracy and response was purchased together with the power sources, connections and software to allow it to be connected to a laptop to give instantaneous readings of pressure. Crank angle was measured using a proximity switch mounted on the engine crankshaft housing and sensing the starter ring which had 118 teeth. This gave a square shaped pulse every 3.27 degrees. Both the pressure trace and the crank angle pulses could be displayed on a continuous basis on a laptop screen and the trace could be captured and printed. Consideration was given to upgrading the software to display pressure vs. swept volume needed to determine indicated power. This was not undertaken because it would have caused another time delay in the programme and for the number of traces anticipated the conversion from pressure vs. crank to pressure vs. swept volume could be undertaken manually and fed into

a spreadsheet The existing thermocouple to measure the temperature of the hot gas was retained and new standard 50 mm dia. 0-10 bar pressure gauges were fitted to measure combustion chamber pressure, external air supply pressure and scroll compressor discharge pressure. Modifications were undertaken on the orifice plate used to measure the external air flow rate in the event that flow rate measurements/calculations were undertaken. This was increased in size to 15 mm dia.

## **4.6 Engine Operation**

### **4.6.1 Expander Performance**

The engine was operated on external compressed air (with no compressor connected) and engine torque/speed and supply pressures were measured. The belt timing of the camshaft was adjusted to achieve a diagram that best represented the anticipated profile. This profile should demonstrate no reductions in pressure around TDC. This was achieved at 10 deg BTDC for the inlet valve which with fixed valve timing between inlet and exhaust advanced the point that the exhaust valve closed and thus increased the amount of recompression. It was observed that the recompression was to 7.5 bar g at a system pressure of 7.5 bar g indicating that there was a degree of throttling on the exhaust valve as it closed. Similarly throttling from the inlet valve reduced the inlet valve opening to an equivalent of less than 60 degrees.

To increase the power new inlet cams of 90 deg opening were manufactured and fitted and the engine retimed. In addition it was realised that output power was low at higher speeds indicating that there was limited external supply air. This was partially overcome by the addition of a second larger bore air supply and the

introduction of a 120 litre reservoir to reduce pressure fluctuations. To achieve this extra flow the system to measure the air flow to the engine had to be by-passed.

#### 4.6.2 Readings Taken

A number of runs were conducted on external compressed air and with the scroll compressor disconnected with the following readings recorded

1. Pressure vs. crank angle traces
2. RPM and torque from the dynamometer
3. Supply pressure to the cylinder
4. Temperature of gas after the combustion chamber

The first objective was to generate the pressure/ swept volume diagrams of the engine from which the indicated work, along with the brake power engine friction characteristics could be determined.

The second objective was to determine the maximum gas temperature that could be achieved.

#### 4.6.3 PV Indicator Diagrams

Traces were recorded for pressure against crank angle along with the associated square wave trace from 118 tooth starter ring. These were manually converted into a spreadsheet for pressure vs. swept volume from which PV diagrams could be produced and indicated power calculated. The pressure vs. crank angle diagrams the PV diagrams and the spreadsheets generated (not all) are shown at Annex 4.

#### **4.7 Interpretation of the Indicator Diagrams**

Selected PV diagrams are shown at Figs 4.26a and 4.26b and clearly show the effect of fixed exhaust valve timing on the recompression with each characteristic

representing a different supply pressure and measured torque. At low system pressures the recompression remains at 7.5 bar g illustrated by the rapid rise and fall of cylinder pressure around TDC. The PV diagram at 700 RPM and 7.5 bar representing the maximum indicated work achieved was analysed in more detail Fig 4.27 where comparison is also made with an ideal cycle.. The throttling of the poppet valves at opening and closing had a noticeable effect on in cylinder pressures. For the exhaust valve whilst actual closure was at 70 deg BTDC (120 deg cam angle and set to open 10 deg BBDC) recompression started earlier at 77degrees BTDC. The inlet valve with a 90 degree cam (although retimed at 10 deg before TDC) also showed throttling before closure. So even though the inlet valve has a theoretical opening over 80 degrees from TDC its opening was only equivalent to 64 degrees. This difference is termed 'apparent valve opening' and is detailed in Table 4.5.

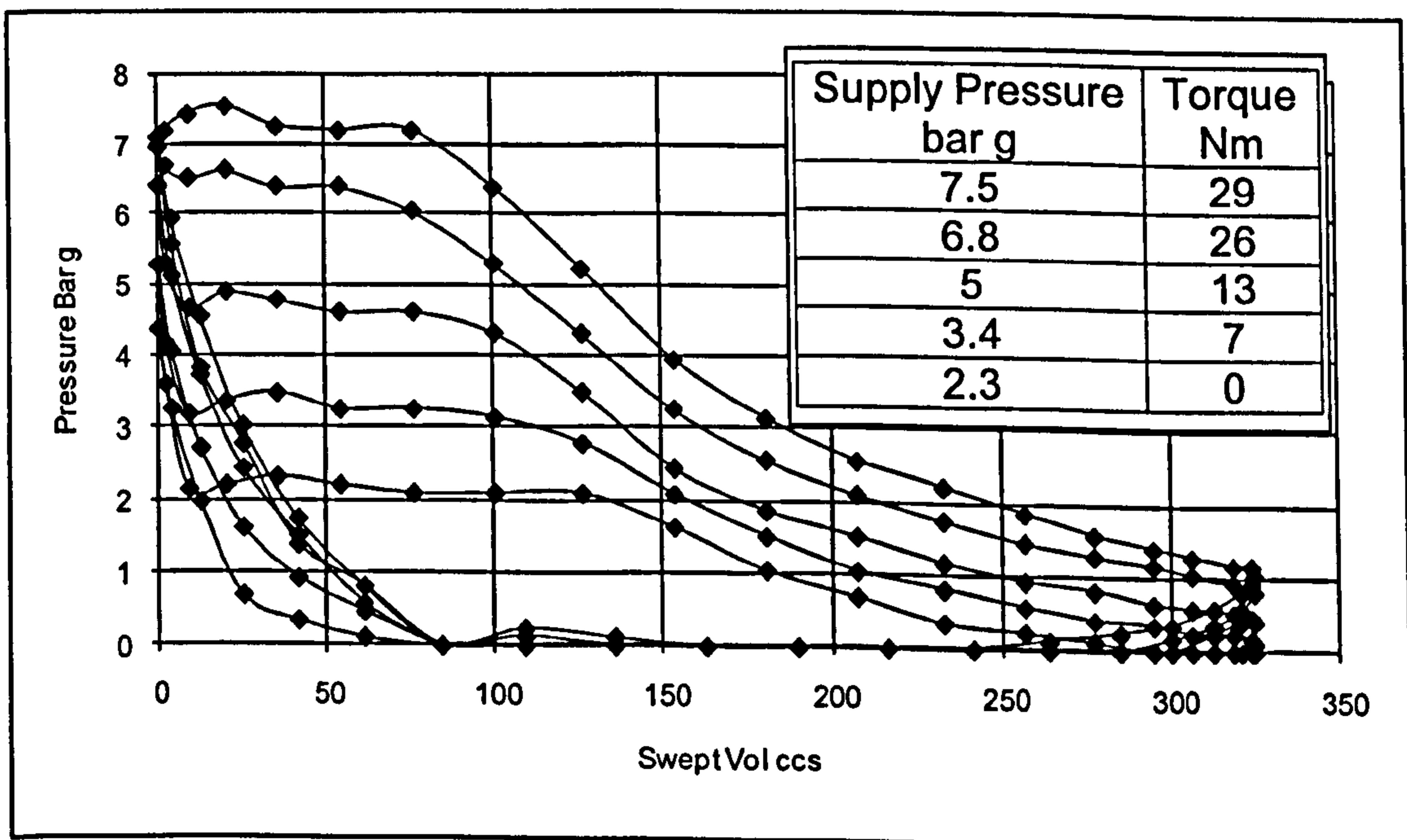


Fig 4.26 a. PV Diagrams 700 RPM @ Increasing Torque

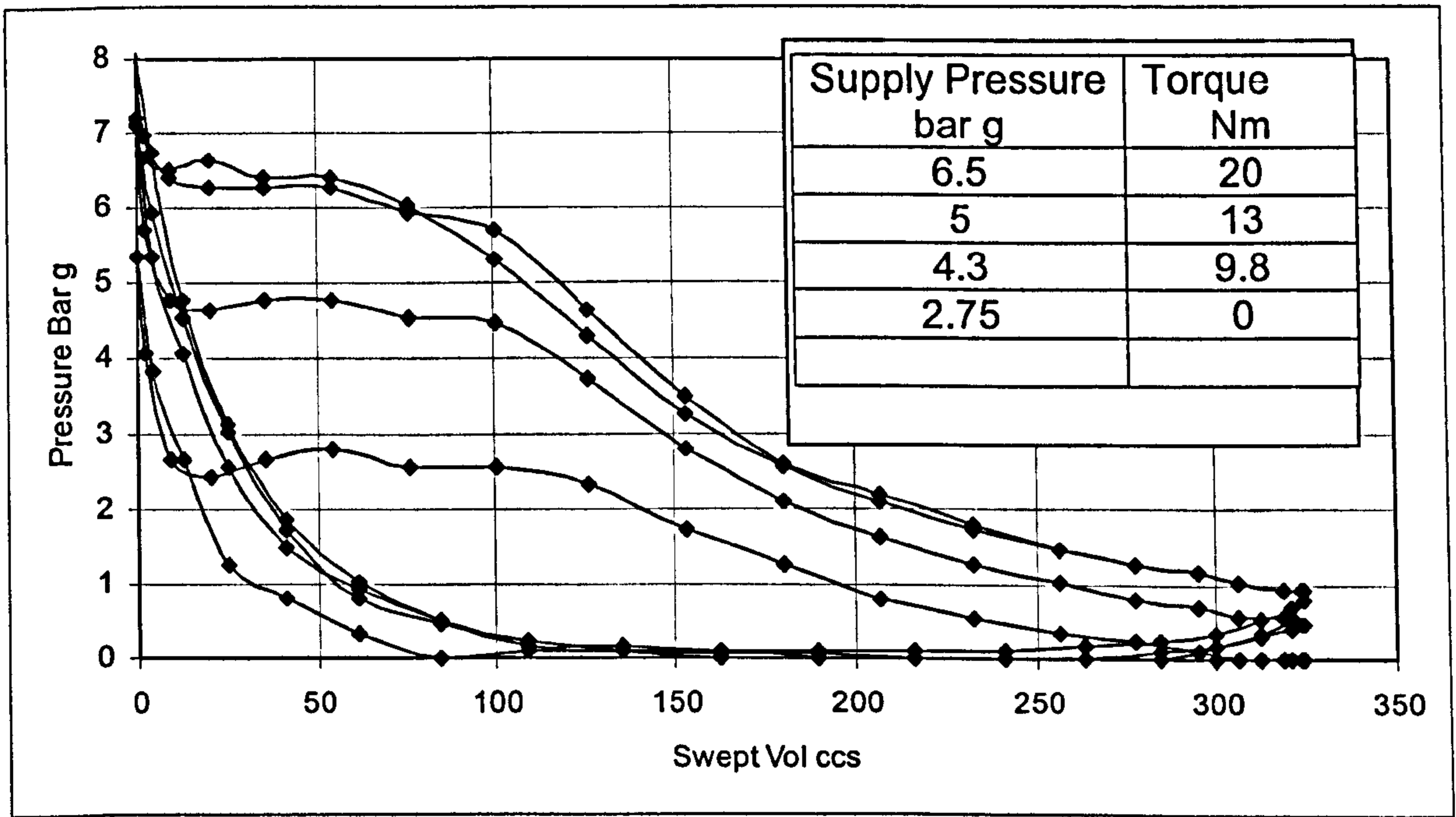


Fig 4.26 b. PV Diagrams 1000 RPM @ Increasing Torque & Supply Pressure

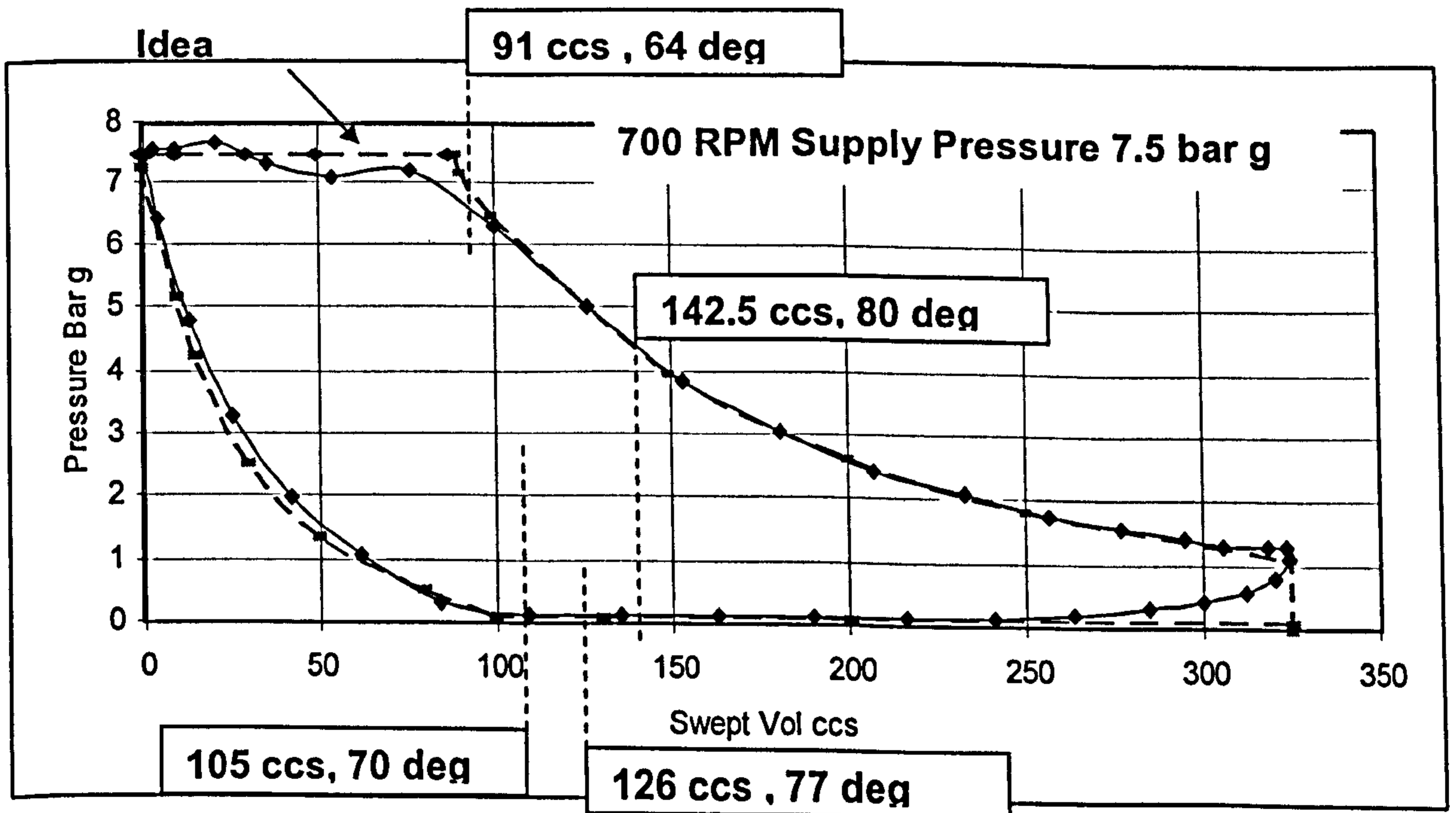


Fig 4.27 Differences Between Actual and Ideal Valve Openings

Valve timing	Actual PV Diagram	Ideal PV Diagram	Diff between Actual and Ideal
	Inlet set to open at 10 deg BTDC		
Inlet Cam angle	90 deg	64 degs	
Inlet valve shut	80 deg ATDC	64 degs ATDC	16 Deg
Exhaust set to open 10 deg BBDC			
Exhaust valve Angle	120 deg	103 deg	
Exhaust valve shut	70 deg BTDC	77 deg BTDC	7 Deg

Table 4.5 Difference Between Actual and Ideal Valve Openings

#### 4.7.1 Selected PV Diagrams

Only the PV diagrams where recompression matched the supply inlet conditions were considered for further detailed analysis. This was based on:

1. A system pressure of 7.5 bar g represented a reasonable maximum for single stage compressor.
2. The exhaust valve timing that gave a recompression that matched supply pressure.
3. The PV diagrams that gave the maximum indicated power for the engine speed achieved.

#### 4.7.2 Polytropic Values for Expansion and Recompression

From the PV spreadsheets of the selected PV diagrams it was possible to calculate the polytropic values of  $n$ . Plotting the absolute supply pressure against swept volume on loge, loge axis the slope of the graph would represent  $n$ . The average and most consistent values obtained from several PV diagrams were:

$$n \text{ expansion} = 1.22$$

**n recompression = 1.3**

These values are on cold air (15 C) where the isentropic value is 1.4. The difference being due to heat transfer.

#### 4.7.3 Friction

The PV diagrams and associated spreadsheets produced the Indicated power which along with the brake power measured allowed the frictional power to be determined from the relationship:

$$\text{Frictional power} = \text{Indicated Power} - \text{Brake Power}$$

The frictional power is made up of several components these being:

1. Piston ring / cylinder friction
2. Crankcase bearing friction
3. Oil pump power required
4. Cam box friction – bearings, cams
5. Transmission friction, drive to dynamometer and belt drives to cam boxes
6. Engine seals

The exact contribution of each of these to the whole could not be determined but Ref. 10 which examined the friction in a range of large commercial engines, and the contribution from the different parts of the engine, stated that the piston ring / cylinder friction would account for between 80% to 40% of the total friction.

To be able to compare Indicated brake and friction power with other published data on engine performance mean effective pressures, in bars, were used i.e.

IMEP: Indicated Mean Effective Pressure



BMEP: Brake Mean Effective pressure

FMEP: Frictional Mean Effective pressure

That have the relationship

$$\text{IMEP} = \text{BMEP} + \text{FMEP}$$

And are derived from the relationship

$$\text{Power} = \text{Mean Effective Pressure} \times \text{Swept Volume} \times \text{Revs /Sec}$$

$$\text{Power} = \text{PLAN}$$

Mechanical efficiency is defined as:

$$\text{Mech eff.} = \text{Brake Power} / \text{Indicated Power} \quad \text{or} \quad \text{BMEP} / \text{IMEP}$$

All the measured data and calculated values are compiled in Table 4.5

**Data Recorded And results From PV Diagrams**

RPM	Supply P Bar	Torque Nm	Brake W	BMEP Bar	Indicated W	IMEP Bar	Friction W	FMEP Bar	Eff %
700	2.3	0	0	0	800	1.052	800	1.052	0
	3.4	7	513	0.68	1197	1.58	684	0.9	42.8
	5	13	952	1.25	1620	2.13	668	0.88	58
	6.8	22	1620	2.13	2216	2.92	596	0.79	73
	7.5	29	2125	2.8	2746	3.62	621	0.62	77.3
800	2.5	0	0	0	897	1.036	897	1.063	0
	3.5	6.4	536	0.62	1280	1.19	744	0.85	42
	4.25	10	837	0.96	1328	1.47	691	0.78	63
	6.7	24.6	2060	2.38	2610	3.01	550	0.63	79
	7.5	29	2429	2.8	2914	3.36	485	0.56	83
900	2.7	0	0	0	1131	1.16	1131	1.16	0
	4.4	10.8	1017	1.04	1956	2	939	0.98	52
	6	18.6	1753	1.8	2524	2.56	771	0.76	69
	7	24.8	2337	2.4	2752	2.822	415	0.422	85
	7.25	25	2356	2.41	2752	2.822	398	0.41	85
1000	2.75	0	0	0	1280	1.19	1280	1.19	0
	4.3	9.8	1022	0.94	2216	2.04	1194	1.1	46
	5	13	1356	1.25	2328	2.15	972	0.9	58
	6.5	20	2212	2.08	3057	2.82	805	0.74	74
1143	2.6	0	0	0	1605	1.29	1605	1.29	0
1200	2.6	0	0	0	1757	1.351	1757	1.351	0

**Table 4.5 Data From PV Diagrams and Torque / Speed**

#### 4.7.4 Understanding Friction

From earlier modelling Ref 7 it was always understood that as the RJC engine operating with low IMEPs friction would have a major influence on the net power the engine would produce. Mechanical efficiencies of the order of 90% would be required for the engine to produce a net power output to be comparable with other micro CHP power generators i.e. the Stirling engine.

From Table 4.5 several characteristics were observed and the following conclusions drawn.

1. From Fig 4.28 Frictional power increases with RPM. This was only constructed for the zero torque condition (motoring) and shows a rising characteristic which is as expected.

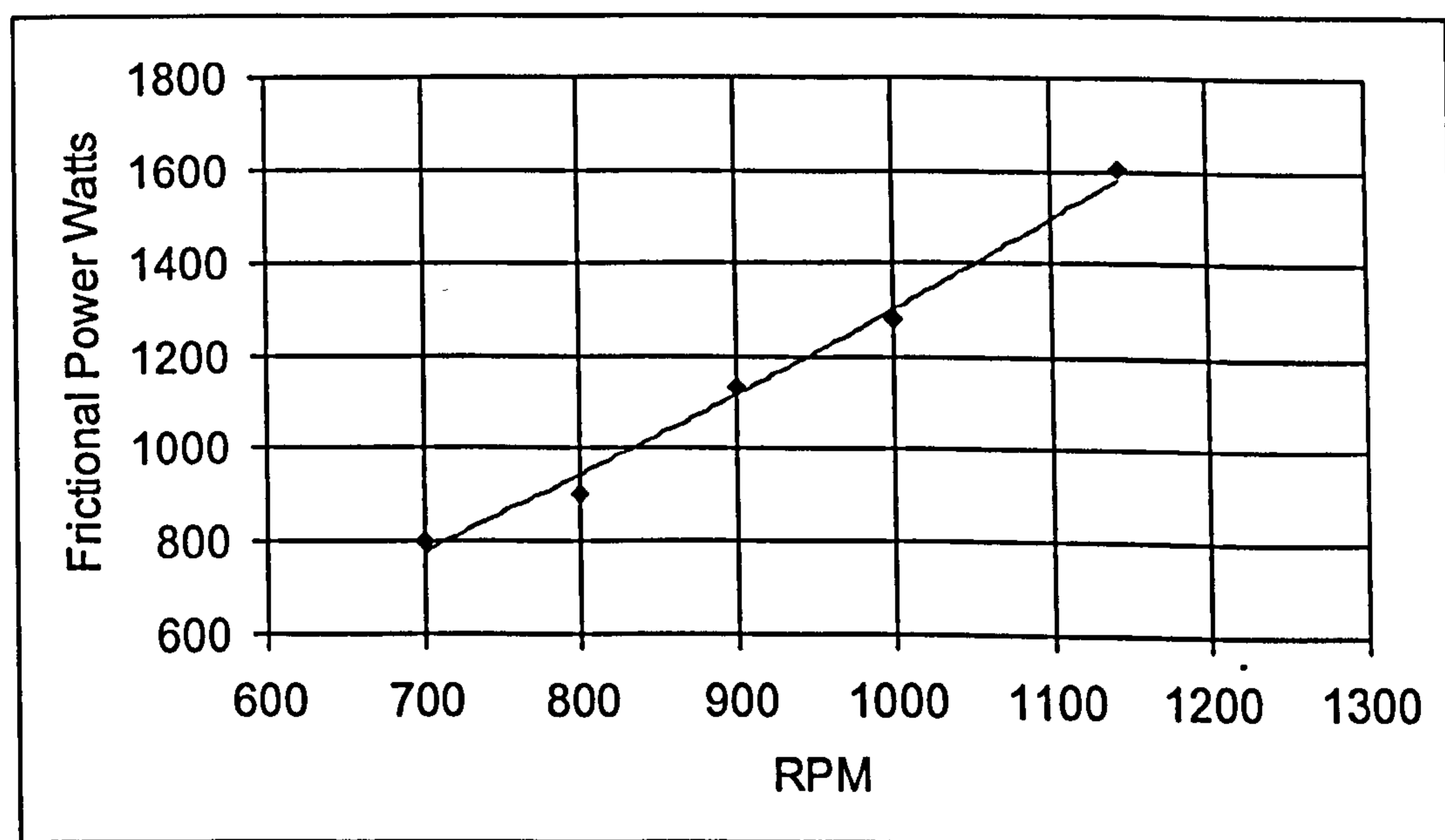


Fig 4.28 Zero Torque Friction Characteristic

2. In Fig. 4.29 with the zero torque values omitted brake power increases with increasing supply pressure whilst frictional power remains sensibly constant but with some scatter. As the higher indicated powers are achieved at higher supply pressures then it would be expected that with higher pressures higher friction power would be encountered. No firm conclusions can be drawn on the frictional

power characteristic except that it is derived over a narrow speed range from 700 to 1000 RPM and that the 'shape' of the indicator diagrams must have an effect.

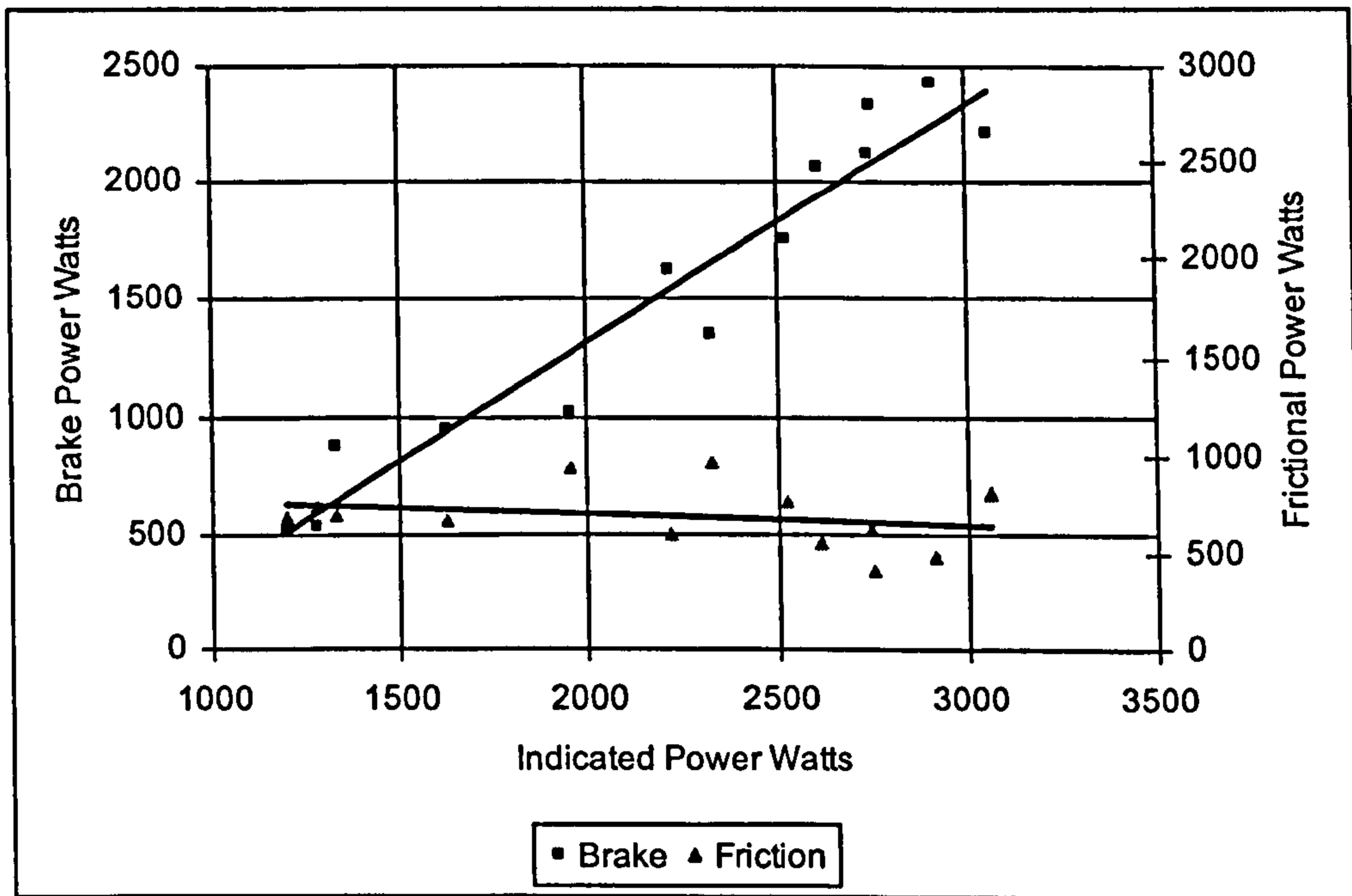


Fig 4.29 Indicated power vs. brake and frictional power

In Fig 4.30 the mechanical efficiency is drawn against supply pressure. This shows that mechanical efficiency increases with increasing supply pressure reaching a maximum of up to 85% at 7.5 bar supply pressure.

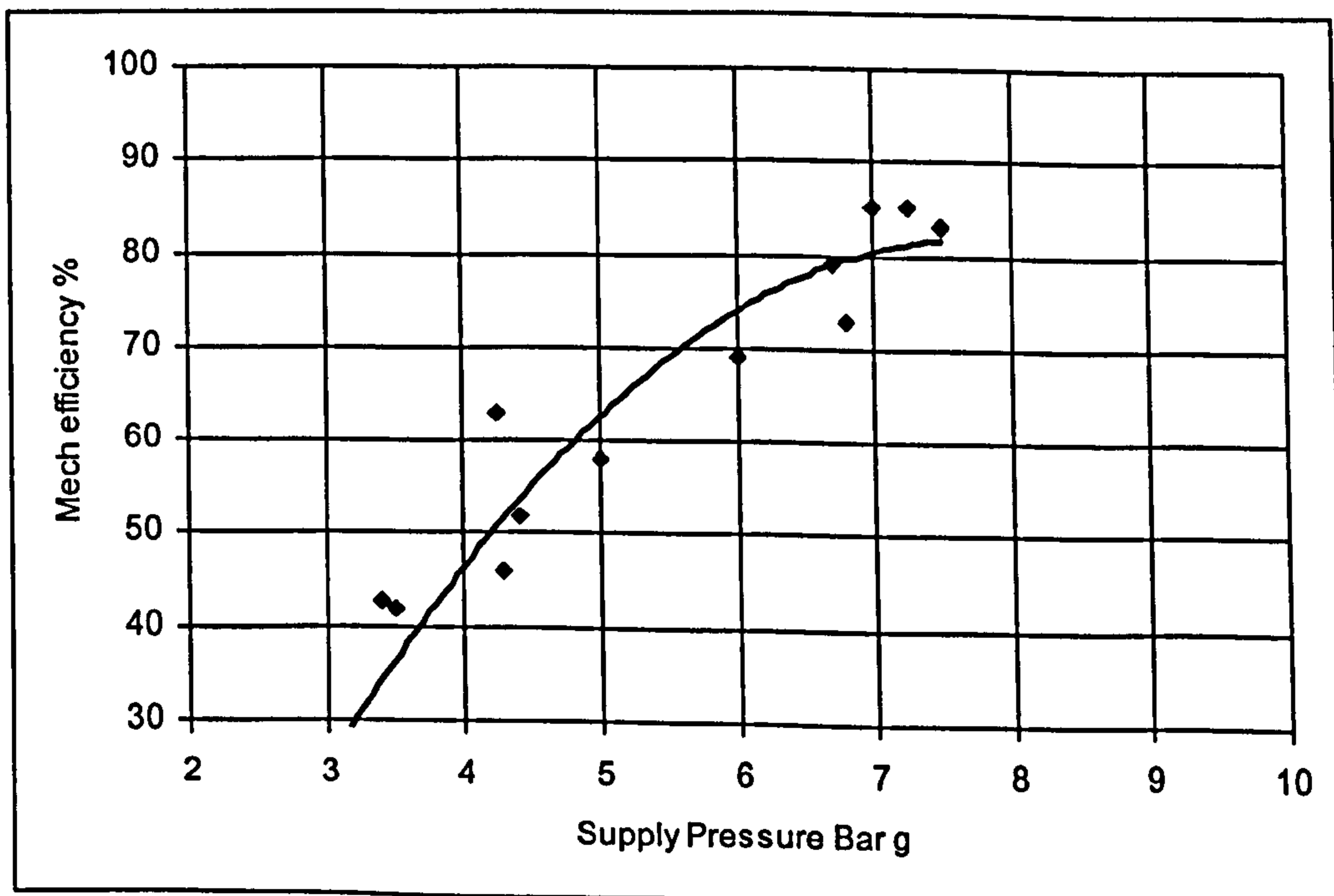


Fig 4.30 Supply pressure vs. mechanical efficiency

The conclusion was that to improve the brake power then there had to be an improvement in indicated power and a reduction in frictional power. Hence in order to examine the influence of all the parameters detail modelling of the expander performance was undertaken and is reported in Part 3.

#### 4.7.5 Engine Operation with Combustion

It was not possible to achieve self sustaining combustion with the scroll compressor connected. The problems with regard to matching compressor power requirements with compressor output could not be overcome.

The engine was operated with combustion and on an external air supply with the objective of determining the effect of hot oil on frictional work and to assess the maximum temperature that could be safely achieved in the combustion chamber as measured by the temperature of the hot gas discharge.

Fig. 4.31 shows the characteristic of power output against supply pressure both on cold air and with combustion. Only 3 readings were taken with combustion at supply pressures between 5 and 6 bar with an extrapolation made to a supply pressure of 7.5 bar

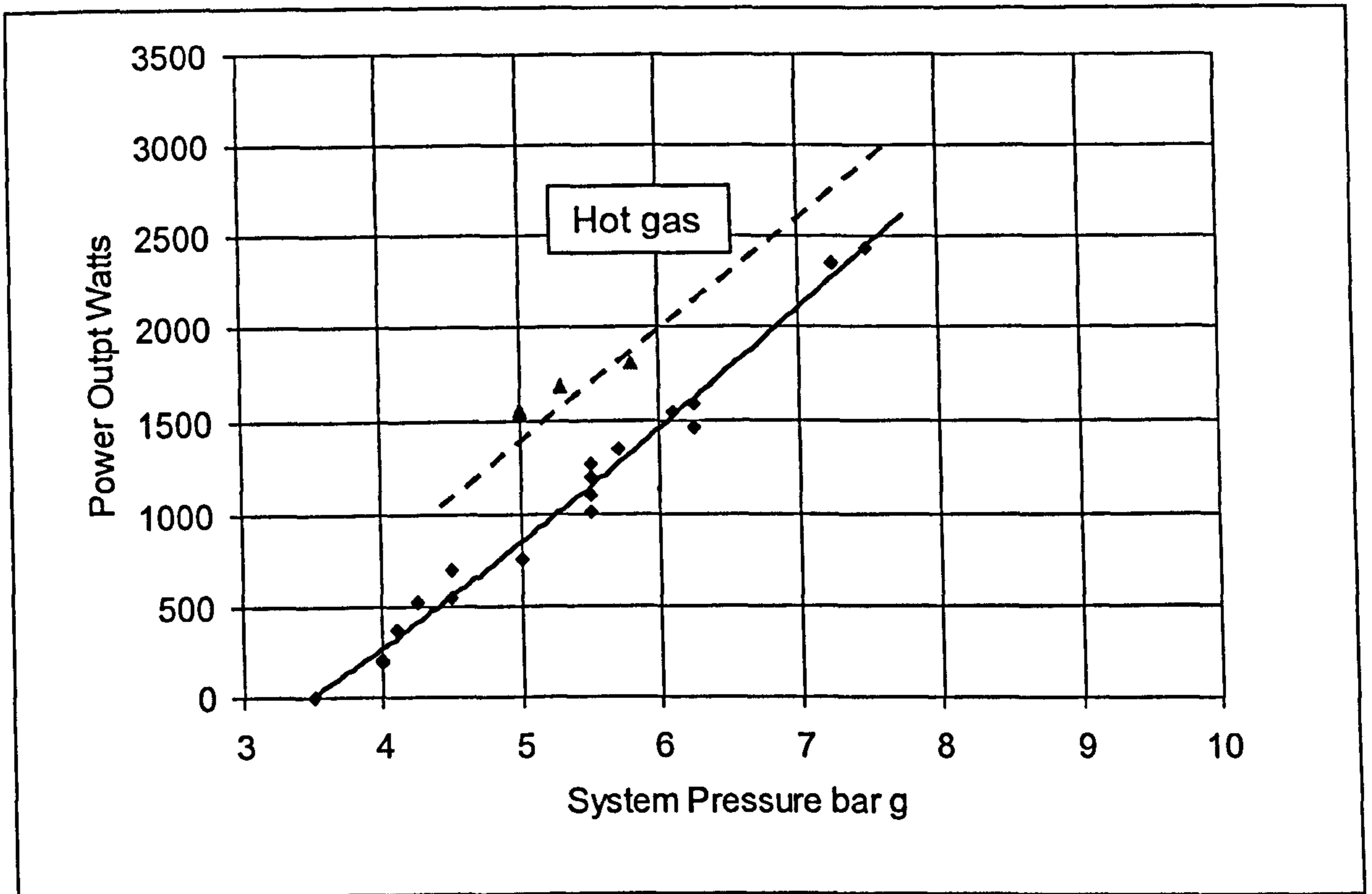


Fig 4.31 Engine operation on Cold Air and Hot Gas. (Various engine RPMs)

At a supply pressure of 7.5 bar there is a increase in power output of 500 Watts. This indicates that under hot conditions, with hot oil, improvements to the mechanical efficiency are possible and that a mechanical efficiency of 90% is readily achievable.

The combustion chamber was operated at 1000 deg C for a short period and stable combustion conditions were observed.

#### 4.7.6 Further Understanding of Engine Friction

Using air standard equations the various parts of the expander cycle were analysed and plotted against supply pressure Fig 4.32 noting that fixed exhaust valve timing was set to give 7.5 bar g recompression. A percentage correction of 2.5% was made for the full admission stage of expansion to allow for the

difference between test engine data and an ideal cycle (derived from the PV diagram at 700 RPM on 7.5 bar g cold air). Polytropic values for expansion and recompression derived from the test data was used and the air inlet temperature was 15 deg C. Also included in Fig 4.32 is the indicated and brake engine test data. The following observations are made from Fig 4.31

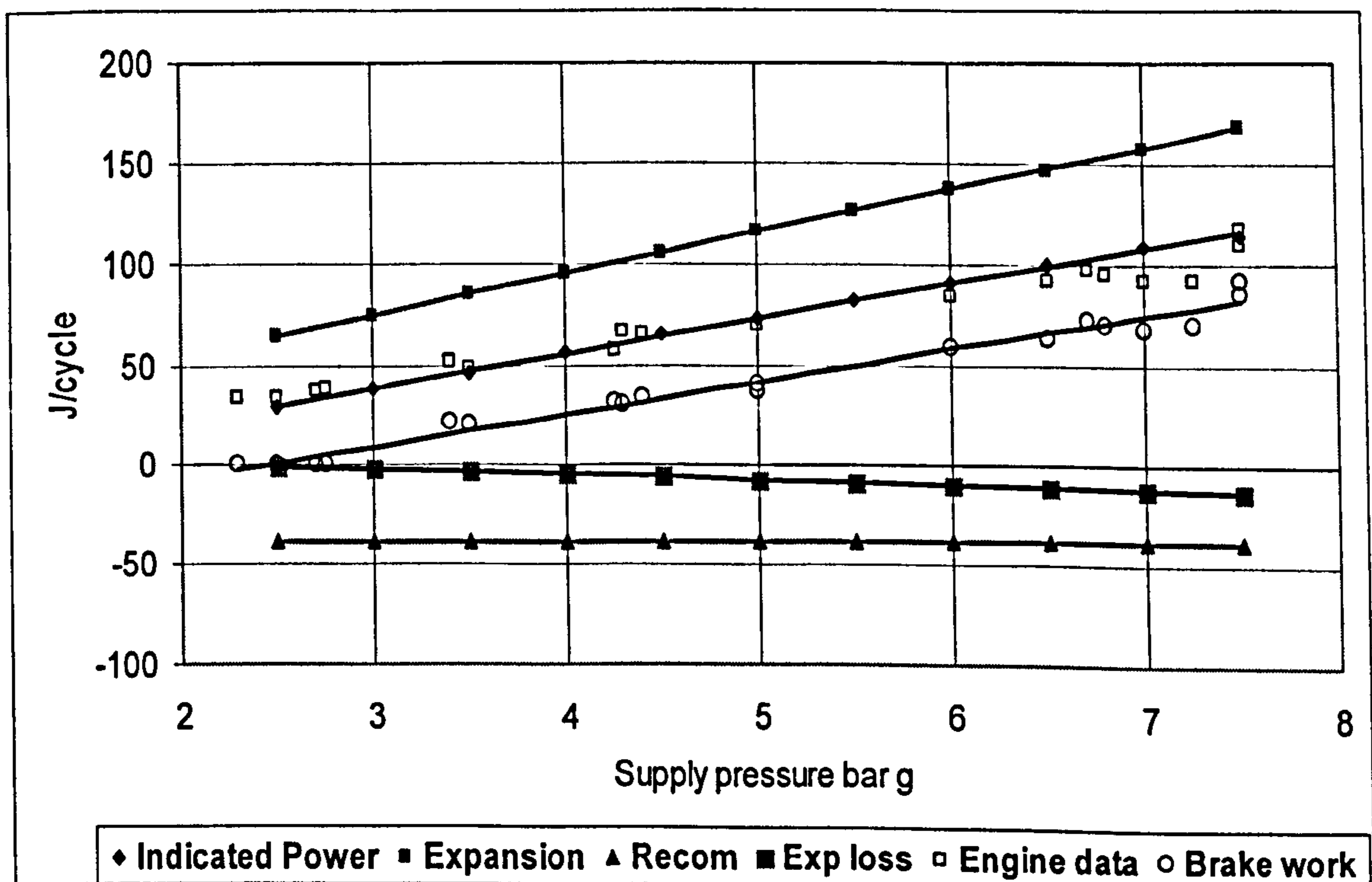


Fig 4.32 Engine Cycle work vs. Supply Pressure

1. There is a good correlation between the derived indicated work and the measured indicated work
2. The frictional work being the difference between indicated and brake work remains sensibly constant but at higher pressures represents a reducing percentage of indicated power. This is in line with the test data in that the maximum mechanical efficiency attained was at 7.5 bar air supply pressure.

#### **4.8 Reciprocating Compressor Performance**

The use of a scroll compressor in the design of an RJC engine had been discounted and that for practical purposes a reciprocating compressor would offer a solution. An engine design based on the two cylinder BMW R650 engine was considered with one cylinder as the expander and one cylinder as the compressor. To provide a better understanding of the pressure volume relationship in a reciprocating compressor work was carried out on a small compressor to determine typical characteristics. The compressor used had a single cylinder with a stroke of 47 mm and a bore of 37 mm with a calculated clearance volume of 2%. The compressor used 'reed' type valves for both suction and discharge and was directly driven a single phase AC motor rated at 1.1 kW at 2860 RPM. The nominal compressor delivery was 200 litres /min FAD.

Modifications to the compressor were undertaken to fit the pressure sensor to the head to directly measure the pressure vs. crank angle relationship and record the trace over a single cycle. The objective was to create a PV diagram from which the polytropic n values for compression and expansion could be determined.

PV diagrams for 7.5 bar and 2.5 bar discharge pressures are shown at Fig. 4.33 with the spreadsheet and pressure traces contained at Annex 4

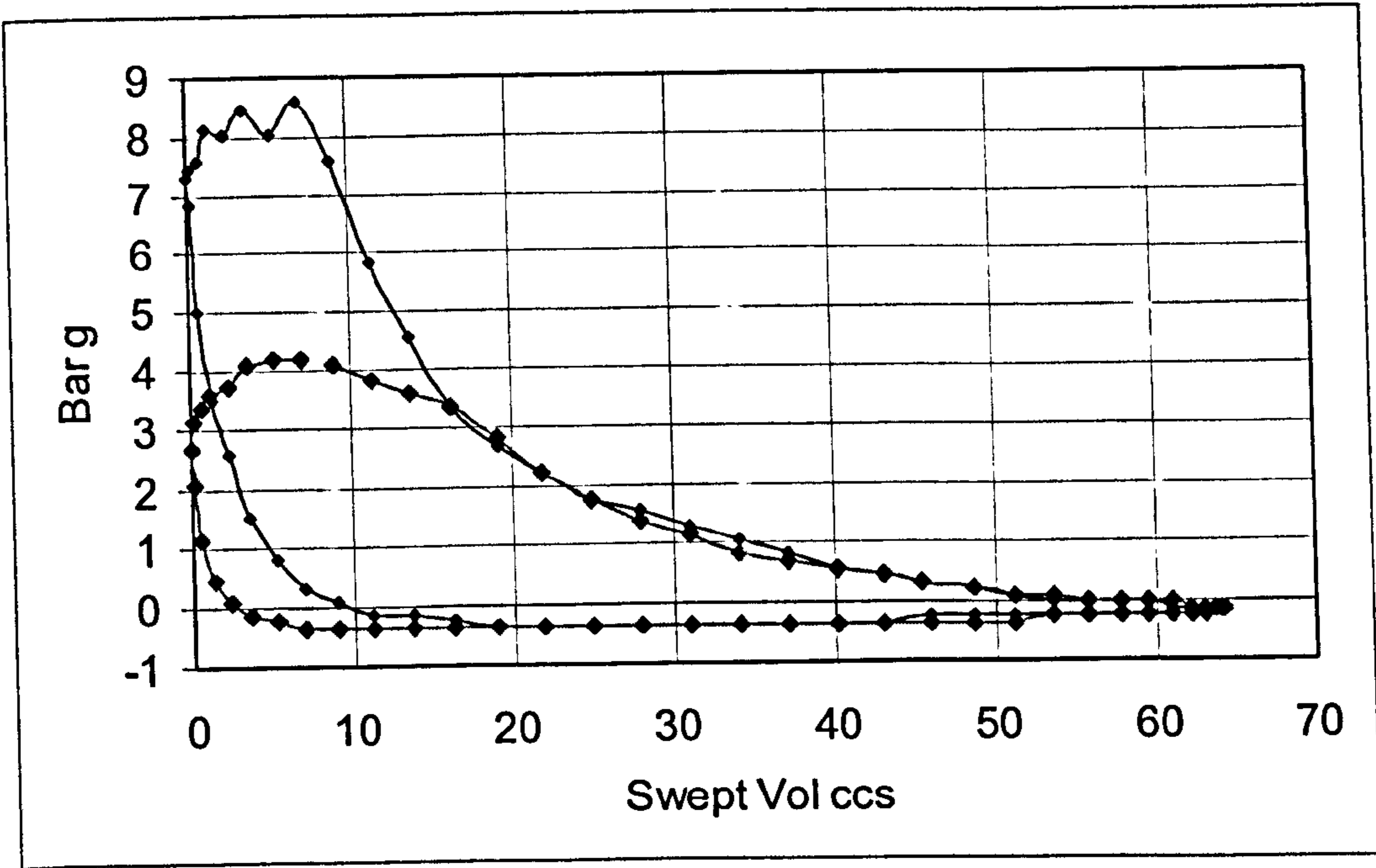


Fig 4.33 PV Diagrams for Portable Compressor

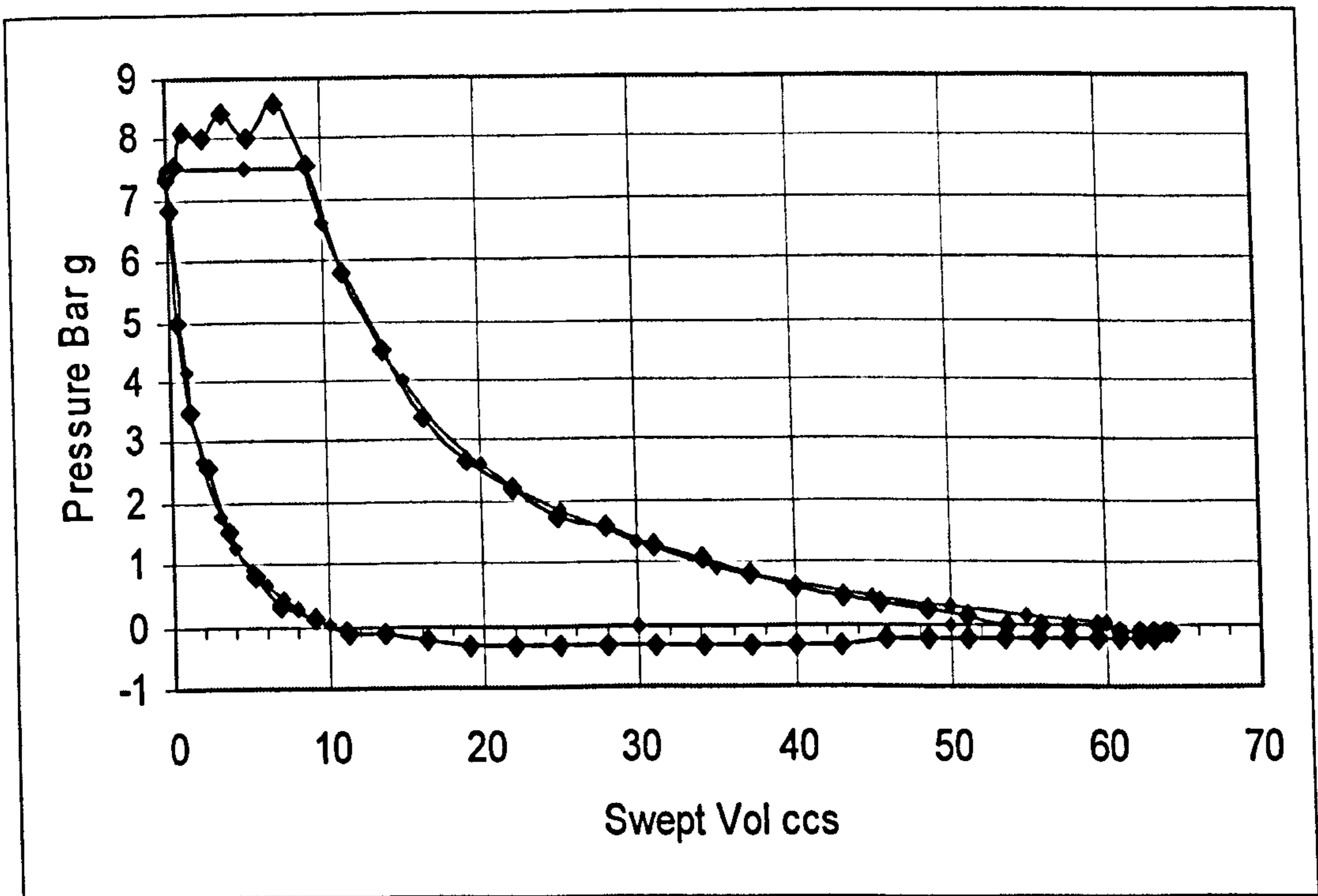


Fig 4.34 Compressor Performance 7.5 bar Supply

On the PV diagram for a 7.5 bar discharge pressure an ideal diagram is superimposed, Fig 4.34, the result of which clearly show the differences during



suction and discharge with these differences being the energy losses from the ideal. The polytropic  $n$  values calculated from the spreadsheet were 1.21 for compression and 1.1 for expansion. Again using the spreadsheet the discharge and suction energy losses were calculated as 6.5 % and 8.5% of the cycle work giving a total loss per cycle of 15%. Hence the actual cycle required 15% more work than the ideal cycle. The indicated work from the PV diagram was calculated as 727.7 Watts resulting in an ideal cycle work of 617.5 watts.

It was not possible to determine the friction characteristics of the reciprocating compressor so a mechanical efficiency of 90% was assumed this being similar to the ideal mechanical efficiency of the engine.

From the above analysis the work to drive the compressor cylinder in the opposed piston configuration for a required mass flow rate can be determined.

#### **4.9 Influence of Friction and Clearance Volumes on Expander Performance**

A compressor cycle efficiency of 85% and the polytropic values were then used for the evaluation of the BMW engine configuration of one cylinder as the expander and one cylinder as the compressor. This evaluation used a simple model, Annex 3, of the expander cycle and matching the mass flow from a compressor model that used the cycle and efficiencies derived from the portable compressor.

The output from this model are shown at Fig 4.35

Even though the evaluation extrapolates the engine characteristics to a gas inlet temperature of 850 C at 1000 RPM the simple model shows the significant effect both overall mechanical efficiency and clearance volumes have on net power output. For a clearance volume of 30 ccs (~10% of swept volume) and an overall mechanical efficiency of 80 % the net output is 50 Watts. By comparison for a

## Part4

clearance volume of 10 ccs and a mechanical efficiency of 90% the net output rises to 583 Watts. This represents a specific net power output of 2.57 Watts per ccs of swept volume per 1000 RPM.

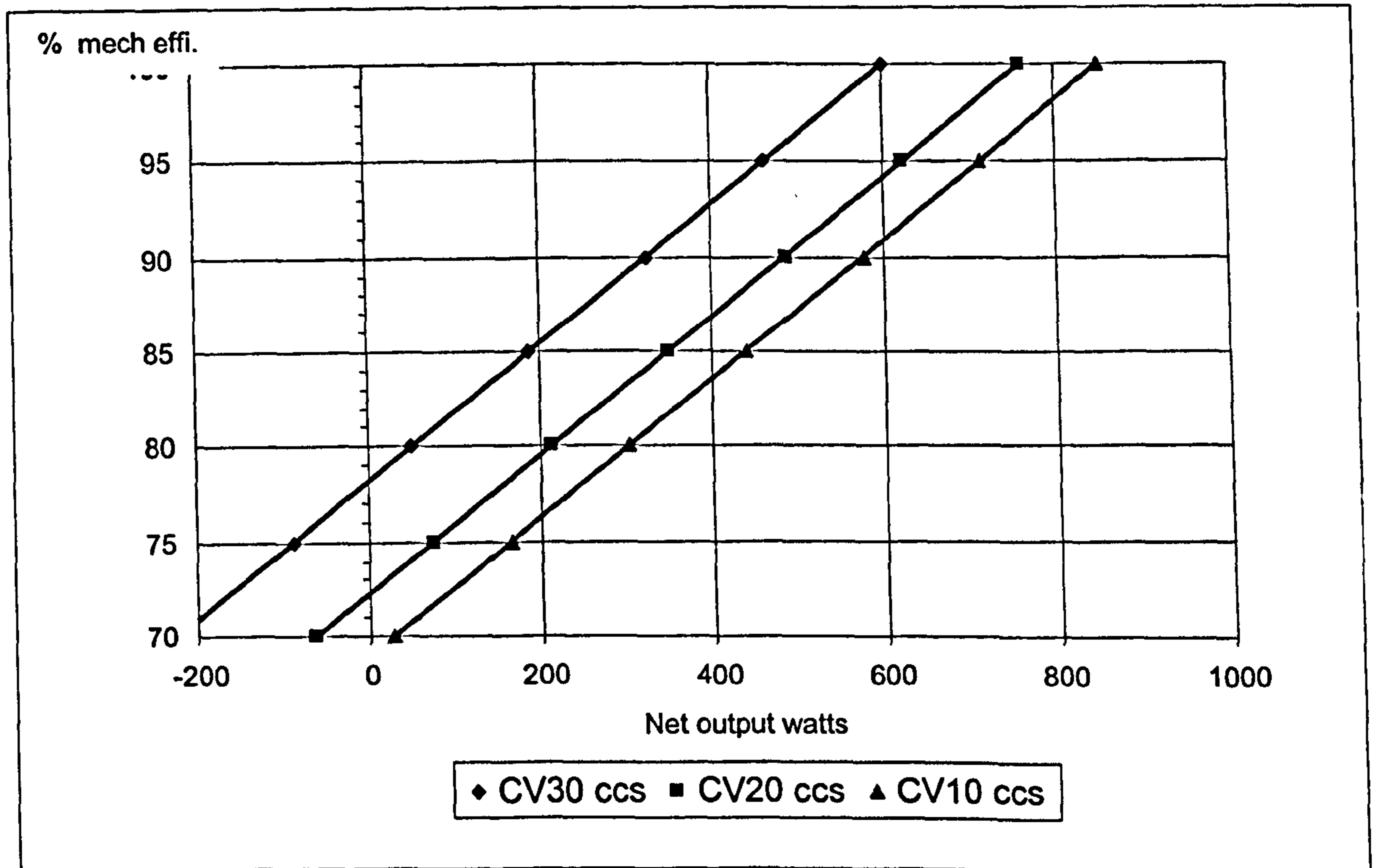


Fig 4.35 Influence of System Efficiencies and Clearance Volume on Output

Configuration: 1 cyl as an expander and 1 cyl as a compressor

and 850 deg C inlet temp at 700 RPM

Matched mass flows between compressor and expander

Best achievable practical output = 583 Watts

In terms of engine swept volume = 2.57 Watts / cc per 1000RPM

### 4.10 Thermal Efficiency

The thermal efficiency was estimated on the net work output as a percentage of the potential work in the hot gas. For the configuration of one cylinder as a compressor and one as an expander (with matched mass flows) the efficiencies

## Part4

were calculated for various values of clearance volumes and mechanical efficiencies Annex 4 and shown at Fig 4.36

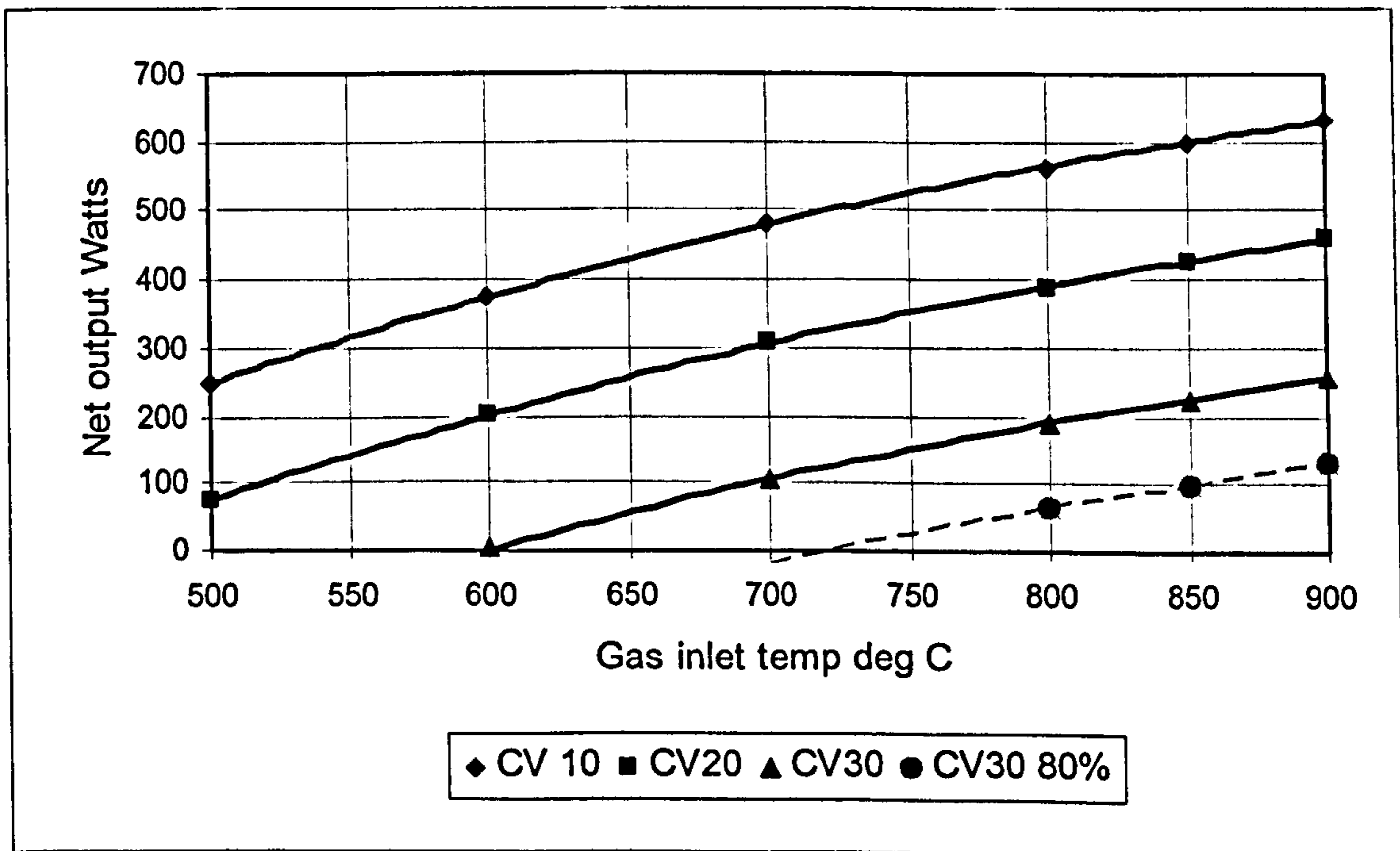


Fig 4.36 Net output against gas inlet temperature

.At 850 C inlet, 7.5 bar supply, an overall mechanical efficiency of 90% a clearance volume of 10cc and air inlet to the combustor of 90C the thermal efficiency is 24 % Fig 4.38. It is noted that this evaluation used a polytropic index of 1.22 which will be an underestimate for hot gas operation.

If thermal efficiency is however assessed on the basis of the amount of fuel burnt and its calorific value (assumed to be 40,000 kJ/kg) and using the exhaust gas to preheat the air to the combustor (regeneration) then the results are shown at Fig 4.37.

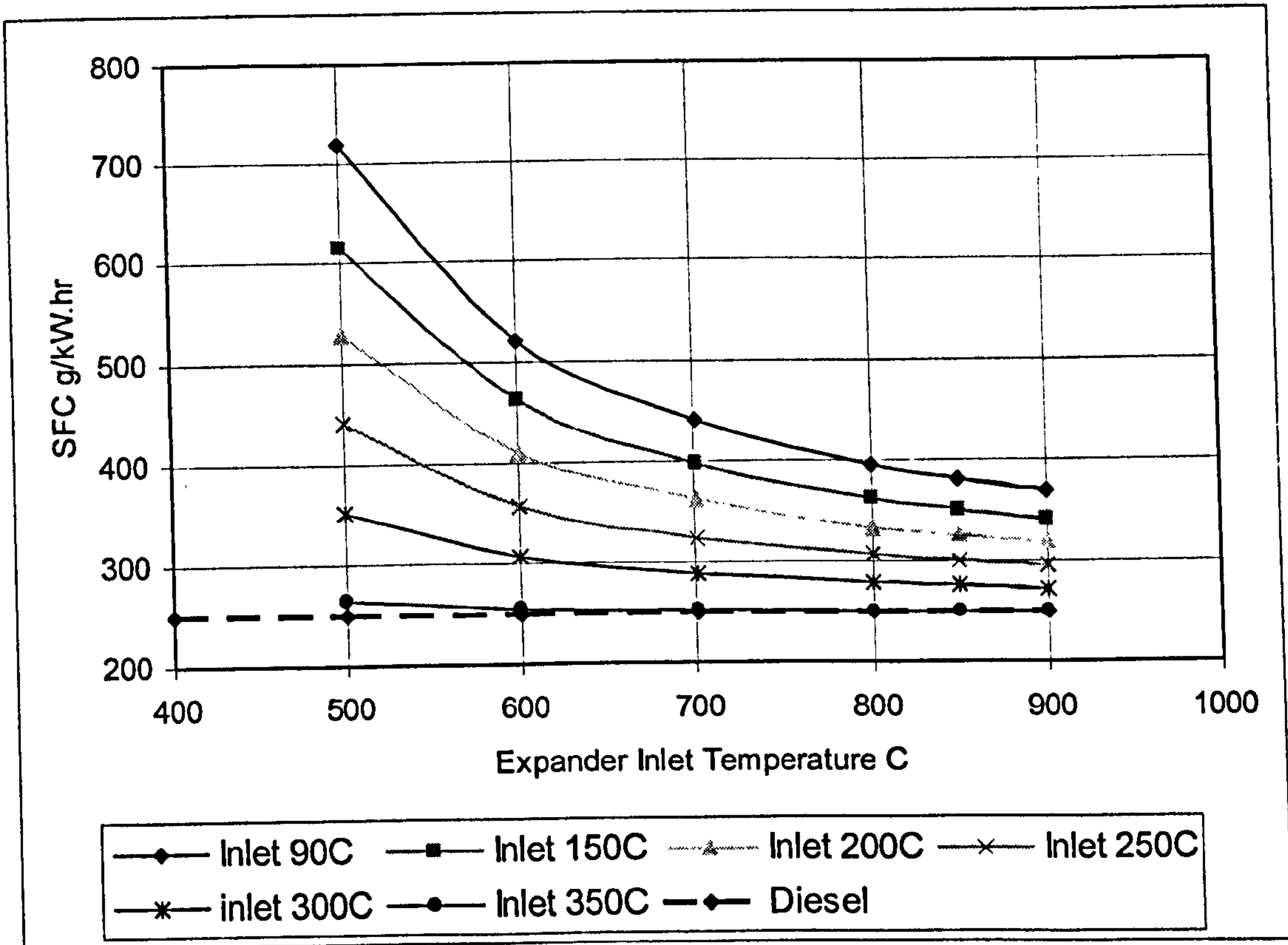


Fig 4.37 Specific Fuel Consumption Vs Expander Inlet Temperature

The Y axis (SFC - specific fuel consumption) has units of g/kW.hr as this is a unit by which comparisons can be made to internal combustion engines. Fig 4.37 shows falling values of SFC as the expander inlet temperature increases (less compressor work) and the amount of regeneration is increased. A comparison is made with a naturally aspirated diesel engine (Perkins 1,8 L, 4 cyl at the University of Plymouth) which has a SFC of 250 g/kW.hr. Only with gas inlet temperatures of 850 C and regeneration to 350C does the RJC engine have a similar SFC to the diesel engine. The falling characteristics are typical of a Joule cycle engine (gas turbine) in that as load reduces the SFC rises rapidly

Thermal efficiencies based on the net work output to the energy in the fuel

are shown at Fig 4.38. A maximum of 36% thermal efficiency is achieved at a gas inlet temperature of 850C and regeneration of 350C. This efficiency is the same as the naturally aspirated diesel engine.

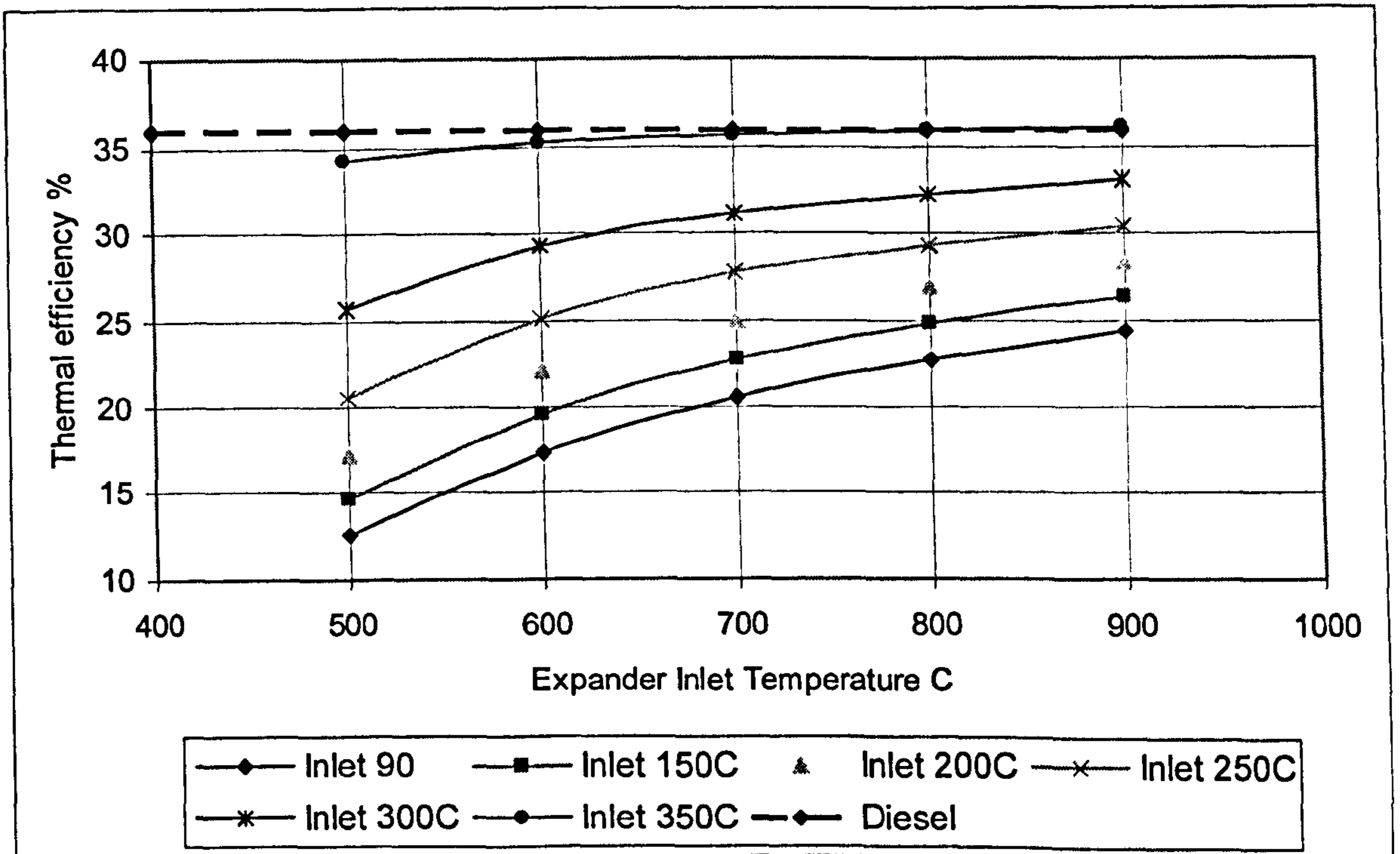


Fig 4.38 Thermal Efficiency Vs Expander inlet temperature Showing Combustor Inlet Temperatures from Regeneration

#### 4.11 Compressor Sizing and Exhaust Valve Control

Further investigations were undertaken to identify the matching of the expander and compressor and what design of compressor control would achieve matching.

Ref. 7 used the parameter 'swept volume ratio' (expander swept vol / compressor swept volume) and concluded that an optimum was 2.5:1. This work however used a  $n$  value for expansion of 1.3. for gas inlet temperatures of 850 C. Fig 4.39 shows the influence of the polytropic value  $n$ , for expansion, on the swept volume

ratio for a range of gas inlet temperatures with the together with the isentropic values

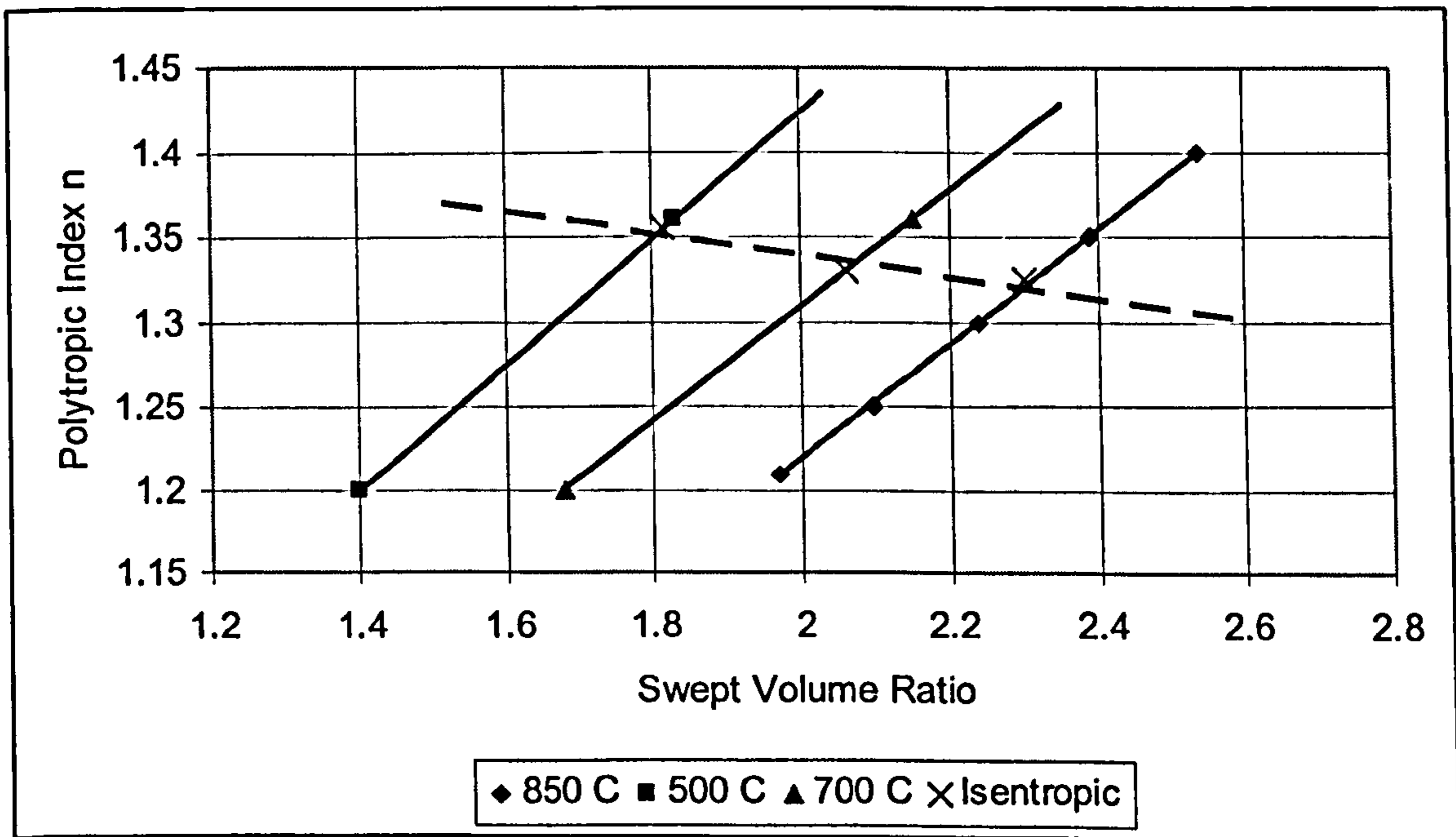


Fig 4.39 Polytopic Index vs. Swept Volume Ratio

The sizing of the compressor (swept volume) thus has to vary as the gas inlet temperature changes in order to balance the mass flow. Compressor design options were further investigated using the following assumptions:

1. Opposed piston RJC engine. One cylinder as the expander and one cylinder as the compressor. Same stroke for expander and compressor.
2. Expander swept volume 325 ccs stroke 82 mm bore 61.5 mm
3. Swept volume of compressor 162.5 ccs
4. Polytopic value for compression  $n=1.21$
5. Gas inlet temperature 850C

Option 1.

Compressor inlet and discharge valves of the reed type. Bore has to be reduced to 58 mm from 82 mm. Mass to be added to compressor piston to reduce out of balance forces. This results in fixed valve timing and matching can only occur at one temperature.

Option 2.

Maintain same bore and stroke but with a variable timed compressor inlet poppet valve and a discharge reed valve. Less out of balance forces but swept area is greater hence friction will be higher. Has the potential to provide matching over a range of temperatures

Option 3.

Similar to option 2 but with a poppet discharge valve. More complicated solution than option 2.

Option 2 has the potential to provide the best solution

#### 4.11.1 Variable Valve Timing for Compressor Inlet Valve

The effect of varying the valve timing to provide matching for varying inlet gas temperatures was investigated. For lower temperatures of the supply gas the compressor has to deliver more mass and thus more work is required.

Varying the inlet valve timing can achieve mass balance for a range of temperatures. The closing point of the inlet valve determines the volume of air, and thus mass, to be compressed.

Inlet valve timing will have to be controlled by temperature. As more fuel is burnt the inlet gas temperature will rise but to maintain a constant speed the inlet valve

timing will have to be advanced. i.e. it will close at a smaller angle before TDC. The compressor will now require less work and thus more net power can be obtained.

By calculation for 850 C conditions the inlet valve has to close at 103 degrees BTDC. By comparison for 700 C the inlet valve has to close at 113 degrees BTDC and for 600 C the inlet valve has to close at 122 degrees BTDC. Hence the inlet valve timing range will need to be 21 degrees for a temp range of 250 degrees.

Varying the inlet valve timing will have an effect on the compressor suction conditions. If the inlet valve closes at 122 degrees before TDC then suction will start earlier and the compressor clearance volume expansion may not have reached atmospheric pressure and some of this work will be lost. As the total suction loss in the portable compressor was calculated as 9.3 % of the cycle work then a 21 degree difference i.e. opening 21 degrees later would only result in a few percent loss of the cycle work. Inlet valve timing should therefore be set for maximum temperature conditions with any losses taken at lower temperatures.

### 4.11.2 Types of Variable Valve Timing Mechanisms

Most of the major automotive engine manufacturers now employ some form of variable valve timing although the degree of variability is less than the 20 plus degrees needed for the RJC engine. A simple design suitable for the RJC engines and giving the 20 plus degrees required is shown at Fig 4.40



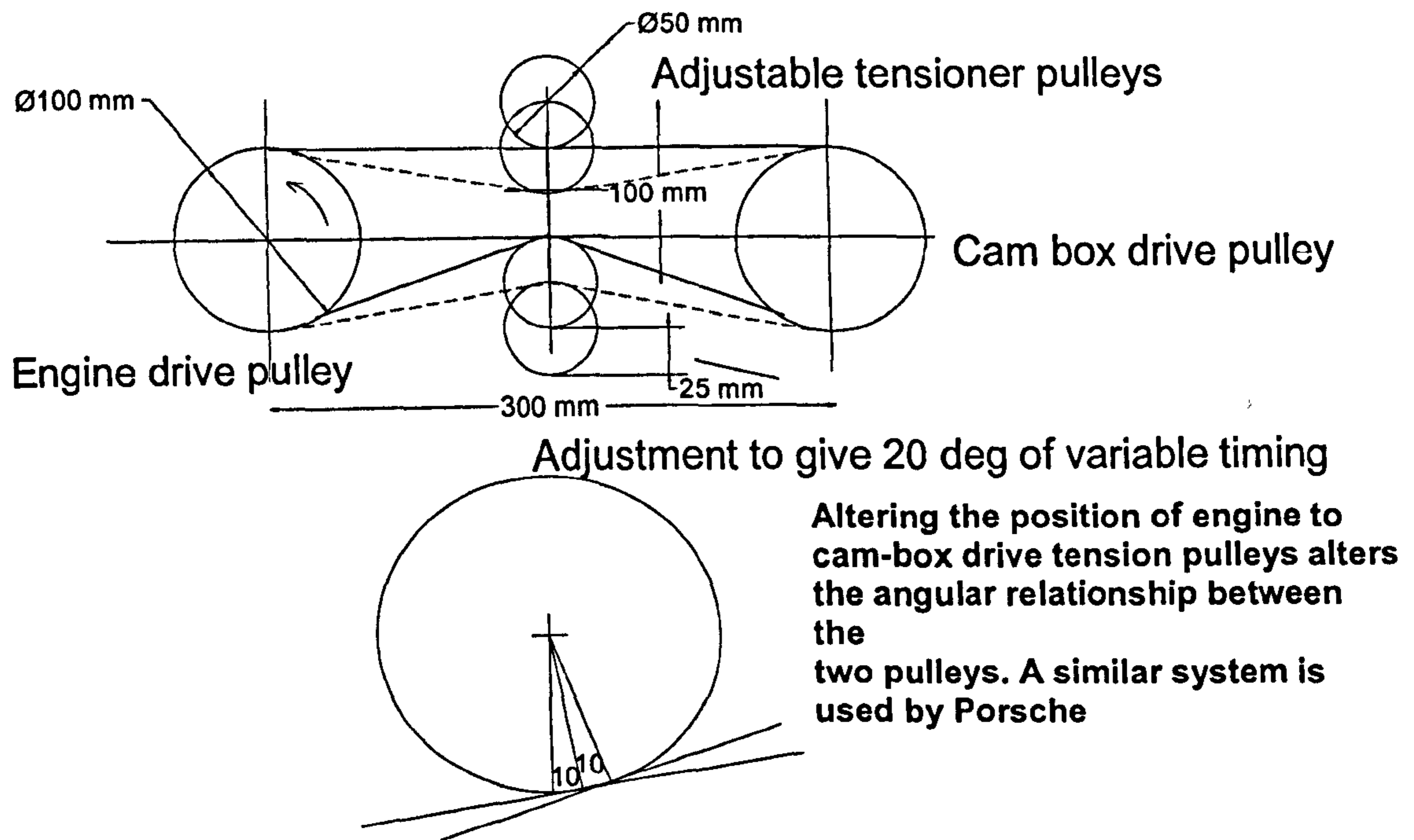


Fig 4.40 Variable Valve Timing Arrangement

## 4.12 Conclusions from Engine Testing and Extrapolation of Data

### 4.12.1 Limits of Operation: Pressure and temperature.

In the evaluation of performance the maximum system pressure used was 7.5 bar g. This represents a balance between what is realistically achievable from a single stage reciprocating pressure with a polytropic  $n$  value of 1.21. Lower pressures result in lower work available from the expander and relatively higher values of friction whilst higher pressures result in higher compressor work from the higher compression and higher discharge temperatures.

A temperature limit of 850 deg C for the inlet gas was assumed. Although such temperatures can be generated in the combustion chamber (1000 C was actually achieved) there would be concerns on the metallurgical limit of pistons and the cylinder lubrication at such temperatures. Piston design could limit the severity of

the conditions and this is discussed in Part 6 on the design of a new engine.

### 4.12.2 Effect of Friction and Clearance Volumes

Mechanical efficiencies of at least 90% are required to achieve sensible values of net power. Some solutions to achieve this 90% including reduced piston ring friction and reduced crankcase bearing friction have been outlined. Again piston/ring design would play a major part in achieving this higher mechanical efficiency together with the use of a hypocycloidal drive Ref.24 to reduce crankcase bearing friction and piston side forces.

The influence of clearance volumes although recognised was not fully appreciated in the earlier design of the cylinder head. Clearance volumes of less than 3% are required to limit the recompression work and thus maximise the indicated power. As a simple estimate every cc reduction from 30ccs to 10 ccs increases the output by 14 watts. Again piston design will heavily influence the clearance volume.

### 4.12.3 True Polytropic Values.

Polytropic values determined from the PV diagrams are on cold air were 1.22 for the expander and 1.21 for a reciprocating compressor.. Earlier hot gas models assumed a  $n$  value for both expansion and compression of 1.3. The lower the  $n$  value for expansion the higher the expansion work but with the consequence that full expansion is not attained resulting in lost work in the exhaust. The extra work however is more than offset by the compressor work required for a given mass flow rate resulting in a decrease in net work. Further work to determine more

exact values of the polytropic index for expansion is required and this is undertaken in Part 3 where detailed engine modelling is undertaken

### 4.12.4 Apparent Valve Opening / Closing

Poppet valves act as variable orifices and restrict flow at positions close to opening and closing. This has to be taken into effect in the design of cams to ensure that increased/reduced opening/closing angles are used to compensate.

### 4.12.5 Power and Size of Low BMEP Engines

The RJC engine using inlet gas pressures of 7.5 bar g will always be a low BMEP engine. By comparison Ref. 25 the BMEP is only 65% of that of a comparable sized single cylinder diesel engine. One major outcome of this is that in terms of the volume envelope an RJC engine it will be significantly larger than a comparable four stroke diesel engine.

### 4.12.6 Thermal efficiencies

The highest thermal efficiency derived from the simple modelling of the BMW RJC engine was 36% and equal to a known naturally aspirated diesel engine. This efficiency was only achieved with a gas inlet temperature of 850C and a regeneration temperature of 350C. The SFC of the RJC engine was typical of other Joule cycle engines (gas turbines) in that at part load the SFC had a rapidly rising characteristic. Increasing the system pressure from 7.5 bar g to 8.5 bar increases the thermal efficiency by only ~1% as the extra net work output is offset by higher compressor work and higher heat input. Operating at higher pressures than 7.5 bar g is not seen as a practical option as it would result in higher leakage

## Part4

losses around compressor and expander piston rings and may possibly negate the small potential improvement in thermal efficiency.

## **Design of a RJC engine**

### **5.1 Engine design**

The modelling undertaken in Part 3 identified the frictional and thermal losses. It also identified limitations imposed by valve pressure losses on the minimum valve area and the maximum RPM. From the results of modelling (Part 3) and testing (Part 4) a number of characteristics were established that set limits on the engine design parameters.

The major parameters in the design of an RJC engine are

1. Cylinder dimensions
2. Piston design
3. Valve and cam design
4. Crankcase design.
5. Combustor

and are described in the following sections.

#### **5.1.1 Cylinder dimensions**

The large valve area on both inlet and exhaust, needed to minimise pressure losses requires an engine with a bore to stroke ratio of greater than unity, ideally a maximum ratio of 1.2:1. As a first iteration in an engine design the modelling determined that the maximum valve area, through which the gasses pass and for all valves, should be in the order of 45% of the cylinder cross sectional area. In order to accommodate this area for a poppet valve configuration four valves per cylinder would be required.

### 5.1.2 Piston Design

The use of conventional automotive pistons requires that some modifications need to be undertaken for use in an RJC engine. The major modification is that the pistons need a flat crown so any piston used that has a profiled crown has to be machined to accept a separate crown. Such an arrangement allows flexibility in the determination of the piston height as the separate crown can be manufactured to result in the required height of the composite piston.

Friction between the cylinder liners and the piston rings is responsible for up to 80% of all friction losses in a conventional reciprocating piston engine. The value of the friction force is not constant and is a function of the pressure in the space above the piston and piston speed.

It is possible to run on a single gas ring and an oil control ring – removing the second ring. Ref 13 details the effect of such a configuration on a diesel engine and the friction between rings and liners and found that higher peak frictions were experienced with a single gas ring but that the overall friction in a cycle was reduced. Because the RJC engine operates at lower peak and mean pressures than a conventional engine a piston with a single gas ring and an oil control could be employed.

The piston would need to have a flat crown and operate against a flat piston head. This is required to achieve a small clearance volume ideally less than 3% of swept volume. The investigations into ring pack friction identified that a single gas tight compression ring and a single oil scraper ring would result in a lower friction than a conventional two compression ring and one scraper ring design. Because of the lower cylinder pressures in an RJC engine, compared to a conventional IC engine, the single gas tight compression ring will not be subject to high differential pressures.

## Part 5

Some consideration was given to the use of an 'anti polish ring' arrangement to provide added protection to the cylinder surfaces from hot gas during the admission and early expansion stages. Anti-polish rings are commonly employed in large diesel engines and have the additional advantage of reducing oil consumption and protecting the upper surfaces of the cylinder from exposure to hot combustion gases. The position of the single gas tight ring would need to be a distance away from the flat piston crown such that the lubricated surface of the cylinder wall only becomes exposed once the piston crown is below the bottom of the anti polish ring and the expansion of the gas has started. There is however a conflict between designs that incorporate an anti polish ring, which necessitate a longer stroke engine, and an engine with a bore greater than the stroke – over square. The ideal situation would be to incorporate a form of anti polish ring with an over square engine and this should be investigated in any detail design work

With gas inlet temperatures up to 850C piston cooling will need to be enhanced. In small automotive engines splash lubrication is used for cooling the underside of the piston crown but this may be inadequate for the RJC engine. Higher oil flow to this area will be required possibly by jetting oil to the piston underside. Such jetting is employed diesel engines with power outputs >250 kW

Piston materials will need to be chosen for their durability under high temperature conditions, have good thermal conductivity for cooling and resist thermal distortion. Additionally the findings from Ref 14 regarding cylinder honing, and piston skirt profile will need to be taken into account.

Piston design, to minimise friction and durability, is an important aspect in the performance of an RJC engine. This aspect will require further development and testing.

### 5.1.3 Valve and Cam Design (Expander)

During the design of the BMW based engine consideration was given to rotary valves as well as poppet type valves. The potential problem associated with a rotary valve arrangement was hot gas sealing. Although preliminary designs were drawn up it was considered that the timescale to test and develop a rotary valve would compromise the programme. Therefore the simpler route of using poppet valves exploiting known technology was employed. Durability of the inlet valve and inlet valve seat, continuously exposed to high gas temperatures, could not be evaluated but is likely to require the use of high temperature materials. The selection of materials will require further investigation and durability testing. It is proposed that both the rotary and poppet valve arrangement be further investigated, both having their merits and demerits.

For a rotary valve arrangement timing is controlled by the valve portages and as such cams are not required. Rotary valves have been developed for automotive engines but their use is currently restricted to demonstration engines and in this application no information on durability or detailed performance is available.

For poppet valves the designs used on the BMW based engine demonstrated that the concept was basically sound. Valve timing and the duration of valve opening, is dictated by cam angles and cam design went through several iterations to achieve the maximum performance from the expander. The throttling effect of poppet valves at opening and closing introduced the concept of 'apparent valve opening' and as such cam angles, valve lift profiles and valve timing have to be carefully designed to compensate.

Modelling demonstrated that at an envisaged speed for a RJC engine of 1500 RPM the required poppet valve area, to minimise pressure losses and thus reduce lost work, needed to be ~45% of the cylinder bore area. Valves of larger size,



although ideal, could not be physically accommodated within the cylinder head area. 'High lift' valves and a small degree of advanced valve timing on the inlet (modelled at 8 deg BTDC) reduced the pressure losses to a minimum and this strategy needs to be further explored. A similar approach is also needed for the exhaust valves.

Rotary valves were also modelled noting that an advantage can be gained in valve area because the Cd value for a slot is  $\sim 0.9$  whilst for a poppet valve is  $\sim 0.75$ . The equivalent to 'high lift' is achieved by having the slot width in the rotary valve smaller than the slot width in the cylinder but this comes with a possible constraint of a large rotary valve diameter. Modelling showed that for an engine of 120 mm bore and 100 mm stroke the rotary valve diameter was 50 mm and the slot dimensions were 13mm wide and 100mm long. The corresponding slot size in the cylinder head was 23 mm wide and 100 mm long.

Reducing the slot length and maintaining the same flow area requires a larger rotary valve diameter.

#### 5.1.4 Crankcase Design

Several designs for a crankcase using a hypocycloidal have been generated at the University of Plymouth including a working model. Such a design lends itself to a two piston horizontal configuration with one piston as the expander and one as a compressor with the potential for reduced vibration and the use of antifriction bearings Ref 24. It is proposed that for the next development stage of the RJC engine that such a crankcase be designed and tested.

### 5.1.5 Combustor Design

From experimental testing stable high temperature combustion under pressure with a fluctuating gas flow has been demonstrated. The combustor design employed an outer air inlet tube and an inner combustion tube with air flows split between a primary air flow, that mixes with the combustion gas in a mixing tube and a secondary air flow that enters the inner combustion tube, via a series of holes, from the outer tube. Whilst recognising that such a combustor demonstrated the concept improvements are possible.

Such improvements would need investigation into the minimum volume (size) of the combustor to maintain stable combustion, the balance and control of primary and secondary air flows and the possibility of using a system employing primary, secondary and tertiary air flow as employed on gas turbines. The inner and outer Tubes of the combustor tested were of stainless steel. Whilst this may be satisfactory for the outer tube the inner tube will need to be manufactured from high temperature alloys. Burner nozzle design went through several iterations to improve the stability of combustion. A key aspect was the need to ensure that the gas velocity was lower than the flame velocity

### 5.1.6 Rotary valves

Some initial design work had already been carried out on rotary valves and the concept has been proven in automotive applications Ref. 23. Such valves are simple in concept and most importantly have a lower overall volume and height than a poppet valve arrangement. However because the RJC engine operates on the principle of supplying hot pressurised gas from an external source the design of the valves at Ref. 23. cannot be easily modified so this particular design was not explored further. The major problem of any rotary valve design is the sealing of

gases at up to 900 C where the leakage paths are from the pressurised gas to the cylinder – valve closed position- and any leakage from the pressurised gas to atmosphere. In addition the rotary valve has to be supported by bearings and such bearings have to be isolated from the hot gases and/or high temperatures. The principle of the rotary valves is that they consist of a rotating barrel in a sleeve with ports in the barrel and sleeve such that when the ports line up gas can pass through. The smaller the clearance between barrel and sleeve then the less gas leakage that can occur both from port to port and axially along the barrel. A method to achieve small clearances is to have both the barrel and sleeve in the form of a taper whereby clearance is controlled by axial movement of the sleeve in the barrel. An outline design of such a cylinder head which incorporates a single tapered barrel for both inlet and exhaust, anti friction bearings and mechanical seals is shown diagrammatically at Fig 5.1

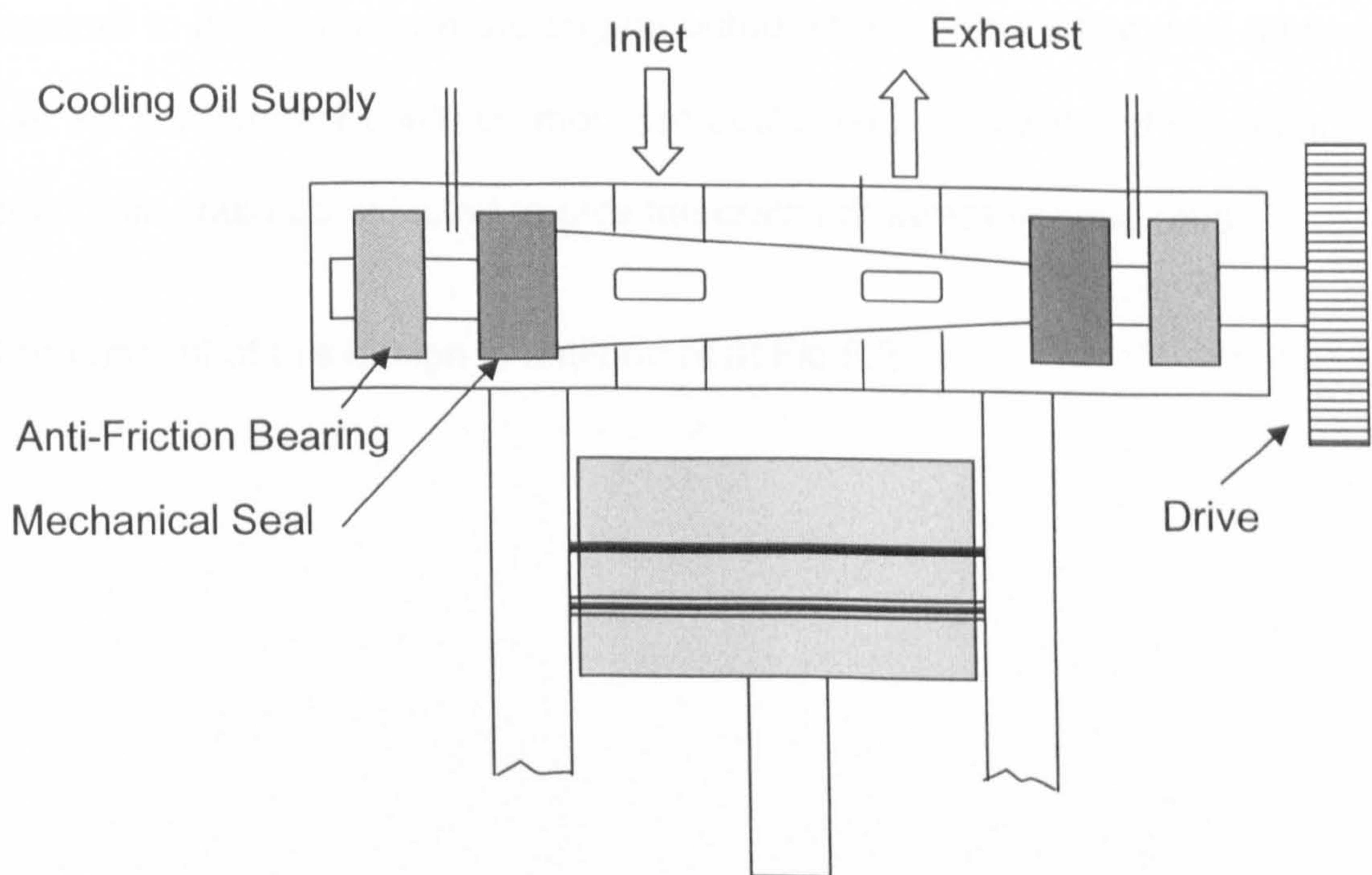


Fig. 5.1 Diagrammatic Representation of Taper Rotary Valve

### 5.1.7 Hypocycloidal Drive

One issue that had been addressed in some detail prior to the start of this project was the use of a hypocycloidal drive, to connect pistons to an output shaft. Ref.24. Such a drive uses anti friction bearings and can provide vibration free operation. A horizontally opposed piston engine utilising a hypocycloidal drive arrangement of one piston as the expander and one as the compressor was drawn in outline. To even meet the power requirements of 3 kW an expander piston of over 100 mm dia was required which in turn for an engine having a stroke of 100 mm ('square) necessitated a large hypocycloidal drive.

If both pistons were used as expanders then it was possible to reduce the size of the engine to fit within the required footprint. Further development of this idea for an engine of 3 kW output resulted in a design overall length of less than 500 mm. The design of twin opposed expanders meant that a separate compressor was required to be driven from the engine output shaft. This had several advantages in that the compressor could be mounted such that it was within the footprint and the drive ratio could be selected to give the optimum swept volume ratio.

The concept of this design is outlined of at Fig 5.2

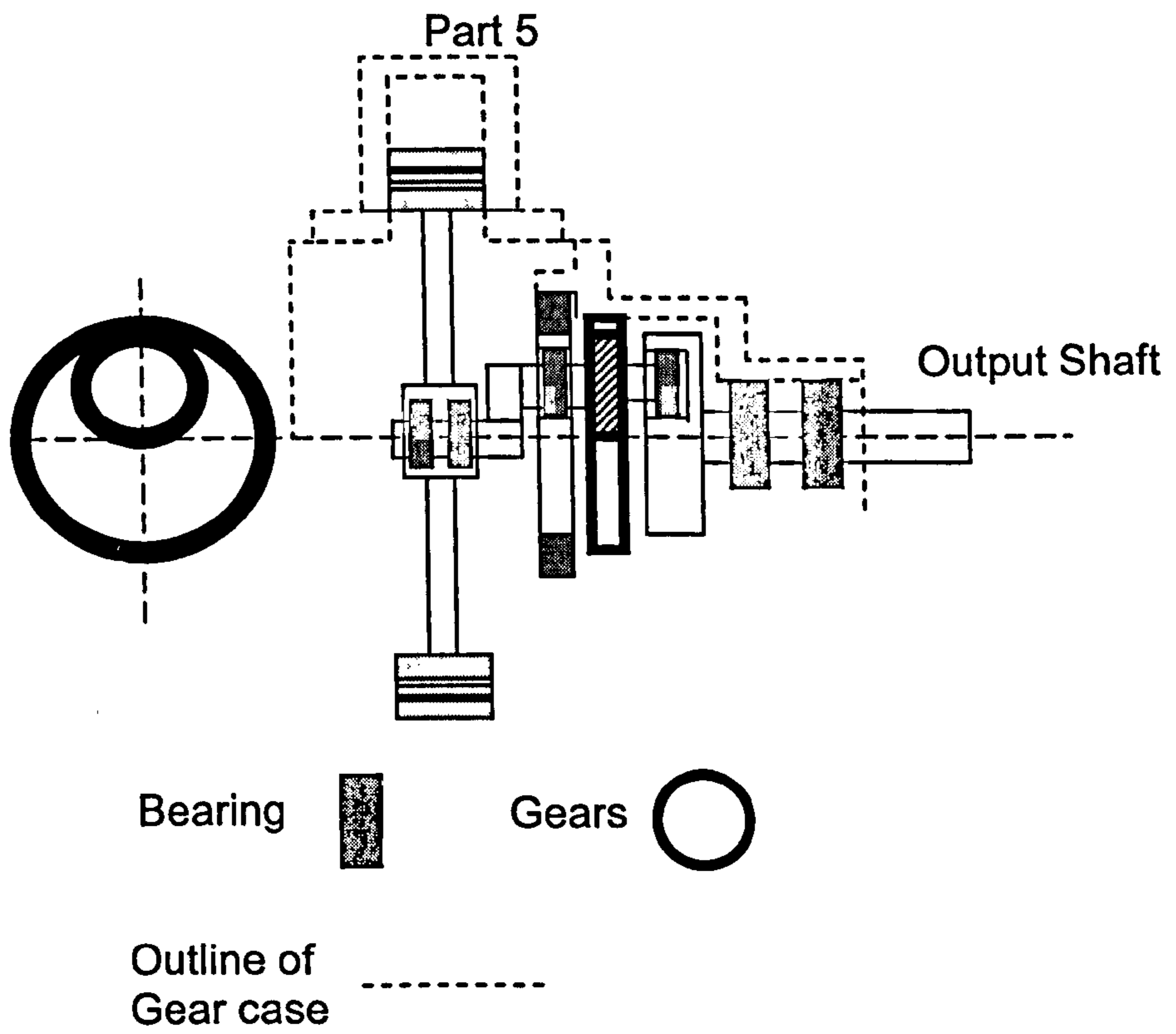


Fig. 5.2 Outline of Design of a Hypocycloidal Drive for an Opposed Piston RJC Engine

## **Summary and Conclusions**

### **6.1 Micro CHP Opportunities**

The trials conducted in the UK on Micro CHP for single dwellings came to an uncertain conclusion. All micro systems evaluated were based on Stirling engines which have poor power to heat ratios because the thermal efficiency of the Stirling engine is at best no more than 20%. Improving the power to heat ratio is the key requirement and this can only be achieved by the use of more thermally efficient prime movers/devices to produce electricity. Stirling engine based micro CHP systems do however have one advantage in that they can be a direct physical replacement for a domestic boiler and installed inside a dwelling. If this condition is removed and the micro CHP system is installed external to a dwelling then other types of prime movers/devices can be employed. In Japan two systems, one based on small gas engines and the other on fuel cells, are on large scale trial these being based external to the dwelling and includes a large hot water storage tank. Such external arrangements are a distinct way forward for an increase in Micro CHP in the UK.

### **6.2 The RJC Engine for Micro CHP Systems**

The research proposed and investigated the use of the RJC engine for micro CHP applications. Detailed modelling and test engine evaluation determined that an RJC could be made to work and with a potential thermal efficiency of 33%, which is equal or better than a small internal combustion gas engine, and with a best power to heat ratio of 1:2. Additionally the work also identified the limitations and constraints of the RJC engine that were taken forward into proposals for the design, and operation of, such an engine.

## **6.3 Engine Design and Operation of Future Engines.**

### **6.3.1 Temperatures and pressures.**

A maximum system temperature of the hot gas at entry to the expander was set at 850C. This is somewhat arbitrary but is considered a safe upper limit for both metallurgical reasons and to safeguard lubrication between the expander piston and cylinder interface. Higher gas inlet temperatures will improve thermal efficiency and power output for a given engine but at a higher risk to longevity.

A maximum system pressure of 7.5 bar g was set as this represented an optimum for a single stage reciprocating compressor. Higher system pressures will result in higher expander power outputs but the increase in compressor work required and the increase in compressor discharge temperature result in only small improvement in thermal efficiency.

### **6.3.2 Efficiencies**

The mechanical efficiency of the RJC engine has a direct relationship with thermal efficiency so the requirement is to have as high a mechanical efficient engine as possible. An overall engine mechanical efficiency of 90% was proven to be achievable. Applying this mechanical efficiency then at gas inlet conditions of 850C and 7.5 bar g an engine thermal efficiency of 24% was realised. This was improved to 33% with regeneration of the combustor inlet air to 350C by heat transfer from the exhaust gas. Incorporating a 33% thermal efficient RJC engine to a micro CHP system resulted in a system efficiency of 79% and a power to heat ratio of 1:2.

### 6.3.3 Compressor Requirements

Matching compressor output to expander requirements at any condition of gas inlet temperature, and system pressure requires control of the mass delivered. A reciprocating compressor was found to be more suitable than a scroll compressor primarily due to the lower discharge temperature for the same mass flow and thus less work required. Control of the mass flow in a reciprocating compressor can be achieved by use of a variable suction valve.

### 6.3.4 Power Output, Speed, Cylinder Dimensions.

The RJC engine is a low BMEP engine when compared to an internal combustion engine. Investigations determined that a RJC engine would produce 3 Watts per cc (at a thermal efficiency of 33%) whilst published performance data for a small single cylinder naturally aspirated diesel engine was 6.8 Watts/cc. Thus for nominal output of 3 kW from a RJC engine an expander displacement of 900 ccs is required.

Pressure losses across the expander inlet valve(s) increased significantly for higher engine speeds resulting in only small increases in power output but at lower thermal efficiencies. To overcome the pressure losses larger inlet valve area are required but this is limited by the size and number of poppet type valves that can be accommodated within the cylinder head for an engine with a given bore size. The work identified that an engine speed of 1500 RPM was achievable but that to maintain the output of 3 Watts/cc the expander cylinder required a bore to stroke ratio of 1.2:1. The use of rotary valves was investigated and highlighted that smaller valve area, when compared to poppet valves, resulted in similar pressure losses. This implied that either different cylinder bore to stroke areas could be used or more importantly the engine could be operated at higher speeds.



### 6.3.5 Foot Print

With an output at 3 Watts/cc, being less than half of that of an internal combustion engine, the physical size of an RJC engine will be larger for the same power output. When the compressor and combustion system are included the overall footprint of a RJC micro CHP system will make it significantly larger. This is likely to detract from the applicability of a RJC engine based micro CHP system.

### 6.3.6 Further Development

Part 5 identified detail design requirements needed for a future engine. Of particular importance is the reduction of friction and the use of a hypocycloidal drive needs to be investigated. Additionally the use of rotary valves is an attractive proposition in that it overcomes the complication of poppet valve actuation and some of the associated pressure losses. A rotary valve working at the required temperatures and pressures, and with minimum leakages, will require extensive development work but if successful will enhance the RJC engine.

With external combustion the use of alternative fuels is a possibility however this has yet to be fully explored and in particular will influence the design of combustor.

### 6.3.7 Overall Applicability and Viability

Whilst the concept of a RJC engine micro CHP system has been proved and that it can be as thermally efficient as an IC engine system its larger foot print will detract from it being a direct replacement for a domestic boiler within a single dwelling. Positioning the micro CHP system external to a building offers a solution. Further development work to produce and test a working prototype RJC engine with high mechanical and thermal efficiencies, incorporating all the design details identified in this work, is needed to determine the long term viability.

# Annex 1

CV of Fuel MJ/Kg 40  
Grid Carbon. KgC/kWh 0.117  
Boiler Efficiency % 80

Fuel CH4  
KgC/Kg Fuel 0.75

RJC @850 C  
Electrical Output W 3387  
Heat Output W 6508  
Overall Efficiency % 78

Total Output W 9895  
Heat Supplied W 12685.9

Carbon Produced Kg 0.856298

Carbon By Grid Kg 0.396279  
Carbon by Boiler Kg 0.549113  
Total Carbon Kg 0.945392

Carbon Saved % 9.423971

RJC @600 C  
Electrical Output W 978  
Heat Output W 6113  
Overall Efficiency % 56

Total Output W 7091  
Heat Supplied W 12662.5

Carbon Produced Kg 0.854719

Carbon by Grid Kg 0.114426  
Carbon by Boiler Kg 0.515784  
Total carbon Kg 0.63021

Carbon Saved % -35.6244

### Carbon Saved Calculations 1.1

## **Annex 2**



## THE DEVELOPMENT OF THE RECIPROCATING JOULE CYCLE ENGINE FOR MICRO CHP APPLICATIONS

PAPER NO.: 61

R.W. Allen, Research Associate, School of Engineering, University of Plymouth (UK)

Dr M.A. Bell, Principal Lecturer, School of Engineering, University of Plymouth (UK)

### SUMMARY

The Reciprocating Joule Cycle (RJC) engine employs the Joule (or Brayton) cycle with its performance determined by the characteristics of a positive displacement compressor and expander as opposed to rotodynamic. Development of an engine by thermodynamic modelling and the building and testing of a basic technology demonstration engine has been an ongoing activity at the University of Plymouth for the last five years.

The thermodynamic modelling shows that an engine with thermal efficiencies higher than both the Otto and Diesel cycles are practically possible. The RJC engine has certain drawbacks that have precluded its development as an automotive prime mover, however it is suitable as a prime mover in Micro Combined Heat and Power (Micro CHP) applications.

Although such an engine requires no new fundamental technologies successful performance depends upon the design of components unique to the engine. Component development was undertaken by using a basic technology demonstration engine adapted from a conventional four cylinder automotive diesel engine. The critical components developed were the external combustion chamber and the inlet/exhaust valve timing and lift mechanism.

Operation of the technology demonstration engine confirmed the predictions from the thermodynamic model notably that high mechanical losses in the form of friction had a major detrimental effect on its overall thermal efficiency.

Knowledge gained from this development is being used in the design of a prototype engine suitable as the prime mover in a domestic dwelling level Micro CHP plant. The design will aim to minimise mechanical losses primarily by their use of anti-friction bearings in a hypocycloidal gearbox that will connect the expander and compressor. Other aspects of the proposed design are detailed in the paper.

### CONCLUSIONS

The RJC engine has been identified as a very suitable prime mover for Micro-CHP systems. It has the potential to deliver high thermal efficiencies, with the energy delivered split approximately equally into electrical and thermal energy. Additionally, a wide range of fuels can be burnt efficiently with low exhaust emissions.

Development of the engine has included thermodynamic modelling and the design and construction of a basic technology demonstration engine for component evaluation.

The major potential problem associated with the RJC engine and highlighted through experience with the technology demonstration engine, is friction the reduction of which will be addressed in the building and testing a prototype engine.

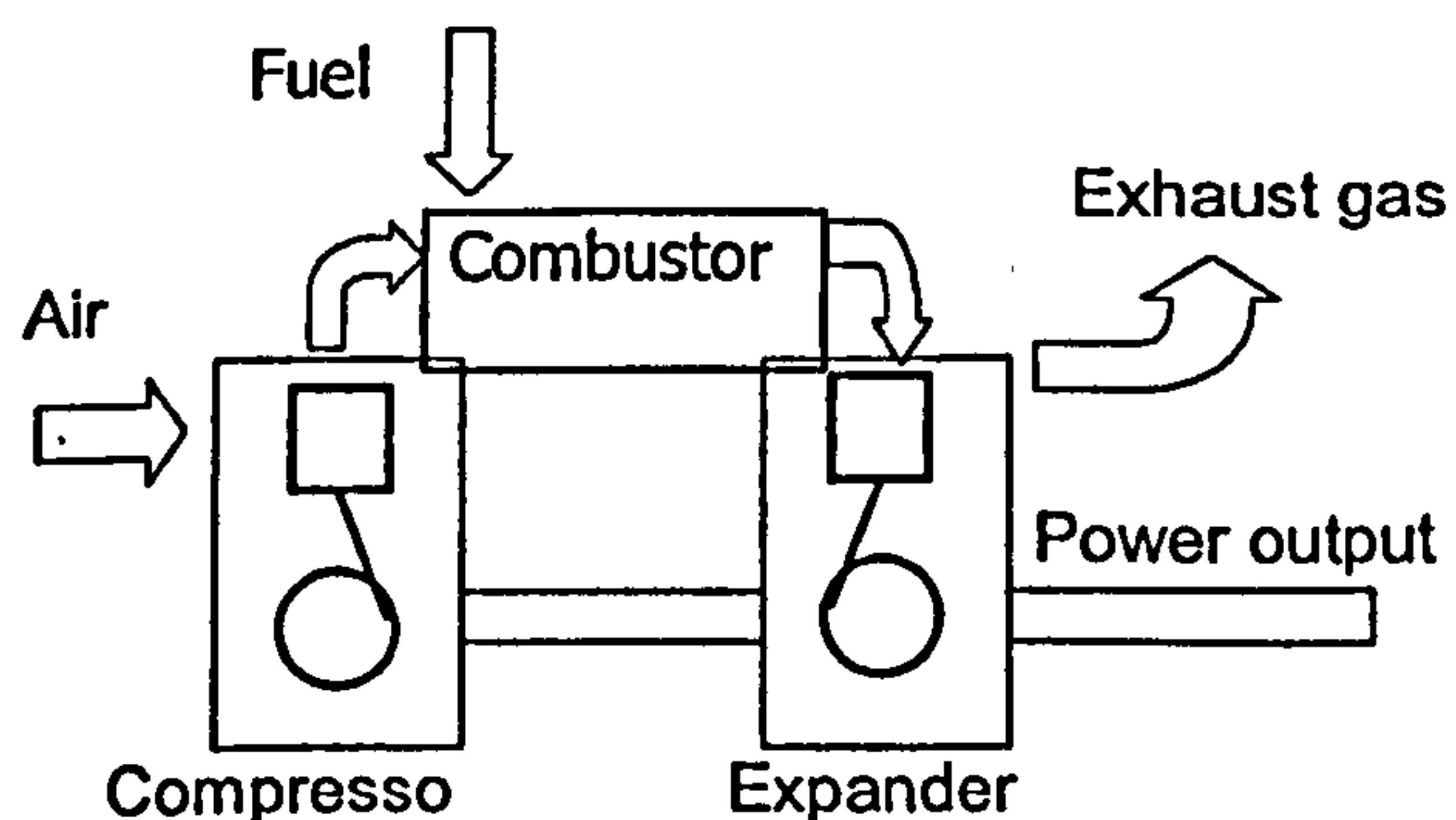
## INTRODUCTION

This paper describes the work undertaken on the development of the Reciprocating Joule Cycle Engine (RJC Engine) at the University of Plymouth (UK). In particular it identifies a specific application to which the engine is ideally suited notably Micro Combined Heat and Power (Micro CHP), and describes the work done to validate the theoretical modeling using a basic demonstration technology engine. The paper also outlines the work being undertaken on the design of a full prototype engine

## THE RJC ENGINE

This type of engine employs the Joule (or Brayton) thermodynamic cycle: the same as a gas turbine. Its performance is determined by the characteristics of a positive displacement compressor and expander as opposed to rotodynamic. A positive displacement compressor is connected mechanically to a reciprocating expander, with energy added to the compressor air delivery in an external continuous combustion process, the whole to produce net power. Fig 1 illustrates the basic components of an RJC engine where both the expander and the compressor are of the conventional reciprocating piston type.

Figure 1. Basic Schematic of an RJC Engine



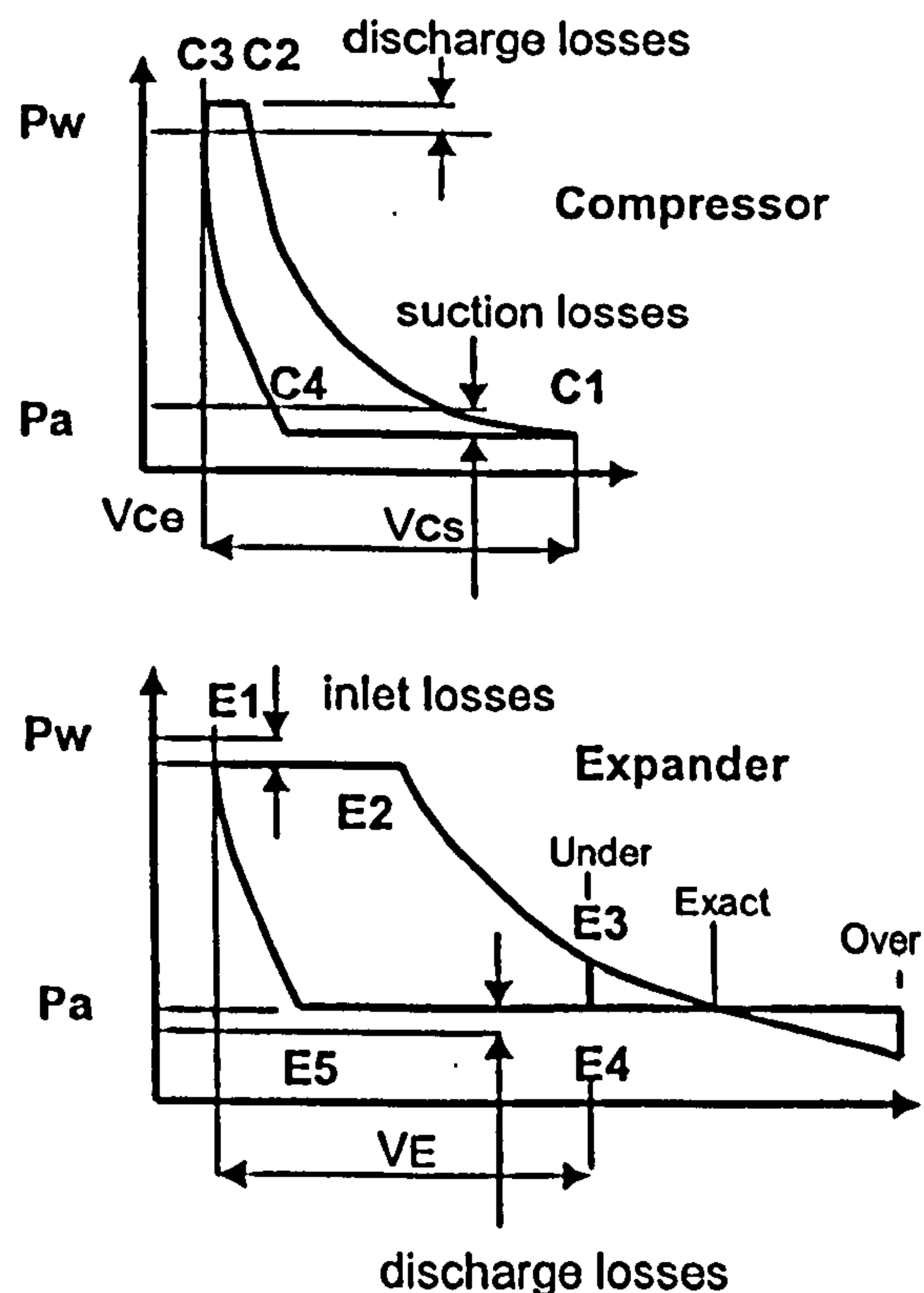
Although the concept of the RJC engine has been well understood for some time its development into a small practical prime mover has not been undertaken even though there are no new fundamental technologies involved. The basic reason is that, like gas turbines, the torque response rate of the Joule cycle is inferior to that of internal combustion engine cycles and is therefore unsuitable for conventional automotive applications.

## THERMODYNAMIC MODELLING

Research into the RJC engine has been an ongoing activity at the University of Plymouth (UOP) for the last 5 years and to the best of current knowledge UOP is a leading authority with an uninterrupted programme of work in this field. This has resulted in the formulation of a basic thermodynamic model, and the construction and testing of a basic technology demonstration engine.

Using air standard formulae a first order assessment has been made of performance. The degree of refinement allows for changes in gas properties, owing to combustion, leakages, pressure losses throughout the system, clearance volumes, and mechanical losses. The model does not allow for heat losses and the processes of compression and expansion are both assumed adiabatic. The manner in which the pressure drops and clearance volumes are incorporated into the model is illustrated by the respective pressure / volume charts at Fig. 2.

Figure 2. PV Diagrams for an RJC Engine



Further details of the thermodynamic modelling are at Ref 1.

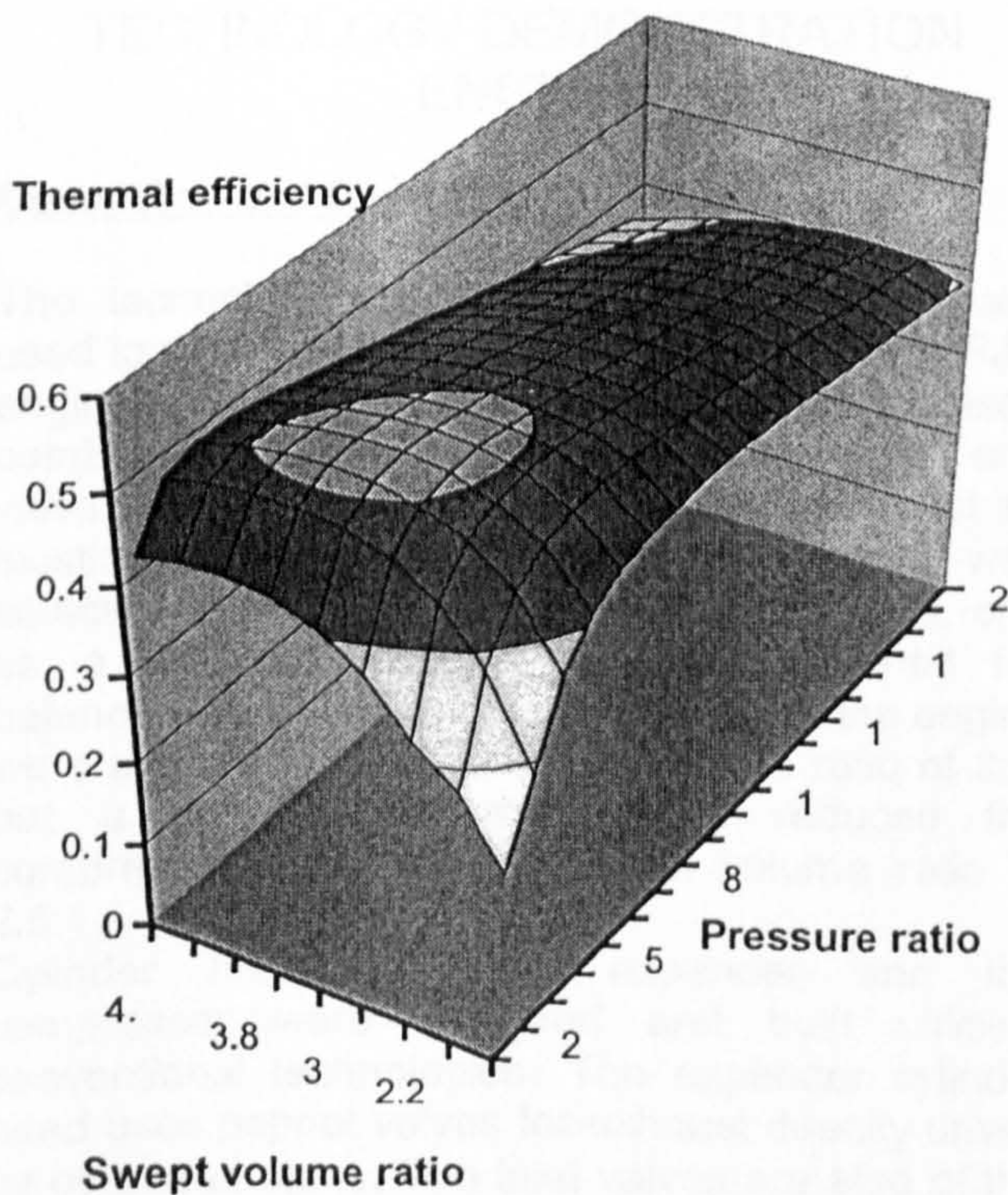
The controlling design factors of the engine are listed in table 1

Table 1 – Controlling Design Factors.

Operating pressure ratio -- controlled by inlet valve timing	$rp$
Maximum temperature controlled by air fuel ratio.	$T_{max}$
Compressor to expander swept volume ratio	$V_{Es} / V_{Cs}$
Clearance volumes	$V_{cc}$ and $V_{ec}$
Mechanical efficiencies	$\eta_m$
Pressure losses and Gas leakages.	$\Delta p$ See Fig 2

The two most important physical factors that influence the overall thermal efficiency and net specific work output are the pressure ratio and swept volume ratio. Using the values from Ref 1 for losses, clearances, valve timings and setting a maximum temperature of 1300 K a theoretical performance map is produced. This is shown at Fig. 3

Figure 3. Performance Mapping RJC Engine

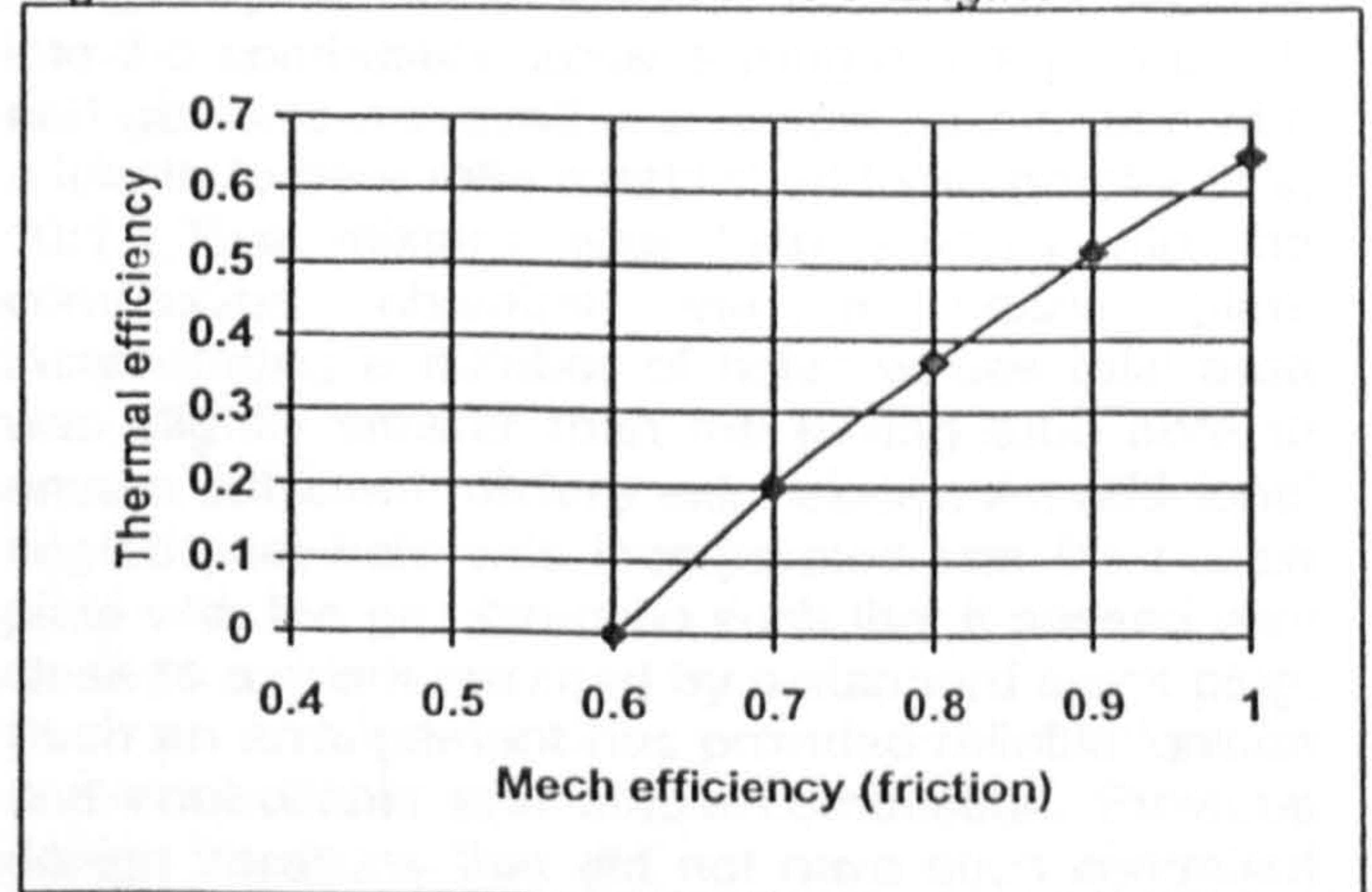


This performance map shows that comparatively high thermal efficiencies are possible with operating pressure ratios above 5 and swept volume ratios of around 2.5:1. This performance is based on the use of a recuperator that uses exhaust energy to pre-heat the combustion air.

The model also shows that losses in the system due to friction (mechanical efficiency), leakages and pressure losses have a significant impact on the thermal efficiency. The greatest impact on net work output comes from the mechanical losses primarily in the form of friction between the lubricated surfaces. This is shown at Fig 4 with the values determined via the thermodynamic model. The reason why friction has such a major impact is that with relatively lower pressures in the expanders, compared to internal combustion engines, high friction can represent a significant percentage of the expander work.

Pressure drops and leakage losses have a lesser effect on the thermal efficiencies and are described in more detail at Ref 1.

Figure 4. Mechanical Losses RJC Engine



By iteration of the design factors in Table 1 optimum values can be identified that result in high thermal efficiencies. The outcome from thermodynamic modelling is that the RJC engine has the potential to be more thermally efficient than the Otto, Diesel or Stirling cycle engines.

## APPLICATION OF THE RJC ENGINE

The RJC engine lends itself best to steady operation with its output specified by its speed and power. It is also best suited to small power outputs (<30 kW) where it is potentially more thermally efficient than other types of engine. The RJC engine employed in a micro-CHP system has the potential

to convert energy at up to 90 % split equally between electrical power and usable heat, reducing reliance on less thermally efficient centrally generated electricity which in turn will reduce overall CO<sub>2</sub> emissions. A conservative estimate of CO<sub>2</sub> emissions based on the electrical generation from a RJC micro-CHP system, utilising natural gas, is ~ 0.24 kgCO<sub>2</sub>/kWh, which is a major reduction when compared with the emission of 0.43 kgCO<sub>2</sub>/kWh from the electricity public supply network. Additionally, the external combustion process of the RJC engine has the potential to efficiently burn a wide range of gaseous and liquid fuels with low emissions of nitrous oxides and other exhaust contaminants. Whilst other micro-CHP systems based on Otto cycle engines or Stirling engines may be more commercially advanced they are not efficient in the production of electrical power and will thus in the longer term have a lower impact on reducing CO<sub>2</sub> emissions.

The RJC engine has applications as the prime mover in micro Combined Heat and Power (CHP) plants with sizes at the single dwelling/domestic level. In such an application it has been estimated that 700,000 units would cut the UK's CO<sub>2</sub> emissions by 5% by reducing the reliance on centrally generated electrical power produced at lower overall thermal efficiency. Ref 2.

## TECHNOLOGY DEMONSTRATION ENGINE

### Description and Development

The technology demonstration engine has been used to solve the major problems unique to the RJC engine notably: the external pressurised combustion system, the expander valve design, and valve timing. For reasons of simplicity and cost an existing four cylinder diesel engine block was selected with two pistons used as expanders, one as a compressor with the other retained for balance. Initially the original pistons from the engine were used resulting in a swept volume ratio of 2:1, but a later design modification reduced the compressor bore giving a swept volume ratio of 2.5:1.

Cylinder heads for the expander and the compressor were designed and built utilising conventional technologies. The expander cylinder head uses poppet valves for exhaust directly driven by overhead cams. The inlet valves are also of the poppet type but open in an upwards direction so that when closed sealing is assisted by system pressure. A simple valve actuating system is employed to open and close the valves utilising a

single cam shaft for both inlet and exhaust valves. Pressure ratios are determined by the degree of admission of the combustion gasses via the inlet cam profiles. Cam profiles giving openings from 70 deg to 100 deg were evaluated. For initial development work this arrangement was found to be adequate but is unlikely to be used in a prototype engine and the area of expander valves will be the subject of future detail design activities. The compressor cylinder head uses two reed valves for suction and three for delivery.

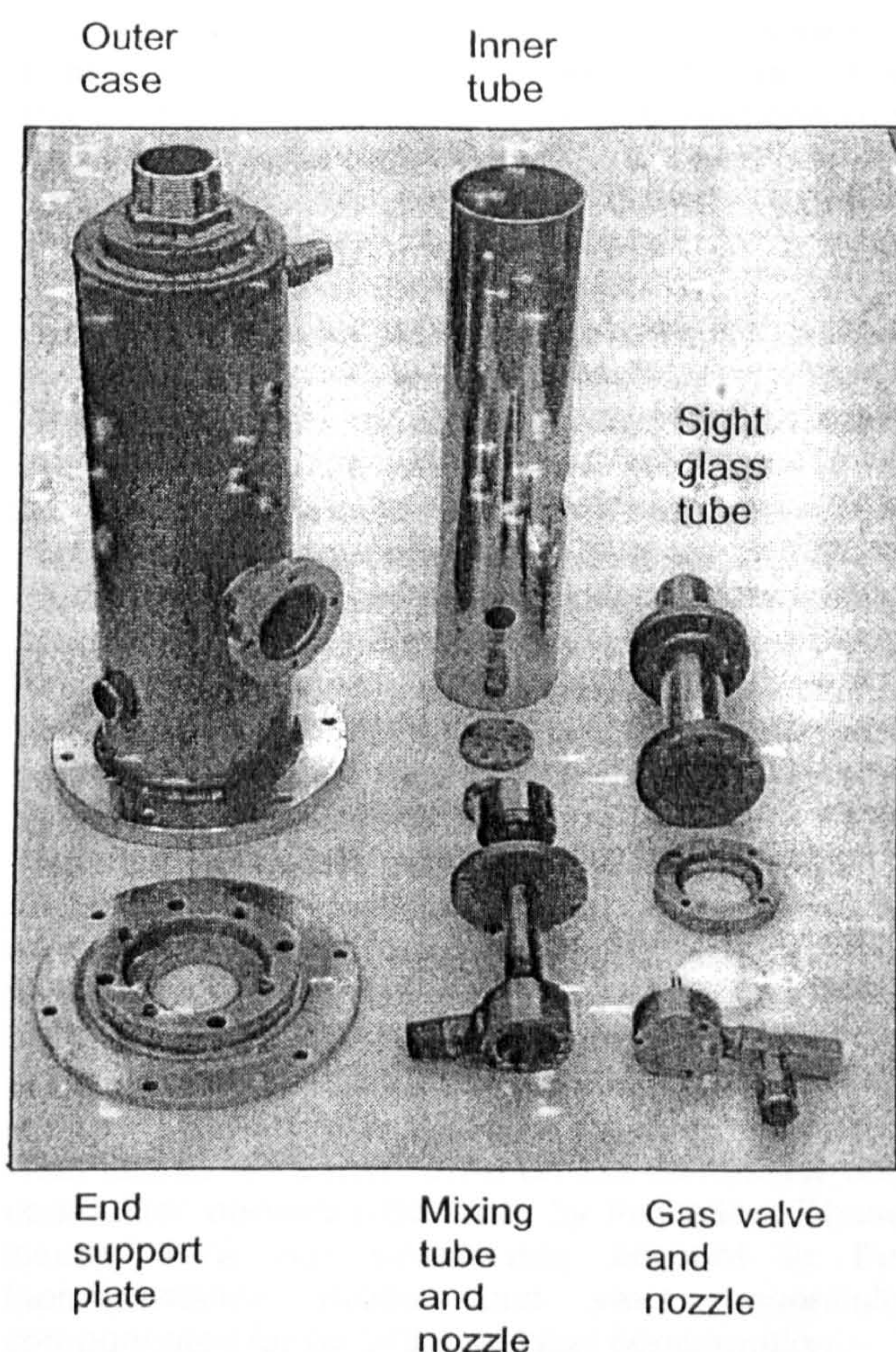
The design of the combustion chamber to provide reliable ignition and stable combustion represented a major part of the engine development. Although broadly based on gas turbine combustor chamber design the much lower air flow rates in the RJC engine required several major differences and these differences were established primarily by a process of design and test. As gas was used as the fuel and with a weak air to fuel ratio it was established that the gas had to be thoroughly mixed with some of the air, to stoichiometric conditions, before being injected into the combustion chamber. This air was termed primary air. The extra air, or secondary air, was then fed via an outer chamber into the combustion zone. Mixing of the primary air and gas was achieved in a simple mixing tube with a length to bore ratio established to be greater than 10:1. This mixture was then emitted into the combustion chamber via a nozzle plate incorporating a number of holes whose total area was slightly smaller than the mixing tube bore to ensure sufficient mixture exit velocity. An additional angled pilot hole was incorporated into the nozzle plate with the gas direction such that it passed very close to a spark provided by a standard spark plug. Such an arrangement has provided reliable ignition and controllable and stable combustion. Previous design iterations that did not have such controlled mixing and ignition gave rise to explosive ignition and pulsating combustion. The whole combustion chamber and delivery pipe-work were insulated to reduce heat losses.

Engine start is achieved using the existing starter motor and the use of an external supply of compressed air introduced upstream of the combustion chamber. The compressed air motors the engine prior to ignition and continue to be supplied until self-sustaining conditions are established.

Expander inlet and exhaust temperatures, engine speed and both combustor inlet and combustion zone pressures are monitored during operation. In addition, combustion conditions are observed via a sight tube. The components of the combustion chamber are shown in Fig 5

Figure 5. Components of Combustion Chamber





From an early stage in the development of the technology demonstration engine it was recognised that it was a 'high friction' engine and this would have a significant effect on performance. In fact, the friction was such that only self-sustaining conditions at engine speeds up to 1000 RPM were expected. However, this did not compromise the aims of developing and testing components that could be taken forward into the design of a full prototype engine. Major aspects of the technology demonstration engine's performance are described under the following headings.

#### Compressor performance.

The volumetric efficiency was determined and gave results averaging out at 75%. Further detail design on ring sealing and reduced clearance volumes could improve on this value. A higher volumetric efficiency higher will require more work from the expander but give increased airflow allowing more fuel to be burnt. The result is that the increase in work from the expander is greater than the work required to drive a more efficient compressor. For the demonstration engine a volumetric efficiency of ~ 75% was deemed acceptable.

#### Combustion conditions

Reliable ignition conditions were achieved with fuel gas pressures down to one bar above system pressure. Once ignition occurred then combustion could be controlled from a very lean to a rich condition. The condition of combustion was assessed visually via the combustion chamber sight glass and by observation of the exhaust gas.

#### Combustion temperatures

Under stable combustion conditions temperatures up to 1150 K were achieved. The maximum temperatures were achieved when, by observation via the sight glass, the walls of the inner combustion tube were clearly visible and the exhaust was clear. There was some concern that the expander liners and piston crowns (aluminium) would suffer undue wear/damage under these conditions but subsequent inspections found them to be in a good and very acceptable condition. Exhaust temperatures were measured up to 700 K.

#### Valve timing

The opening angle of the inlet valves determines the engine operating pressure. The exhaust valve cams were profiled to give a 6 mm lift over 170 degrees of crank angle to achieve close to a full stroke exhaust. Inlet valve cams giving openings of 70, 80 and 100 degrees of crank angle were evaluated. The longer the opening the lower the engine operating pressure. An opening of 70 deg was shown by the thermodynamic model to be the optimum for maximum power production. The optimum valve timing was determined using a pressure transducer, motoring the engine on compressed air and adjusting the timing to give a balance between recompression and lost work as indicated by the transducer output. The valve timing was found to be critical and even 3 degrees of retard resulted in lost work. Table 2 shows the achieved pressure ratios for various inlet cam openings.

Table 2 Pressure Ratios vs. Inlet Valve Opening

Inlet cam opening	Predicted pressure ratio $r_p$	Measured pressure ratio $r_p$
70 deg	3.52	4
80 deg	3.00	3.4
100 deg	2.34	2.8

The difference between predicted and measured pressure ratios can be explained by the fact that the predicted assumes a square shaped opening and closing profile with no pressure losses.

### Evaluation of Losses

Losses are inherent in the design of the engine and the aim was to minimise these wherever possible. Losses due to gas leakage are evident at the valve guides and via the piston rings. The use of oil pressurised valve guide seals with both inlet valves shut reduced the overall system leakage loss to 7% of compressor delivery volume. With the inlet valves open with leakage past the expander rings this increased to 12% of compressor delivery volume. The basic design of the technology demonstration engine did not allow for these losses to be reduced by any significant amount.

Pressure losses are again inherent in the design. These were minimised by pipe lengths being kept to a minimum, but pressure losses will also occur in the combustion chamber and at the inlet and exhaust valves. An overall assessment of the pressure losses was estimated as 10% of compressor discharge pressure.

Heat losses were minimised on the combustor and combustor delivery pipe work by insulation. These losses were not taken into account in the thermodynamic model and were essentially compensated for by additional fuel consumption.

Friction losses were identified as having the largest negative effect on net power output. Frictional power increases both with engine speed and engine pressure ratio, primarily due to friction at the expander and compressor ring / liner interface. A determination of this loss was assessed to be ~3 kW at 1000 rpm, and taking into account the method employed to measure friction power, it corresponded well with empirical and other published test data for engines of a similar size Ref 3. These large proportional losses are inherent in the design of the demonstration engine and very little can be done to reduce them without major design changes.

The combination of these measured and estimated losses when applied in the thermodynamic model indicated that a self-sustaining condition could be achieved. In actual operation self-sustaining conditions with clean combustion were achieved at the conditions in table 3

Table 3 *Self-Sustaining Performance*

The cumulative experience gained from development of this technology demonstration engine is being fed forward into a first iteration of a prototype design.

	Swept volume ratio 2:1	Swept volume ratio 2.5:1
Engine RPM. N	750	750
Pressure ratio $r_p$	2.8	3.4
T max (exp inlet) deg K	1120	1050

### PROTOTYPE DESIGN RJC ENGINE FOR MICRO CHP

The basic design parameters set for the prototype engines are:

- Nominal output of 5 kWe at >40% thermal efficiency
- Overall system thermal efficiency ~90%
- 3000 rpm constant output with minimal noise and vibration
- Minimal size and weight – footprint the same as a domestic boiler.
- Reliable and durable.

Additionally the design will have a pressure ratio of 5:1 and a nominal swept volume ratio of 2.5:1.

The influence of frictional losses on net work output as demonstrated by the technology demonstration engine drives much of the detail design to minimise these losses. Some of the major aspects of the proposed design are outlined below:

#### Expander Pistons

Similar sized pistons to those used in the technology demonstration engine will be employed but modified with a higher crown land and an anti-polish ring. This will give the greater protection to the lubricated surfaces of the liner. Friction from the ring/liner interfaces will always be present and cannot be eliminated. However, because of lower pressures consideration will be given to reducing friction by using only a single gas tight ring together with an oil scraper ring. Ref 4. In addition the piston liners will

require water cooling with the waste heat being recovered in the heating system.

### Gearbox

The 'gearbox' comprises the mechanical linkage from the expander pistons to the power output shaft and the power take-offs needed to drive cam shafts and pumps.

Connecting the pistons to the power take-off to minimise friction and vibration will be achieved using a hypocycloidal drive employing anti-friction bearings. Such a drive is applicable to the RJC engines due to the lower pressures in the expanders giving overall lower loadings. Demonstration models have been completed for this aspect of the prototype engine. Such a gearbox lends itself to two diametrically opposed reciprocating expander pistons, and the employment of a hypocycloidal drive can theoretically eliminate out-of-balance vibration and minimise side thrust between piston and liner.

### Inlet and exhaust valves

These will entail further detailed design and development and two alternatives are under evaluation. The first is the use of conventional poppet valves using *desmodronic* valve activation and a conventional cam shaft. In this instance the inlet valve lifts upwards and back seating is assisted by system pressure. The second is the use of rotary valves which will require less work to activate and although more difficult to seal represents a more ideal solution for this type of engine with its relatively low internal pressures. Rig testing of a basic design is being undertaken.

### Combustion chamber

The combustion chamber developed for the prototype engine will need further detail design but the concept developed and most of the components and materials used will remain the same.

### Positive displacement compressor

Although the technology demonstration engine employed a reciprocating compressor such a compressor will have reduced performance in terms of friction and volumetric efficiency at 3000 RPM. Consideration is being given to the use of a scroll compressor driven directly from the gearbox. Such compressors are now widely used for 'lower pressure' applications and exhibit low friction and low noise. In addition, the necessary swept volume

ratio can be achieved by alteration of the drive ratios.

### Heat exchangers

Heat exchangers will be incorporated for waste heat recovery from cooling water and exhaust gas. In addition, to obtain a high overall thermal efficiency an air-to-air recuperator will use some of the exhaust gas energy to preheat the combustion air.

### Control

For electrical generation accurate speed control under varying load conditions is required. Primary control can be provided by variation in fuel supply, but the strategy for more precise control still needs to be determined. It could include variable timing of the inlet valves and/or variation in delivery volume from the positive displacement compressor.

A major factor in realising a successful design of a prototype engine is the use of existing rather than completely new technologies. Detail design of the critical components such as the inlet valves, and friction reduction are the major design challenges.

## CONCLUSIONS

The RJC engine has been identified as a very suitable prime mover for micro-CHP systems. It has the potential to deliver high thermal efficiencies, with the energy delivered split approximately equally into electrical and thermal energy. Additionally a wide range of fuels can be burnt efficiently with low exhaust emissions.

Development of the engine has included thermodynamic modelling and the design and construction of a basic technology demonstration engine for component evaluation.

The major potential problems associated with the RJC engine, highlighted through experience with the technology demonstration engine is friction the reduction of which will be addressed in the building and testing of a prototype engine.

## NOMENCLATURE

See Ref 1

## ACKNOWLEDGEMENTS

The authors gratefully acknowledge the support of the School of Engineering of the University of Plymouth in carrying out the studies described.

## REFERENCES

- [1] M.A.Bell, and T Partridge. "Thermodynamic design of a reciprocating Joule Cycle Engine". Proc. Instn. Mech. Engrs. Vol. 217 Part A: J. Power and Energy. 2003
- [2] Combined Heat and Power Association (UK). Confernece on "Future opportunities of Domestic, or Micro-CHP" London, 10 July 2002
- [3] J.B. Heywood. "Internal combustion engine fundamentals". McGraw-Hill, New York, 1988
- [4] Y Wakuri, M Soejima and T Kiatahara. "Studies on the friction characteristics of piston ring in a diesel engine". CIMAC 20<sup>th</sup> International Congress on Combustion Engines" London 1993.

## **Annex 3**

Stroke mm	100	pamb	101325	Inlet Temp 850 C				
Bore mm	120	n exp	1.3734	Inlet pressure bar g	7.5			ccs
Clearance ccs	30	n recom	1.2	Inlet closing ATDC deg	70	1.221111	371.561	
Dispalced vol ccs	1130	mech eff	0.9	Exhaust closing BTDC de	35		140	
R	287	n exhaust	1.3					
T amb	288							
Supply Press Bar	7.5	Pabs N/m2	861262.5	Work Watts	304.97126	200632.7	1.980	Work exp J/c
		Vol to inlet close ccs	371.5612984	Work J/c	302.935			J/c
		Recompression Work		IMEP Expansion abs	3.994186			3.075938
		J/c		IMEP recompression				
		43.063						
		J/c						
		-43.803						
		11						
		Loss						
		Total Work Calculated						
		J/c						
		553.843						
		13.84						

Notes: Loss of 2.6 % of work done with inlet valve open measured from PV diagram

### 3.1 Expander Performance Model (1 cyl)

7.5 bar Supply Pressure

Gas inlet 1123 deg K

Compressor  
Pamb = 101325 Vcc/Vcs = 0.018  
Tamb = 288 Vcs = 0.000624  
Cp = 1010 Vcc = 0.000011232  
Cv = 723 vcs + Vcc = 0.000635232  
n = 1.3 nmechc = 0.8  
R = 287

Expander 2-cylinders  
Cpg = 1200 c/Ves = 0.018  
Cvg = 923 Ves = 0.000624  
\*ng = 1.3 Vec = 1.1232E-05  
Rg = 277 + Vec = 0.00063523  
nmeche = 0.8

Regenerator e = 0

Nat gas LCV = 42.0 MJ/kg

\*Mattingly p. 346

rp	Dpci (Pa)	Dpcd (Pa)	rpc	nvol	mdel kg	T2c K	wc J/cycle	V2c m³	T4 K	T3 K	AFR	q J/cycle	Dpei	Dped	rpe	2 <<%DP
2.061411	4177	4177	2.19	0.925	0.0006782	360.4	58.06	0.0003917	1123.0	360.4	31.82	217.00724	4177	4177.4	1.93765	
2.193701	4446	4446	2.34	0.916	0.0006703	367.2	62.73	0.000374	1123.0	367.2	27.55	246.49194	4446	4445.5	2.05699	
2.323229	4708	4708	2.49	0.908	0.0006626	373.6	66.99	0.0003582	1123.0	373.6	24.24	275.61808	4708	4708	2.17325	
<del>2.45011</del>	<del>4965</del>	<del>4965</del>	<del>2.63</del>	<del>0.901</del>	<del>0.0006551</del>	<del>379.6</del>	<del>70.89</del>	<del>0.0003442</del>	<del>1123.0</del>	<del>379.6</del>	<del>21.60</del>	<del>304.37319</del>	<del>4965</del>	<del>4965.1</del>	<del>2.28657</del>	
2.574451	5217	5217	2.77	0.893	0.0006479	385.3	74.47	0.0003317	1123.0	385.3	19.45	332.74962	5217	5217.1	2.39710	
2.696349	5464	5464	2.91	0.886	0.000641	390.7	77.77	0.0003203	1123.0	390.7	17.66	360.74329	5464	5464.2	2.50495	
2.815897	5706	5706	3.04	0.879	0.0006342	395.8	80.81	0.00031	1123.0	395.8	16.15	388.35283	5706	5706.4	2.61023	
2.933182	5944	5944	3.18	0.872	0.0006276	400.8	83.63	0.0003005	1123.0	400.8	14.86	415.57886	5944	5944.1	2.71306	
3.048283	6177	6177	3.31	0.865	0.0006212	405.5	86.23	0.0002919	1123.0	405.5	13.74	442.42357	6177	6177.3	2.81353	
3.161263	6406	6406	3.44	0.858	0.000615	410.0	88.65	0.0002839	1000.0	410.0	12.77	468.89114	6406	6406.3	2.91174	
3.271397	6629	6629	3.57	0.852	0.0006089	414.3	90.89	0.0002766	1123.0	414.3	11.92	495.04188	6629	6629.5	3.00804	

### 3.2 Prototype Reciprocating Joule Cycle Engine (fixed valve timing)

Based on Ford 2.5 DI Engine

con rod len = 154 mm ratio =  
 crank radius = 45.27 mm 3.401811  
 Over expansion No regeneration  
 inlet crank  
 angle ° stroke %  
 80 48.60%

RPM =  
700

Ve2 = 0.000315

2 << %leak

pe2 kPa	Vexact m³	Ve5 m³	Pe3 Pa	Te3 K	Te4 = T5 K	we12 J	we23 J	we51 J	wnet J/cycle	spec. work kJ/kg	eta thermal	power (kW)
204426.9	0.000523	1.8981E-05	81966	909.47	561.29	58	28	-1	35	-23	-0.106	-0.38
217568.7	0.000548	1.9915E-05	87236	909.47	594.69	62	29	-1	43	-20	-0.080	-0.33
230436	0.000571	2.0818E-05	92395	909.47	628.08	65	30	-1	51	-16	-0.059	-0.27
243040.3	0.000594	2.1692E-05	97449	909.47	661.45	69	31	-1	58	-13	-0.043	-0.22
255392	0.000616	2.2539E-05	102401	909.47	694.80	72	32	-1	65	-9	-0.028	-0.16
267501.1	0.000637	2.336E-05	107257	909.47	728.14	75	33	-1	72	-6	-0.017	-0.10
279376.7	0.000658	2.4158E-05	112018	909.47	761.46	78	34	-1	78	-2	-0.006	-0.04
291027.3	0.000678	2.4933E-05	116690	909.47	794.77	82	35	-1	85	1	0.003	0.02
302460.9	0.000697	2.5688E-05	121274	909.47	828.06	85	36	-1	91	5	0.010	0.08
313685.5	0.000716	2.6423E-05	125775	809.86	861.35	88	36	-1	97	8	0.017	0.13
324731.2	0.000734	2.7141E-05	130203	909.47	894.61	90	37	-1	102	12	0.023	0.19

### 3.2 Prototype Reciprocating Joule Cycle Engine (fixed valve timing)

Based on Ford 2.5 DI Engine



Blair 150xLstxN

Small 2T industrial engines with rolling element bearings ie chain saws

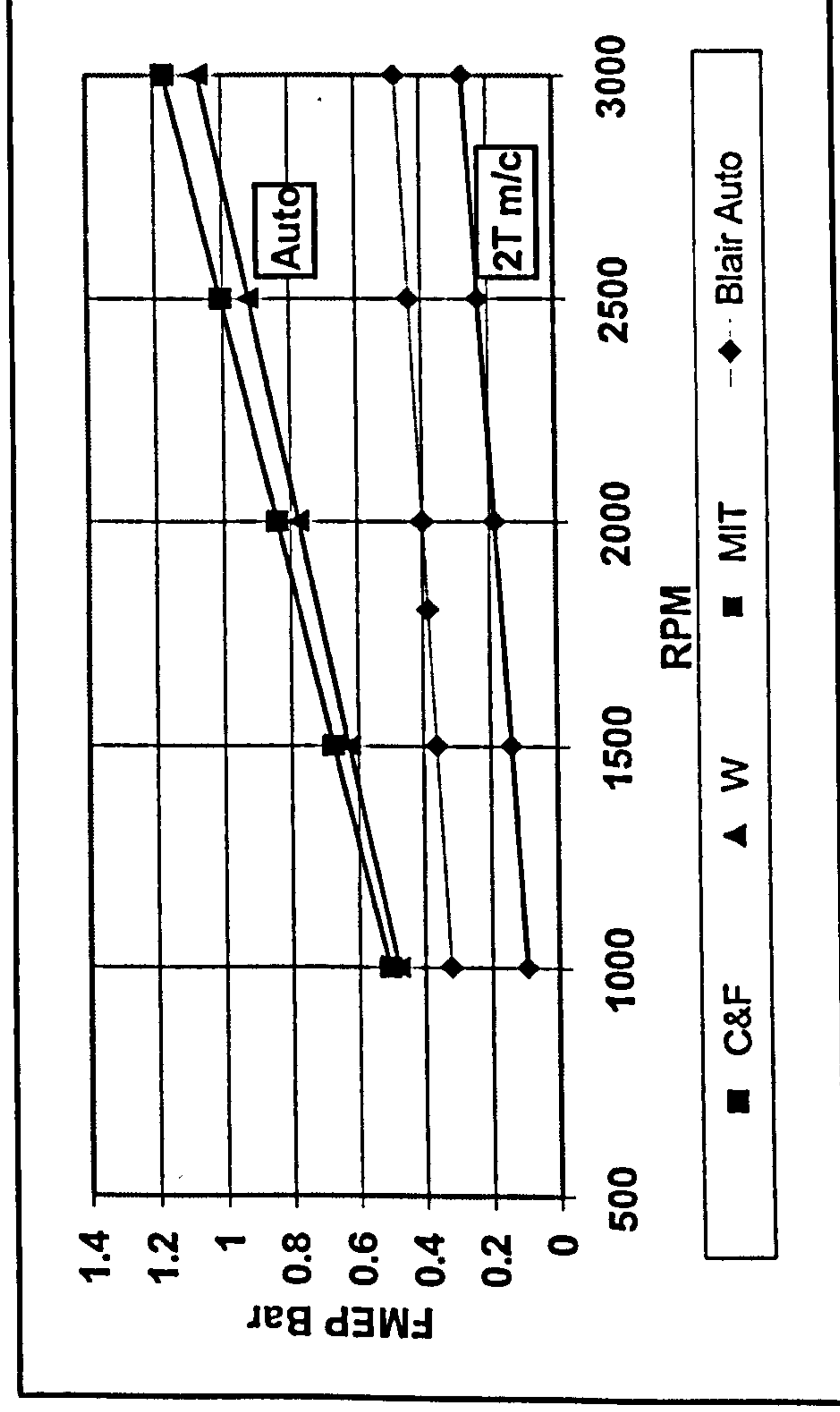
Chen and Flynn

$$0.137 + p_{max}/200 + .162x_{mp}$$

Winterbourne

$$0.061 + p_{max}/60 + .294x_{N}/1000$$

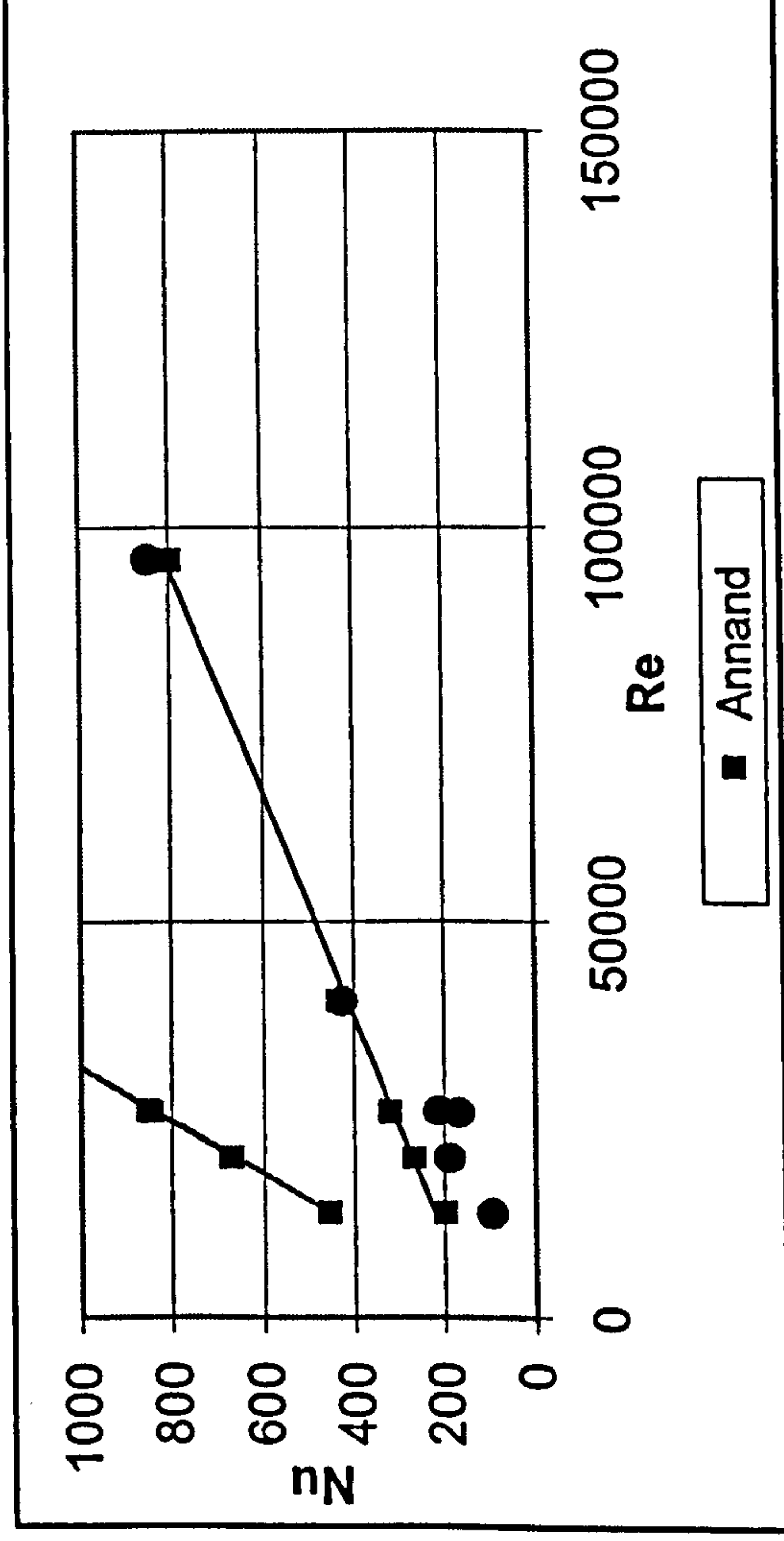
RPM	Blair		Blair Auto		C&F		Blair F		W	
	FMEP	FMEP	FMEP	FMEP	FMEP	FMEP	FMEP	FMEP	FMEP	FMEP
1000	0.091044	0.322601	0.5066	49.31532	0.48					
2000	0.182087	0.399752	0.8387	197.2613	0.774					
3000	0.273131	0.475866	1.1708	443.8379	1.068					
1500	0.136566	0.361696	0.67265	110.9595	0.627					
2500	0.227609	0.437809	1.00475	308.2208	0.921					
1800	0.163879	0.38453	0.77228	159.7816	0.7152					



### 3.3 Friction Modelling

Re	Annand	Q	F	Q+F	h Pis A	Nu Pis. A	FullADT	h Full A	Fit Pis A	NU Full A	Fit Full A
20090	267.3371	787.8	110.96	898.7595	528.682	942.4332	8.48	105.9858	671.3121	188.9312	168.7466
40180	434.2905	1575.6	443.84	2019.438	1187.905	2117.569	8.48	238.1413	1252.713	424.5127	283.7968
13085	198.0227	774.8	110.96	885.7595	328.0591	480.3722	13.6	65.12937	456.3929	95.36801	122.3433
26171	321.6974	1528.8	443.84	1972.638	730.6066	1069.817	13.6	145.0469	851.6885	212.3901	205.762
25948	319.7762	1853.8	436.01	2289.81	565.3853	1009.617	24.3	94.23088	845.1543	168.2694	204.4457
96019	799.1409	3941.6	2552.55	6494.154	1599.545	3824.999	18.35	353.9048	2743.873	846.2942	545.4662
0	0	0	0	0	0	0	0	0	0	0	0

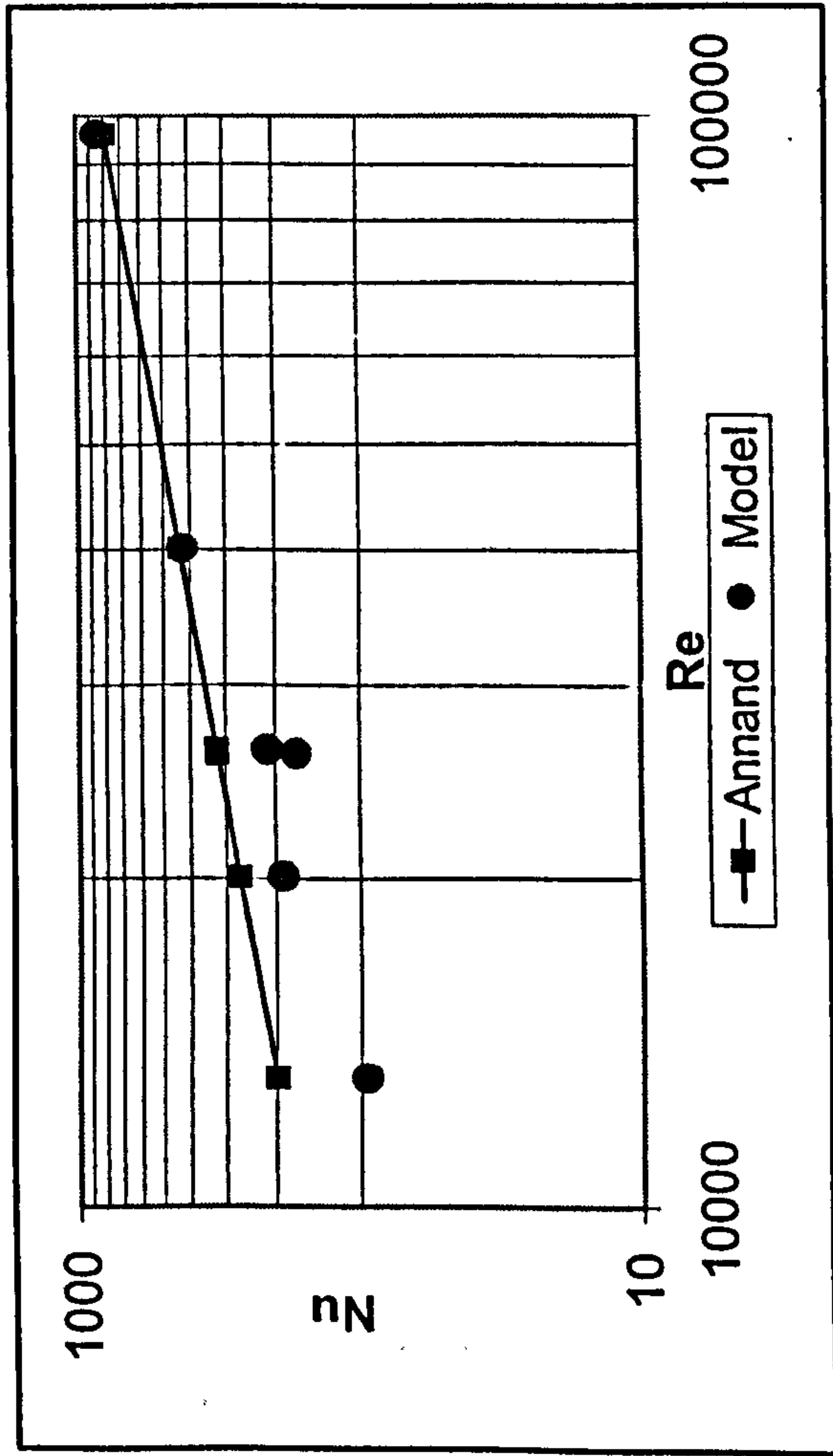
$$h(\text{Taylor}) = h_{\text{Ap}} \cdot (T_g - T_c)$$



### Thermal Modelling 3.4

	101325		Nu 90%	Nu 87%	Nu 86%
1500	FMEP	F	606	787.8	848.4
3000	0.136566	110.9595	1212	1575.6	1696.8
1500	0.136566	110.9595	596	774.8	834.4
3000	0.273131	443.8379	1176	1528.8	1646.4
1500	0.222058	436.0104	1426	1853.8	1996.4
3000	0.488527	2552.554	3032	3941.6	4244.8

87% polytropic efficiency



### Thermal Modelling 3.4

### 3.5 Engine modelling Inlet Opens 8 deg BTDC (1)

Bore m		0.1		RPM		1500		Pa	
Stroke m		0.12						Ps	
Vc ccs		0.00003		942				Valve lift	
Area cm2		0.00785						0.01 valve dia (2)	
Cam dia		40						1.50022222 Cd	
Sv ccs	crank ang	rads	dt	crank ang	valve lift	valve area	A*sqrtRT.dt	P1(V1/V2)^n	
8	0.000008	1	0	0.000294	0	0	0.000000	2.193796373	
6	0.000006	0.995754	0.092188	0.000415	5.28465	0.00191756	0.000485368	2.356596807	
4	0.000004	0.991507	0.130419	0.000802	7.476274	0.00269594	0.000684487	2.689097787	
2	0.000002	0.987261	0.159787	0.001003	9.159782	0.00328239	0.00083531	3.328854875	
8.5	0	0.983015	0.184572	0.001166	10.58057	0.00376776	0.000960658	4.263683892	
8.5	0.000002	0.978769	0.206431	0.001394	11.83365	0.00418748	0.001069429	4.608565698	
8.5	0.000004	0.968153	0.253052	0.001589	14.50616	0.00505226	0.001294652	5.087045289	
8.5	0.000006	0.957537	0.292461	0.001949	16.7653	0.00574611	0.00147644	5.735373284	
8.5	0.000008	0.936306	0.358837	0.002253	20.5703	0.0068241	0.001760783	6.555765917	
8.5	0.00001	0.915074	0.415104	0.002624	23.79578	0.00763569	0.00197639	7.46317197	
8.5	0.000015	0.893843	0.464952	0.002947	26.65333	0.00826666	0.002144922	7.496226067	
8.5	0.00002	0.872611	0.510272	0.003239	29.25129	0.00876244	0.002277906	6.520182589	
8.5	0.00003	0.85138	0.552186	0.003509	31.65396	0.00915093	0.002382452	6.72601161	
8.5	0.00004	0.830149	0.591422	0.00376	33.90318	0.00945087	0.002463377	6.972301296	
8.5	0.00005	0.808917	0.628488	0.003997	36.02799	0.00967574	0.002524165	7.190279819	
8.5	0.00006	0.787686	0.663753	0.004223	38.04952	0.00983566	0.002567457	7.366642928	
8.5	0.00007	0.766454	0.697494	0.004438	39.98372	0.00993854	0.002595336	7.504541749	
8.5	0.00008	0.745223	0.729927	0.004646	41.84296	0.00999074	0.002609488	7.611176173	
8.5	0.00009	0.723992	0.761225	0.004845	43.6371	0.00999748	0.002611316	7.693604844	
8.5	0.0001	0.70276	0.791527	0.005039	45.37414	0.00996314	0.002602005	7.757550601	
8.5	0.00011	0.681529	0.820947	0.005226	47.06064	0.00989147	0.002582578	7.80731177	
8.5	0.00012	0.660297	0.849582	0.005409	48.70214	0.0097857	0.002553928	7.84601477	
8.5	0.00013	0.639066	0.877513	0.005587	50.30331	0.00964867	0.002516843	7.875910146	
8.5	0.00014	0.617834	0.904811	0.005761	51.86813	0.00948289	0.002472028	7.898617402	
8.5	0.00015	0.596603	0.931535	0.005932	53.40008	0.00929062	0.002420119	7.915304459	
8.5	0.00016	0.575372	0.957738	0.006099	54.90218	0.00907387	0.002361691	7.926812793	
8.5	0.00017	0.55414	0.983467	0.006263	56.37707	0.00883449	0.002297273	7.933743083	

### 3.5 Engine modelling Inlet Opens 8 deg BTDC (2)

101325 318.315881 T 1123  
 861262.5 8.5 R 287 Density 2.67223  
 RT 322301 567.7156  
 gamma 1.324  
 gamma Ex 1.324

0.08  
 0.75

Sqrt(Ps-p3/po)	3	0	PV mod	PV ideal	mass
1.536197494	2.19379637	0			
1.516238664	2.49310271	0.136506	-0.505227	0	-1.56756E-06
1.47463603	3.07209999	0.383002	-0.622561	0	-1.93161E-06
1.391093818	3.91448802	0.585633	-0.793271	0	-2.46127E-06
1.25909134	5.01967747	0.755994	-1.017238	0	-2.938297
1.206751671	5.51220193	0.903636	1.117048	1.722525	5.34446E-06
1.130129783	6.18625922	1.099214	1.253645	1.722525	5.34446E-06
1.017141344	7.04226574	1.306892	1.427115	1.722525	5.34446E-06
0.852977025	7.98762	1.431854	1.618691	1.722525	5.34446E-06
0.622897263	8.76130128	1.298129	1.775478	1.722525	1.33612E-05
0.612887853	8.88033752	1.384111	4.499001	4.3063125	1.33612E-05
0.860747217	8.56236195	2.042179	4.337907	4.3063125	2.67223E-05
0.814776405	8.55093678	1.824925	8.664237	8.612625	2.67223E-05
0.756104656	8.58078716	1.608486	8.694483	8.612625	2.67223E-05
0.70008749	8.60984948	1.41957	8.72393	8.612625	2.67223E-05
0.651248051	8.62793959	1.261297	8.74226	8.612625	2.67223E-05
0.610343864	8.63486774	1.130326	8.74928	8.612625	2.67223E-05
0.57672782	8.63300378	1.021828	8.747391	8.612625	2.67223E-05
0.549334674	8.62481217	0.931207	8.739091	8.612625	2.67223E-05
0.527104213	8.61219874	0.854648	8.72631	8.612625	2.67223E-05
0.509133837	8.59647549	0.789164	8.710379	8.612625	2.67223E-05
0.494705829	8.57848869	0.732474	8.692154	8.612625	2.67223E-05
0.48326642	8.55875496	0.682845	8.672158	8.612625	2.67223E-05
0.474393234	8.53756551	0.638948	8.650688	8.612625	2.67223E-05
0.467765243	8.51505725	0.599753	8.627882	8.612625	2.67223E-05
0.463138945	8.49125883	0.564446	8.603768	8.612625	2.67223E-05
0.460330571	8.46611956	0.532376	8.578296	8.612625	2.67223E-05

At 1500 rpm  
 0.000227916 Kg/sec

8.5	180	0.00018	0.532909	1.008762	0.006424	57.82712	0.00857418	0.002227349	1.095405	47.8271201	7.936513606
8.5	190	0.00019	0.511677	1.03366	0.006583	59.25442	0.00829447	0.00215237	1.035376	49.2544221	7.935400043
8.5	200	0.0002	0.490446	1.058195	0.006739	60.66086	0.00799682	0.002072751	0.976380	50.6608616	7.930562572
8.5	210	0.00021	0.469214	1.082395	0.006893	62.04814	0.00768257	0.001988884	0.918385	52.0481397	7.922064112
8.5	220	0.00022	0.447983	1.106288	0.007046	63.4178	0.00735297	0.001901134	0.861366	53.4178004	7.909882253
8.5	230	0.00023	0.426752	1.129899	0.007196	64.77125	0.00700922	0.001809844	0.805304	54.7712523	7.893916569
8.5	240	0.00024	0.40552	1.153249	0.007345	66.10979	0.00665241	0.00171534	0.750182	56.1097871	7.873992466
8.5	250	0.00025	0.384289	1.176359	0.007492	67.43459	0.00628362	0.001617929	0.695990	57.4345945	7.849862319
8.5	260	0.00026	0.363057	1.199249	0.007638	68.74678	0.00590385	0.001517903	0.642719	58.7467757	7.821204455
8.5	270	0.00027	0.341826	1.221937	0.007782	70.04735	0.00551407	0.001415539	0.590363	60.047354	7.787620374
8.5	280	0.00028	0.320594	1.244439	0.007926	71.33728	0.0051152	0.001311102	0.538916	61.3372847	7.74863049
8.5	290	0.00029	0.299363	1.266771	0.008068	72.61746	0.00470812	0.001204846	0.488377	62.6174631	7.703668656
8.5	300	0.0003	0.278132	1.288948	0.008209	73.88873	0.0042937	0.001097013	0.438744	63.888732	7.652075671
8.5	310	0.00031	0.2569	1.310983	0.00835	75.15189	0.00387276	0.000987835	0.390017	65.1518879	7.593091979
8.5	320	0.00032	0.235669	1.33289	0.008489	76.40769	0.0034461	0.000877537	0.342196	66.4076865	7.525849783
8.5	330	0.00033	0.214437	1.354681	0.008628	77.65685	0.00301452	0.000766334	0.295283	67.6568477	7.449364801
8.17058773	340	0.00034	0.193206	1.376368	0.008766	78.90006	0.00257876	0.000654434	0.249279	68.9000601	7.362527921
7.862946023	350	0.00035	0.171975	1.397963	0.008904	80.13798	0.00213957	0.000542039	0.204189	70.1379847	7.264097033
7.575073925	360	0.00036	0.150743	1.419476	0.009041	81.37126	0.00169769	0.000429343	0.160014	71.371259	7.152689339
7.305203274	370	0.00037	0.129512	1.44092	0.009178	82.6005	0.00125383	0.000316534	0.116760	72.6005	7.026774468
7.051766235	380	0.00038	0.10828	1.462303	0.009314	83.82631	0.00080869	0.000203798	0.074430	73.8263071	6.884668703
6.813368063	390	0.00039	0.087049	1.483637	0.00945	85.04927	0.00036298	9.13112E-05	0.033029	75.0492652	6.724530665
6.588764163	400	0.0004	0.065817	1.504931	0.009585	86.26995	-8.263E-05	-2.0751E-05	-0.007437	76.2699474	6.544358743
6.376840671	410	0.00041	0.044586	1.526196	0.009721	87.48892	0	0	0.000000	77.4889171	6.341990567
6.176597948	420	0.00042	0.023355	1.54744	0.009856	88.70673	0	0	0.000000	78.7067309	6.156070251
5.987136492	430	0.00043	0.002123	1.568673	0.009992	89.92394	0	0	0.000000	79.9239404	5.979509584
5.807644864	440	0.00044	-0.01911	1.589906	0.010127	91.1411	0	0	0.000000	81.1410951	5.811648929
5.637389313	450	0.00045	-0.04034	1.611147	0.010262	92.35874	0	0	0.000000	82.358744	5.65188787
5.475704811	460	0.00046	-0.06157	1.632406	0.010398	93.57744	0	0	0.000000	83.5774382	5.499678794
5.321987299	470	0.00047	-0.0828	1.653694	0.010533	94.79773	0	0	0.000000	84.797733	5.35452129
5.175686949	480	0.00048	-0.10403	1.675019	0.010669	96.02019	0	0	0.000000	86.0201905	5.215957238
5.036302286	490	0.00049	-0.12527	1.696392	0.010805	97.24538	0	0	0.000000	87.2453814	5.083566492
4.903375064	500	0.0005	-0.1465	1.717822	0.010942	98.47389	0	0	0.000000	88.4738881	4.956963078
4.776485761	510	0.00051	-0.16773	1.739321	0.011079	99.70631	0	0	0.000000	89.706307	4.835791833
4.65524963	520	0.00052	-0.18896	1.760899	0.011216	100.9433	0	0	0.000000	90.9432513	4.719725433
4.539313217	530	0.00053	-0.21019	1.782567	0.011354	102.1854	0	0	0.000000	92.185354	4.608461755
4.428351284	540	0.00054	-0.23142	1.804336	0.011493	103.4333	0	0	0.000000	93.4332713	4.501721528
4.322064086	550	0.00055	-0.25265	1.826219	0.011632	104.6877	0	0	0.000000	94.6876859	4.399246244
4.220174955	560	0.00056	-0.27389	1.848227	0.011773	105.9493	0	0	0.000000	95.9493111	4.300796286
4.122428152	570	0.00057	-0.29512	1.870374	0.011914	107.2189	0	0	0.000000	97.2188951	4.206149259
4.028586946	580	0.00058	-0.31635	1.892674	0.012056	108.4972	0	0	0.000000	98.4972258	4.115098489

0.459203061	8.43952703	0.503013	8.551351	8.612625	2.67223E-05	2.64435E-05
0.459656576	8.4113174	0.475917	8.522767	8.612625	2.67223E-05	2.63491E-05
0.461621536	8.38128062	0.450718	8.492333	8.612625	2.67223E-05	2.62481E-05
0.46505347	8.34916235	0.427098	8.459789	8.612625	2.67223E-05	2.61396E-05
0.469929161	8.31466341	0.404781	8.424833	8.612625	2.67223E-05	2.60226E-05
0.476243722	8.27743742	0.383521	8.387113	8.612625	2.67223E-05	2.58958E-05
0.484008332	8.23708693	0.363094	8.346228	8.612625	2.67223E-05	2.57577E-05
0.493248447	8.19315847	0.343296	8.301718	8.612625	2.67223E-05	2.56067E-05
0.504002336	8.14513646	0.323932	8.25306	8.612625	2.67223E-05	2.5441E-05
0.516319827	8.09243636	0.304816	8.199661	8.612625	2.67223E-05	2.52585E-05
0.530261189	8.03439693	0.285766	8.140853	8.612625	2.67223E-05	2.50569E-05
0.545896063	7.97027197	0.266603	8.075878	8.612625	2.67223E-05	2.48336E-05
0.563302405	7.89922147	0.247146	8.003886	8.612625	2.67223E-05	2.45855E-05
0.582565389	7.82030246	0.22721	7.923921	8.612625	2.67223E-05	2.43093E-05
0.603776247	7.73245966	0.20661	7.834915	8.612625	2.67223E-05	2.40014E-05
0.627031026	7.6345163	0.185151	7.735674	8.612625	2.67223E-05	2.36576E-05
0.65242926	7.52516516	0.162637	7.624874	8.278848017		2.32734E-05
0.680072549	7.4029603	0.138863	7.50105	7.967130058	0.000908558	2.28438E-05
0.710063078	7.26630969	0.11362	7.362588	7.675443654		2.23633E-05
0.742502082	7.11346902	0.086695	7.207722	7.401997218	0.022713958	2.1826E-05
0.777488298	6.94253715	0.057868	7.034526	7.145202138	Kg/sec	2.12252E-05
0.815116427	6.75145337	0.026923	6.84091	6.90364519		0.000997753
0.855475651	6.53799675	-0.006362	6.624625	6.676065288		0.024943829
0.898648237	6.34199057	0	6.426022	6.46133381		0.025171744
0.936559456	6.15607025	0	6.237638	6.258437871	10.82060161	
0.971193088	5.97950958	0	6.058738	6.06646605		
1.003011815	5.81164893	0	5.888653	5.884596159		
1.032384794	5.65188787	0	5.726775	5.712084721		
1.059612159	5.49967879	0	5.57255	5.548257899		
1.084941777	5.35452129	0	5.425469	5.392503631		
1.108581072	5.21595724	0	5.285069	5.244264801		
1.130705602	5.08356649	0	5.150924	5.103033292		
1.151465411	4.95696308	0	5.022643	4.968344784		
1.170989839	4.83579183	0	4.899866	4.839774197		
1.189391224	4.71972543	0	4.782262	4.716931687		
1.206767787	4.60846175	0	4.669524	4.599459117		
1.223205927	4.50172153	0	4.561369	4.487026938		
1.238782048	4.39924624	0	4.457536	4.379331435		
1.253564052	4.30079629	0	4.357782	4.276092273		
1.267612547	4.20614926	0	4.261881	4.177050325		
1.280981858	4.11509849	0	4.169624	4.081965723		

11.645% more mass flow

3.938431912	590	0.00059	-0.33758	1.915141	0.012199	109.7851	0	0.000000	99.7851361	4.027451679
3.851759391	600	0.0006	-0.35881	1.93779	0.012343	111.0835	0	0.000000	101.08351	3.943029697
3.768380125	610	0.00061	-0.38004	1.960639	0.012489	112.3933	0	0.000000	102.393292	3.861665479
3.688118017	620	0.00062	-0.40127	1.983704	0.012636	113.7155	0	0.000000	103.715488	3.783203051
3.610809027	630	0.00063	-0.42251	2.007004	0.012784	115.0512	0	0.000000	105.051185	3.707496629
3.53630017	640	0.00064	-0.44374	2.03056	0.012934	116.4016	0	0.000000	106.401554	3.634409815
3.46444861	650	0.00065	-0.46497	2.054395	0.013086	117.7679	0	0.000000	107.767864	3.563814865
3.395120849	660	0.00066	-0.4862	2.078532	0.01324	119.1515	0	0.000000	109.1515	3.49559202
3.328191981	670	0.00067	-0.50743	2.102997	0.013396	120.554	0	0.000000	110.553977	3.429628903
3.263545024	680	0.00068	-0.52866	2.12782	0.013554	121.977	0	0.000000	111.976962	3.365819961
3.201070309	690	0.00069	-0.54989	2.153033	0.013715	123.4223	0	0.000000	113.4223	3.304065971
3.140664928	700	0.0007	-0.57113	2.178672	0.013878	124.892	0	0.000000	114.892046	3.244273571
3.082232223	710	0.00071	-0.59236	2.204777	0.014045	126.3885	0	0.000000	116.388498	3.186354842
3.025681328	720	0.00072	-0.61359	2.231393	0.014214	127.9142	0	0.000000	117.914248	3.130226925
2.970926749	730	0.00073	-0.63482	2.258571	0.014388	129.4722	0	0.000000	119.472238	3.075811662
2.917887974	740	0.00074	-0.65605	2.286371	0.014565	131.0658	0	0.000000	121.065832	3.023035278
2.866489126	750	0.00075	-0.67728	2.314859	0.014747	132.6989	0	0.000000	122.698914	2.971828077
2.816658633	760	0.00076	-0.69851	2.344115	0.014933	134.376	0	0.000000	124.37601	2.92212417
2.768328934	770	0.00077	-0.71975	2.374232	0.015126	136.1024	0	0.000000	126.102448	2.873861224
2.721436206	780	0.00078	-0.74098	2.40532	0.015324	137.8846	0	0.000000	127.884579	2.826980224
2.675920112	790	0.00079	-0.76221	2.437514	0.01553	139.7301	0	0.000000	129.730082	2.781425263
2.63172357	800	0.0008	-0.78344	2.470977	0.015743	141.6484	0	0.000000	131.648389	2.737143339
2.588792538	810	0.00081	-0.80467	2.505917	0.015967	143.6513	0	0.000000	133.651311	2.694084174
2.547075819	820	0.00082	-0.8259	2.542597	0.016202	145.754	0	0.000000	135.753972	2.652200043
2.506524877	830	0.00083	-0.84713	2.581364	0.01645	147.9763	0	0.000000	137.976294	2.611445616
2.467093671	840	0.00084	-0.86837	2.622693	0.016715	150.3454	0	0.000000	140.345434	2.571777811
2.428738496	850	0.00085	-0.8896	2.667258	0.017002	152.9001	0	0.000000	142.900114	2.533155659
2.391417841	860	0.00086	-0.91083	2.716082	0.017319	155.699	0	0.000000	145.698963	2.49554018
2.355092254	870	0.00087	-0.93206	2.770853	0.017678	158.8387	0	0.000000	148.83868	2.458894259
2.31972422	880	0.00088	-0.95329	2.834746	0.018109	162.5014	0	0.000000	152.501379	2.423182545
2.285278039	890	0.00089	-0.97452	2.915378	0.018739	167.1236	0	0.000000	157.123555	2.388371345
2.251719727	900	0.0009	-0.99575	3.049405	0.009285	174.8066	0	0.000000	164.806649	2.354428529
2.219016911	910	0.00091	1	0	0.009711	0	0	0.000000	-10	2.321323442
2.187138735	920	0.00092	1	0	0	0	0	0.000000	-10	2.289026824
2.156055778	930	0.00093	1	0	0	0	0	0.000000	-10	2.257510728
2.125739966	940	0.00094	1	0	0	0	0	0.000000	-10	2.226748453

### 3.5 Engine modelling Inlet Opens 8 deg BTDC (5)



1.293720852	4.02745168	0	4.080815	3.990616135
1.305873644	3.9430297	0	3.995275	3.902795203
1.317480182	3.86166548	0	3.912833	3.818311161
1.32857675	3.78320305	0	3.83333	3.73698558
1.339196393	3.70749663	0	3.756621	3.658652247
1.349369287	3.63440981	0	3.682566	3.583156147
1.359123048	3.56381487	0	3.611035	3.510352555
1.368483015	3.49559202	0	3.541909	3.4401062
1.377472479	3.4296289	0	3.475071	3.372290525
1.386112897	3.36581996	0	3.410417	3.306786995
1.394424073	3.30406597	0	3.347845	3.243484491
1.402424316	3.24427357	0	3.28726	3.182278738
1.410130584	3.18635484	0	3.228574	3.1230718
1.417558609	3.13022692	0	3.171702	3.065771606
1.424723008	3.07581166	0	3.116566	3.010291528
1.43163738	3.02303528	0	3.06309	2.95654999
1.438314398	2.97182808	0	3.011205	2.904470107
1.444765886	2.92212417	0	2.960842	2.85397936
1.451002891	2.87386122	0	2.91194	2.805009292
1.457035745	2.82698022	0	2.864438	2.757495235
1.462874124	2.78142526	0	2.818279	2.711376053
1.468527103	2.73714334	0	2.77341	2.666593907
1.474003195	2.69408417	0	2.729781	2.623094039
1.479310403	2.65220004	0	2.687342	2.580824573
1.48445625	2.61144562	0	2.646047	2.539736332
1.489447822	2.57177781	0	2.605854	2.499782662
1.494291794	2.53315566	0	2.56672	2.460919281
1.498994464	2.49554018	0	2.528606	2.423104127
1.503561775	2.45889426	0	2.491475	2.386297227
1.507999344	2.42318255	0	2.45529	2.350460565
1.512312482	2.38837135	0	2.420017	2.315557973
1.516506214	2.35442853	0	2.385625	2.281555014
1.520585301	2.32132344	0	2.352081	2.248418885
1.524554254	2.28902682	0	2.319356	2.216118324
1.528417353	2.25751073	0	2.287423	2.184623517
1.532178658	2.22674845	0	2.256253	2.153906021

Work

528.7254 533.3267347

### 3.5 Engine modelling Inlet Opens 8 deg BTDC (6)

### 3.6 Exhaust Valve Modelling (1)

Vol ccs	Vol m3	P	deg	Rads	Deg	dt	180 - deg	Valve lift	Valve area	ACddt
1130	0.00113	1	-0.9993	3.10397	177.9345	0.0001	0.036032	0.000495582	3.08E-04	0.000000
1122	0.001122	1	-0.9851	2.96897	170.1958	0.0001	0.171028	0.002337948	1.45E-03	0.000175
1092	0.001092	1	-0.9321	2.77085	158.8387	0.0001	0.369147	0.004928452	3.06E-03	0.000392
1062	0.001062	1	-0.8790	2.64452	151.5965	0.0001	0.495483	0.006456069	4.01E-03	0.000548
1032	0.001032	1	-0.8259	2.54260	145.754	0.0001	0.597403	0.007591338	4.72E-03	0.000689
1002	0.001002	1	-0.7728	2.45408	140.6795	0.0001	0.685925	0.008493869	5.28E-03	0.000825
972	0.000972	1	-0.7197	2.37423	136.1024	0.0001	0.765768	0.009233181	5.74E-03	0.000962
942	0.000942	1	-0.6667	2.30052	131.8772	0.0001	0.839476	0.009847176	6.12E-03	0.001103
912	0.000912	1	-0.6136	2.23139	127.9142	0.014224	0.908607	0.010359254	6.44E-03	0.177774
882	0.000882	1	-0.5605	2.16580	124.154	0.013804	0.974203	0.010785053	6.70E-03	0.174736
852	0.000852	1	-0.5074	2.10300	120.554	0.013402	1.037003	0.011135606	6.92E-03	0.172560
822	0.000822	1	-0.4544	2.04244	117.0826	0.013015	1.097559	0.011419004	7.10E-03	0.171427
792	0.000792	1	-0.4013	1.98370	113.7155	0.01264	1.156296	0.011641339	7.24E-03	0.171339
762	0.000762	1	-0.3482	1.92644	110.433	0.012274	1.213558	0.011807292	7.34E-03	0.172175
732	0.000732	1	-0.2951	1.87037	107.2189	0.011916	1.269626	0.012	7.46E-03	0.174880
702	0.000702	1	-0.2420	1.81526	104.0596	0.011565	1.324738	0.012	7.46E-03	0.175889
672	0.000672	1	-0.1890	1.76090	100.9433	0.011218	1.379101	0.012	7.46E-03	0.177901
642	0.000642	1	-0.1359	1.70710	97.85918	0.010874	1.432901	0.012	7.46E-03	0.180642
612	0.000612	1	-0.0828	1.65369	94.79773	0.010534	1.486306	0.012	7.46E-03	0.183962
582	0.000582	1	-0.0297	1.60052	91.74982	0.010195	1.539475	0.012	7.46E-03	0.187801
552	0.000552	1	0.0234	1.54744	88.70673	0.009856	1.592560	0.012	7.46E-03	0.192153
522	0.000522	1	0.0764	1.49429	85.65986	0.009517	1.645711	0.012	7.46E-03	0.197049
492	0.000492	1	0.1295	1.44092	82.6005	0.009177	1.699080	0.012	7.46E-03	0.202550
462	0.000462	1	0.1826	1.38718	79.51964	0.008834	1.752824	0.012	7.46E-03	0.208741
432	0.000432	1	0.2357	1.33289	76.40769	0.008487	1.807110	0.012	7.46E-03	0.215737
402	0.000402	1	0.2887	1.27788	73.25416	0.008136	1.862122	0.012	7.46E-03	0.223687
372	0.000372	1	0.3418	1.22194	70.04735	0.007779	1.918063	0.012	7.46E-03	0.232785
342	0.000342	1	0.3949	1.16483	66.77384	0.007415	1.975168	0.012	7.46E-03	0.243291
312	0.000312	1	0.4480	1.10629	63.4178	0.007041	2.033712	0.0115	7.15E-03	0.244905
282	0.000282	1	0.5011	1.04597	59.96014	0.006655	2.094029	0.011	6.84E-03	0.248798
252	0.000252	1	0.5541	0.98347	56.37707	0.006255	2.156533	0.01	6.22E-03	0.242881

Bore mm 0.12 Pend 1.5

Stroke mm 0.1

C vol ccs 0.00003 Valve dia 0.07

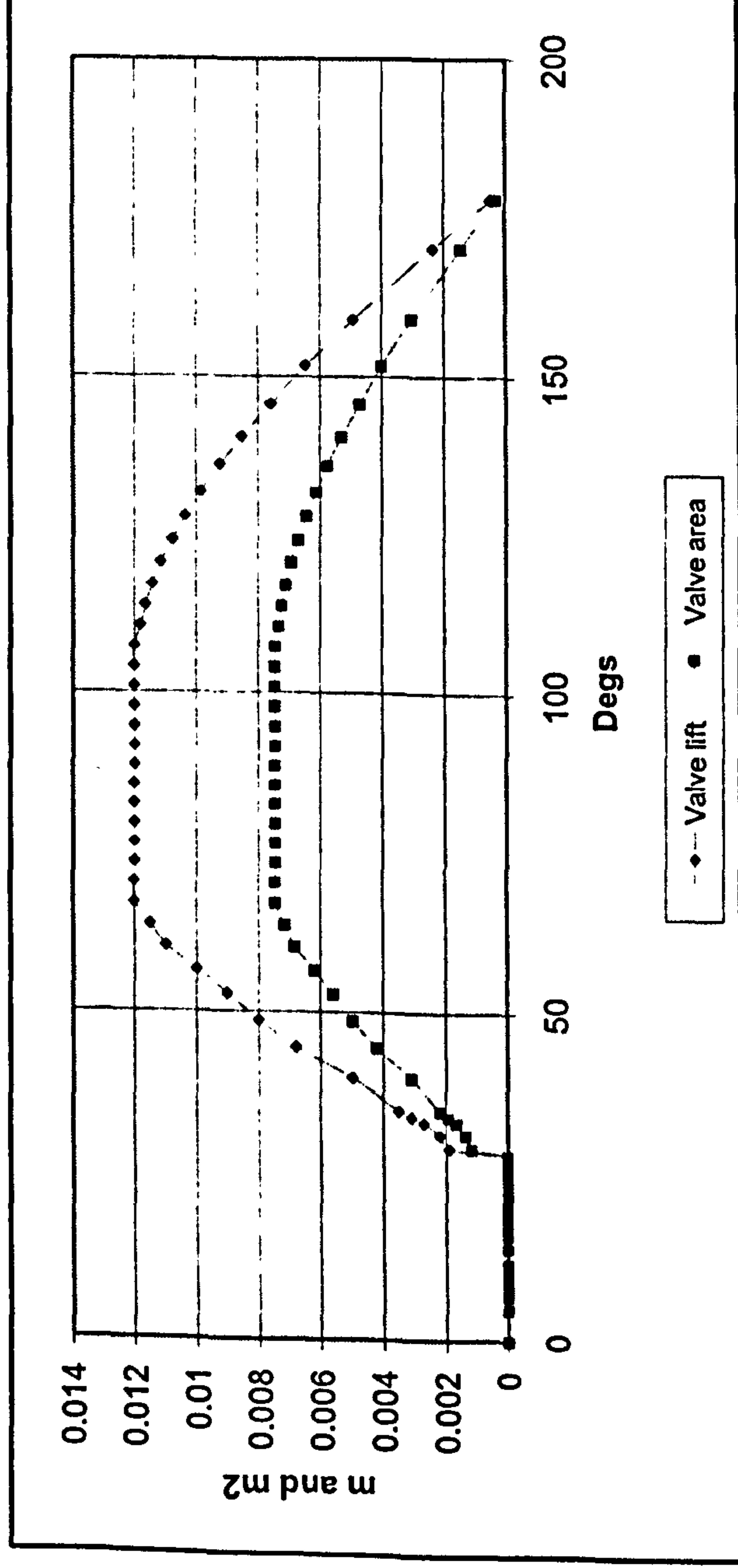
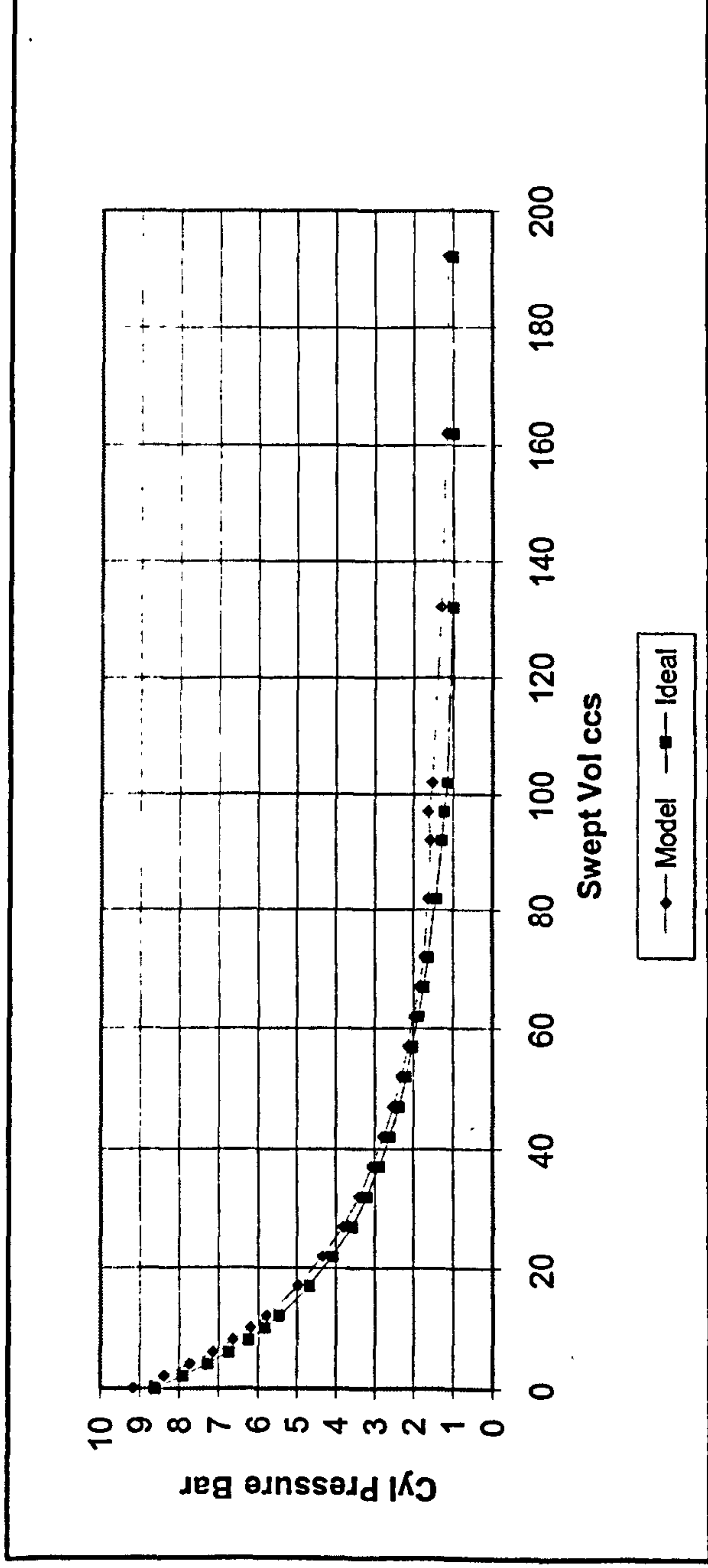
Swept vol 0.0011304 Area 0.011304 Cam dia 0.03

Gamma 1.36

RPM 1500

222	0.000222	1	0.6072	0.91824	52.63802	0.005838	2.221759	0.009	5.59E-03	0.239249
192	0.000192	1	0.6603	0.84958	48.70214	0.005397	2.290418	0.008	4.97E-03	0.237867
162	0.000162	1	0.7134	0.77649	44.51232	0.004927	2.363507	0.0068	4.23E-03	0.232573
132	0.000132	1	0.7665	0.69749	39.98372	0.004416	2.442506	0.005	3.11E-03	0.205445
102	0.000102	1.15	0.8195	0.61020	34.97967	0.004064	2.529799	0.0035	2.18E-03	0.165474
97	0.000097	1.212	0.8284	0.59459	34.08466	0.004064	2.545412	0.0031	1.93E-03	0.154465
92	0.000092	1.28	0.8372	0.57861	33.1685	0.00368	2.561394	0.0027	1.68E-03	0.125264
82	0.000082	1.438	0.8549	0.54540	31.26511	0.003468	2.594598	0.0022	1.37E-03	0.109094
72	0.000072	1.633	0.8726	0.51027	29.25129	0.003303	2.629728	0.0019	1.18E-03	0.099631
67	0.000067	1.749	0.8815	0.49186	28.19556	0.003002	2.648144	0	0.00E+00	0.000000
62	0.000062	1.879	0.8903	0.47278	27.10223	0.002725	2.667217	0	0.00E+00	0.000000
57	0.000057	2.027	0.8992	0.45297	25.9665	0.002494	2.687029	0	0.00E+00	0.000000
52	0.000052	2.197	0.9080	0.43232	24.78254	0.002725	2.707682	0	0.00E+00	0.000000
47	0.000047	2.394	0.9168	0.41069	23.54302	0.002494	2.729305	0	0.00E+00	0.000000
42	0.000042	2.622	0.9257	0.38794	22.23864	0.002334	2.752059	0	0.00E+00	0.000000
37	0.000037	2.892	0.9345	0.36384	20.85719	0.002365	2.776158	0	0.00E+00	0.000000
32	0.000032	3.214	0.9434	0.33811	19.38217	0.002199	2.801889	0	0.00E+00	0.000000
27	0.000027	3.603	0.9522	0.31034	17.79028	0.00205	2.829658	0	0.00E+00	0.000000
22	0.000022	4.082	0.9611	0.27993	16.04675	0.001771	2.860073	0	0.00E+00	0.000000
17	0.000017	4.684	0.9699	0.24589	14.09535	0.001549	2.894114	0	0.00E+00	0.000000
12	0.000012	5.458	0.9788	0.20643	11.83365	0.001383	2.933569	0	0.00E+00	0.000000
10	0.00001	5.833	0.9823	0.18839	10.79939	0.001194	2.951611	0	0.00E+00	0.000000
8	0.000008	6.254	0.9858	0.16845	9.656403	0.001064	2.971549	0	0.00E+00	0.000000
6	0.000006	6.731	0.9894	0.14584	8.360213	0.000916	2.994161	0	0.00E+00	0.000000
4	0.000004	7.276	0.9929	0.11904	6.824066	0.000732	3.020958	0	0.00E+00	0.000000
2	0.000002	7.901	0.9965	0.08415	4.823918	0.000379	3.055849	0	0.00E+00	0.000000
0	0	8.626	1.0000	0.00000	0	0.000268	3.140000	0	0.00E+00	0.000000

### 3.6 Exhaust Valve Modelling (3)



3.6 Exhaust Valve Modelling (5)

P ideal	Sv ccs	crank ang	rads	dt secs	crank ang	valve lift	valve area	A*SqrtRT.dt	P1(V1/V2)^1.4
8.5	0	0	0	0	0	0	0	0	0
8.5	2	0.987678	0.157147	0.0005	9.008419	0.00157132	0.000125817	0.000000	7.551035216
8.5	4	0.975356	0.222469	0.002934	12.75301	0.00216364	0.000174527	0.019755	7.022831357
8.5	6	0.963033	0.272751	0.00367	15.63541	0.00257898	0.000209101	0.141237	6.865738242
8.5	8	0.950711	0.315275	0.004269	18.07306	0.00289696	0.000235804	0.196042	6.90291498
8.5	10	0.938389	0.352857	0.004792	20.22749	0.00314936	0.000257143	0.245663	7.081039962
8.5	12	0.926067	0.386943	0.005263	22.18145	0.00335296	0.00027445	0.293770	7.347996114
8.5	14	0.913745	0.418389	0.005696	23.98407	0.00351804	0.000288542	0.341102	7.642566133
8.5	16	0.901423	0.447752	0.0061	25.66732	0.00365149	0.000299975	0.386129	7.892108947
8.5	18	0.8891	0.47542	0.006479	27.2534	0.00375824	0.000309146	0.425397	8.032471431
8.5	20	0.876778	0.501675	0.006839	28.75845	0.003842	0.000316358	0.455007	8.067204797
8.5	22	0.864456	0.526729	0.007182	30.19466	0.00390564	0.000321846	0.474617	8.085074484
8.5	24	0.852134	0.550747	0.007511	31.57148	0.00395146	0.000325804	0.489375	8.100414927
8.5	26	0.839812	0.57386	0.007827	32.89644	0.00398137	0.000328388	0.500511	8.110003385
8.5	28	0.827489	0.596175	0.008132	34.17562	0.00399692	0.000329734	0.508192	8.119032632
8.5	30	0.815167	0.617778	0.008428	35.41404	0.00399947	0.000329954	0.513067	8.124254932
8.5	32	0.802845	0.638744	0.008714	36.6159	0.00399017	0.00032915	0.515225	8.13054659
8.5	34	0.790523	0.659134	0.008993	37.78475	0.00397002	0.000327408	0.515237	8.132674357
8.5	36	0.778201	0.679001	0.009264	38.9236	0.00393992	0.000324807	0.513007	8.138313125
8.5	38	0.765879	0.69839	0.009529	40.03508	0.00390064	0.000321416	0.509226	8.136997437
8.5	40	0.753556	0.717341	0.009788	41.12145	0.00385291	0.000317298	0.503428	8.144466593
8.5	42	0.741234	0.735889	0.010041	42.18473	0.00379734	0.000312511	0.496757	8.137269536
8.5	44	0.728912	0.754065	0.01029	43.22665	0.00373453	0.000307107	0.487930	8.151071628
8.5	46	0.71659	0.771895	0.010533	44.24878	0.00366499	0.000301134	0.479229	

Pa  
Ps  
0.004 cam ang  
vale dia  
Cd

700  
73.26666667  
Valve lift

RPM  
rad/s

Bore m 0.082  
Stroke m 0.0615  
Vc ccs 0.00003  
Area cm2 0.005278  
Cam dia 25

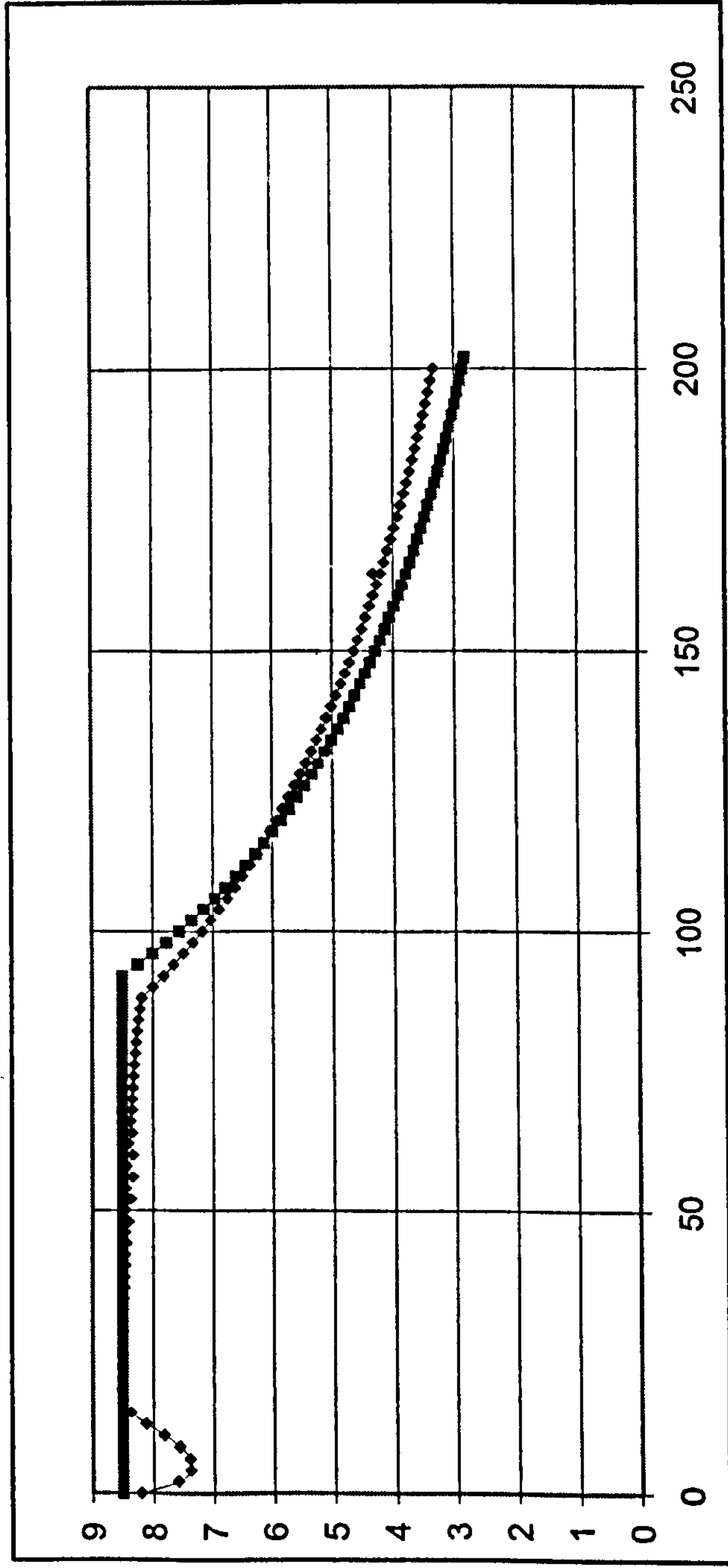
### 3.7 BMW Test Engine on Cold Air



5.859602907	120	0.00012	0.260669	1.307081	0.01784	74.92821	0	0.000000	6.037432606
5.725562632	122	0.000122	0.248347	1.319823	0.018014	75.65863	0	0.000000	5.929650941
5.596694174	124	0.000124	0.236025	1.332523	0.018187	76.38668	0	0.000000	5.825164953
5.472719312	126	0.000126	0.223703	1.345185	0.01836	77.11249	0	0.000000	5.723833004
5.353378893	128	0.000128	0.211381	1.357809	0.018532	77.83619	0	0.000000	5.625521256
5.238431252	130	0.00013	0.199058	1.370399	0.018704	78.55793	0	0.000000	5.530103147
5.127650787	132	0.000132	0.186736	1.382957	0.018875	79.27782	0	0.000000	5.437458915
5.020826665	134	0.000134	0.174414	1.395486	0.019046	79.996	0	0.000000	5.347475148
4.917761656	136	0.000136	0.162092	1.407986	0.019217	80.71258	0	0.000000	5.260044381
4.818271069	138	0.000138	0.14977	1.420461	0.019387	81.4277	0	0.000000	5.175064715
4.722181789	140	0.00014	0.137447	1.432912	0.019557	82.14147	0	0.000000	5.092439465
4.629331399	142	0.000142	0.125125	1.445342	0.019727	82.85401	0	0.000000	5.012076839
4.53956738	144	0.000144	0.112803	1.457753	0.019896	83.56544	0	0.000000	4.933889634
4.45274638	146	0.000146	0.100481	1.470146	0.020066	84.27586	0	0.000000	4.857794961
4.368733547	148	0.000148	0.088159	1.482523	0.020235	84.98539	0	0.000000	4.78371398
4.287401919	150	0.00015	0.075837	1.494887	0.020403	85.69415	0	0.000000	4.711571665
4.208631866	152	0.000152	0.063514	1.507239	0.020572	86.40224	0	0.000000	4.641296577
4.132310575	154	0.000154	0.051192	1.519582	0.02074	87.10978	0	0.000000	4.572820657
4.058331581	156	0.000156	0.03887	1.531916	0.020909	87.81687	0	0.000000	4.506079028
3.986594333	158	0.000158	0.026548	1.544245	0.021077	88.52362	0	0.000000	4.441009817
3.917003797	160	0.00016	0.014226	1.55657	0.021245	89.23014	0	0.000000	4.377553988
3.849470088	162	0.000162	0.001903	1.568893	0.021413	89.93653	0	0.000000	4.315655179
3.783908132	164	0.000164	-0.01042	1.581215	0.021413	90.64291	0	0.000000	4.255259555
3.849470088	162	0.000162	0.001903	1.568893	0.021582	89.93653	0	0.000000	4.315655179
3.783908132	164	0.000164	-0.01042	1.581215	0.021582	90.64291	0	0.000000	4.255259555
3.720237354	166	0.000166	-0.02274	1.593539	0.02175	91.34938	0	0.000000	4.196315674
3.658381391	168	0.000168	-0.03506	1.605867	0.021918	92.05604	0	0.000000	4.138774356
3.598267821	170	0.00017	-0.04739	1.618199	0.022086	92.76302	0	0.000000	4.082588559
3.539827921	172	0.000172	-0.05971	1.630539	0.022255	93.4704	0	0.000000	4.027713269
3.482996434	174	0.000174	-0.07203	1.642888	0.022423	94.17831	0	0.000000	3.974105394
3.427711359	176	0.000176	-0.08435	1.655248	0.022592	94.88685	0	0.000000	3.921723662
3.373913753	178	0.000178	-0.09667	1.667621	0.022761	95.59614	0	0.000000	3.870528527
3.321547548	180	0.00018	-0.109	1.680009	0.02293	96.30627	0	0.000000	3.820482084
3.270559382	182	0.000182	-0.12132	1.692414	0.0231	97.01737	0	0.000000	3.771547983
3.220898439	184	0.000184	-0.13364	1.704838	0.023269	97.72956	0	0.000000	3.723691355
3.172516301	186	0.000186	-0.14596	1.717282	0.023439	98.44293	0	0.000000	3.676878733

### 3.7 BMW Test Engine on Cold Air

3.125366813	188	0.000188	-0.15828	1.72975	0.023609	99.15762	0	0.000000	3.63107799
3.079405952	190	0.00019	-0.17061	1.742242	0.02378	99.87375	0	0.000000	3.586258266
3.03459171	192	0.000192	-0.18293	1.754761	0.023951	100.5914	0	0.000000	3.542389917
2.990883979	194	0.000194	-0.19525	1.76731	0.024122	101.3108	0	0.000000	3.499444445
2.948244448	196	0.000196	-0.20757	1.77989	0.024294	102.0319	0	0.000000	3.457394454
2.906636506	198	0.000198	-0.2199	1.792504	0.024466	102.755	0	0.000000	3.416213592
2.86602515	200	0.0002	-0.23222	1.805154	0.024638	103.4801	0	0.000000	3.375876507
2.826376899	202	0.000202	-0.24454	1.817842	0.012319	104.2075	0	0.000000	3.336358794
	204	0.000204							



3.7 BMW Test Engine on Cold Air



101325	T	288	Density	10.41984
861262.5	8.5 R	287		
1.222277778	RT	82656	406.5858	
0.025	gamma	1.36		
0.67	gamma Ex	1.4		

Sqrt(1 - p3/po)	P
0.000	8.2
0.149174418	7.591
0.0991887026	7.390
1.345971282	7.402
1.695787848	7.567
2.080195888	7.828
2.50641903	8.119
2.951014055	8.362
3.357281877	8.491
3.654828102	8.509
3.828835177	8.511
3.956634874	8.511
4.05434764	8.506
4.121436947	8.502
4.165605244	8.495
4.185819787	8.489
4.189162014	8.480
4.172115811	8.476
4.144242642	8.464
4.096396179	8.463
4.045820702	8.446
3.970418986	8.452
3.906229396	8.424

### 3.7 BMW Test Engine on Cold Air

3.802523205	0.083	0.314	8.446
3.735578989	0.063	0.236	8.396
3.598795355	0.090	0.325	8.444
3.540290209	0.053	0.188	8.360
3.366273549	0.102	0.344	8.440
3.321109014	0.044	0.146	8.327
3.120331737	0.112	0.349	8.425
3.076073745	0.048	0.147	8.324
2.883809665	0.108	0.312	8.396
2.809754482	0.064	0.180	8.339
2.647038909	0.096	0.254	8.363
2.534439922	0.080	0.203	8.339
2.39169124	0.091	0.218	8.335
2.259622988	0.091	0.205	8.323
2.122435742	0.095	0.202	8.312
1.985650397	0.099	0.196	8.299
1.848346899	0.103	0.190	8.285
1.710937783	0.108	0.185	8.269
1.573645837	0.113	0.179	8.251
1.436700927	0.120	0.172	8.230
1.300336881	0.127	0.165	8.206
1.164800227	0.135	0.157	8.178
0	0.144	0.000	7.996
0	0.199	0.000	7.821
0	0.241	0.000	7.653
0	0.278	0.000	7.491
0	0.310	0.000	7.335
0	0.340	0.000	7.184
0	0.367	0.000	7.038
0	0.392	0.000	6.898
0	0.416	0.000	6.762
0	0.439	0.000	6.631
0	0.461	0.000	6.505
0	0.482	0.000	6.382
0	0.502	0.000	6.263
0	0.522	0.000	6.149

0	0.541	0.000	6.037
0	0.559	0.000	5.930
0	0.577	0.000	5.825
0	0.594	0.000	5.724
0	0.611	0.000	5.626
0	0.628	0.000	5.530
0	0.644	0.000	5.437
0	0.660	0.000	5.347
0	0.675	0.000	5.260
0	0.691	0.000	5.175
0	0.706	0.000	5.092
0	0.720	0.000	5.012
0	0.735	0.000	4.934
0	0.749	0.000	4.858
0	0.763	0.000	4.784
0	0.777	0.000	4.712
0	0.791	0.000	4.641
0	0.804	0.000	4.573
0	0.818	0.000	4.506
0	0.831	0.000	4.441
0	0.844	0.000	4.378
0	0.857	0.000	4.316
0	0.870	0.000	4.255
0	0.857	0.000	4.316
0	0.870	0.000	4.255
0	0.882	0.000	4.196
0	0.895	0.000	4.139
0	0.907	0.000	4.083
0	0.919	0.000	4.028
0	0.931	0.000	3.974
0	0.943	0.000	3.922
0	0.955	0.000	3.871
0	0.967	0.000	3.820
0	0.979	0.000	3.772
0	0.990	0.000	3.724
0	1.002	0.000	3.677

### 3.7 BMW Test Engine on Cold Air

0	1.013	0.000	3.631
0	1.024	0.000	3.586
0	1.036	0.000	3.542
0	1.047	0.000	3.499
0	1.058	0.000	3.457
0	1.069	0.000	3.416
0	1.080	0.000	3.376
0	1.090	0.000	3.336

### 3.8 BMW Test Engine Modelling on Cold Air (1)

Advanced Timing and high Lift Cam

		Bore m	0.082	RPM		700	Pa	
		Stroke m	0.0615				Ps	
		Vc ccs	0.00003	324.6179		Valve lift		0.005 valve dia (2)
		Area m2	0.0052783			Cam angle		1.2211111 Cd
Sv ccs	crank ang	rads	dt	crank ang	valve lift	valve area	A*sqrtRT.dt	P1(V1/V2)^n
8.5	0	0	0	0	0	0	0.000000	0
8.5	2	0.000002	0.987678	0.1571469	0.003036	9.008419	0.003	2.758569398
8.5	4	0.000004	0.975356	0.2224691	0.001578	12.75301	0.0038	6.787040723
8.5	6	0.000006	0.963033	0.272751	0.001267	15.63541	0.0043	7.755501985
8.5	8	0.000008	0.950711	0.3152745	0.001093	18.07306	0.0047	8.060117859
8.5	10	0.00001	0.938389	0.3528573	0.002544	20.22749	0.005	8.115951266
8.5	20	0.00002	0.876778	0.5016752	0.003616	28.75845	0.005	6.135229818
8.5	30	0.00003	0.815167	0.6177783	0.002944	35.41404	0.005	6.706305074
8.5	40	0.00004	0.753556	0.7173409	0.002577	41.12145	0.005	6.874616238
8.5	50	0.00005	0.691946	0.8066159	0.00234	46.23913	0.005	7.137920038
8.5	60	0.00006	0.630335	0.8888121	0.002173	50.95101	0.005	7.133310463
8.5	65	0.000065	0.599529	0.9278836	0.001556	53.19078	0.005	7.555235487
8.5	70	0.00007	0.568724	0.9658429	0.001516	55.36679	0.0047	7.580783865
8.5	75	0.000075	0.537918	1.0028306	0.001955	57.4871	0.0043	7.554890767
8.5	80	0.00008	0.507113	1.0389647	0.001955	59.55849	0.0037	7.111542135
8.5	90	0.00009	0.445502	1.1090615	0.001881	63.57677	0.0027	6.820036502
7.411979454	100	0.0001	0.383891	1.1767898	0.001823	67.45929	0.0018	6.477147339
6.54822708	110	0.00011	0.32228	1.2426592	0.001778	71.23524	0.001	6.098234896
5.847882194	120	0.00012	0.260669	1.307081	0.001743	74.92821	0	5.693095666
5.269966905	130	0.00013	0.199058	1.3703994	0.001717	78.55793	0	5.234933161
4.785946162	140	0.00014	0.137447	1.4329124	0.001699	82.14147	0	4.838196697
4.375378481	150	0.00015	0.075837	1.4948869	0.001688	85.69415	0	4.491721924
4.023261792	160	0.00016	0.014226	1.5565702	0.001683	89.23014	0	4.18685034
3.718353529	170	0.00017	-0.04739	1.6181993	0.001685	92.76302	0	3.916770491
3.452073432	180	0.00018	-0.109	1.6800094	0.001693	96.30627	0	3.676055294
3.217767092	190	0.00019	-0.17061	1.742242	0.001708	99.87375	0	3.46033092

### 3.8 BMW Test Engine Modelling on Cold Air (2)

Advanced Timing and high Lift Cam

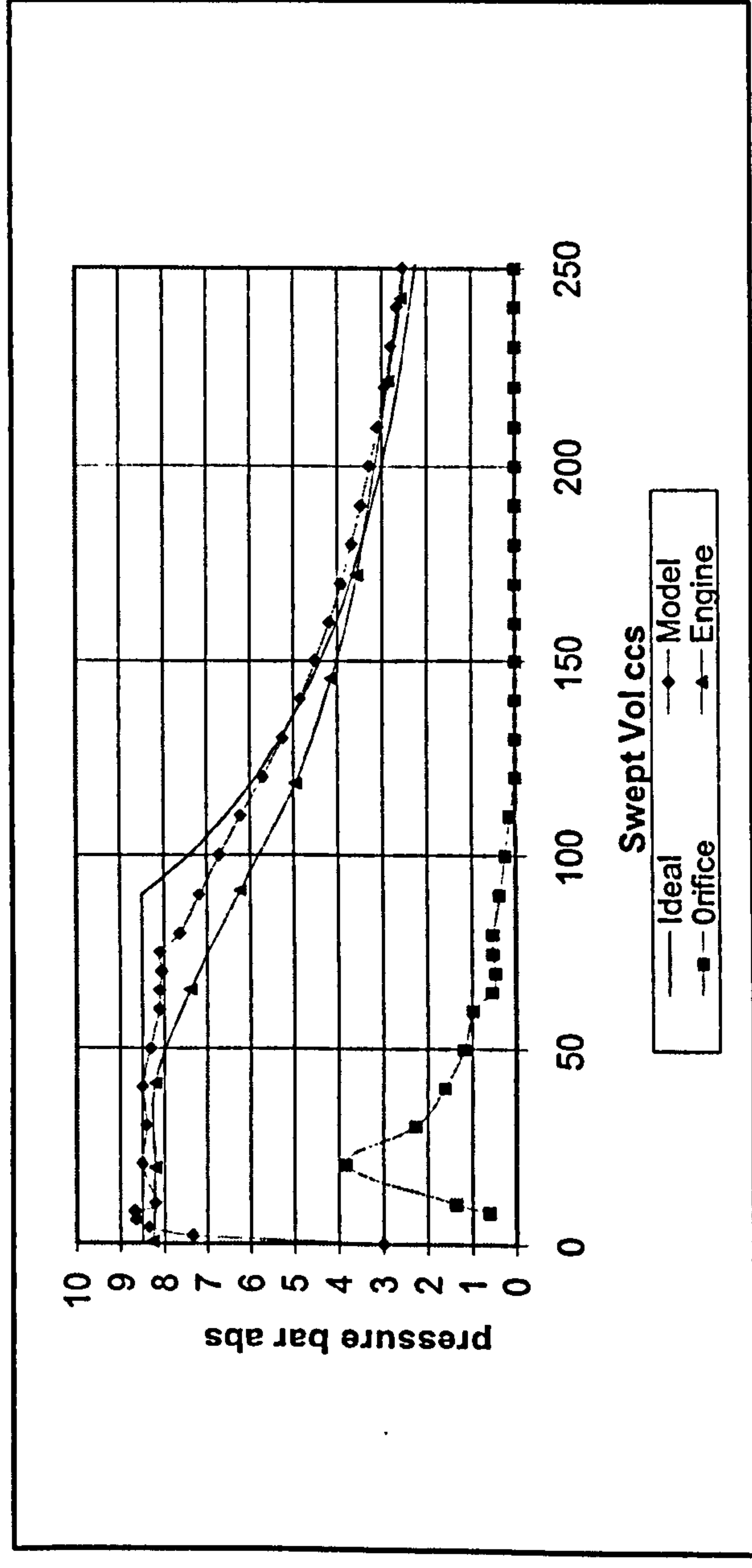
101325	T	288	Density	10.41984
861262.5	8.5 R	287		
	RT	82656	406.5858	
0.025	gamma	1.3		
0.725	gamma Ex	1.3		
Sqrt(Ps-p3/po)	0	3	0	-35
0.82186521	7.34358414	4.585015	1.80045E-05	1.488177
0.448914937	8.35373265	1.566692	2.04811E-05	1.692884
0.295952702	8.64702704	0.891525	2.12002E-05	1.75232
0.22748811	8.67558449	0.615467	2.12702E-05	1.758107
0.212561059	8.2	1.357279	2.01042E-05	1.66173
0.527454507	8.5	3.829388	0.000104198	8.612625
0.459372324	8.4	2.262522	0.000102973	8.5113
0.437288942	8.49104631	1.61643	0.000104089	8.603553
0.40030576	8.31360537	1.175685	0.000101913	8.423761
0.400982549	8.10538092	0.97207	9.93609E-05	8.212777
0.333389811	8.10351477	0.548279	4.9669E-05	4.105443
0.328851144	8.0495996	0.468816	4.93386E-05	4.078128
0.333450628	8.08636453	0.531474	4.95639E-05	4.096754
0.404163314	7.63680723	0.525265	9.36169E-05	7.737995
0.444570314	7.18744467	0.367408	8.81083E-05	7.282678
0.487834671	6.71497248	0.237825	8.23164E-05	6.803946
0.531564296	6.22731267	0.129078	7.63384E-05	6.309825
0.574651233	5.69309567	0	6.97896E-05	5.768529
0.619778598	5.23493316	0	6.41732E-05	5.304296
0.656353859	4.8381967	0	5.93097E-05	4.902303
0.686703813	4.49172192	0	5.50624E-05	4.551237
0.712340769	4.18685034	0	5.13251E-05	4.242326
0.734304754	3.91677049	0	4.80143E-05	3.968668
0.753341162	3.67605529	0	4.50634E-05	3.724763
0.770001458	3.46033092	0	4.24189E-05	3.50618
				7.973501
				8.205951
				8.438401
				8.554626
				8.264063
				8.205951
				8.205951
				7.392376
				6.230126
				4.95165
				4.138075
				3.55695
				2.8596
				2.569038
				2.3947
				2.278475
				2.16225
				2.16225
				256.66
				277.1673
				294.7152
				306.0798
				318.3881
				323.7495
				221.66
				242.1673
				259.7152
				271.0798
				283.3881
				288.7495
				91.2073
				118.2512
				145.4974
				172.2879
				65.21316
				40.97433
				19.13283
				25.89592
				0.413168

3.010199624	200	0.0002	-0.23222	1.8051536	0.00173	103.4801	0	0.000000	3.266035731
2.825200096	210	0.00021	-0.29383	1.8690263	0.001761	107.1416	0	0.000000	3.090242096
2.65940704	220	0.00022	-0.35544	1.9341808	0.001801	110.8766	0	0.000000	2.930522817
2.510083193	230	0.00023	-0.41705	2.0009941	0.001853	114.7067	0	0.000000	2.784849733
2.374978549	240	0.00024	-0.47866	2.0699259	0.001919	118.6582	0	0.000000	2.651515835
2.252227708	250	0.00025	-0.54027	2.1415571	0.002003	122.7644	0	0.000000	2.52907482
2.140271945	260	0.00026	-0.60188	2.2166536	0.002112	127.0693	0	0.000000	2.416293698
2.037799353	270	0.00027	-0.66349	2.2962757	0.002257	131.6336	0	0.000000	2.312115299
1.94369839	280	0.00028	-0.72511	2.3819833	0.002457	136.5468	0	0.000000	2.215628365
1.857021451	290	0.00029	-0.78672	2.4762673	0.002752	141.9516	0	0.000000	2.126043502
1.776956059	300	0.0003	-0.84833	2.5836136	0.003244	148.1052	0	0.000000	2.042673697
1.702801874	310	0.00031	-0.90994	2.7139303	0.004352	155.5756	0	0.000000	1.964918431
1.633952215	320	0.00032	-0.97155	2.9024805	#NUM!	166.3842	0	#NUM!	1.89225064
1.601348859	325	0.000325	-1.00235	#NUM!	-0.039615	#NUM!	0	0.000000	

slot  
0.00041  
0.0082

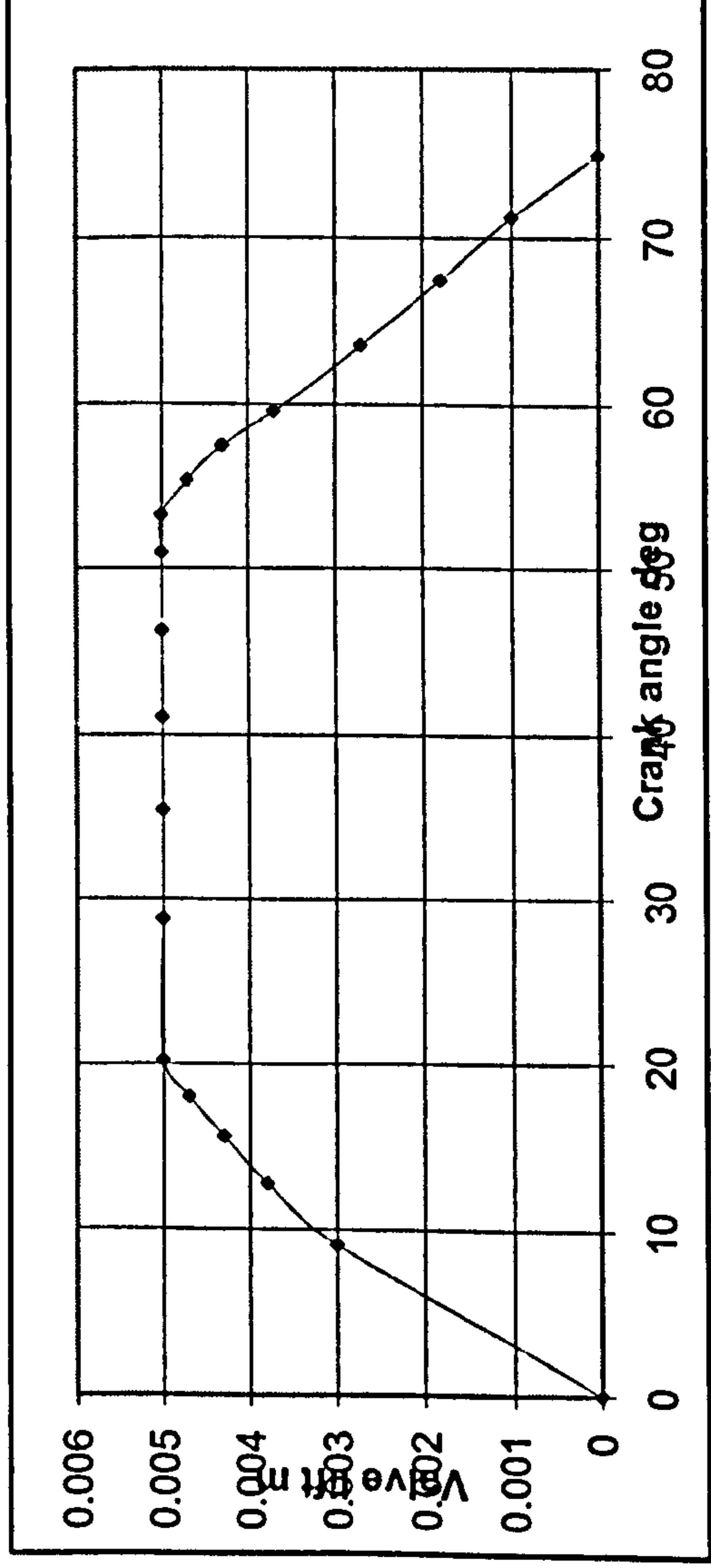
slot length  
0.05

Valve area Slot width  
0  
0.000245 0.00489  
0.000313 0.006255  
0.000356 0.007121  
0.000391 0.007821  
0.000418 0.00835  
0.000418 0.00835  
0.000418 0.00835  
0.000418 0.00835  
0.000418 0.00835  
0.000418 0.00835  
0.000391 0.007821  
0.000356 0.007121  
0.000304 0.006083  
0.000219 0.004385  
0.000145 0.002891  
7.95E-05 0.00159



**3.8 BMW Test Engine Modelling on Cold Air (3)**  
Advanced Timing and high Lift Cam

0.784704086	3.26603573	0	4.00372E-05	3.309311
0.797773217	3.0902421	0	3.78822E-05	3.131188
0.809464397	2.93052282	0	3.59242E-05	2.969352
0.819982085	2.78484973	0	3.41385E-05	2.821749
0.829491989	2.65151583	0	3.2504E-05	2.686648
0.838129934	2.52907482	0	3.1003E-05	2.562585
0.846008365	2.4162937	0	2.96205E-05	2.44831
0.853221211	2.3121153	0	2.83434E-05	2.342751
0.859847568	2.21562837	0	2.71606E-05	2.244985
0.865954522	2.1260435	0	2.60624E-05	2.154214
0.871599362	2.0426737	0	2.50404E-05	2.069739
0.876831298	1.96491843	0	2.40872E-05	1.990954
0.881692848	#NUM!	#NUM!	#NUM!	#NUM!



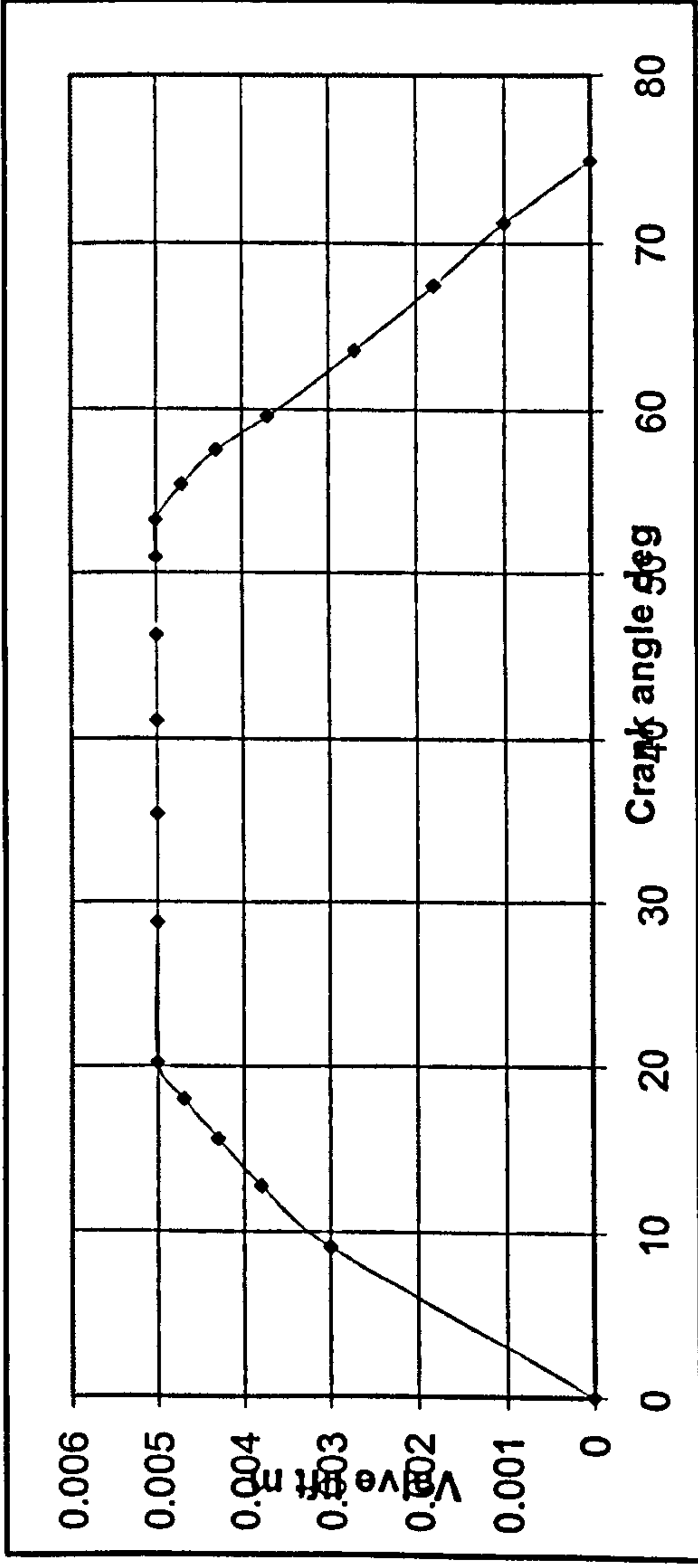
**3.8 BMW Test Engine Modelling on Cold Air (4)**  
Advanced Timing and high Lift Cam



### 3.9 Valve Modelling and Influence of Advanced Valve Timing (1)

Bore m		0.12		RPM		1500		Pa					
Stroke m		0.1		Length		0.1		Ps					
Vc ccs		0.000034		1130.4		0.523333333		0.01 valve dia					
Area cm2		0.011304		Slot angle30		0.837333333		1.34322222 Cd					
Cam dia		40		Head ang 48		valve area		A*sqrtRT.dt					
Sv ccs		crank ang		rads		dt		crank ang		valve lift		P1(V1/V2)^n	
10	0.00001	1	0	0.000268	0	0.004	0	0.00210376	#VALUE!	#VALUE!	6.405380173		
8	0.00008	0.996461	0.0841506	#VALUE!	4.823918	0.004	0.000297605	0.187506	5.355750947				
6	0.00006	0.992923	0.119042	0.0007325	6.824066	0.004	0.000364598	0.302262	5.976853599				
4	0.00004	0.989384	0.1458393	0.0009156	8.360213	0.004	0.000421126	0.428430	6.769711344				
2	0.00002	0.985846	0.1684506	0.0010644	9.656403	0.004	0.000470973	0.606176	6.589892385				
8.5	0	0.982307	0.1883893	0.0012718	10.79939	0.004	0.000577251	0.799833	6.578711046				
8.5	0.00002	0.973461	0.2309004	0.0014497	13.23633	0.005	0.000667049	1.073674	6.749742848				
8.5	0.00004	0.964614	0.2668197	0.0017776	15.2954	0.006	0.000818191	1.446372	7.112612149				
8.5	0.00006	0.946921	0.3272763	0.0020551	18.76106	0.0065	0.000946192	1.854112	7.638694512				
8.5	0.00008	0.929229	0.3784767	0.0023919	21.69611	0.007	0.001059483	2.225440	7.986314127				
8.5	0.0001	0.911536	0.423793	0.0026861	24.29387	0.0082	0.001162381	2.409084	7.358389372				
8.5	0.00015	0.893843	0.4649524	0.0029515	26.65333	0.009	0.00125745	2.560579	6.46007967				
8.5	0.0002	0.87615	0.5029799	0.0031958	28.83324	0.0096	0.001346356	2.478267	6.76932552				
8.5	0.0003	0.858457	0.5385424	0.0034238	30.87186	0.01	0.001373283	2.323412	6.997285375				
8.5	0.0004	0.840764	0.5721029	0.0036387	32.79571	0.01	0.001373283	2.161549	7.172246163				
8.5	0.0005	0.823071	0.6039982	0.0038426	34.6241	0.01	0.001373283	2.029516	7.310748523				
8.5	0.0006	0.805379	0.6344824	0.0040374	36.3716	0.01	0.001373283	1.919302	7.423104507				
8.5	0.0007	0.787686	0.6637528	0.0042244	38.04952	0.01	0.001373283	1.825595	7.516074904				
8.5	0.0008	0.769993	0.6919663	0.0044045	39.66686	0.01	0.001373283	1.744718	7.594275854				
8.5	0.0009	0.7523	0.71925	0.0045786	41.23089	0.01	0.001373283	1.674041	7.660966337				
8.5	0.001	0.734607	0.7457087	0.0047474	42.74763	0.01	0.001373283	1.611624	7.718512576				
8.5	0.0011	0.716914	0.7714301	0.0049115	44.22211	0.01	0.001373283	1.556007	7.768674033				
8.5	0.0012	0.699222	0.7964883	0.0050713	45.65857	0.01	0.001373283	1.506064	7.812786118				
8.5	0.0013	0.681529	0.8209468	0.0052272	47.06064	0.01	0.001245905	1.325406	7.851880646				
8.5	0.0014	0.663836	0.8448602	0.0053797	48.43148	0.01	0.001187364	1.227627	7.886767454				
8.5	0.0015	0.646143	0.8682764	0.005529	49.77381	0.0098	0.001129962	1.137391	7.894667767				
8.5	0.0016	0.62845	0.8912373	0.0056753	51.09003	0.0096	0.001073606	1.053710	7.886546122				
8.5	0.0017	0.610757	0.9137797	0.005819	52.38228	0.009	0.001018214	0.975765	7.870185209				
8.5	0.0018	0.593064	0.9359368	0.0059602	53.65243								

0.784704086	3.26603573	0	4.00372E-05	3.309311
0.797773217	3.0902421	0	3.78822E-05	3.131188
0.809464397	2.93052282	0	3.59242E-05	2.969352
0.819982085	2.78484973	0	3.41385E-05	2.821749
0.829491989	2.65151583	0	3.2504E-05	2.686648
0.838129934	2.52907482	0	3.1003E-05	2.562585
0.846008365	2.4162937	0	2.96205E-05	2.44831
0.853221211	2.3121153	0	2.83434E-05	2.342751
0.859847568	2.21562837	0	2.71606E-05	2.244985
0.865954522	2.1260435	0	2.60624E-05	2.154214
0.871599362	2.0426737	0	2.50404E-05	2.069739
0.876831298	1.96491843	0	2.40872E-05	1.990954
0.881692848	#NUM!	#NUM!	#NUM!	#NUM!



**3.8 BMW Test Engine Modelling on Cold Air (4)**  
Advanced Timing and high Lift Cam

### 3.9 Valve Modelling and Influence of Advanced Valve Timing (1)

		Bore m	0.12	RPM	1500	Pa	
		Stroke m	0.1	Length	0.1	Ps	
		Vc ccs	0.000034	Slot angle30	0.5233333333	Valve lift	
		Area cm2	0.011304	Head ang 48	0.8373333333	Slot angle	
		Cam dia	40			1.34322222 Cd	
Sv ccs	crank ang	rads	dt	crank ang	valve lift	A*sqrtRT.dt	P1(V1/V2)^n
10	0.00001	1	0	0.000268	0.004	0	
8	0.000008	0.996461	0.0841506	#VALUE!	4.823918	0.000210376	#VALUE!
6	0.000006	0.992923	0.119042	0.0007325	6.824066	0.000297605	0.187506
4	0.000004	0.989384	0.1458393	0.0009156	8.360213	0.000364598	0.302262
2	0.000002	0.985846	0.1684506	0.0010644	9.656403	0.000421126	0.428430
0	0	0.982307	0.1883893	0.0012718	10.79939	0.000470973	0.606176
2	0.000002	0.973461	0.2309004	0.0014497	13.23633	0.000577251	0.799833
4	0.000004	0.964614	0.2668197	0.0017776	15.2954	0.000667049	1.073674
6	0.000006	0.946921	0.3272763	0.0020551	18.76106	0.000818191	1.446372
8	0.000008	0.929229	0.3784767	0.0023919	21.69611	0.000946192	1.854112
10	0.00001	0.911536	0.423793	0.0026861	24.29387	0.001059483	2.225440
15	0.000015	0.893843	0.4649524	0.0029515	26.65333	0.001162381	2.409084
20	0.00002	0.87615	0.5029799	0.0031958	28.83324	0.00125745	2.560579
30	0.00003	0.858457	0.5385424	0.0034238	30.87186	0.001346356	2.478267
40	0.00004	0.840764	0.5721029	0.0036387	32.79571	0.001373283	2.323412
50	0.00005	0.823071	0.6039982	0.0038426	34.6241	0.001373283	2.161549
60	0.00006	0.805379	0.6344824	0.0040374	36.3716	0.001373283	2.029516
70	0.00007	0.787686	0.6637528	0.0042244	38.04952	0.001373283	1.919302
80	0.00008	0.769993	0.6919663	0.0044045	39.66686	0.001373283	1.825595
90	0.00009	0.7523	0.71925	0.0045786	41.23089	0.001373283	1.744718
100	0.0001	0.734607	0.7457087	0.0047474	42.74763	0.001373283	1.674041
110	0.00011	0.716914	0.7714301	0.0049115	44.22211	0.001373283	1.611624
120	0.00012	0.699222	0.7964883	0.0050713	45.65857	0.001373283	1.556007
130	0.00013	0.681529	0.8209468	0.0052272	47.06064	0.001373283	1.506064
140	0.00014	0.663836	0.8448602	0.0053797	48.43148	0.001245905	1.325406
150	0.00015	0.646143	0.8682764	0.005529	49.77381	0.001187364	1.227627
160	0.00016	0.62845	0.8912373	0.0056753	51.09003	0.001129962	1.137391
170	0.00017	0.610757	0.9137797	0.005819	52.38228	0.001073606	1.053710
180	0.00018	0.593064	0.9359368	0.0059602	53.65243	0.001018214	0.975765

### 3.9 Valve Modelling and Influence of Advanced Valve Timing (2)

101325 318.3158808 T 1123  
 861262.5 8.5 R 287  
 RT 322301 567.7156 Density 2.672230306  
 gamma 1.34 2.63729E-05  
 gamma Ex 1.34

Sqrt(Ps-p3/po)	6	5	#VALUE!	#VALUE!	PV model	PV ideal
0.885351368					0	-13.23633
1.084729689	5.55914433	0.203393			4.823918	-8.412412
0.971704654	6.270563192	0.29371			6.824066	-6.412264
0.804678389	7.114459717	0.344748			8.360213	-4.876117
0.845457878	7.102388324	0.512496			9.656403	-3.579928
0.847928827	7.256912654	0.678202		0	10.79939	-2.436941
0.809308288	7.61867585	0.868933		1.5	13.23633	0
0.72054648	8.154790396	1.042178		1.5	15.2954	2.059069
0.567729766	8.5	1.052635		1.5	18.76106	5.524729
0.438441716	8.5	0.975726		1.5	21.69611	8.459784
0.653615073	8.5	1.574614		1.5	24.29387	11.05754
0.873714736	8.5	2.237216		3.75	26.65333	13.41699
0.804768098	8.5	1.99443		3.75	28.83324	15.59691
0.749896478	8.5	1.742318		7.5	30.87186	17.63553
0.704890796	8.5	1.523656		7.5	32.79571	19.55938
0.667113773	8.5	1.353918		7.5	34.6241	21.38777
0.634818884	8.5	1.218409		7.5	36.3716	23.13527
0.60679791	8.5	1.107767		7.5	38.04952	24.81319
0.582185025	8.5	1.015749		7.5	39.6686	26.43053
0.560341451	8.5	0.938034		7.5	41.23089	27.99456
0.540784274	8.5	0.871541		7.5	42.74763	29.5113
0.523140755	8.5	0.814011		7.5	44.22211	30.98578
0.507117992	8.5	0.763752		7.5	45.65857	32.42224
0.492482216	8.5	0.652739		7.5	47.06064	33.82431
0.479044276	8.474855334	0.588088		7.5	48.43148	35.19515
0.475948494	8.436007433	0.54134	0.0098	7.5	49.77381	36.53748
0.479130719	8.391410843	0.504865	0.0096	7.5	51.09003	37.8537
0.485477923	8.3438976	0.473712	0.009	7.5	52.38228	39.14595
				7.5	53.65243	40.4161



0.493734727	8.29435975	0.44578	0.0085	7.29435975	7.5	54.90218	41.66585
0.503384628	8.242920809	0.420054	0.008	7.242920809	7.5	56.13304	42.89671
0.514214274	8.189378931	0.39596	0.007195	7.189378931	7.5	57.3464	44.11007
0.526142312	8.133380962	0.373123	0.006847	7.133380962	7.5	58.54349	45.30716
0.539149191	8.074492416	0.351261	0.006488	7.074492416	7.5	59.72547	46.48914
0.553246759	8.012225132	0.330147	0.006119	7.012225132	7.5	60.89336	47.65703
0.568464333	7.946046876	0.309583	0.005739	6.946046876	7.5	62.04814	48.81181
0.584841915	7.875382926	0.289393	0.005352	6.875382926	7.5	63.19069	49.95436
0.602426668	7.799613967	0.269414	0.004957	6.799613967	7.5	64.32182	51.08549
0.621270929	7.718072224	0.249493	0.004555	6.718072224	7.5	65.44231	52.20598
0.641430989	7.630036764	0.229482	0.004147	6.630036764	7.5	66.55286	53.31653
0.662966251	7.534728382	0.209238	0.003734	6.534728382	7.5	67.65414	54.41781
0.685938582	7.431304321	0.18862	0.003317	6.431304321	7.5	68.74678	55.51045
0.71041178	7.318852919	0.167487	0.002897	6.318852919	7.5	69.83136	56.59502
0.736451083	7.196388292	0.1457	0.002474	6.196388292	7.156638579	70.90843	57.6721
0.764122717	7.062845064	0.123116	0.002049	6.062845064	6.836788957	71.97854	58.74221
0.793493459	6.917073219	0.099595	0.001623	5.917073219	6.538218516	73.04217	59.80584
0.824630228	6.757833079	0.07499	0.001196	5.757833079	6.258962495	74.0998	60.86347
0.85759968	6.583790453	0.049155	0	5.583790453	5.99728551	75.15189	61.91556
0.892467837	6.393511967	0.02194	0	5.393511967	5.751649475	76.19887	62.96254
0.929299737	6.185460598	-0.006807	0	5.185460598	5.520686703	77.24116	64.00482
0.968159112	5.995232845	0	0	4.995232845	5.30317726	78.27916	65.04283
1.002388001	5.81499188	0	0	4.81499188	5.098029798	79.31326	66.07693
1.033812359	5.644005779	0	0	4.644005779	4.904265281	80.34384	67.10751
1.062797869	5.481610821	0	0	4.481610821	4.721003086	81.37126	68.13493
1.089642774	5.327203838	0	0	4.327203838	4.547449112	82.39588	69.15955
1.114593978	5.18023555	0	0	4.18023555	4.382885551	83.41805	70.18172
1.137858492	5.04020477	0	0	4.04020477	4.226662062	84.43811	71.20178
1.159611776	4.906653318	0	0	3.906653318	4.078188139	85.45638	72.22005
1.180003956	4.779161571	0	0	3.779161571	3.936926473	86.47321	73.23688
1.199164547	4.657344548	0	0	3.657344548	3.802387179	87.48892	74.25259
1.2172061	4.540848455	0	0	3.540848455	3.674122746	88.50382	75.26749
1.234227063	4.429347635	0	0	3.429347635	3.551723618	89.51824	76.28191
1.250314048	4.322541861	0	0	3.322541861	3.434814308	90.53249	77.29616
1.265543657	4.220153941	0	0	3.220153941	3.323049973	91.5469	78.31057
1.279983963	4.121927576	0	0	3.121927576	3.216113402	92.56177	79.32544
1.293695718	4.027625459	0	0	3.027625459	3.113712332	93.57744	80.34111
1.306733364	3.937027572	0	0	2.937027572	3.015577082	94.59422	81.35789
1.319145859	3.84992966	0	0	2.84992966	2.921458445	95.61243	82.3761
1.330977387	3.766141865	0	0	2.766141865	2.831125801	96.63241	83.39608
1.342267939	3.685487499	0	0	2.685487499	2.744365451	97.65449	84.41816

1220.55

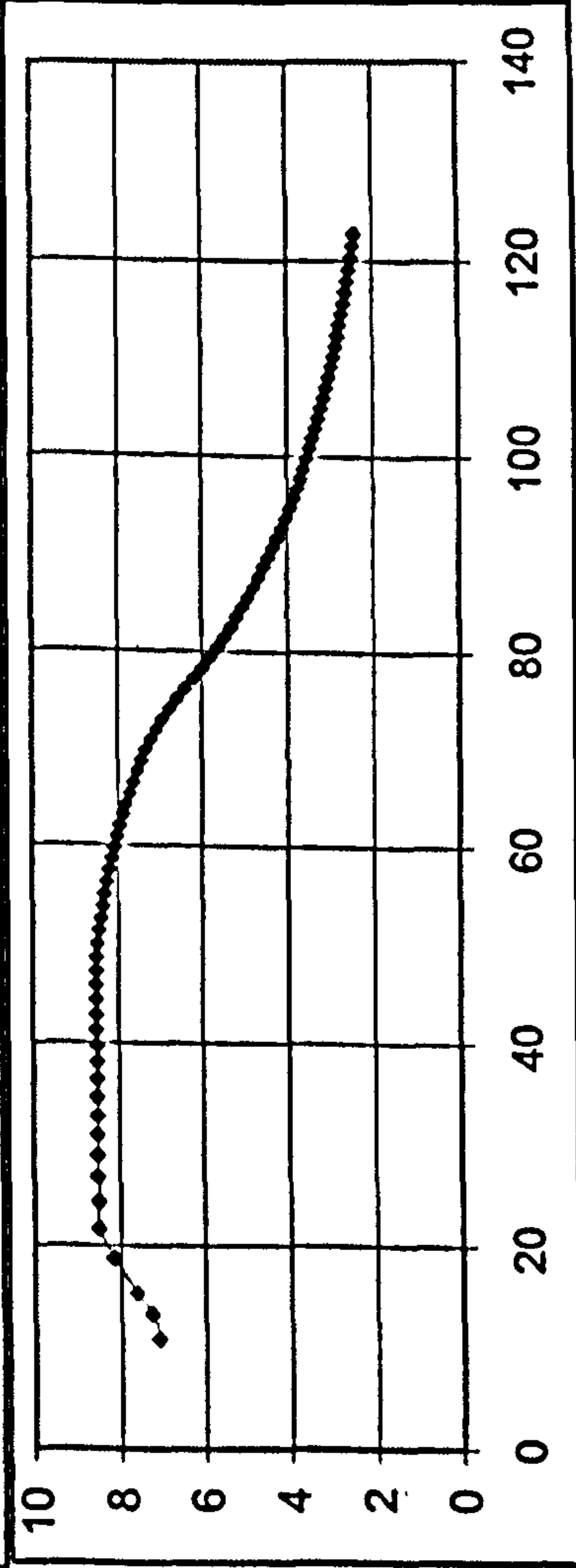
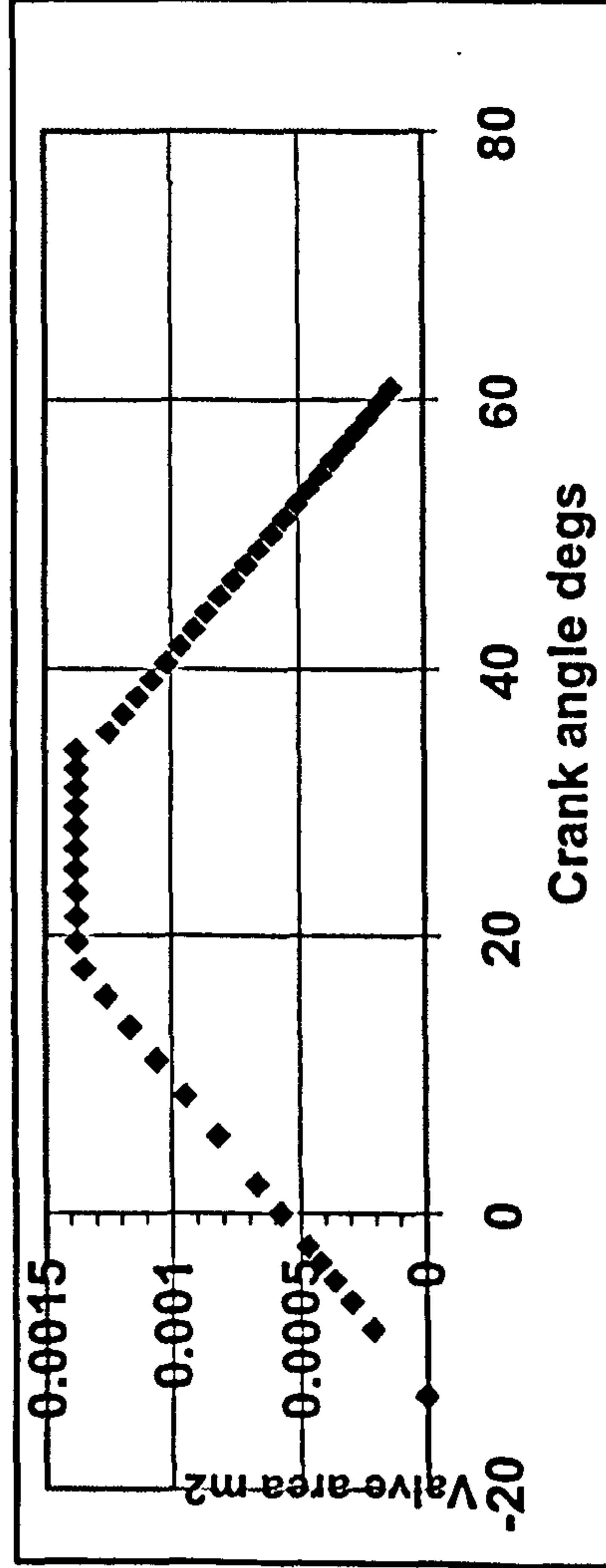
1236.722

3.660979104	600	0.0006	-0.15004	1.7214004	0.0109645	98.679	0	0	0.000000	3.607801934
3.580782539	610	0.00061	-0.16773	1.7393211	0.0110787	99.70631	0	0	0.000000	3.532931608
3.503604397	620	0.00062	-0.18542	1.7572967	0.0111932	100.7368	0	0	0.000000	3.460733124
3.429285087	630	0.00063	-0.20311	1.7753334	0.0113081	101.7707	0	0	0.000000	3.391072432
3.357675814	640	0.00064	-0.22081	1.7934379	0.0114234	102.8085	0	0	0.000000	3.323824091
3.288637693	650	0.00065	-0.2385	1.8116169	0.0115392	103.8507	0	0	0.000000	3.2588706
3.222040944	660	0.00066	-0.25619	1.8298775	0.0116556	104.8974	0	0	0.000000	3.196101789
3.157764175	670	0.00067	-0.27389	1.8482269	0.0117725	105.9493	0	0	0.000000	3.135414261
3.095693722	680	0.00068	-0.29158	1.8666726	0.01189	107.0067	0	0	0.000000	3.076710891
3.03572305	690	0.00069	-0.30927	1.8852227	0.0120081	108.0701	0	0	0.000000	3.01990036
2.977752217	700	0.0007	-0.32696	1.9038854	0.012127	109.1399	0	0	0.000000	2.964896738
2.921687371	710	0.00071	-0.34466	1.9226694	0.0122467	110.2167	0	0	0.000000	2.911619095
2.867440307	720	0.00072	-0.36235	1.9415839	0.0123672	111.301	0	0	0.000000	2.859991149
2.814928051	730	0.00073	-0.38004	1.9606385	0.0124886	112.3933	0	0	0.000000	2.809940941
2.764072482	740	0.00074	-0.39774	1.9798435	0.012611	113.4942	0	0	0.000000	2.761400539
2.714799992	750	0.00075	-0.41543	1.9992098	0.0127344	114.6044	0	0	0.000000	2.714305762
2.667041164	760	0.00076	-0.43312	2.0187489	0.0128589	115.7245	0	0	0.000000	2.66859593
2.620730488	770	0.00077	-0.45081	2.0384732	0.0129845	116.8552	0	0	0.000000	2.624213632
2.575806089	780	0.00078	-0.46851	2.0583961	0.0131115	117.9972	0	0	0.000000	2.581104512
2.532209484	790	0.00079	-0.4862	2.0785317	0.0132398	119.1515	0	0	0.000000	2.53921707
2.489885357	800	0.0008	-0.50389	2.0988956	0.0133695	120.3189	0	0	0.000000	2.498502479
2.448781349	810	0.00081	-0.52159	2.1195043	0.0135009	121.5002	0	0	0.000000	2.458914422
2.408847865	820	0.00082	-0.53928	2.140376	0.0136339	122.6967	0	0	0.000000	2.420408926
2.370037899	830	0.00083	-0.55697	2.1615306	0.0137687	123.9094	0	0	0.000000	2.382944226
2.332306687	840	0.00084	-0.57466	2.1829897	0.0139054	125.1395	0	0	0.000000	2.346480626
2.295612468	850	0.00085	-0.59236	2.2047771	0.0140443	126.3885	0	0	0.000000	2.310980375
2.259914511	860	0.00086	-0.61005	2.2269194	0.0141854	127.6578	0	0	0.000000	2.27640755
2.225174822	870	0.00087	-0.62774	2.2494459	0.014329	128.9491	0	0	0.000000	2.242727951
2.1913571	880	0.00088	-0.64544	2.2723893	0.0144753	130.2644	0	0	0.000000	2.209908998
2.158426813	890	0.00089	-0.66313	2.2957865	0.0146244	131.6056	0	0	0.000000	2.177919639
2.126351089	900	0.0009	-0.68082	2.3196792	0.0147768	132.9752	0	0	0.000000	2.146730262
2.095098621	910	0.00091	-0.69851	2.3441148	0.0149326	134.376	0	0	0.000000	2.116312613
2.064639578	920	0.00092	-0.71621	2.3691479	0.0150922	135.811	0	0	0.000000	2.086639722
2.034945517	930	0.00093	-0.7339	2.3948414	0.0152561	137.2839	0	0	0.000000	2.057685831
2.005989307	940	0.00094	-0.75159	2.4212691	0.0154247	138.7989	0	0	0.000000	2.029426329
1.977745052	950	0.00095	-0.76929	2.4485179	0.0155986	140.3609	0	0	0.000000	2.001837685
1.950188026	960	0.00096	-0.78698	2.476692	0.0157785	141.976	0	0	0.000000	1.974897397
1.923294609	970	0.00097	-0.80467	2.5059173	0.0159651	143.6513	0	0	0.000000	1.948583934
1.897042222	980	0.00098	-0.82236	2.5363495	0.0161596	145.3958	0	0	0.000000	1.922876682
1.871409276	990	0.00099	-0.84006	2.5681839	0.0163631	147.2207	0	0	0.000000	1.897755902
1.846375117	1000	0.001	-0.85775	2.601672	0.0165775	149.1404	0	0	0.000000	1.873202681

1.353053825	3.607801934	0	0	2.607801934	2.660979104	98.679	85.44267
1.363368097	3.532931608	0	0	2.532931608	2.580782539	99.70631	86.46998
1.373240922	3.460733124	0	0	2.460733124	2.503604397	100.7368	87.50042
1.382699896	3.391072432	0	0	2.391072432	2.429285087	101.7707	88.53438
1.391770321	3.323824091	0	0	2.323824091	2.357675814	102.8085	89.57221
1.400475445	3.2588706	0	0	2.2588706	2.288637693	103.8507	90.61432
1.408836672	3.196101789	0	0	2.196101789	2.222040944	104.8974	91.66111
1.416873745	3.135414261	0	0	2.135414261	2.157764175	105.9493	92.71298
1.424604907	3.076710891	0	0	2.076710891	2.095693722	107.0067	93.77038
1.432047043	3.01990036	0	0	2.01990036	2.03572305	108.0701	94.83376
1.43921581	2.964896738	0	0	1.964896738	1.977752217	109.1399	95.9036
1.446125744	2.911619095	0	0	1.911619095	1.921687371	110.2167	96.98039
1.452790363	2.85991149	0	0	1.85991149	1.867440307	111.301	98.06466
1.459222255	2.809940941	0	0	1.809940941	1.814928051	112.3933	99.15696
1.465433158	2.761400539	0	0	1.761400539	1.764072482	113.4942	100.2579
1.471434033	2.714305762	0	0	1.714305762	1.714799992	114.6044	101.3681
1.477235124	2.66859593	0	0	1.66859593	1.667041164	115.7245	102.4881
1.482846021	2.624213632	0	0	1.624213632	1.620730488	116.8552	103.6188
1.488275708	2.581104512	0	0	1.581104512	1.575806089	117.9972	104.7609
1.493532614	2.53921707	0	0	1.53921707	1.532209484	119.1515	105.9152
1.498624654	2.498502479	0	0	1.498502479	1.489885357	120.3189	107.0825
1.503559266	2.458914422	0	0	1.458914422	1.448781349	121.5002	108.2639
1.50834345	2.420408926	0	0	1.420408926	1.408847865	122.6967	109.4604
1.512983799	2.382944226	0	0	1.382944226	1.370037899	123.9094	110.6731
1.517486526	2.346480626	0	0	1.346480626	1.33230687	125.1395	111.9032
1.521857494	2.310980375	0	0	1.310980375	1.295612468	126.3885	113.1522
1.526102241	2.27640755	0	0	1.27640755	1.259914511	127.6578	114.4215
1.530225998	2.242727951	0	0	1.242727951	1.225174822	128.9491	115.7128
1.534233713	2.209908998	0	0	1.209908998	1.1913571	130.2644	117.028
1.538130073	2.177919639	0	0	1.177919639	1.158426813	131.6056	118.3693
1.541919514	2.146730262	0	0	1.146730262	1.126351089	132.9752	119.7389
1.545606242	2.116312613	0	0	1.116312613	1.095098621	134.376	121.1397
1.549194249	2.086639722	0	0	1.086639722	1.064639578	135.811	122.5747
1.552687324	2.057685831	0	0	1.057685831	1.034945517	137.2839	124.0476
1.556089064	2.029426329	0	0	1.029426329	1.005989307	138.7989	125.5625
1.559402891	2.001837685	0	0	1.001837685	0.977745052	140.3609	127.1246
1.562632059	1.974897397	0	0	0.974897397	0.950188026	141.976	128.7396
1.565779664	1.948583934	0	0	0.948583934	0.923294609	143.6513	130.415
1.568848655	1.922876682	0	0	0.922876682	0.897042222	145.3958	132.1595
1.571841844	1.897755902	0	0	0.897755902	0.871409276	147.2207	133.9844
1.574761909	1.873202681	0	0	0.873202681	0.846375117	149.1404	135.9041



1.821919978	1010	0.00101	-0.87544	2.6371466	0.0168049	151.174	0	0.000000	1.849198891
1.79802493	1020	0.00102	-0.89314	2.6750643	0.0170485	153.3476	0	0.000000	1.82572715
1.77467184	1030	0.00103	-0.91083	2.7160819	0.017313	155.699	0	0.000000	1.802770784
1.751843333	1040	0.00104	-0.92852	2.7612053	0.0176057	158.2857	0	0.000000	1.780313789
1.729522749	1050	0.00105	-0.94621	2.812122	0.0179405	161.2044	0	0.000000	1.758340804
1.70769411	1060	0.00106	-0.96391	2.8721018	0.018349	164.6428	0	0.000000	1.736837075
1.686342082	1070	0.00107	-0.9816	2.9494611	0.0190321	169.0774	0	0.000000	1.715788427
1.665451952	1080	0.00108	-0.99929	3.1039683	0.0093932	177.9345	0	0.000000	1.695181237
1.645009586	1090	0.00109	1	0	0.0098852	0	0	0.000000	1.675002407
1.625001411	1100	0.0011	1	0	0	0	0	0.000000	1.655239339
1.605414381	1110	0.00111	1	0	0	0	0	0.000000	1.635879913
1.586235958	1120	0.00112	1	0	0	0	0	0.000000	1.616912464
1.56745408	1130	0.00113	1	0	0	0	0	0.000000	1.59832576



3.9 Valve Modelling and Influence of Advanced Valve Timing (5)

1.577611407	1.849198891	0	0	0.849198891	0.821919978	151.174	137.9377
1.580392776	1.82572715	0	0	0.82572715	0.79802493	153.3476	140.1113
1.583108348	1.802770784	0	0	0.802770784	0.77467184	155.699	142.4626
1.585760348	1.780313789	0	0	0.780313789	0.751843333	158.2857	145.0493
1.588350904	1.758340804	0	0	0.758340804	0.729522749	161.2044	147.9681
1.590882052	1.736837075	0	0	0.736837075	0.70769411	164.6428	151.4064
1.59335574	1.715788427	0	0	0.715788427	0.686342082	169.0774	155.8411
1.595773831	1.695181237	0	0	0.695181237	0.665451952	177.9345	164.6982
1.598138112	1.675002407	0	0	0.675002407	0.645009586	0	-13.23633
1.600450295	1.655239339	0	0	0.655239339	0.625001411	0	-13.23633
1.602712019	1.635879913	0	0	0.635879913	0.605414381	0	-13.23633
1.604924858	1.616912464	0	0	0.616912464	0.586235958	0	-13.23633
1.607090322	1.59832576	0	0	0.59832576	0.56745408	0	-13.23633

418.3429312 434.6139314

IMEP bar 3.70215

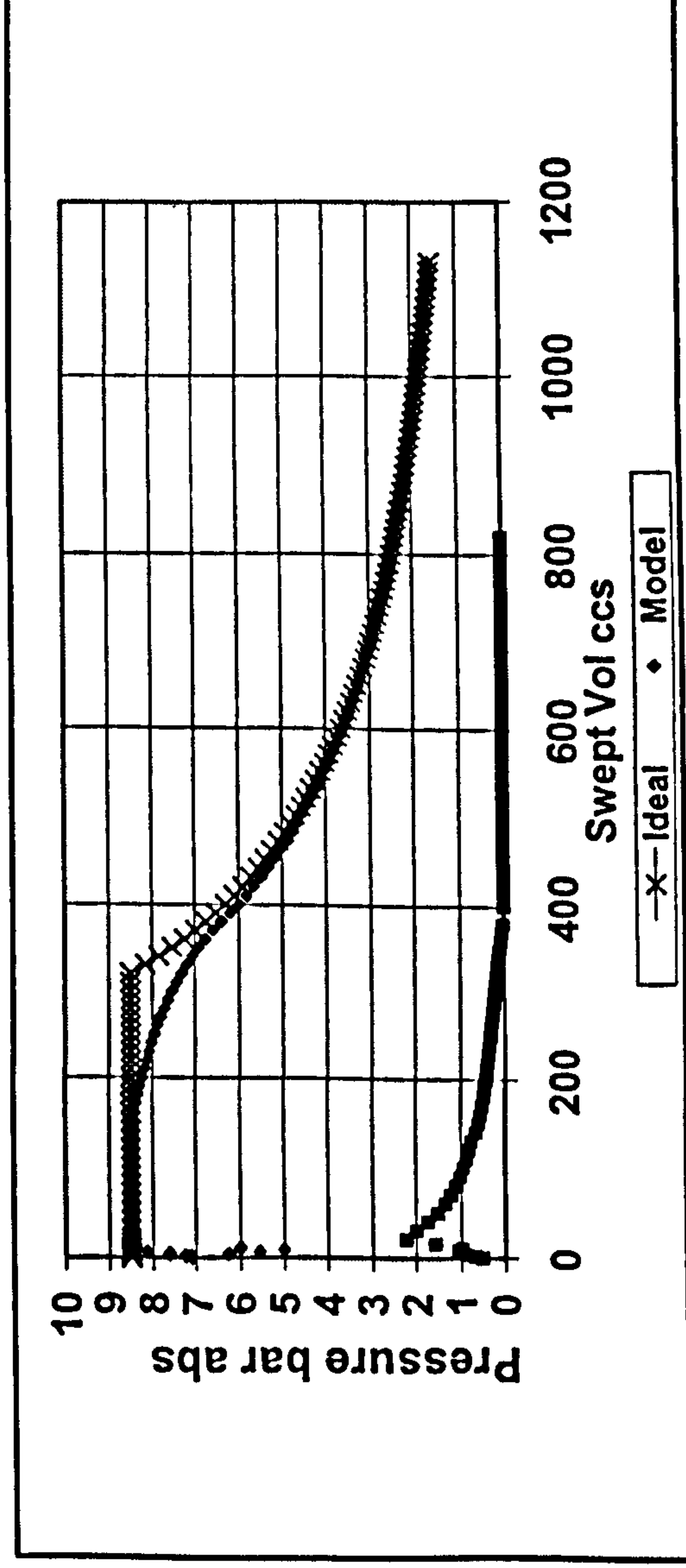
W at 15 10458.57328

931

3.372592

0.329558

3.515486817

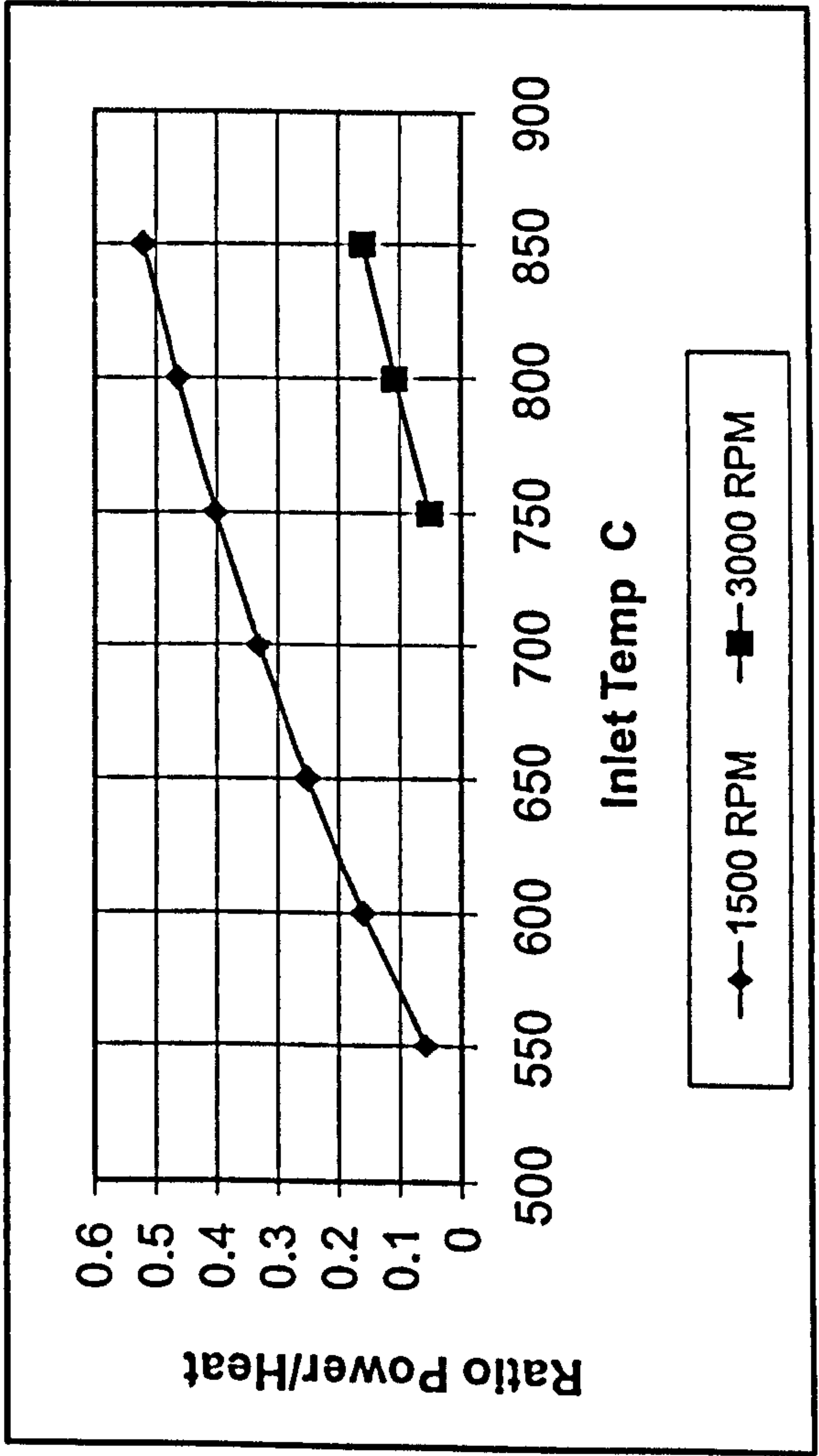
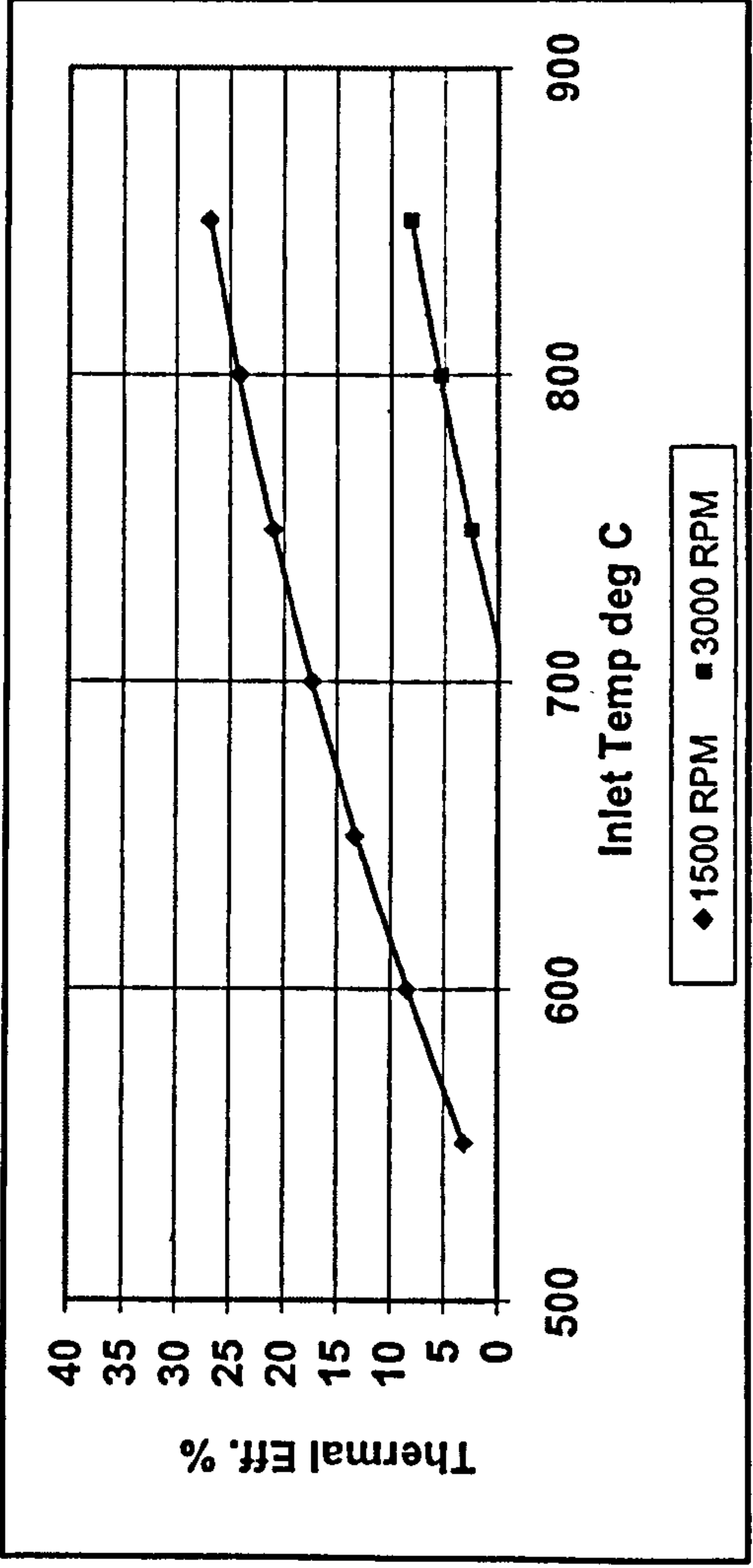


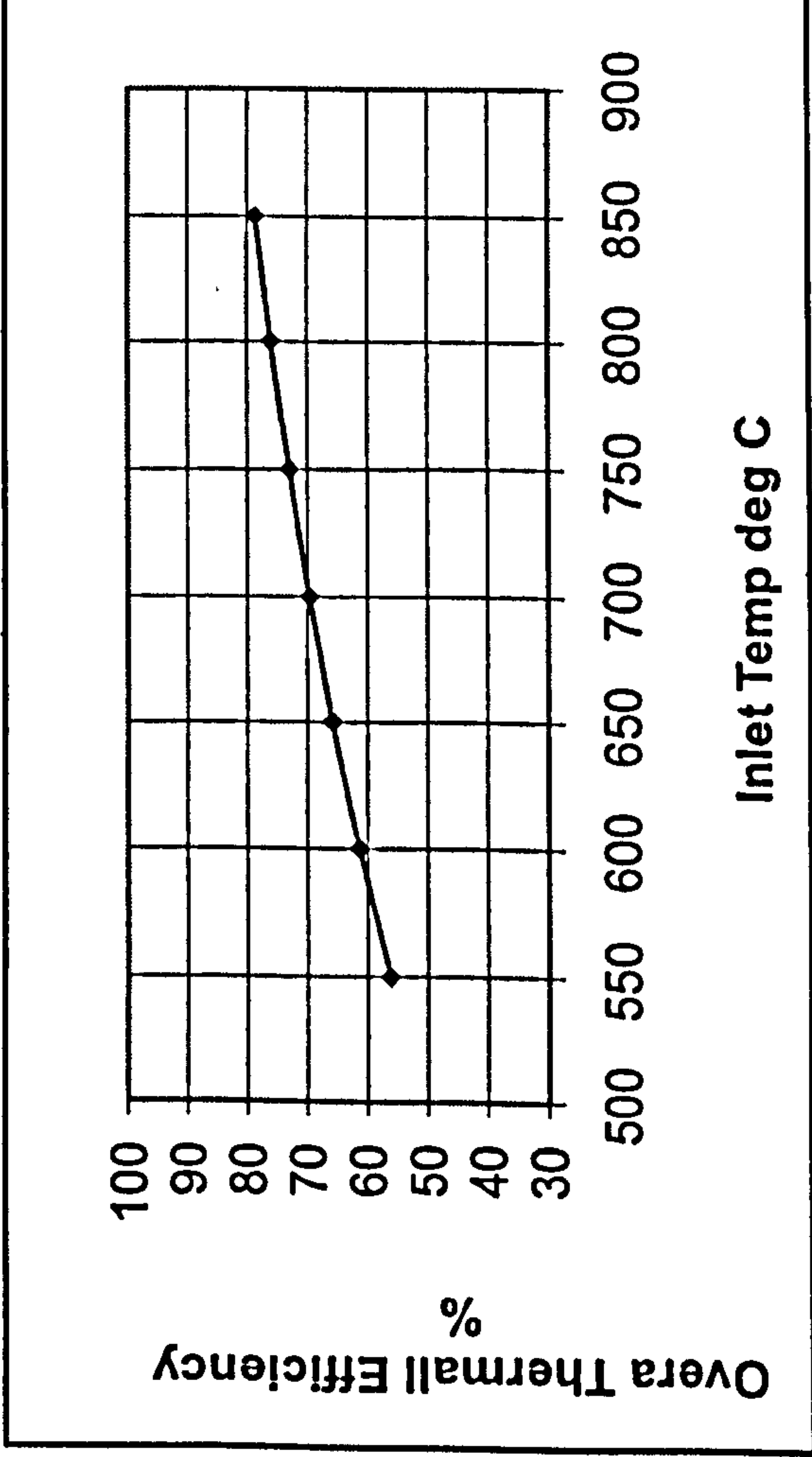
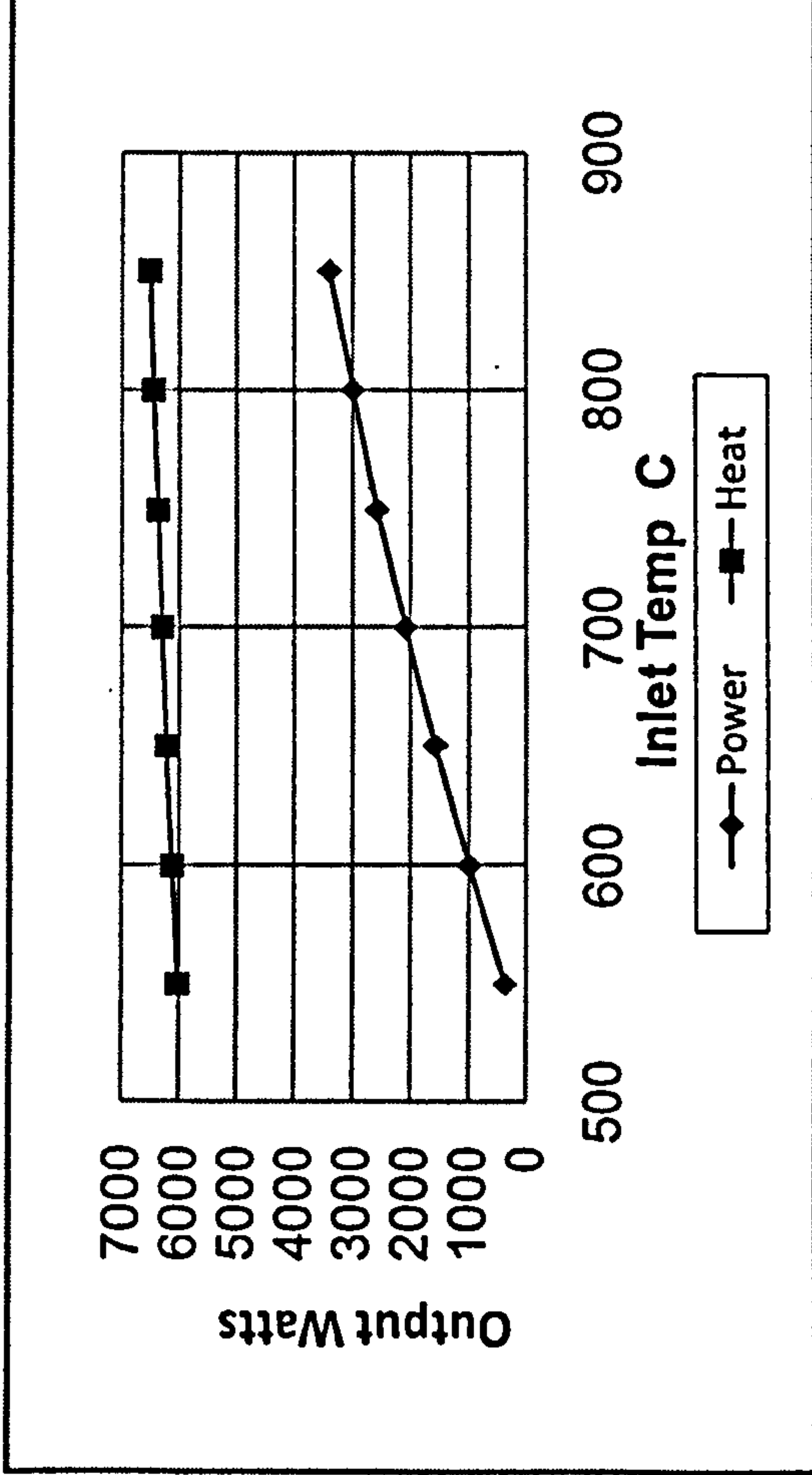
3.9 Valve Modelling and Influence of Advanced Valve Timing (6)

Tin	Effectiveness		313		3387		Ex temp				
	Comp deg K	363	0.7	0.6	CP ex	1.025	W out	%	T Ex	Syst Heat jacket	3000
	Tc Out K	Heat in	mass	473	cp						
1123	711	606.6	12580.51	0.020822	1.17	3387	26.9	467.4	3508.744	3000	
1073	677	582.8	12391.89	0.021792	1.16	2985	24.1	457.2	3444.406	3000	
973	642	558.3	12215.2	0.022858	1.15	2556	20.9	446.7	3366.75	3000	
923	608	534.5	12013.44	0.024032	1.14	2074.5	17.3	436.5	3288.502	3000	
873	575	511.4	11783.06	0.025334	1.13	1558	13.2	426.6	3209.567	3000	
823	541	487.6	11561.69	0.026785	1.12	978	8.5	416.4	3113.354	3000	
	508	464.5	11306.24	0.028412	1.11	349	3.1	406.5	3014.187	3000	
1123	675	581.4	29555.52	0.020822	1.17	2409	8.2	581.4	13564.73	1500	
1073	642	558.3	29145.15	0.021792	1.16	1559	5.3	558.3	12907.58	1500	
973	609	535.2	28722.21	0.022858	1.15	701	2.4	535.2	12207.32	1500	
923	576	512.1	28284.76	0.024032	1.14	-217	-0.8	512.1	11457.29	1500	
873	544	489.7	27785.57	0.025334	1.13	-1250	-4.5	489.7	10689.49	1500	
823	512	467.3	27262.31	0.026785	1.12	-2366	-8.7	467.3	9857.735	1500	
	480	444.9	26710.6	0.028412	1.11	-3443	-12.9	444.9	8950.377	1500	

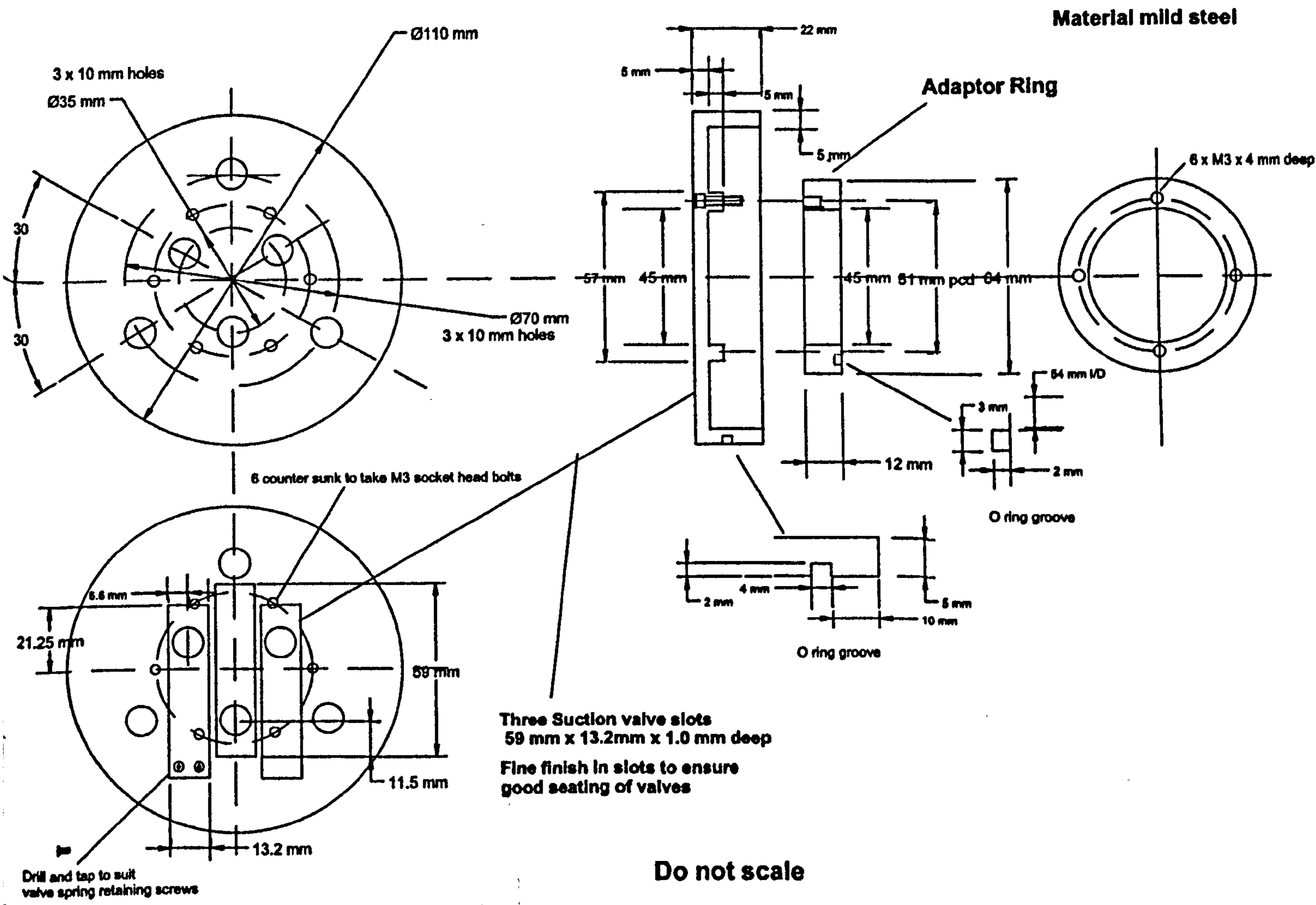
	Tc Out K	Tc out C	Th out K	Th out C	Cp
1123	711	0.02082217	467.4	194.4	
1073	677	0.02179245	457.2	184.2	
973	642	0.02285758	446.7	173.7	
923	608	0.02403217	436.5	163.5	
873	575	0.02533402	426.6	153.6	
823	541	0.026785	416.4	143.4	
	508	0.02841227	406.5	133.5	

Ratio	1500 RPM				3000 Rpm				Overall eff
	Ratio	5253	418	384	8640	3387	850	78.7	
6508.744	0.520377	1123	5253	418	384	8640	3387	850	78.7
6444.406	0.463192	1073	5520	412	378	8505	2985	800	76.1
6366.75	0.401461	1023	5814	406	372	8370	2556	750	73.0
6288.502	0.329888	973	6138	399	365	8212.5	2074.5	700	69.6
6209.567	0.250903	923	6497	392	358	8055	1558	650	65.9
6113.354	0.159978	873	6897	384	350	7875	978	600	61.3
6014.187	0.058029	823	7346	376	342	7695	349	550	56.3
15064.73	0.15991	1123	10506	355	287	12915	2409	850	
14407.58	0.108207	1073	11041	348	280	12600	1559	800	
13707.32	0.051141	1023	11629	342	274	12330	701	750	
12957.29		973	12277	336	268	12060	-217	700	
12189.49		923	12995	329	261	11745	-1250	650	
11357.74		873	13796	322	254	11430	-2366	600	
10450.38		823	14693	318	250	11250	-3443	550	



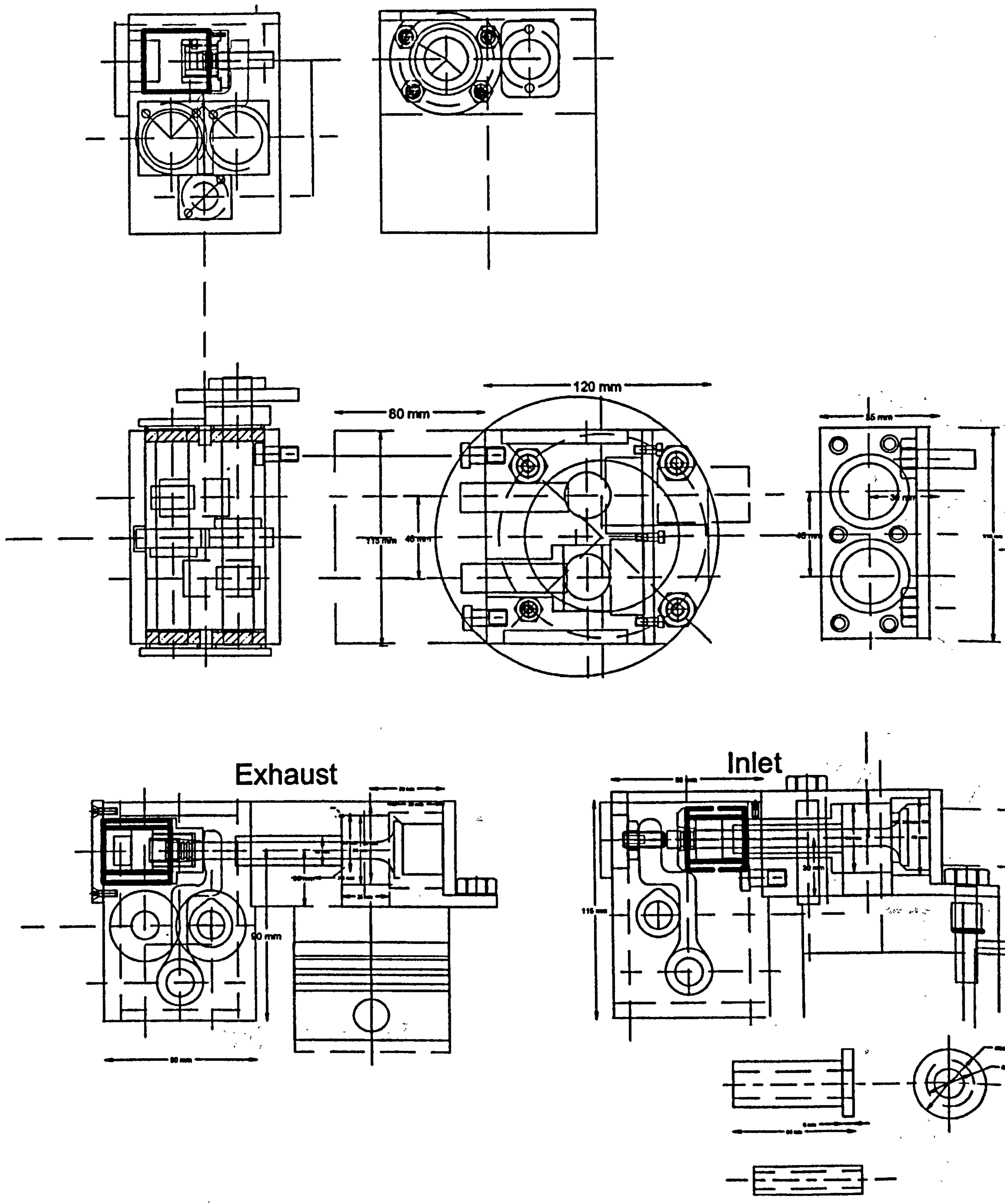


## **Annex 4**

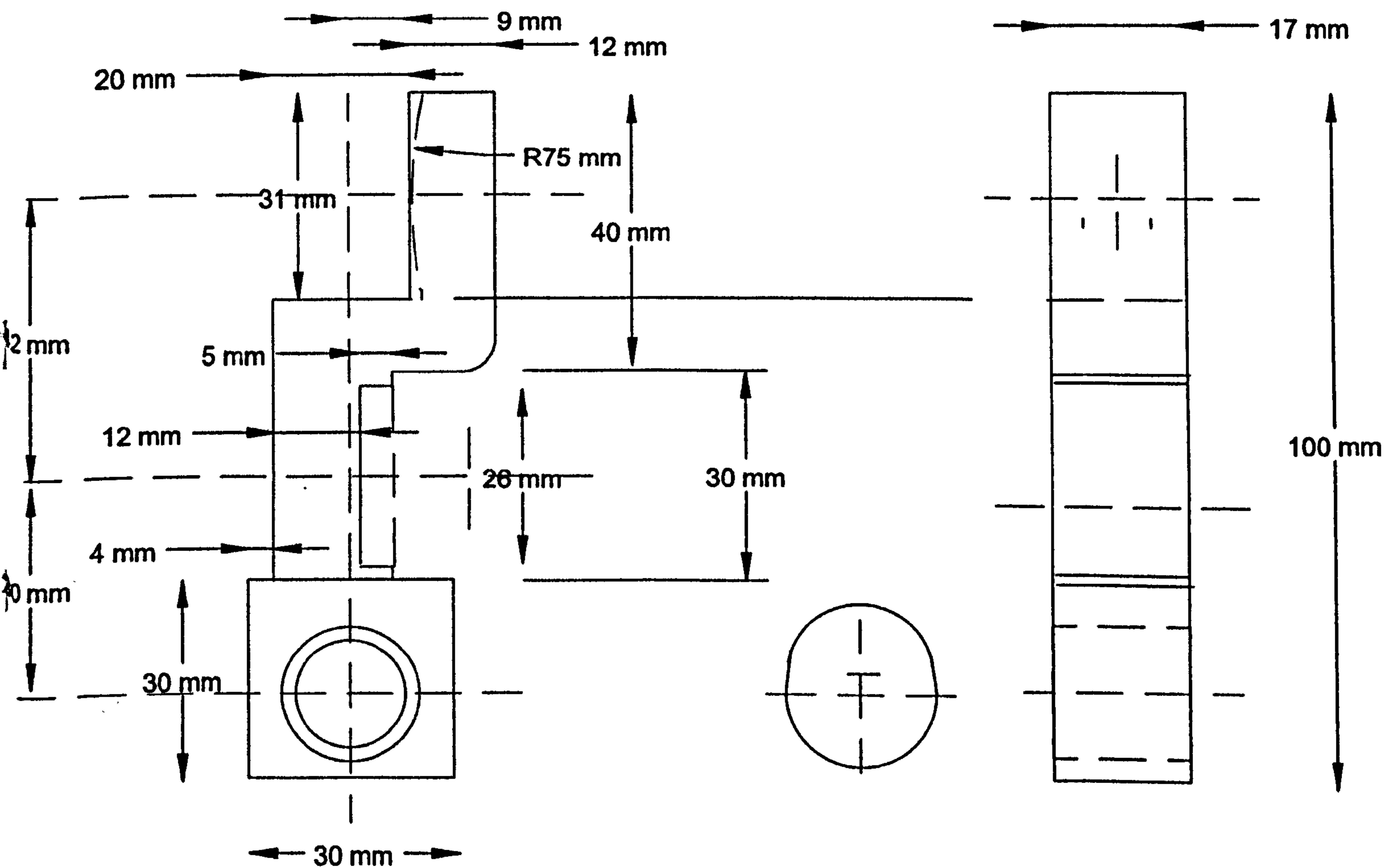


**Dwg 4.1 Compressor Valve Plate and Adaptor Ring**

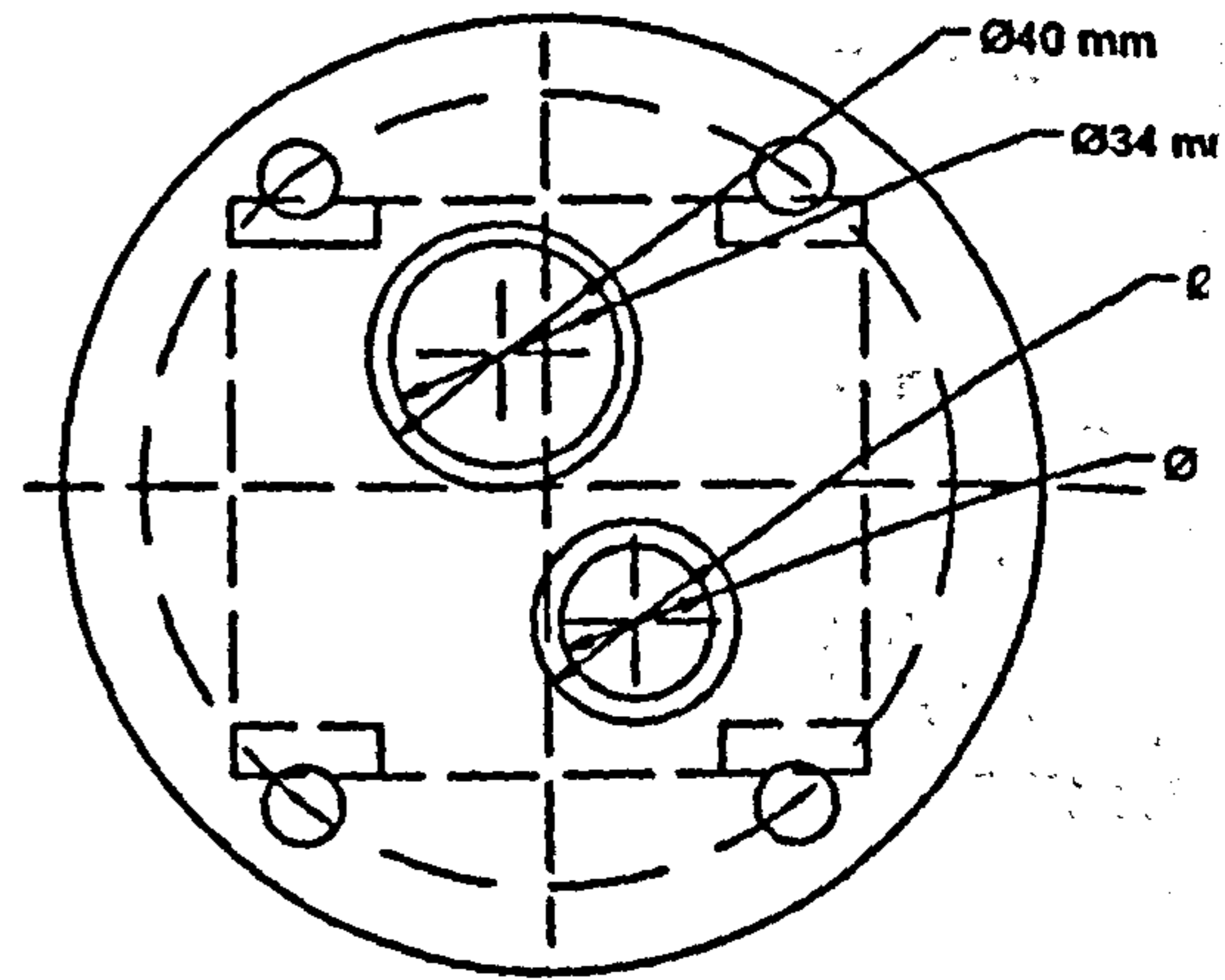
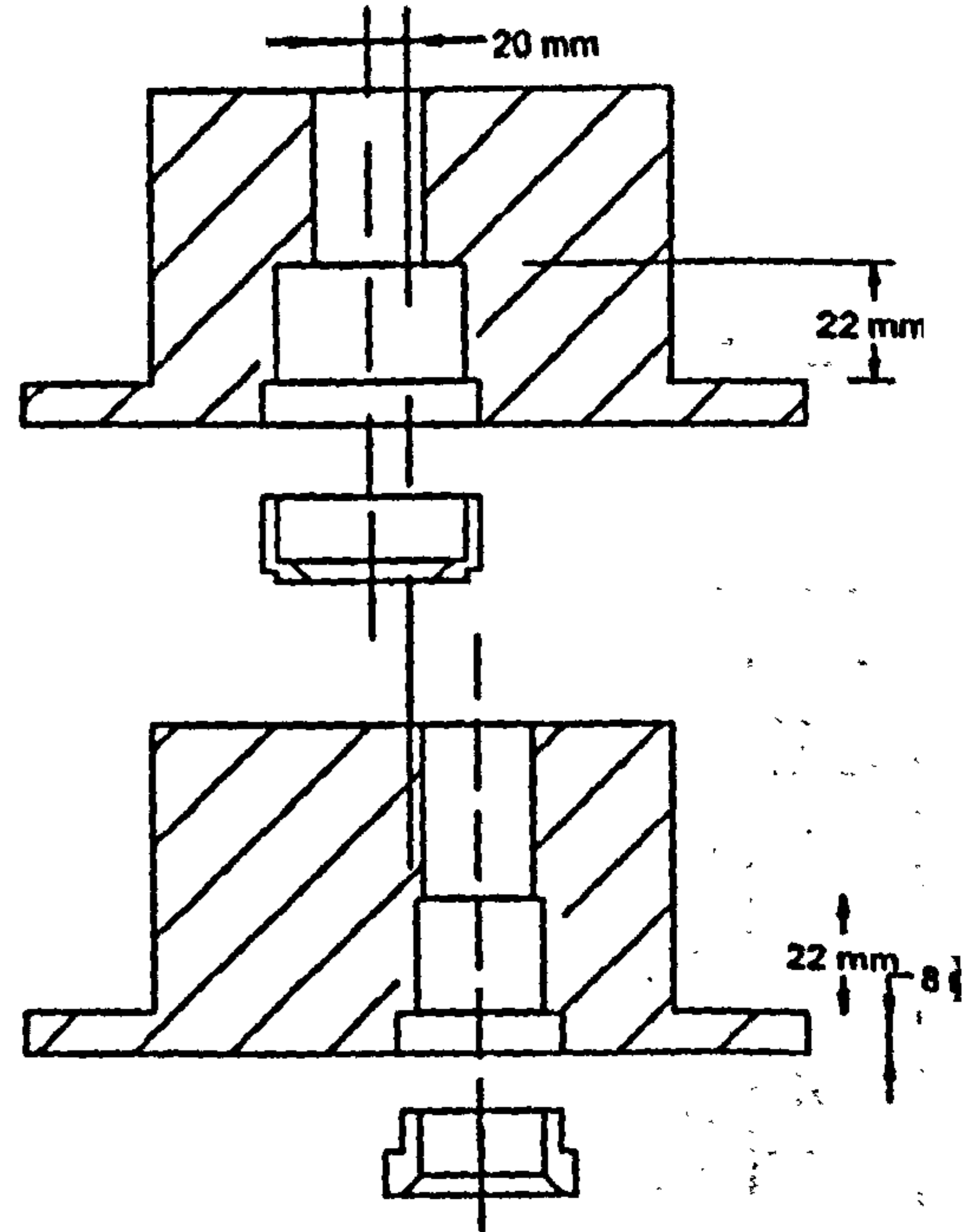
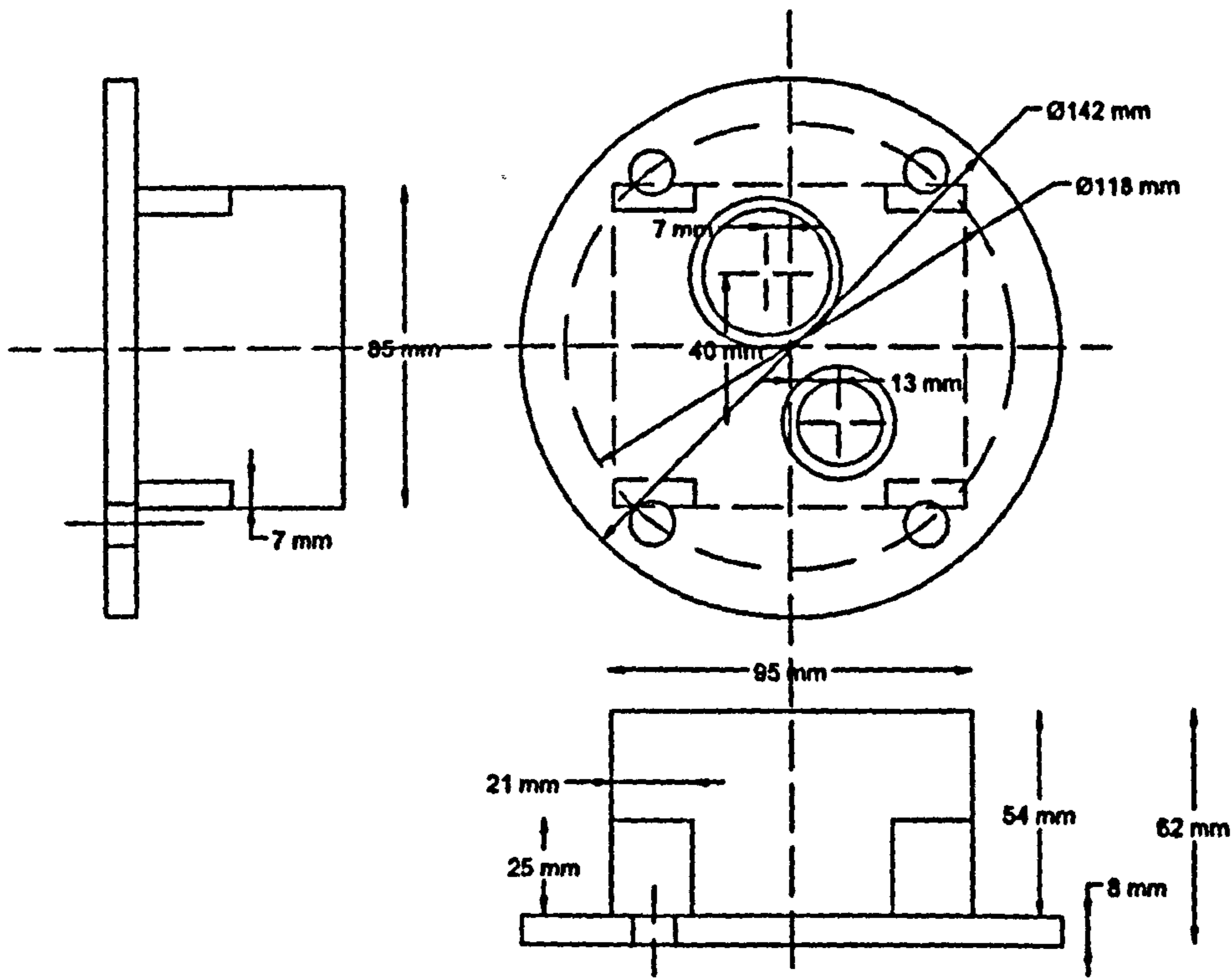




Dwg 4.2 Head and Cambox Assembly (SV)



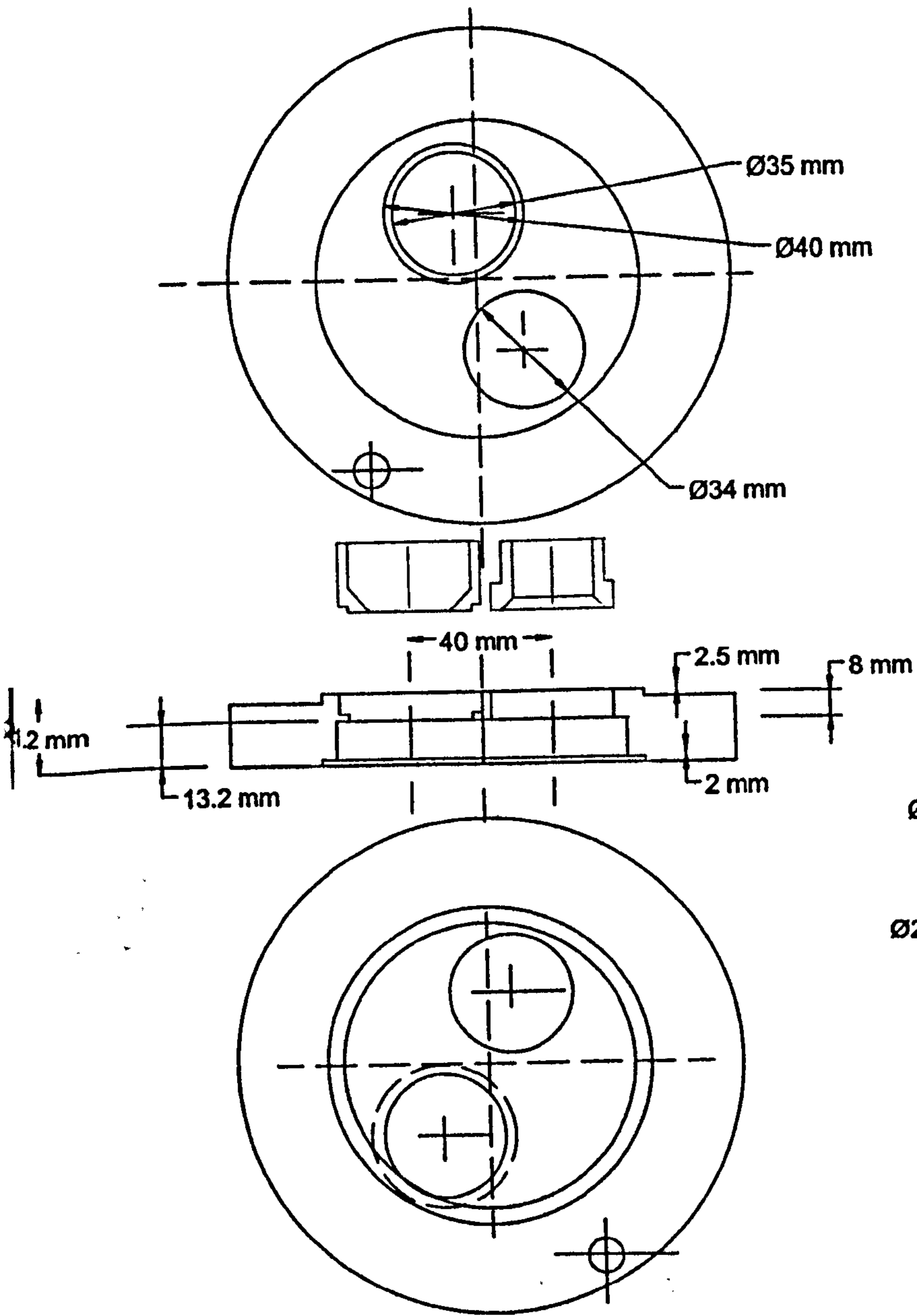
**Dwg 4.3 Exhaust Rocker Arm (SV)**



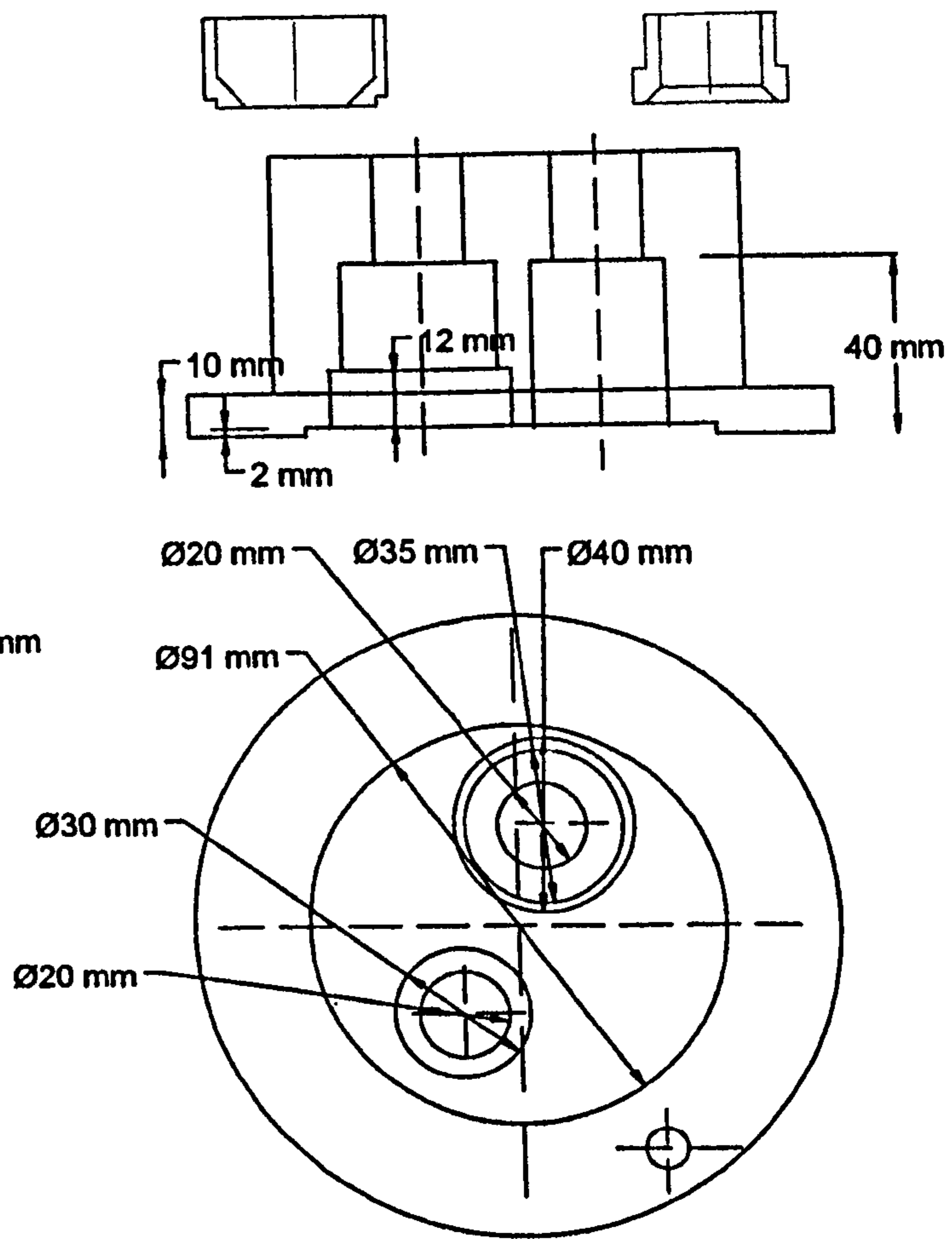
Material: MS

Do not Scale

**Dwg 4.4 Cylinder Head**

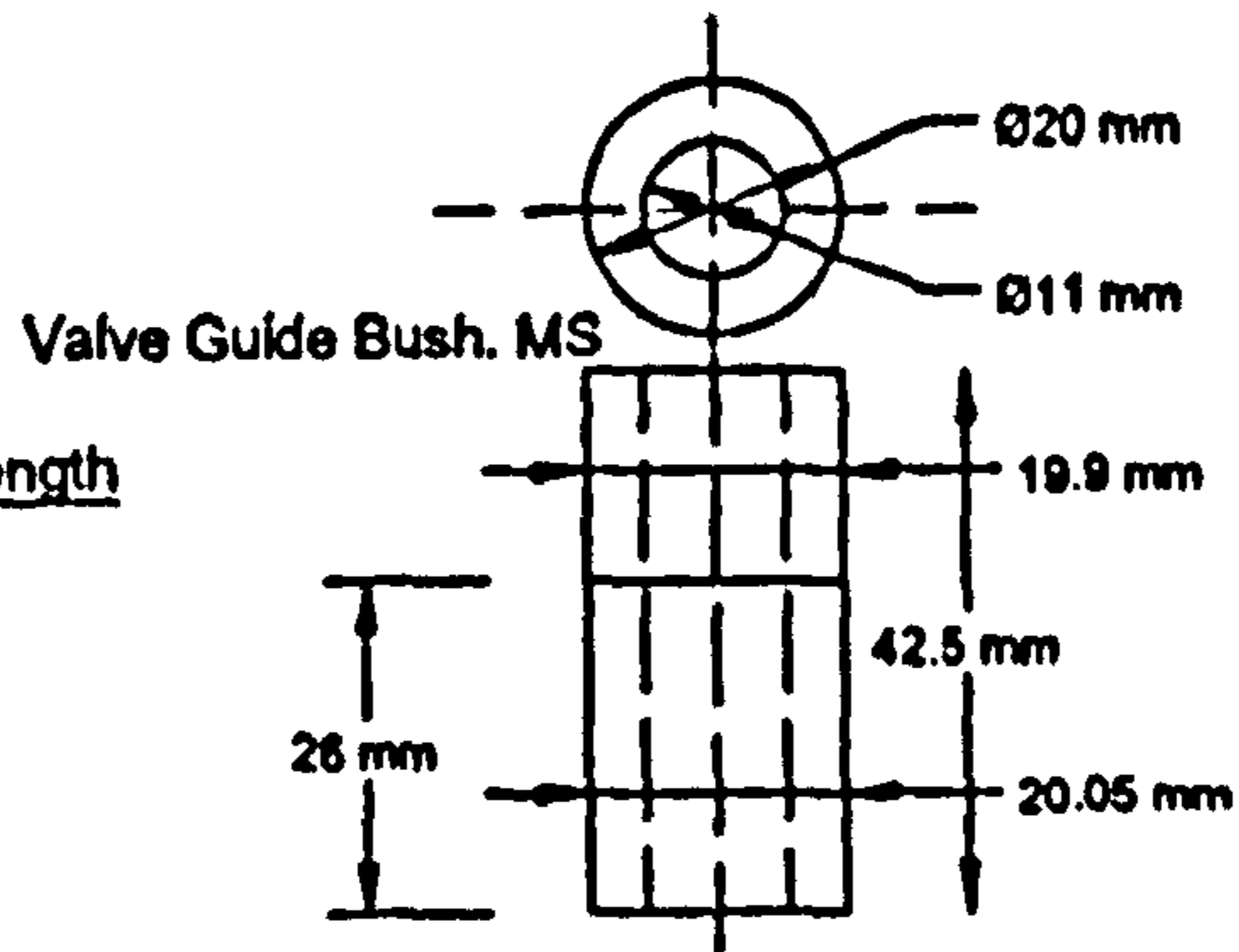
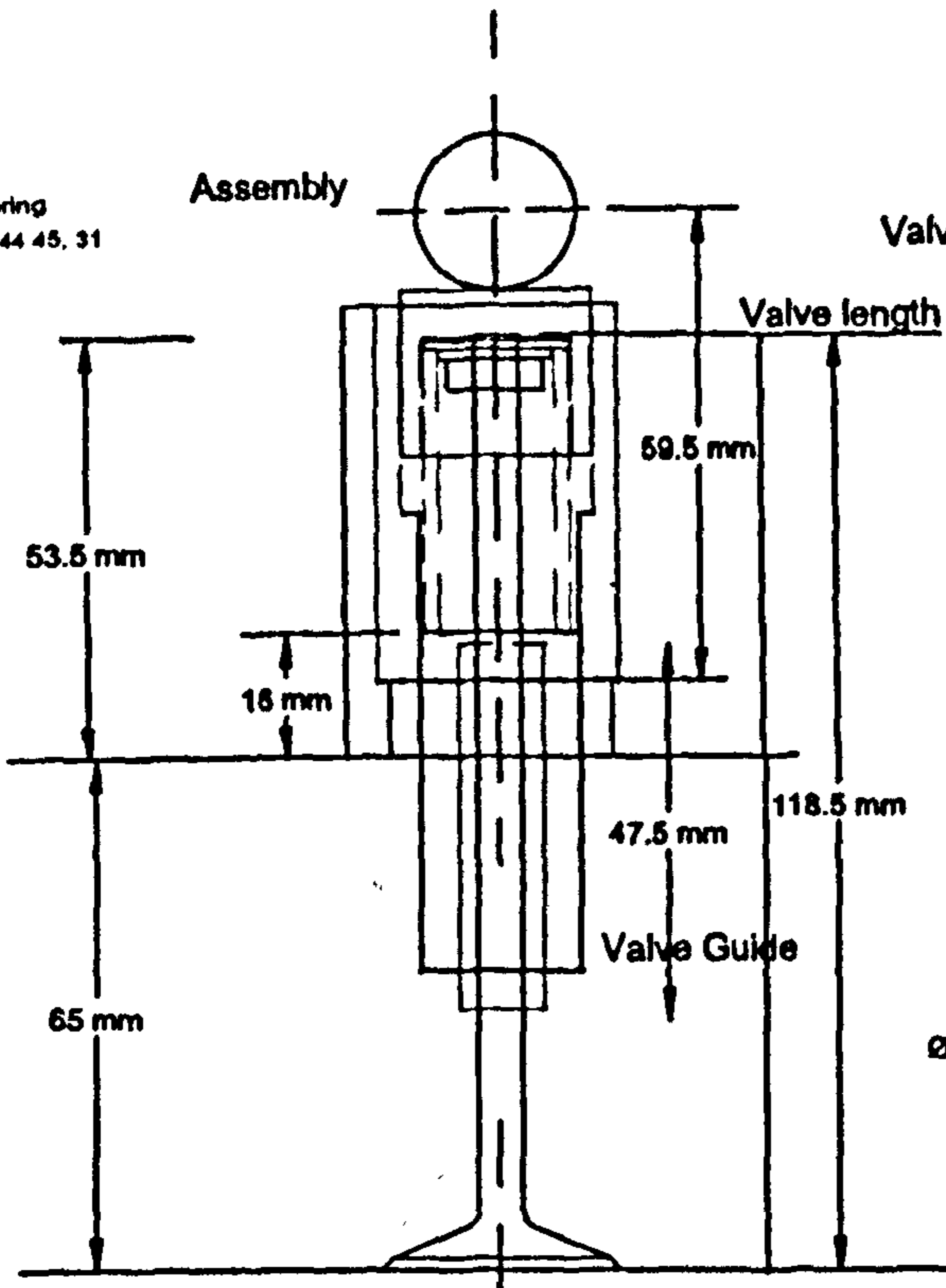


### Right hand Head

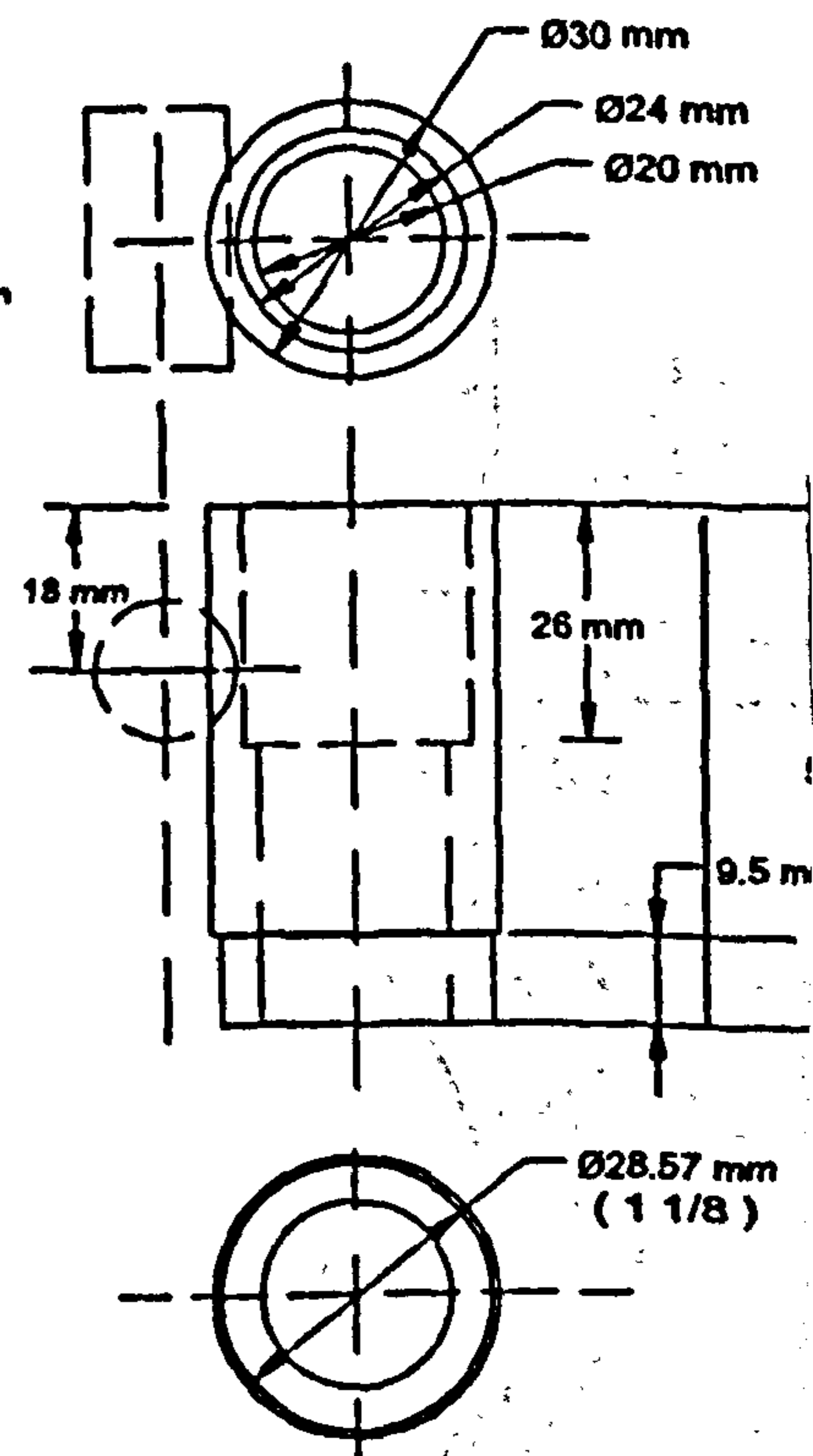


Dwg 4.5 Cylinder Head Details

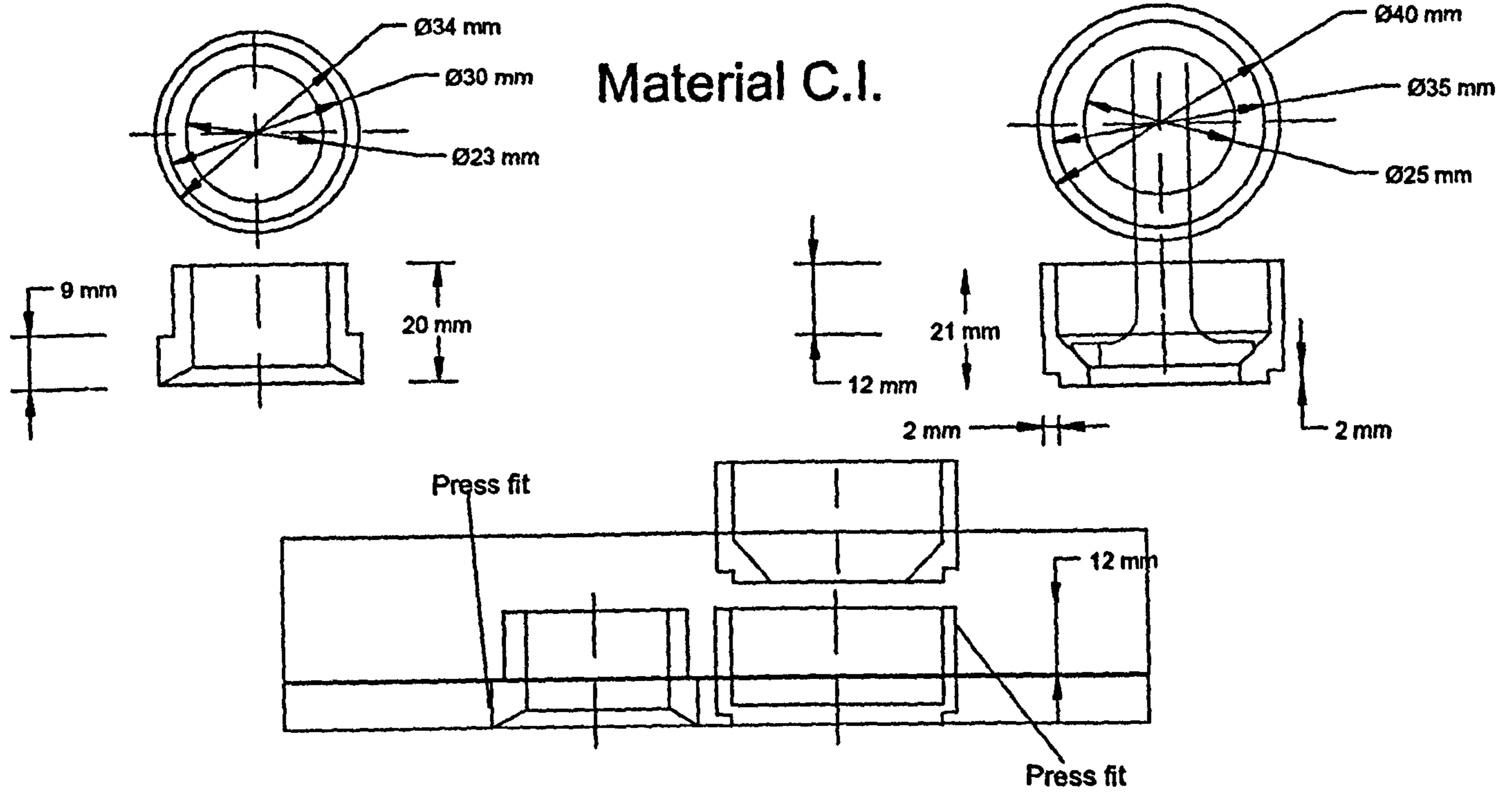
Valve spring  
18 29, 13 5, 44 45, 31  
LC 380J-5



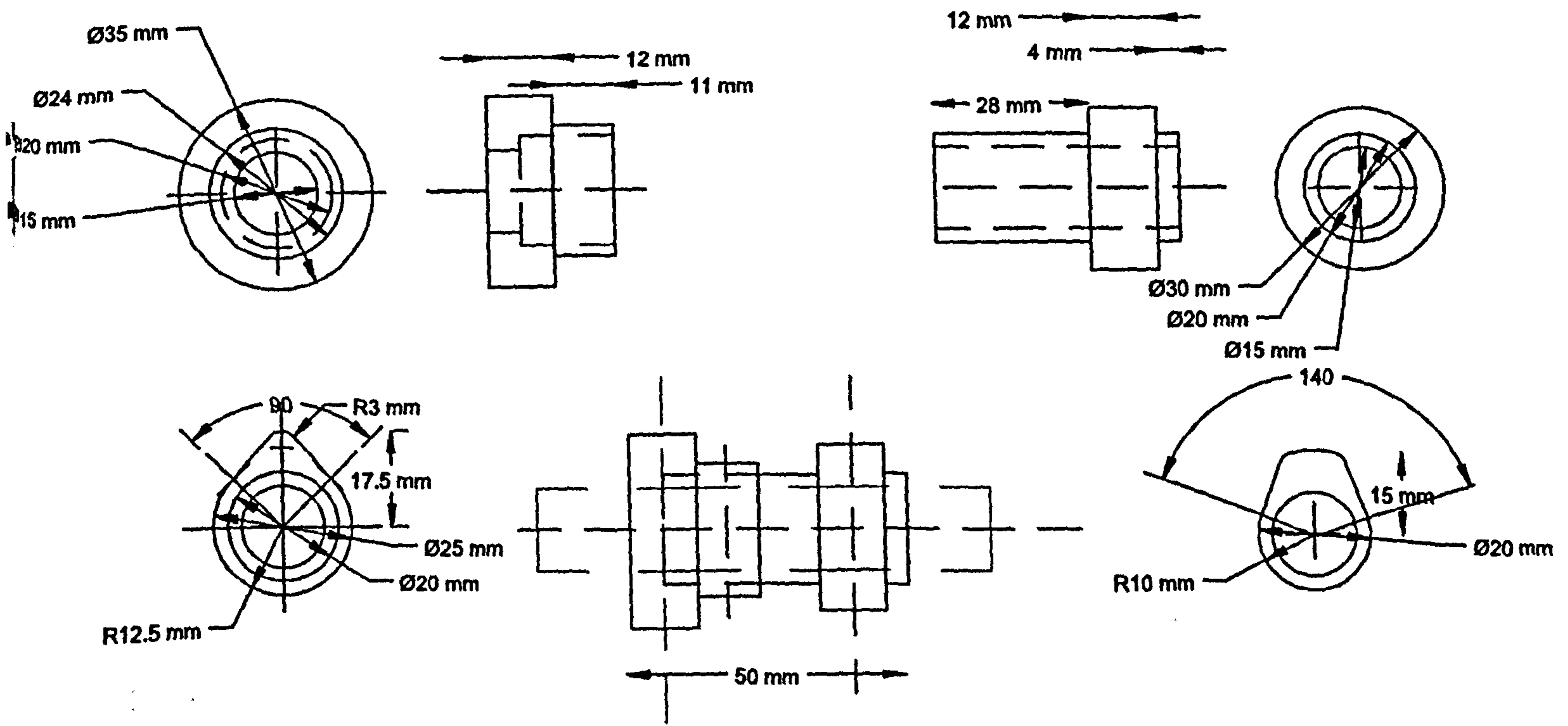
Bucket Guide. MS



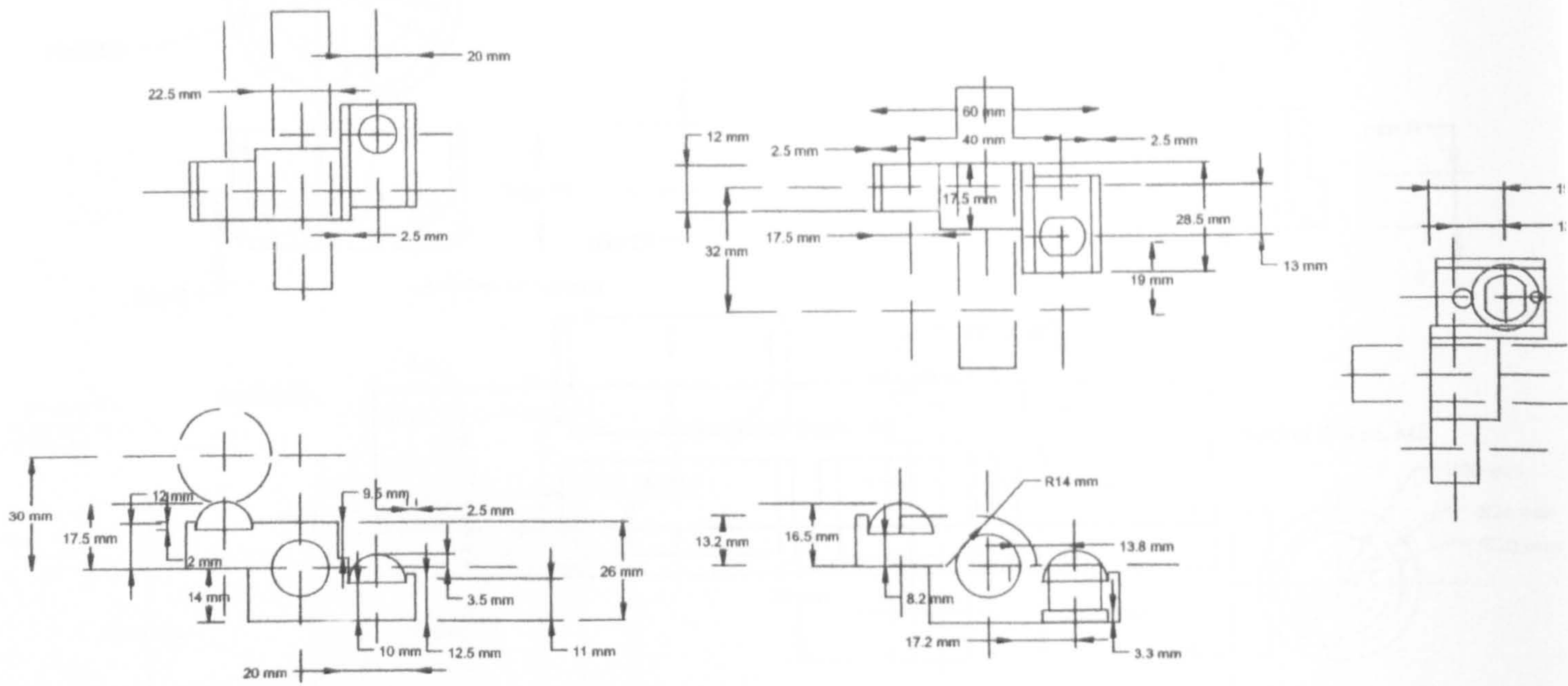
Dwg 4.6 Exhaust Valve Details



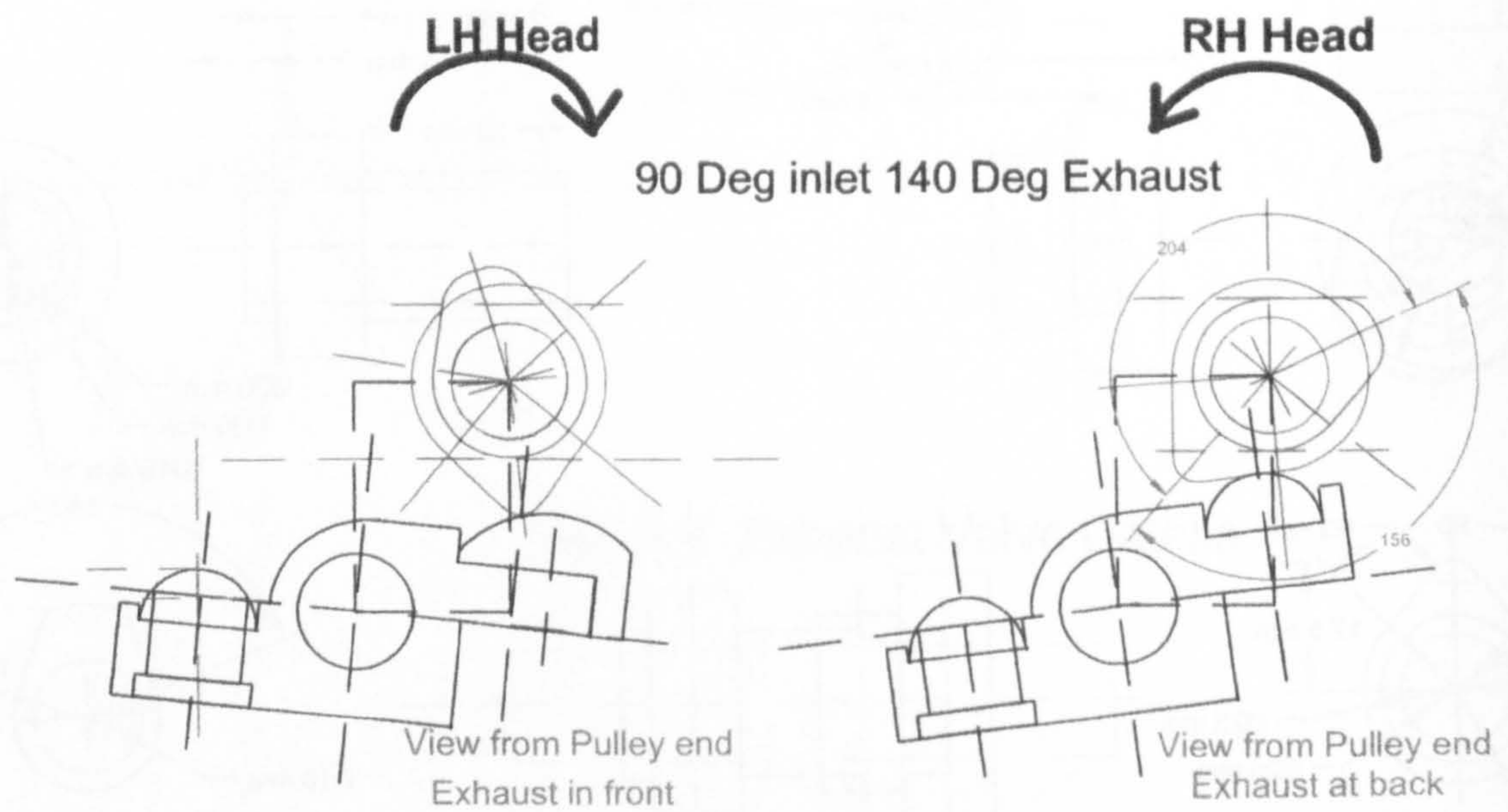
Dwg 4.7 Valve Seats



Dwg 4.8 Cam Blanks



Dwg 4.9 Rocker Arms



Dwg 4.10 Cam Set Up

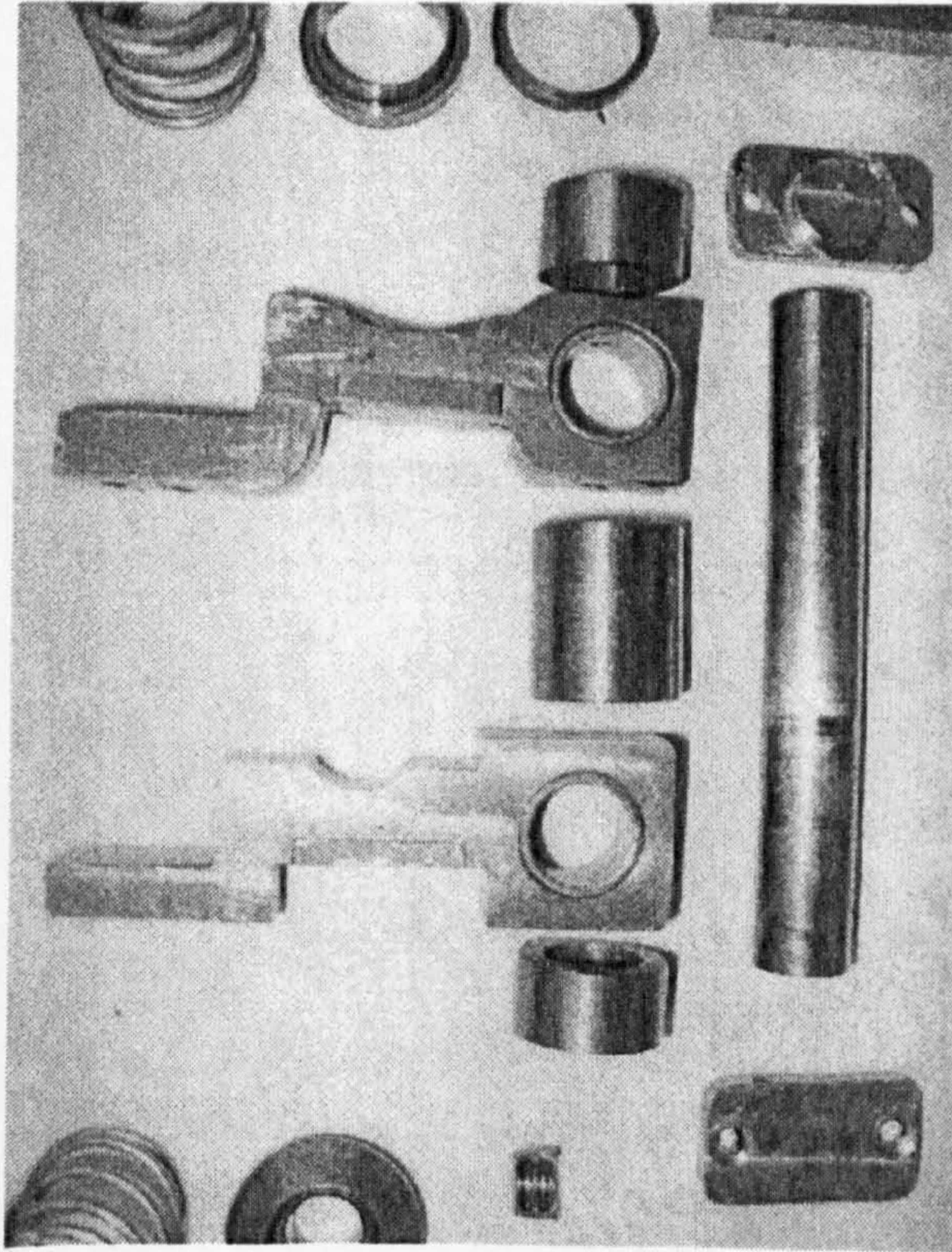


Photo 4.5 Cam Box, Rocker Arms, and Rocker Shaft

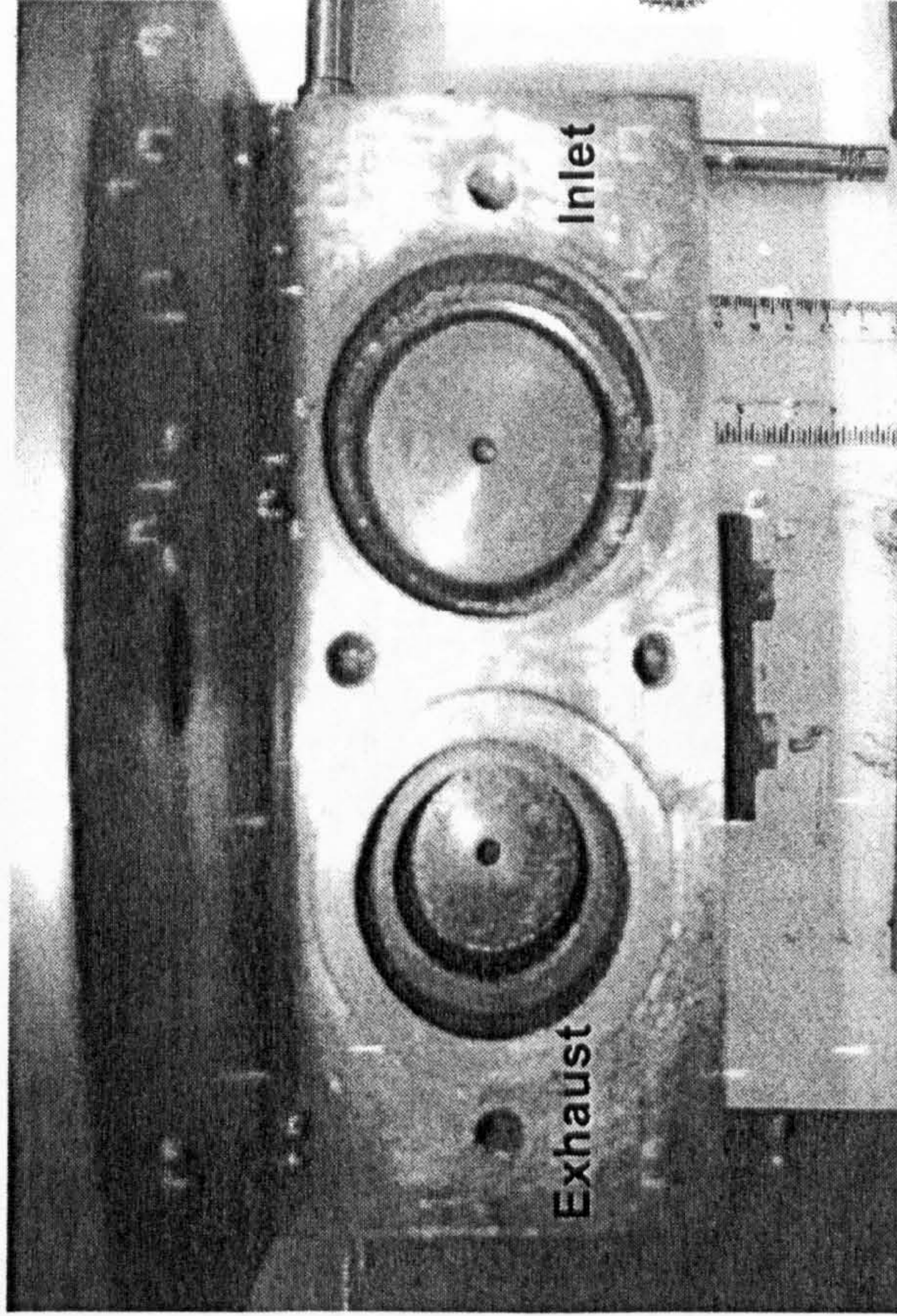


Photo 4.6 View of Valves from Inlet / Exhaust Cylinder Head Flange

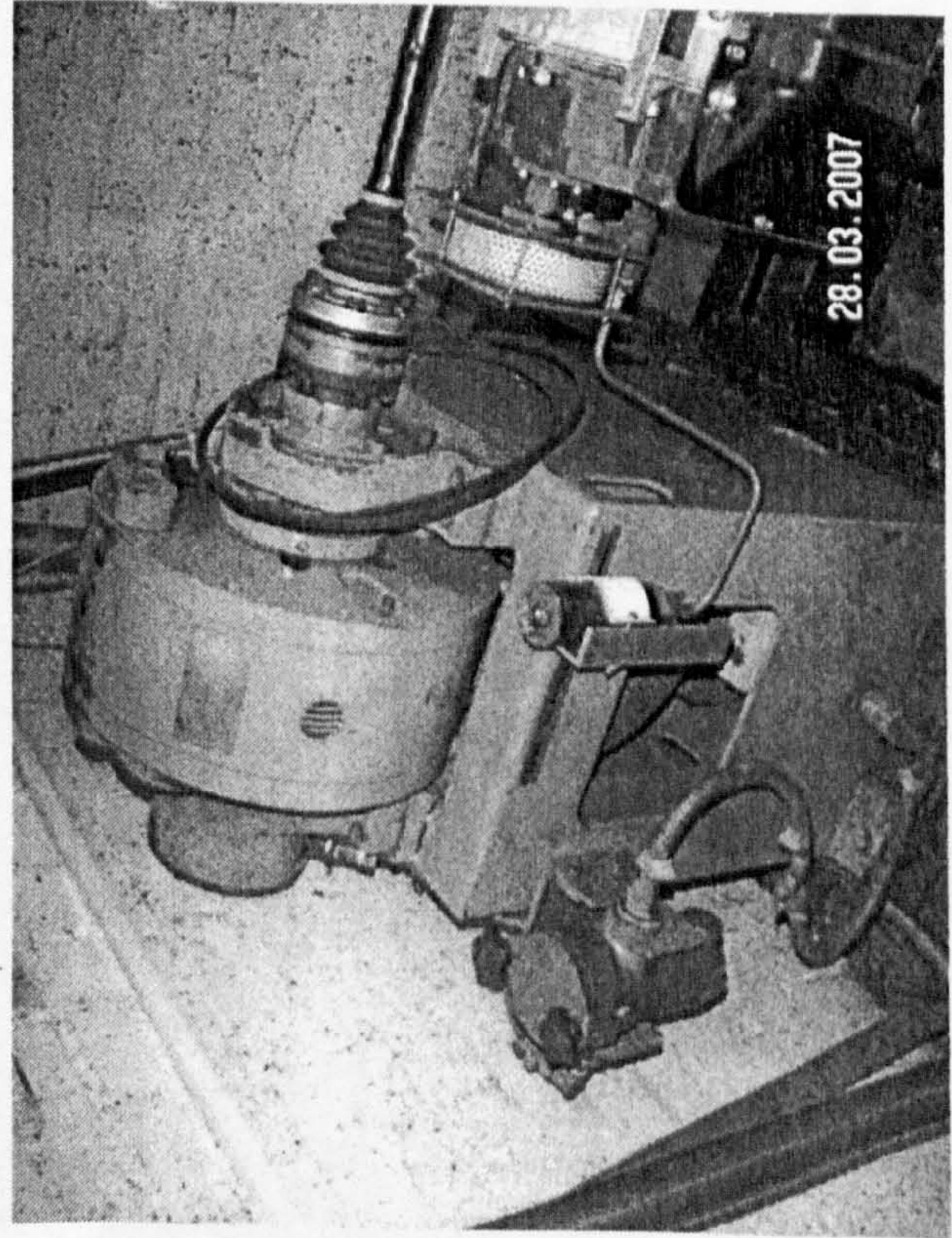


Photo 4.7 Dynamometer

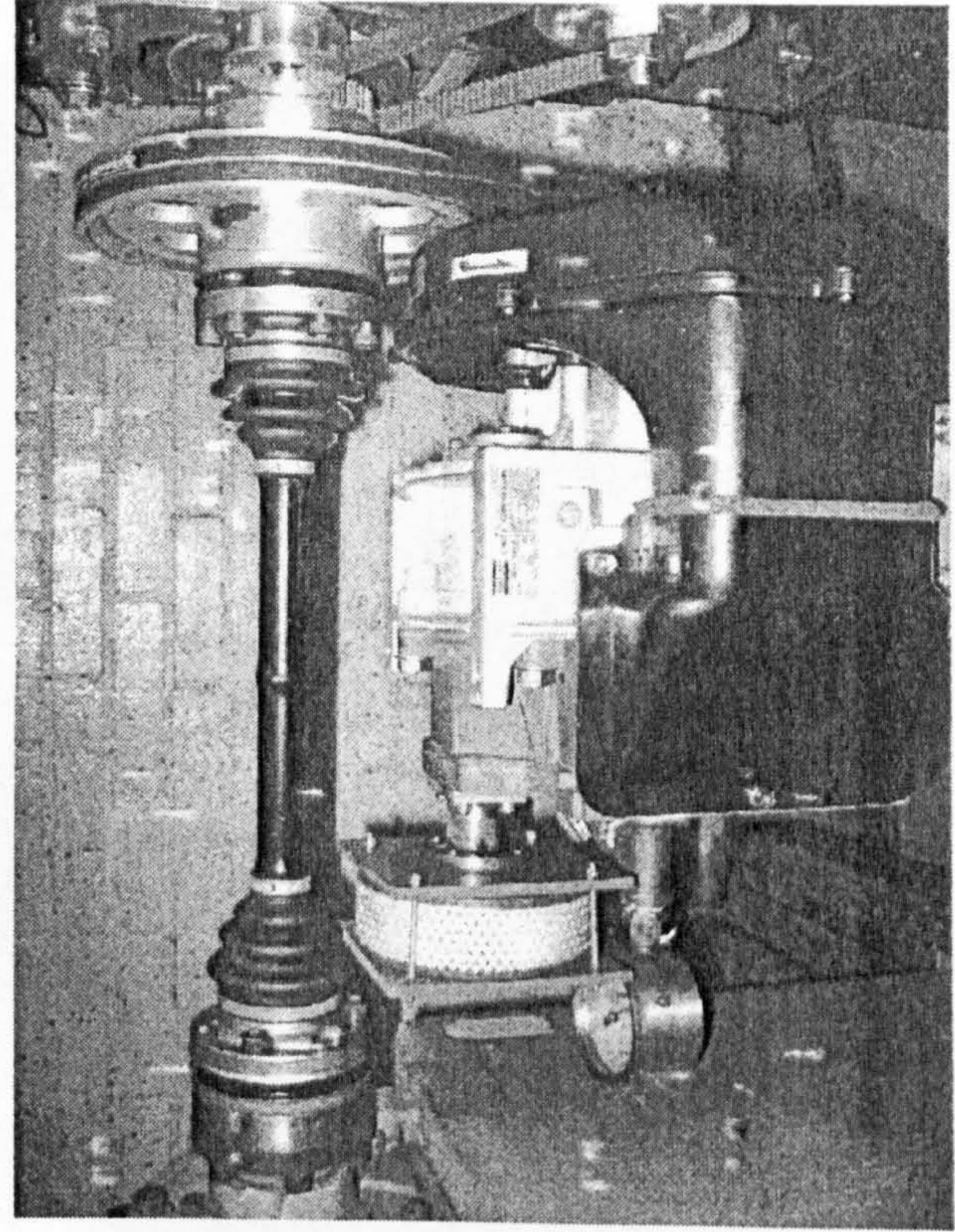


Photo 4.8 Dynamometer and Scroll Compressor Drive



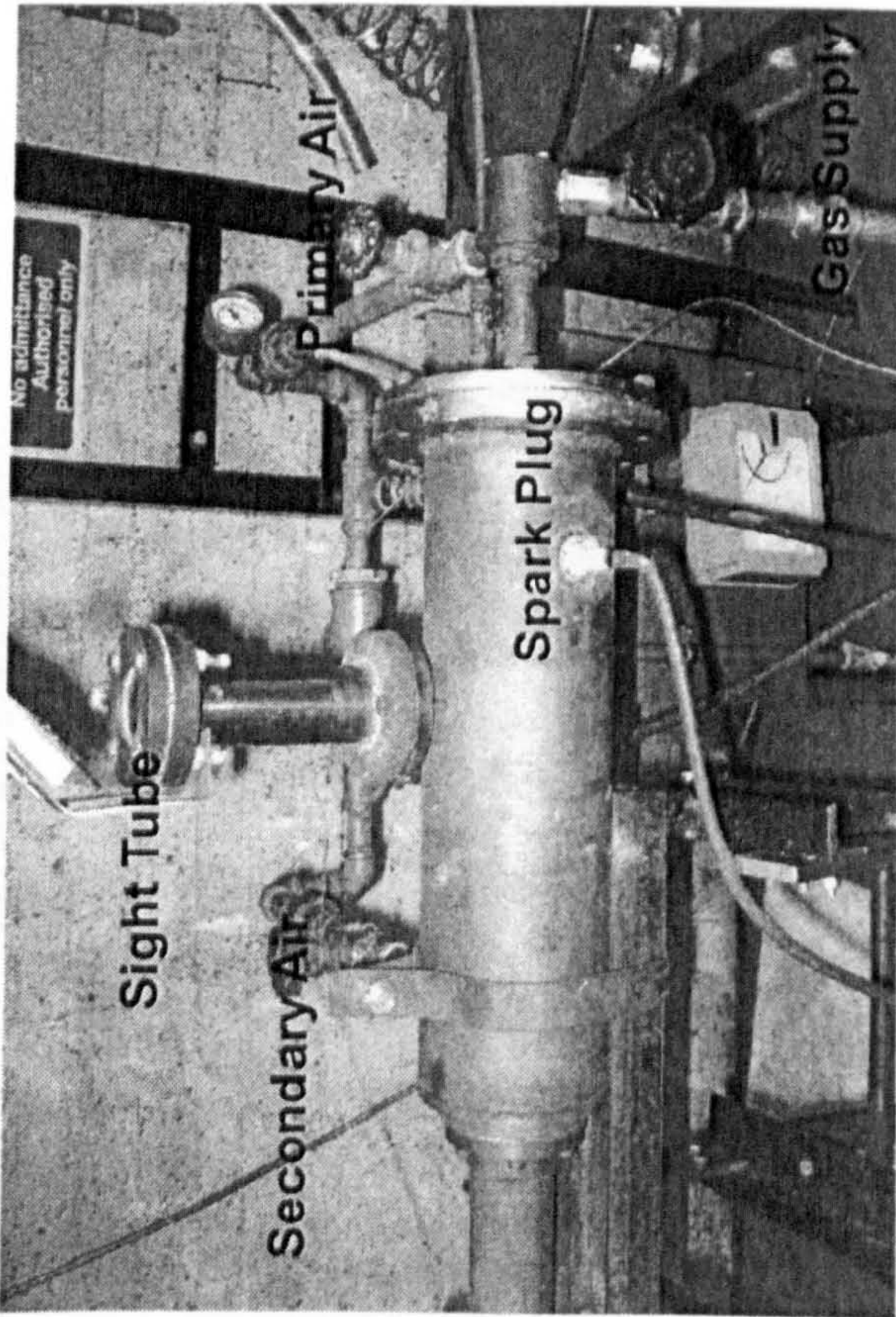


Photo 4.9 Combustion Chamber

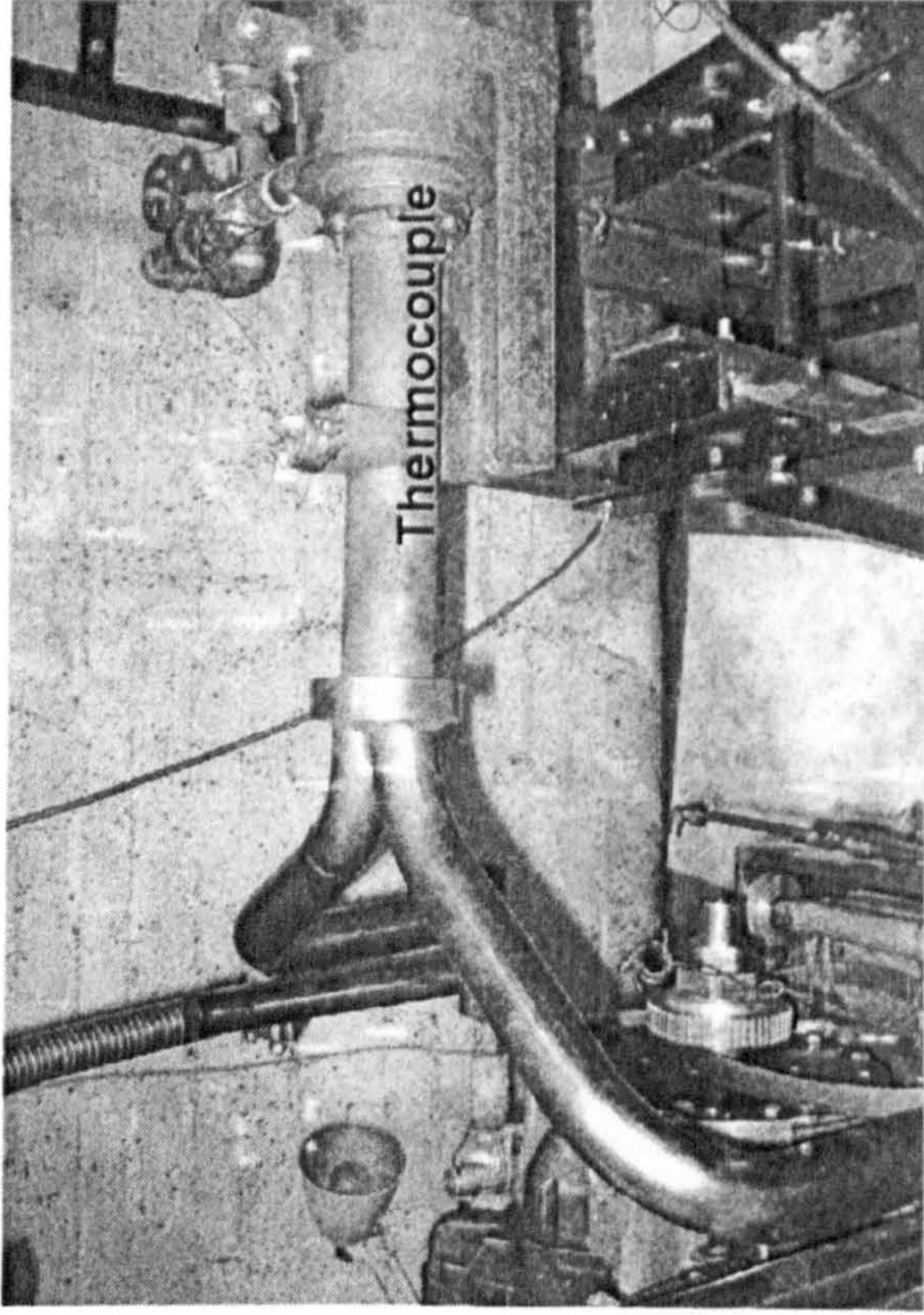


Photo 4.10 Hot Gas Supply Pipe Work



Photo 4.11 Burner Flame Test In Air

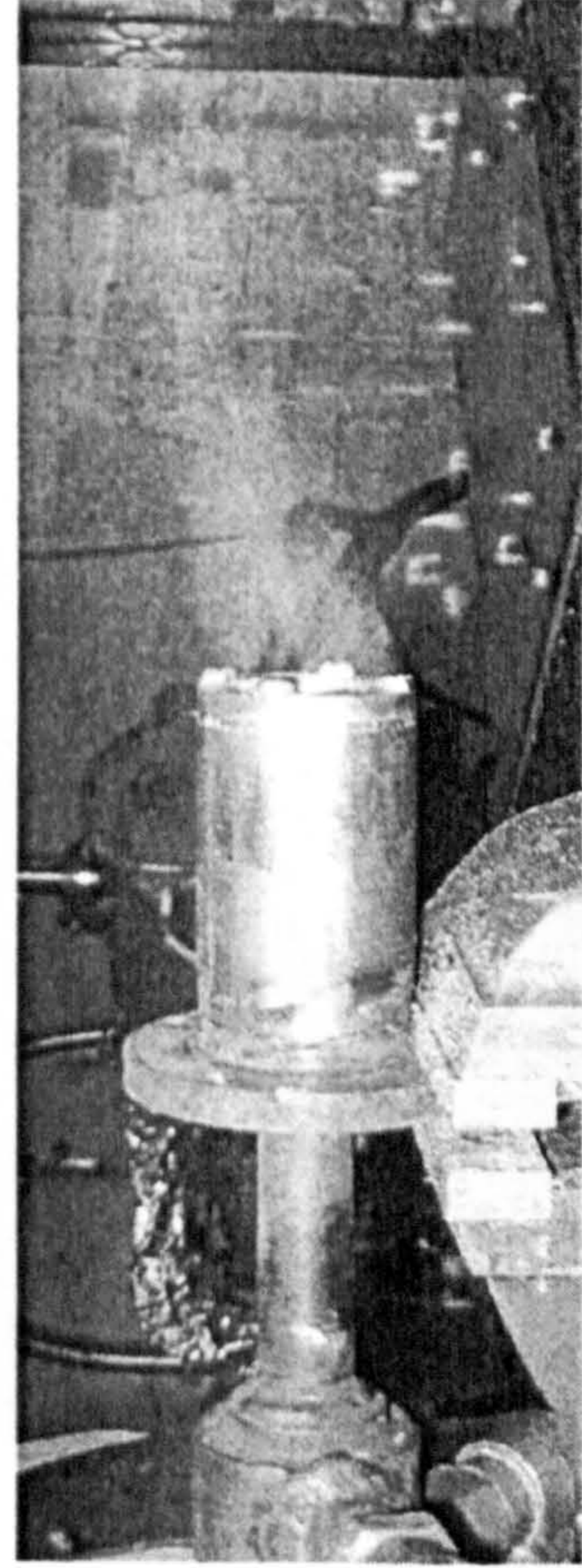


Photo 4.11 Burner Flame Test In Air

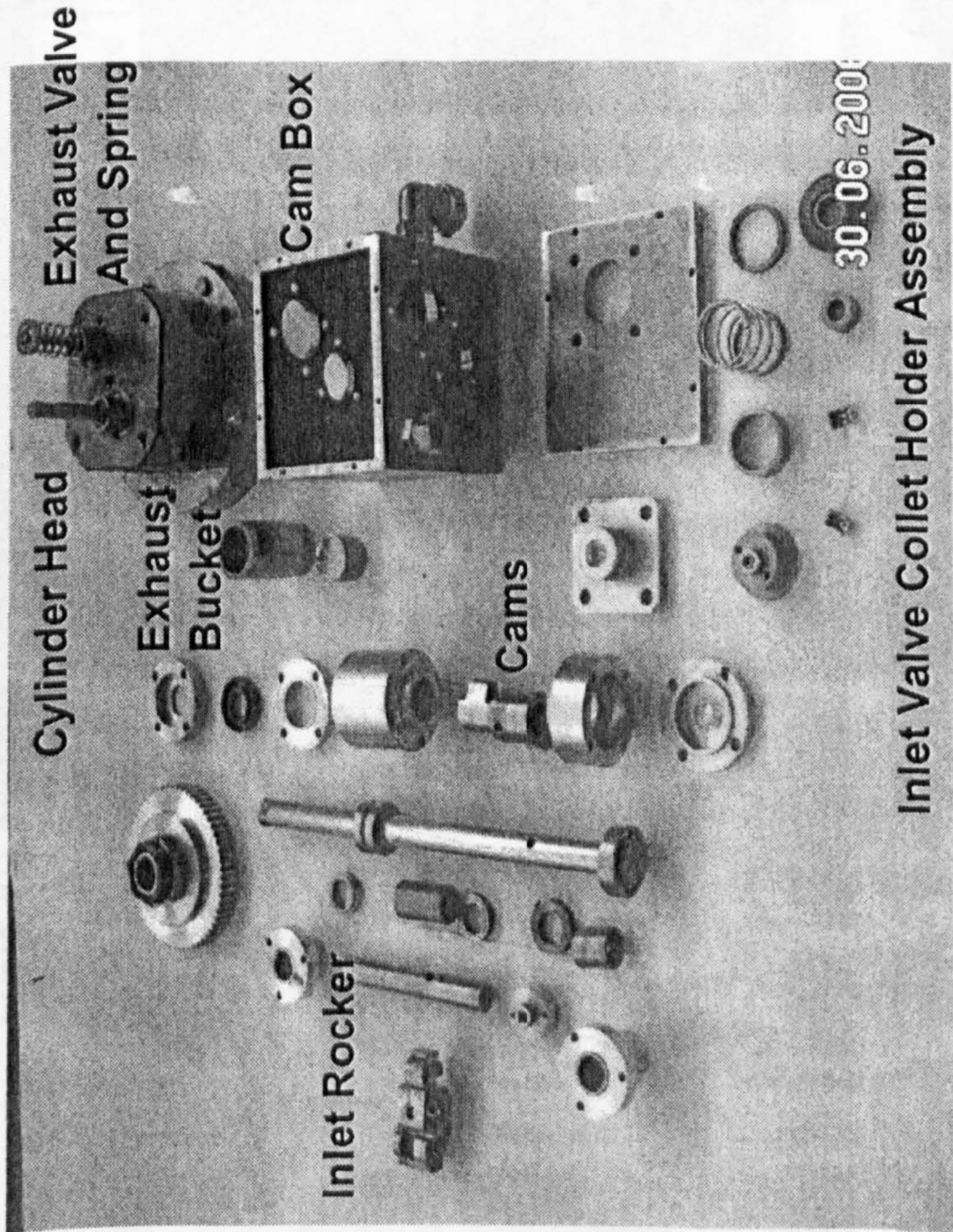


Photo 4.12 Cylinder Head, Cam Box and Cam Box Components

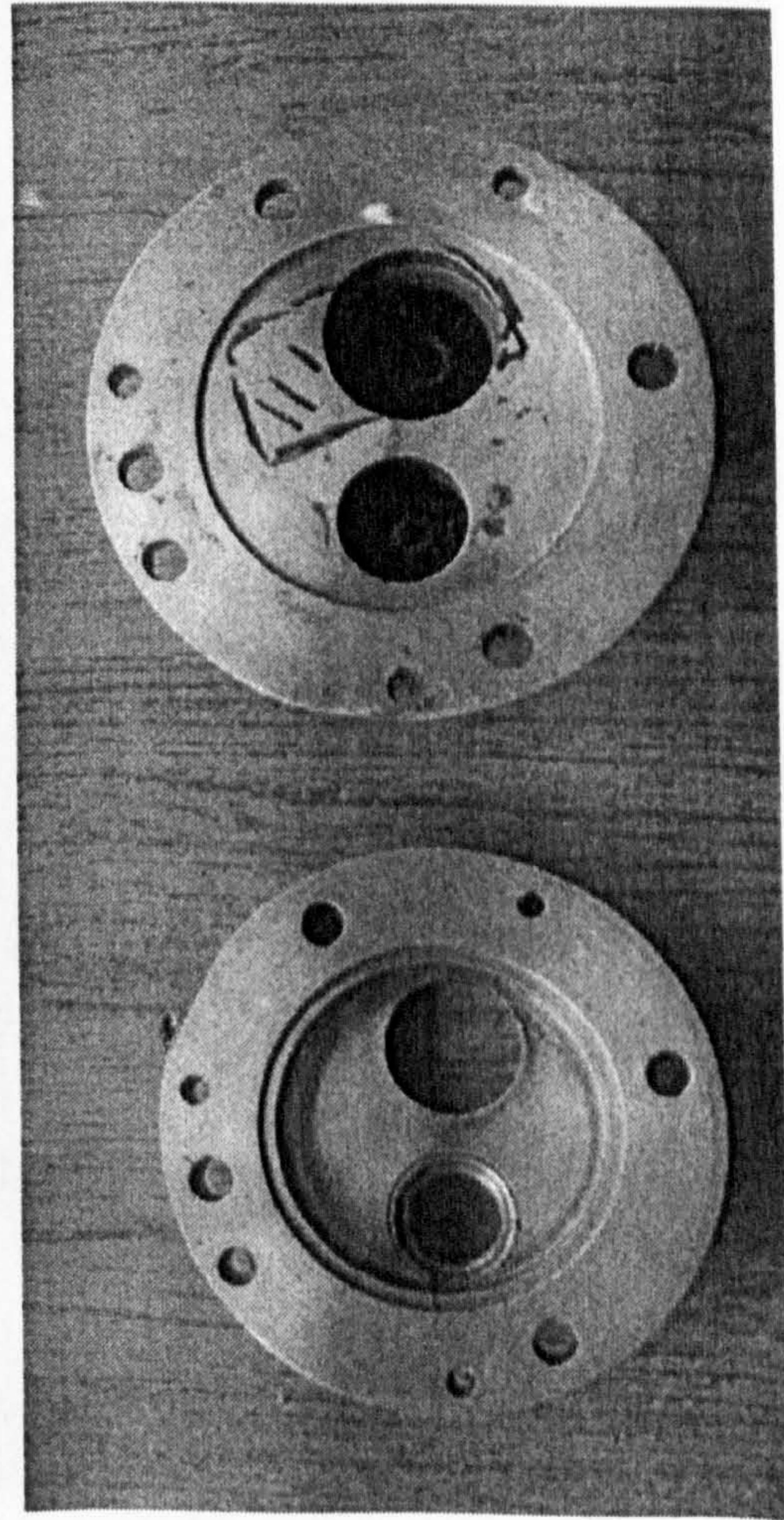


Photo 4.14 Two Part Cylinder Head

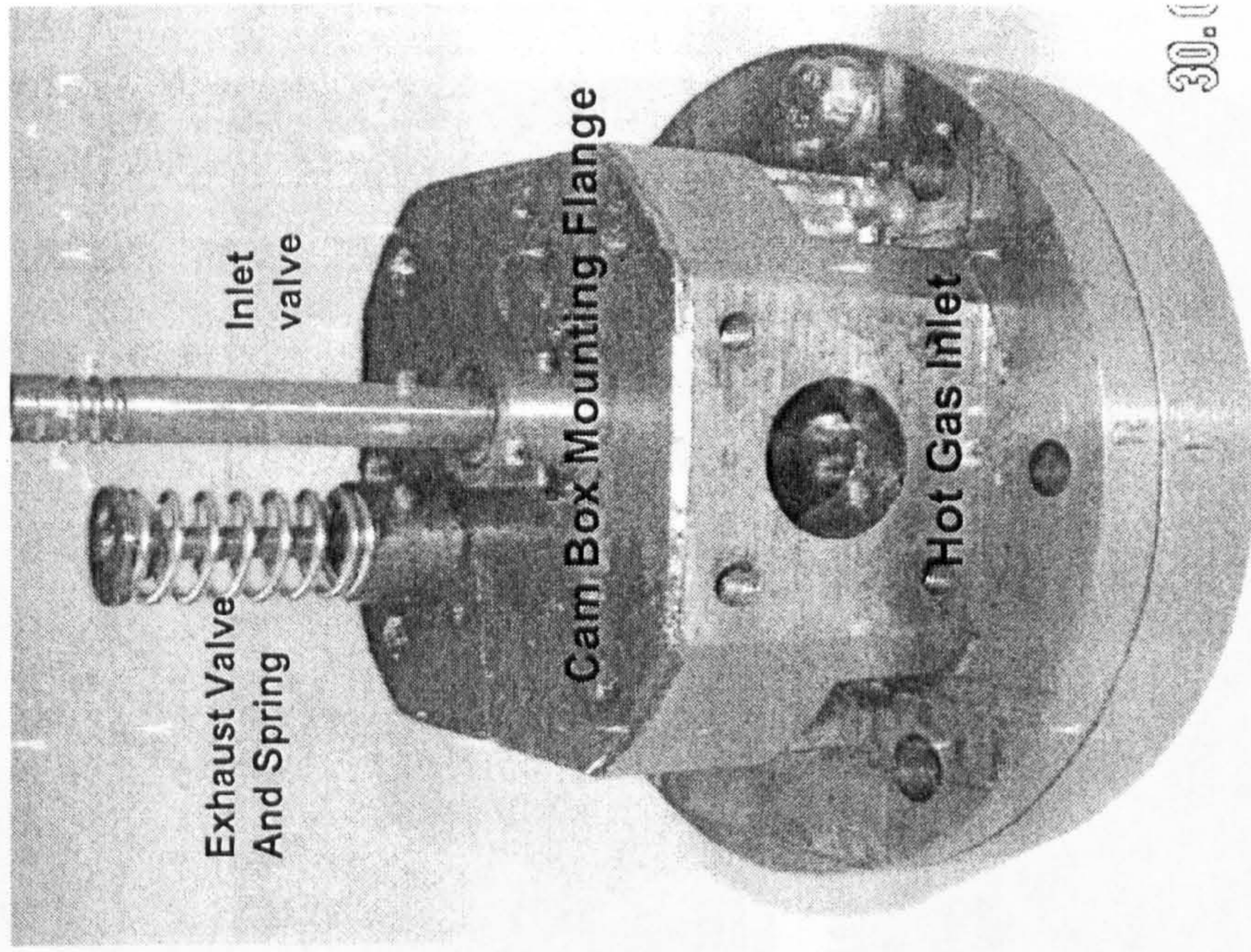


Photo 4.13 Cylinder Head Assembly

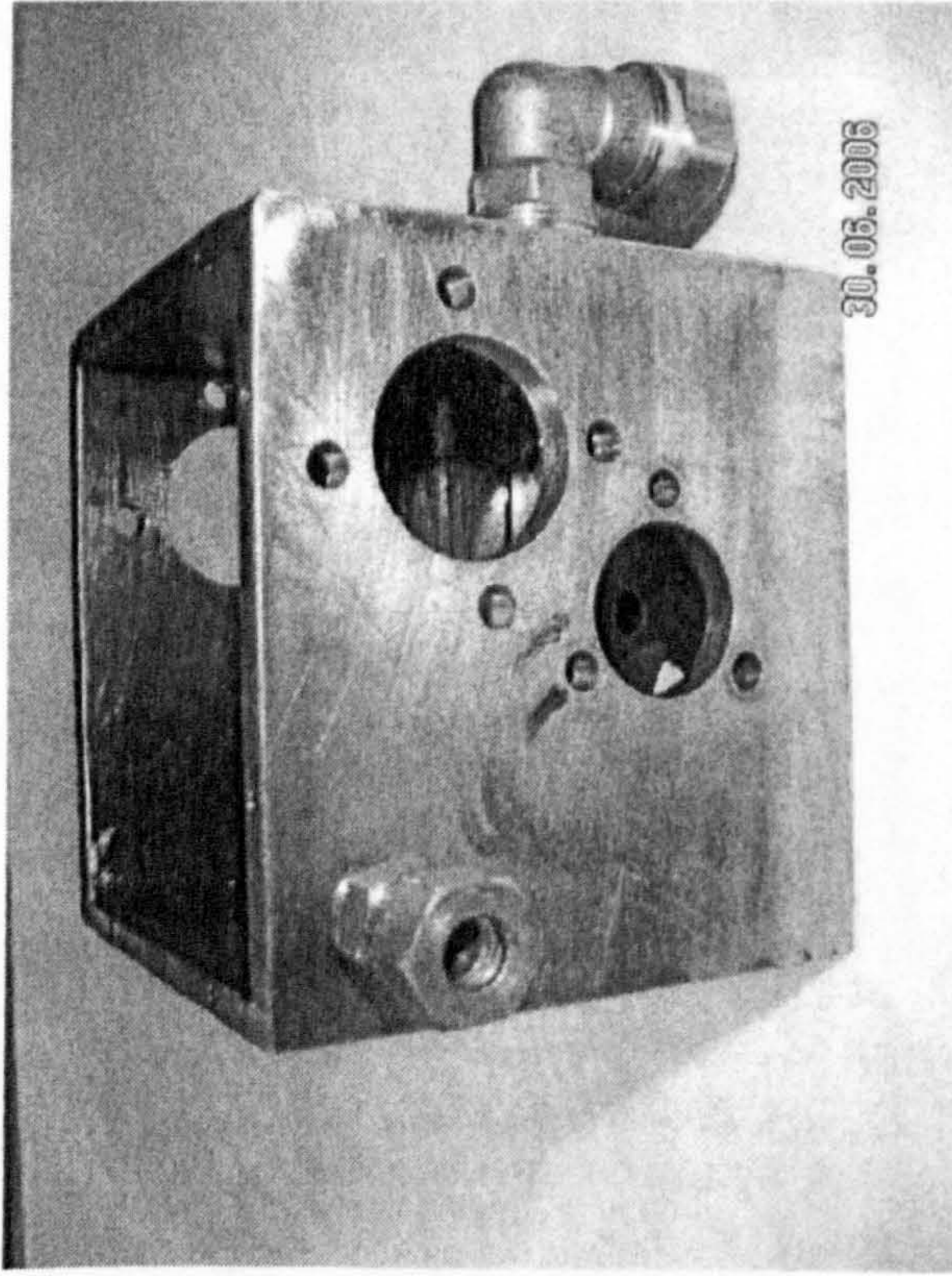


Photo 4.15 Cam Box

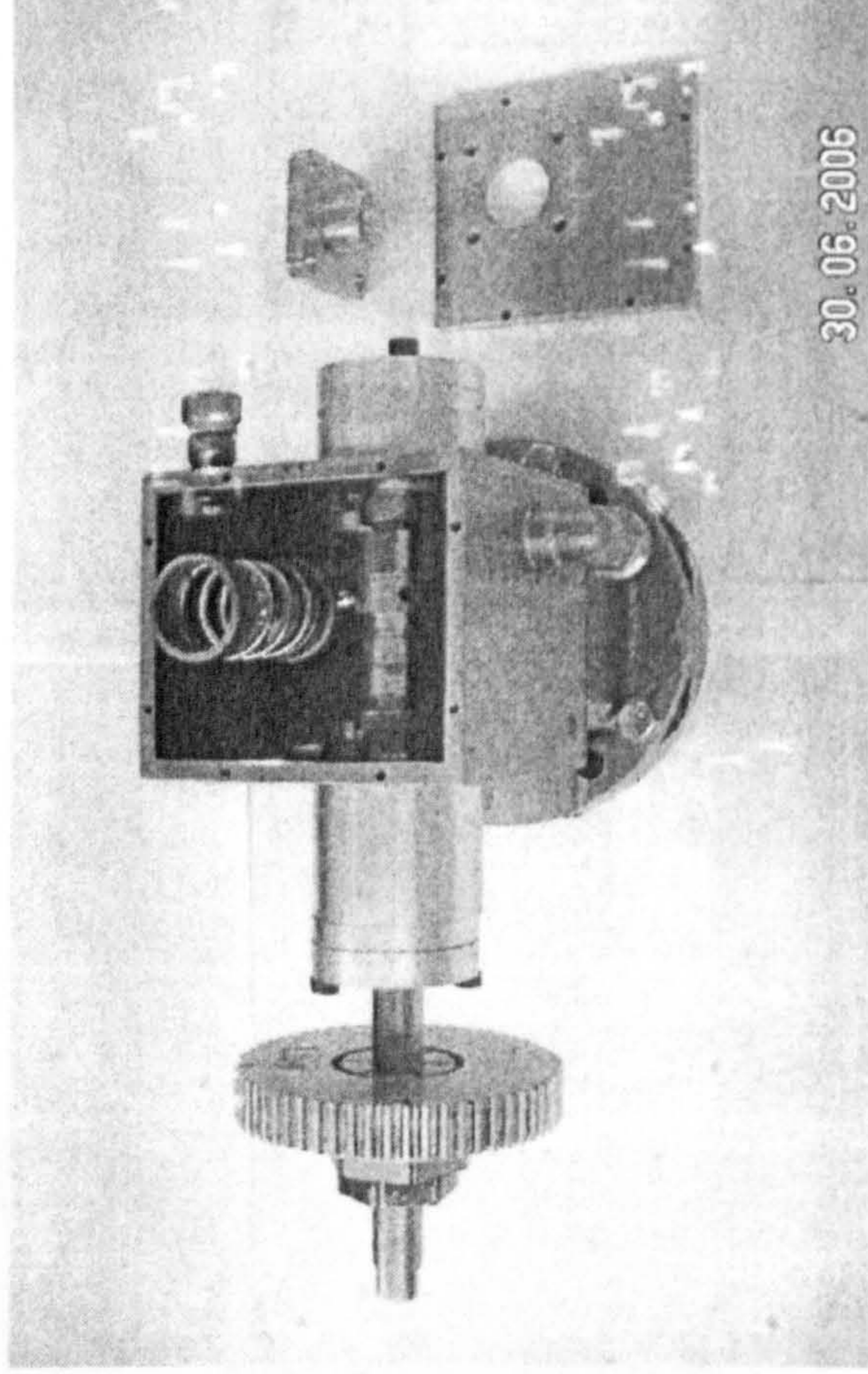


Photo 4.16 Cam Box Mounted On Cylinder Head

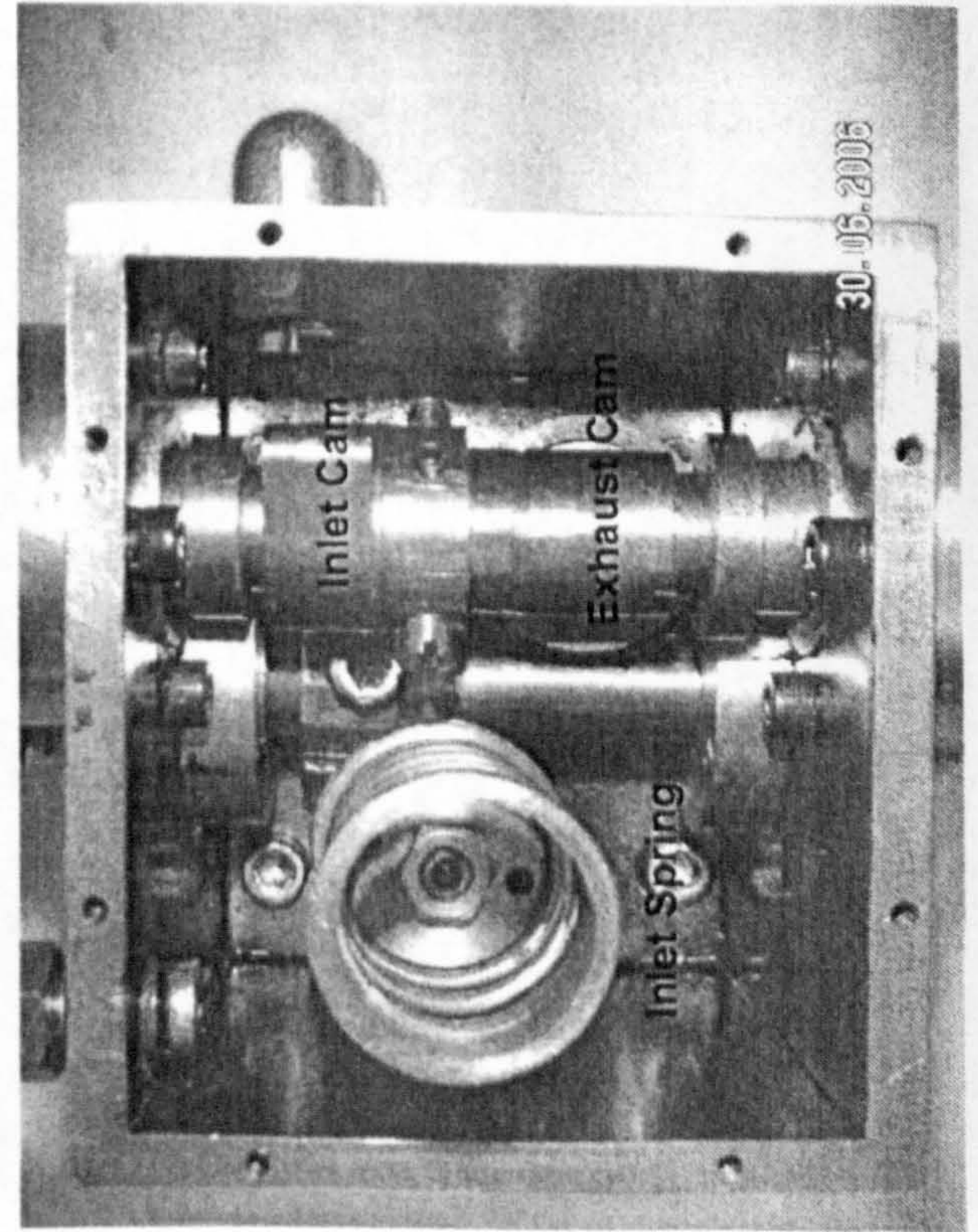


Photo 4.17 Cam Box Mechanisms

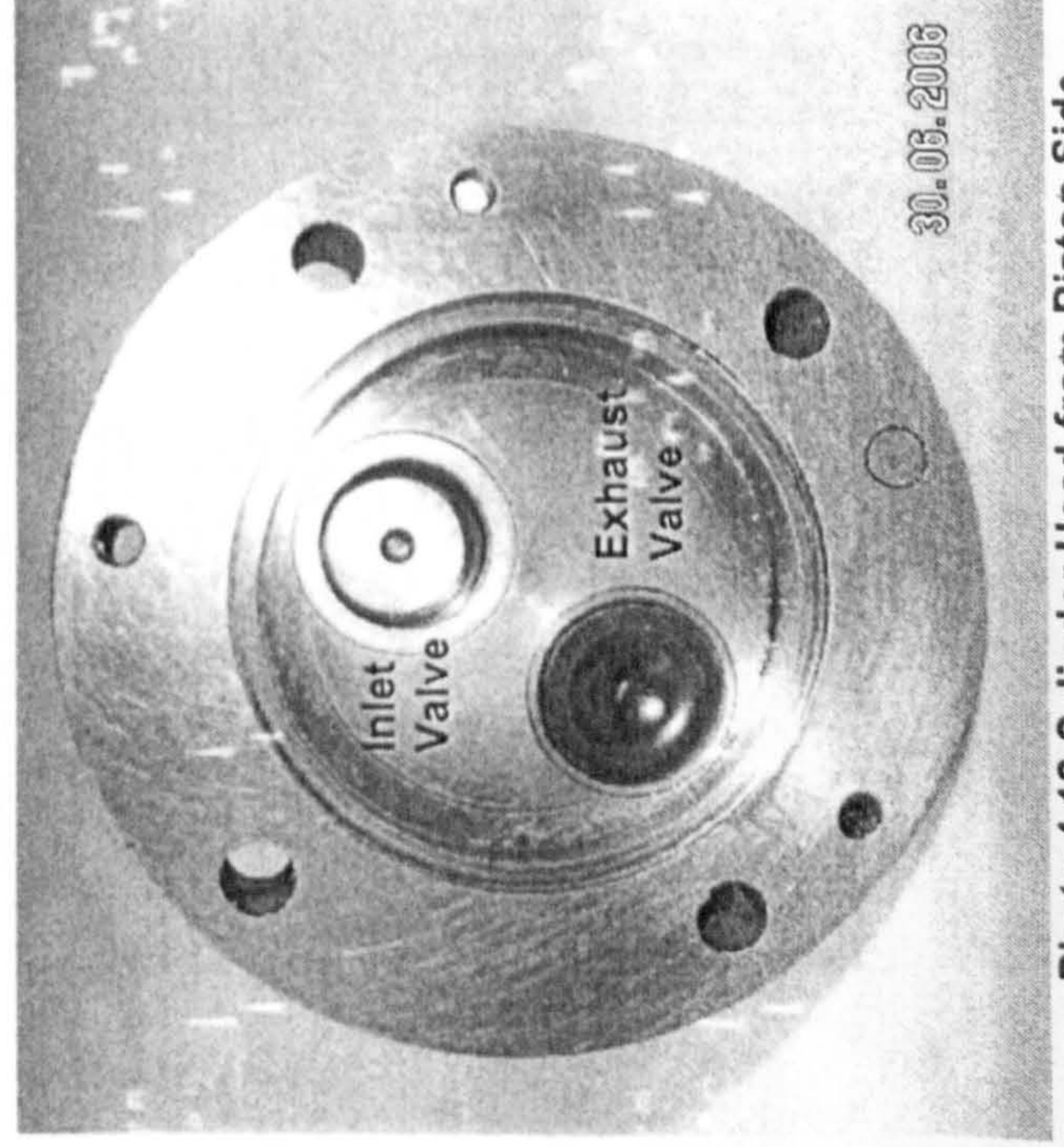


Photo 4.18 Cylinder Head from Piston Side

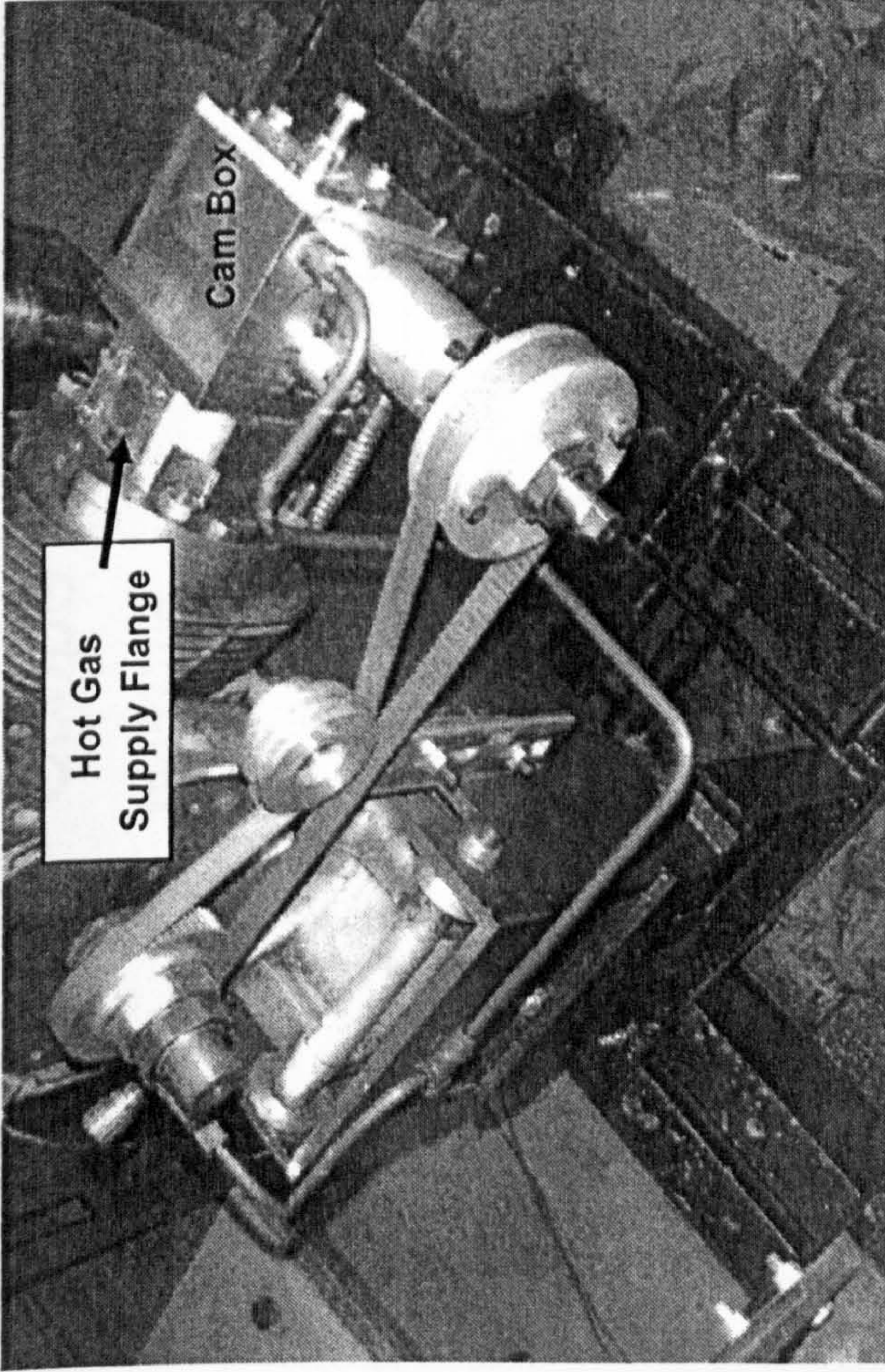


Photo 4.19 Cylinder Head and Cam Box Mounted on Engine

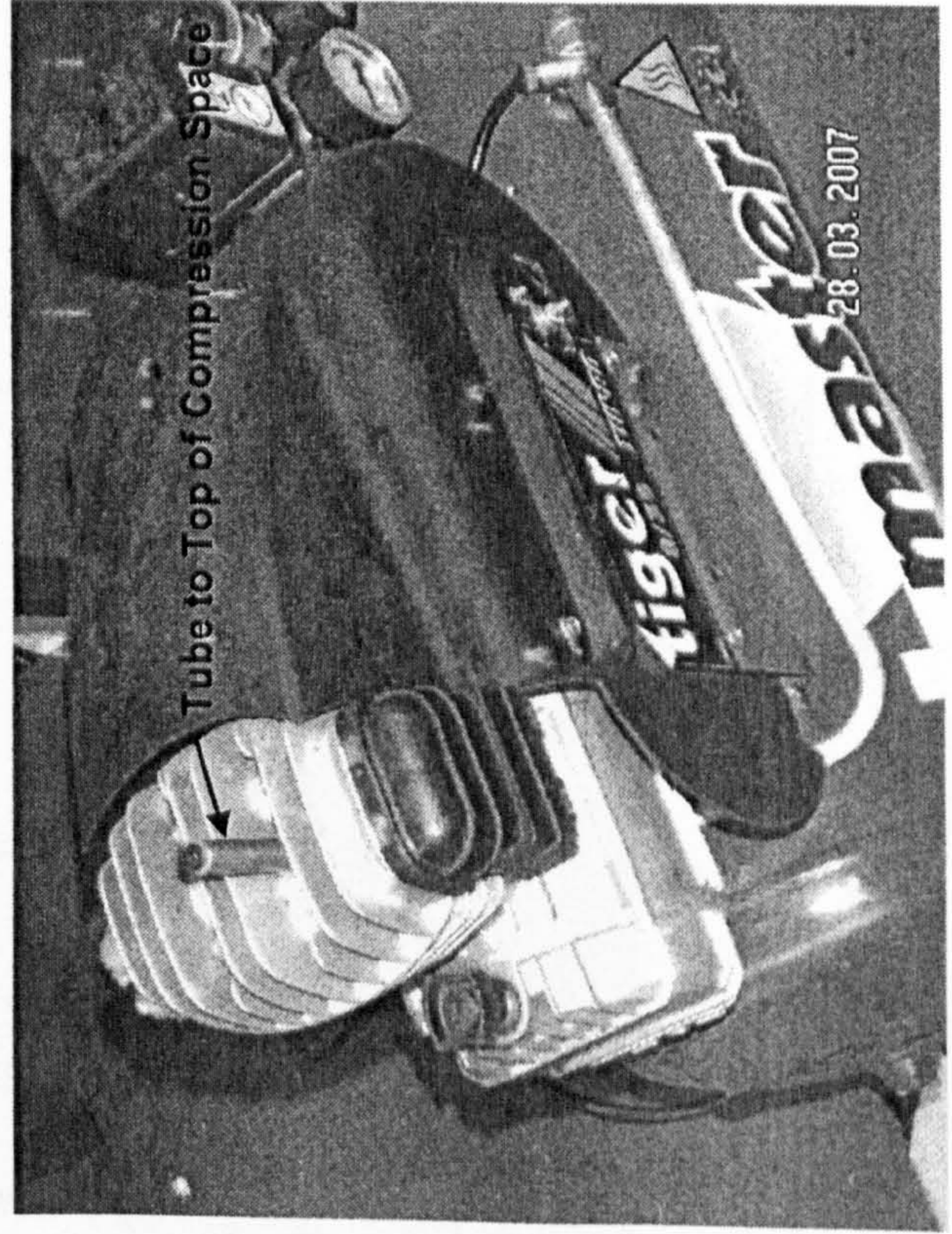
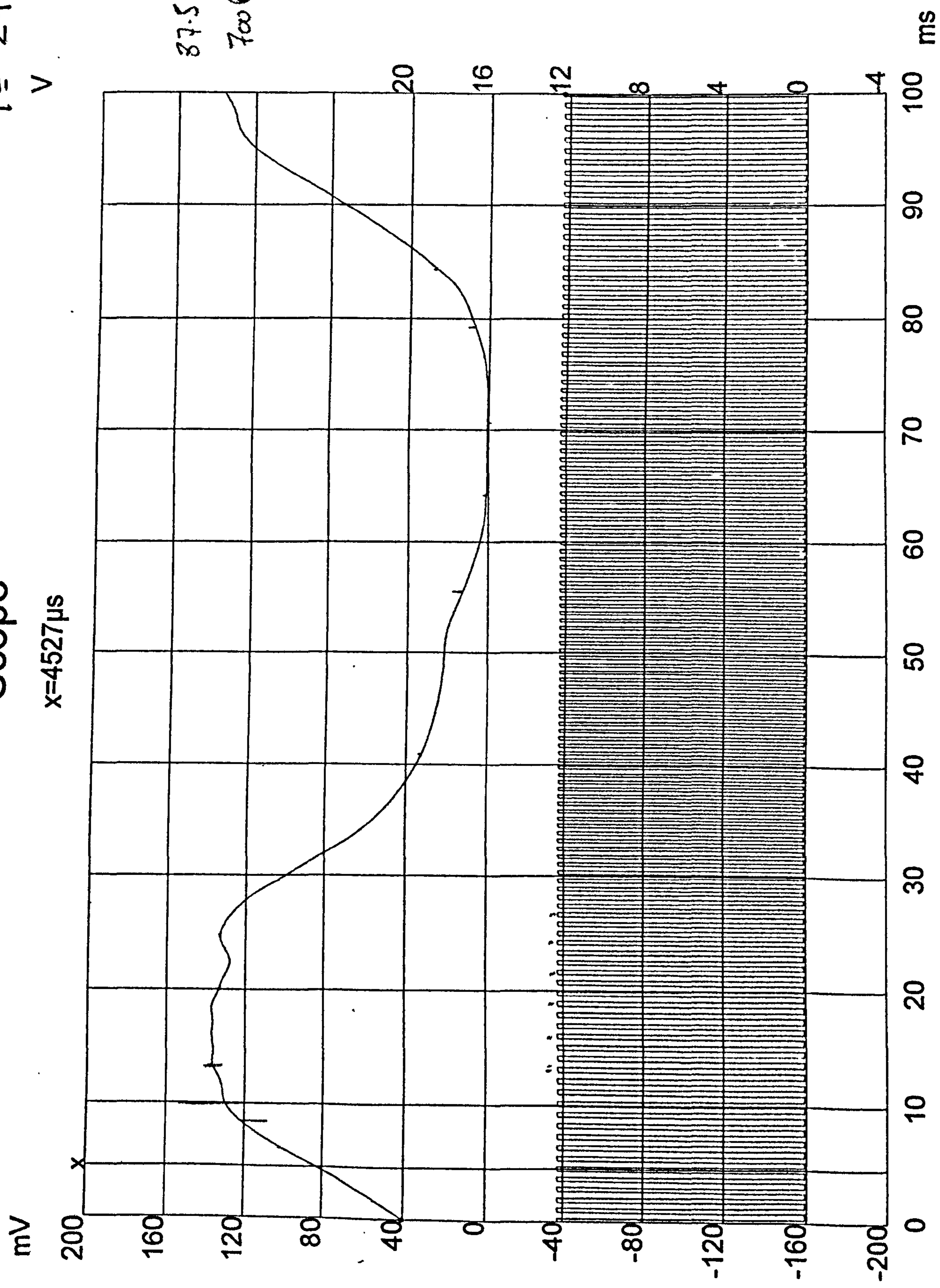


Photo 4.20 Portable Compressor and Pressure Sensing Modifications

700 RPM  
T = 29 Nm.  
V

Scope  
x=4527 μs

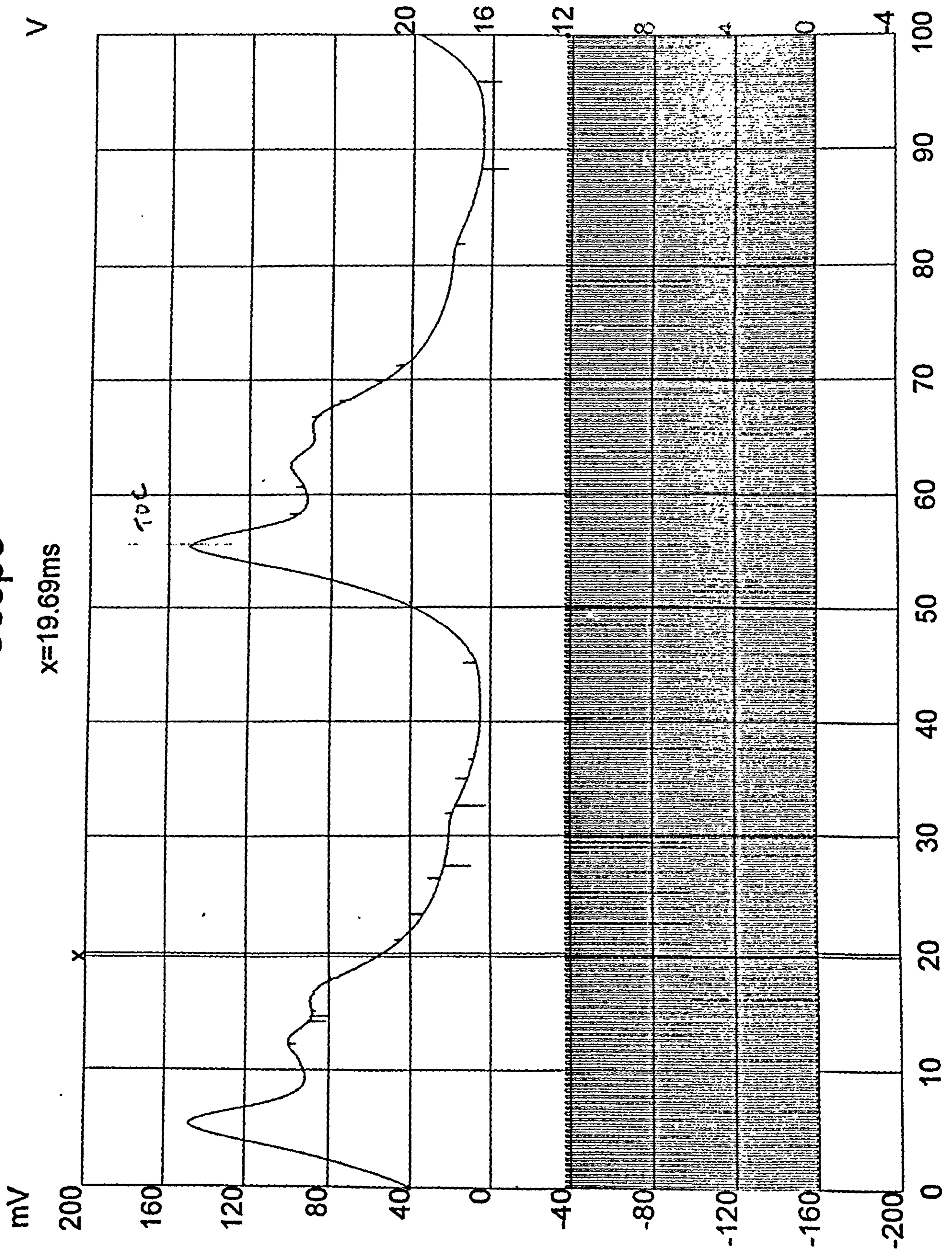


Pressure vs. Crank Angle 700 RPM 29 Nm Torque

# Scope

1200 RPM  
V Tz 0

x=19.69ms



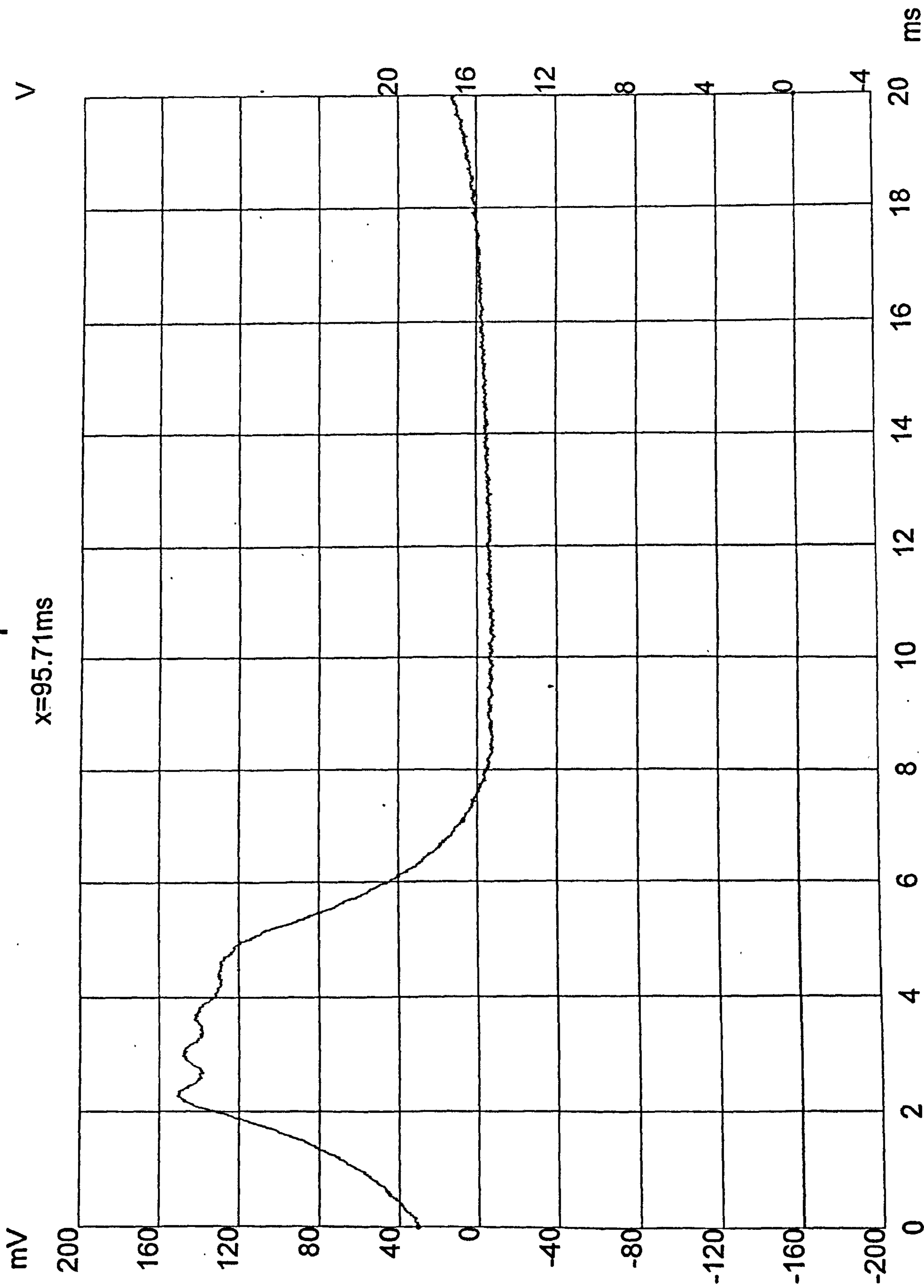
Pressure vs. Crank Angle 1200 RPM Zero Torque

Comp Pressure

Discharge Pressure = 7.5 bar

# Scope

x=95.71ms



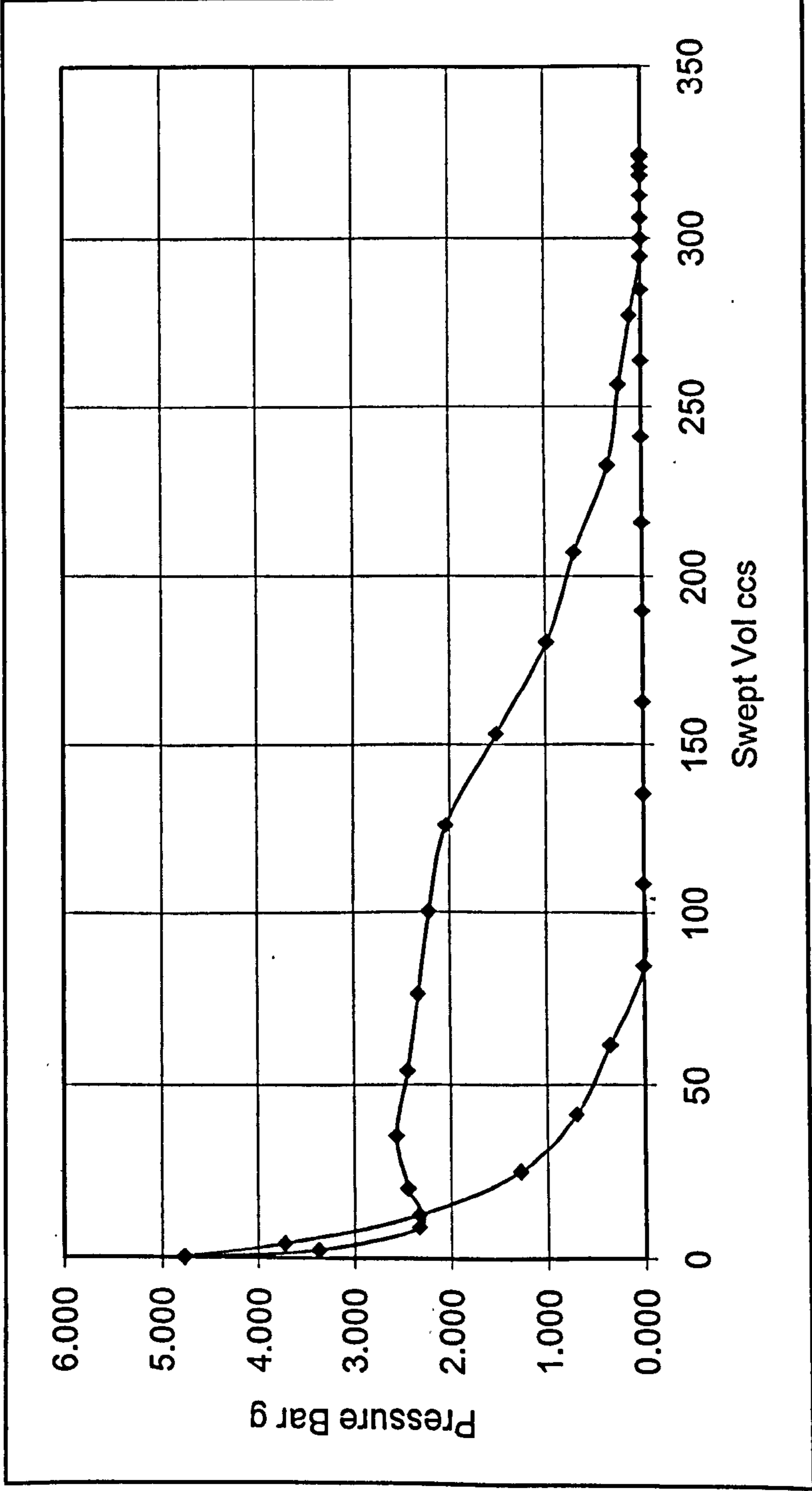
Pressure vs. Crank Angle Compressor 7.5 bar Discharge Pressure

Crank angle	Rads	1-Cos	Stroke cm	Swept Vol cc	hight	Bar G	ccs	P	PV
0	0	1	0	0	41	4.765	0		
1	9.64	0.985884685	0.043404594	2.292196618	29	3.371	2.2922	4.06787541	0.932437
2	19.28	0.943937224	0.172393038	9.104076317	20	2.325	6.8119	2.84751278	1.939691
3	28.92	0.875341819	0.383323905	20.24333544	21	2.441	11.1393	2.38261274	2.654054
4	38.57	0.781926198	0.670576942	35.41316833	22	2.557	15.1698	2.49883775	3.790695
5	48.2	0.666650768	1.025048887	54.13283172	21	2.441	18.7197	2.49883775	4.67774
6	57.86	0.532151153	1.438635203	75.97432509	20	2.325	21.8415	2.38261274	5.203982
7	67.5	0.382888751	1.897617092	100.2131586	19	2.208	24.2388	2.26638773	5.493459
8	77.14	0.222817157	2.389837242	126.2073048	17.5	2.034	25.9941	2.12110646	5.513635
9	86.79	0.056281072	2.901935703	153.2512245	13	1.511	27.0439	1.77243143	4.793349
10	96.42	-0.111500336	3.417863534	180.4973732	8.5	0.988	27.2461	1.24941887	3.404185
11	106.07	-0.276475945	3.92516353	207.287886	6	0.697	26.7905	0.84263133	2.257453
12	115.71	-0.433473053	4.407929638	232.7827642	3	0.349	25.4949	0.52301255	1.333414
13	125.51	-0.580508601	4.860063947	256.659977	2	0.232	23.8772	0.29056253	0.693782
14	135	-0.706792409	5.248386659	277.1672994	1	0.116	20.5073	0.17433752	0.35752
15	144.6	-0.814851909	5.580669619	294.7151626	0	0.000	17.5479	0.05811251	0.101975
16	152.26	-0.884835434	5.795868959	306.0798397	0	0.000	11.3647	0	0
17	163.9	-0.960629363	6.028935291	318.3880727	0	0.000	12.3082	0	0
18	173.57	-0.993645256	6.130459161	323.7495483	0	0.000	5.3615	0	0
19	183.16	-0.998512553	6.145426101	324.5399524	0	0.000	0.7904	0	0
20	192.8	-0.975289796	6.074016124	320.7687915	0	0.000	-3.7712	0	0
21	202.5	-0.924134476	5.916713513	312.4616406	0	0.000	-8.3072	0	0
22	212.15	-0.847029362	5.679615288	299.9404834	0	0.000	-12.5212	0	0
23	221.15	-0.753468378	5.391915262	284.747045	0	0.000	-15.1934	0	0
24	231.43	-0.624065885	4.994002596	263.7332771	0	0.000	-21.0138	0	0
25	241	-0.485503476	4.567923188	241.2320236	0	0.000	-22.5013	0	0
26	250.71	-0.331128675	4.093220677	216.162984	0	0.000	-25.0690	0	0
27	260.37	-0.168130122	3.592000125	189.6935266	0	0.000	-26.4695	0	0
28	270	-0.00088898	3.077733614	162.5351122	0	0.000	-27.1584	0	0
29	279.56	0.165172607	2.567094233	135.5682465	0	0.000	-26.9669	0	0
30	289.3	0.329615248	2.061433113	108.8642827	0	0.000	-26.7040	0	0
31	298.84	0.481503202	1.594377655	84.19908396	1	0.000	-24.6652	0	0
32	308.57	0.622675651	1.160272373	61.27398402	3	0.349	-22.9251	0.17433752	-0.39967
33	318.21	0.744893713	0.784451833	41.4269013	6	0.697	-19.8471	0.52301255	-1.03803
34	327.76	0.845244756	0.475872377	25.13082021	11	1.278	-16.2961	0.9879126	-1.60991
35	337.4	0.922782735	0.237443089	12.53936953	20	2.325	-12.5915	1.80148768	-2.26833
36	347.14	0.974661789	0.077915	4.114691155	32	3.719	-8.4247	3.0218503	-2.54581
37	356.7	0.998273523	0.005308918	0.280363974	41	4.765	-3.8343	4.24221292	-1.6266

4.1 PV 800 Zero Torque

33.65902





Indicated Power = 897  
 Brake power = 0.0 Watts

IMEP 1.036 Bar

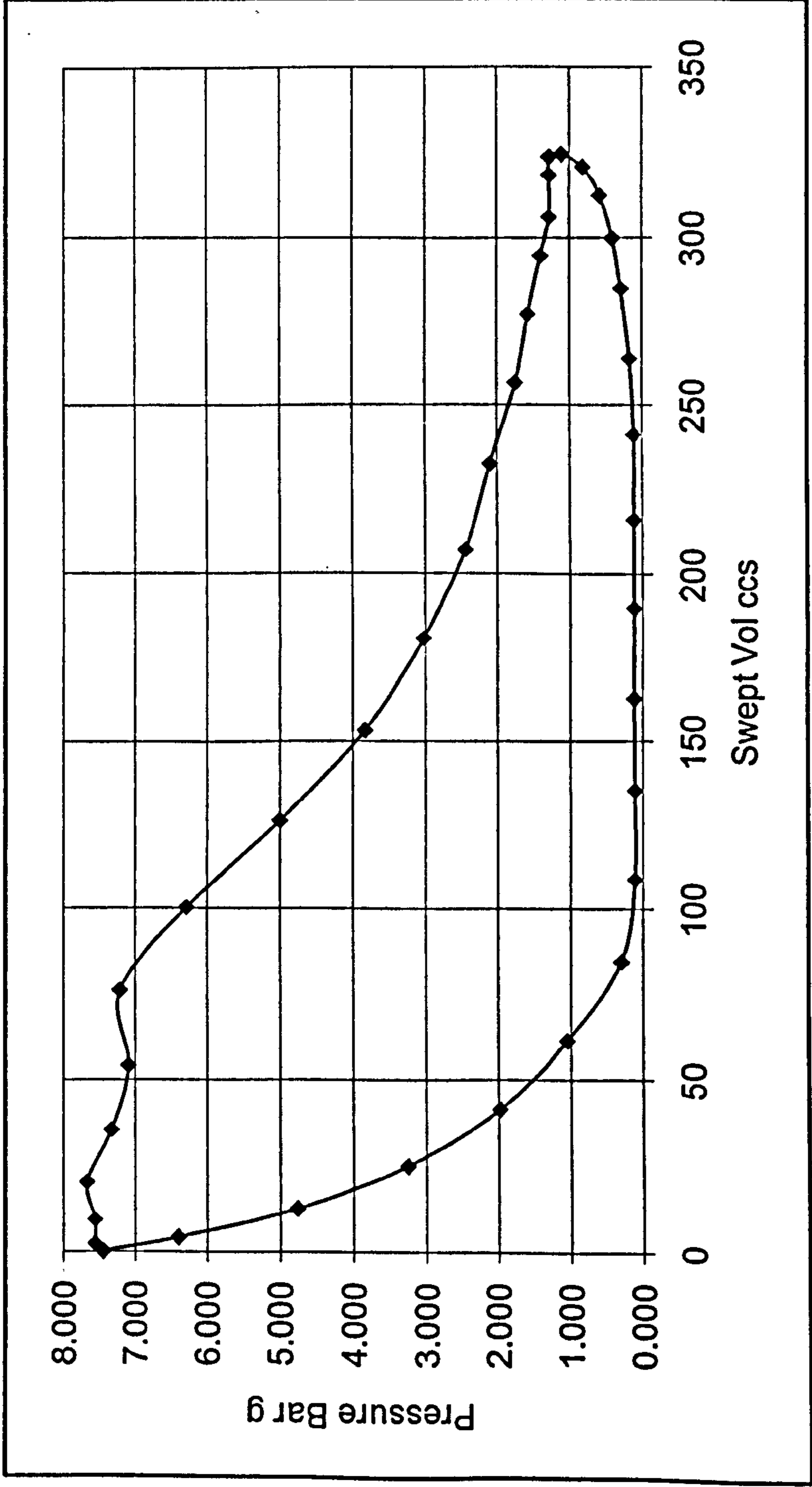
Friction power = 897

### 4.1 PV 800 Zero Torque

	Crank angle	Rads	1-Cos	Stroke cm	Swept Vol cc	height	Bar G	ccs	P	PV
0	0	0	1	0	0	64	7.438	0		
1	9.64	0.168	0.986	0.0434	2.2922	65	7.555	2.29	7.4965	1.72
2	19.28	0.336	0.944	0.1724	9.1041	65	7.555	6.81	7.5546	5.15
3	28.92	0.505	0.875	0.3833	20.2433	66	7.671	11.14	7.6127	8.48
4	38.57	0.673	0.782	0.6706	35.4132	63	7.322	15.17	7.4965	11.37
5	48.2	0.841	0.667	1.0250	54.1328	61	7.090	18.72	7.2060	13.49
6	57.86	1.010	0.532	1.4386	75.9743	62	7.206	21.84	7.1478	15.61
7	67.5	1.178	0.383	1.8976	100.2132	54	6.276	24.24	6.7411	16.34
8	77.14	1.346	0.223	2.3898	126.2073	43	4.998	25.99	5.6369	14.65
9	86.79	1.514	0.056	2.9019	153.2512	33	3.835	27.04	4.4166	11.94
10	96.42	1.683	-0.112	3.4179	180.4974	26	3.022	27.25	3.4286	9.34
11	106.07	1.851	-0.276	3.9252	207.2879	21	2.441	26.79	2.7313	7.32
12	115.71	2.019	-0.433	4.4079	232.7828	18	2.092	25.49	2.2664	5.78
13	125.51	2.190	-0.581	4.8601	256.6600	15	1.743	23.88	1.9177	4.58
14	135	2.356	-0.707	5.2484	277.1673	13.5	1.569	20.51	1.6562	3.40
15	144.6	2.523	-0.815	5.5807	294.7152	12	1.395	17.55	1.4819	2.60
16	152.26	2.657	-0.885	5.7959	306.0798	11	1.278	11.36	1.3366	1.52
17	163.9	2.860	-0.961	6.0289	318.3881	11	1.278	12.31	1.2785	1.57
18	173.57	3.029	-0.994	6.1305	323.7495	11	1.278	5.36	1.2785	0.69
19	183.16	3.196	-0.999	6.1454	324.5400	9.5	1.104	0.79	1.1913	0.09
20	192.8	3.364	-0.975	6.0740	320.7688	7	0.814	-3.77	0.9589	-0.36
21	202.5	3.534	-0.924	5.9167	312.4616	5	0.581	-8.31	0.6974	-0.58
22	212.15	3.702	-0.847	5.6796	299.9405	3.5	0.407	-12.52	0.4940	-0.62
23	221.15	3.859	-0.753	5.3919	284.7470	2.5	0.291	-15.19	0.3487	-0.53
24	231.43	4.038	-0.624	4.9940	263.7333	1.5	0.174	-21.01	0.2325	-0.49
25	241	4.205	-0.486	4.5679	241.2320	1	0.116	-22.50	0.1453	-0.33
26	250.71	4.375	-0.331	4.0932	216.1630	1	0.116	-25.07	0.1162	-0.29
27	260.37	4.543	-0.168	3.5920	189.6935	1	0.116	-26.47	0.1162	-0.31
28	270	4.712	-0.001	3.0777	162.5351	1	0.116	-27.16	0.1162	-0.32
29	279.56	4.878	0.165	2.5671	135.5682	1.5	0.110	-26.97	0.1131	-0.31
30	289.3	5.048	0.330	2.0614	108.8643	1.5	0.110	-26.70	0.1100	-0.29
31	298.84	5.215	0.482	1.5944	84.1991	5.5	0.300	-24.67	0.2050	-0.51
32	308.57	5.385	0.623	1.1603	61.2740	9	1.046	-22.93	0.6730	-1.54
33	318.21	5.553	0.745	0.7845	41.4269	17	1.976	-19.85	1.5109	-3.00
34	327.76	5.719	0.845	0.4759	25.1308	28	3.254	-16.30	2.6151	-4.26
35	337.4	5.888	0.923	0.2374	12.5394	41	4.765	-12.59	4.0098	-5.05
36	347.14	6.058	0.975	0.0779	4.1147	55	6.392	-8.42	5.5788	-4.70
37	356.7	6.224	0.998	0.0053	0.2804	64	7.438	-3.83	6.9154	-2.65

**4.2 PV 800 RPM 29 Nm**

109.512



Indicated Power = 2914  
 Brake power = 2429 Watts

IMEP 3.36 Bar

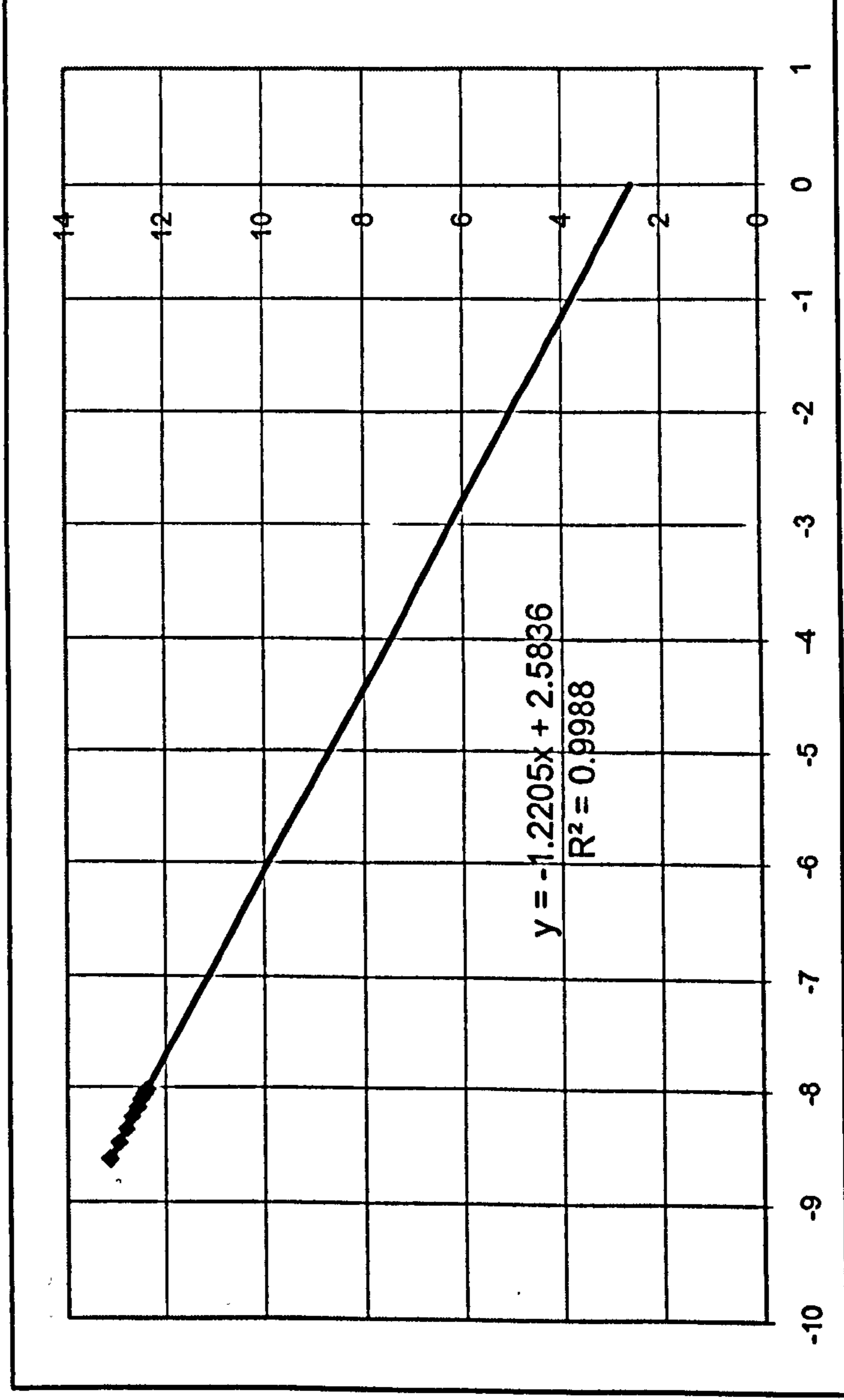
Friction power = Frition power = 485 Watts

Eff 83%

4.2 PV 800 RPM 29 Nm

Determination of Polytropic Value n for expansion

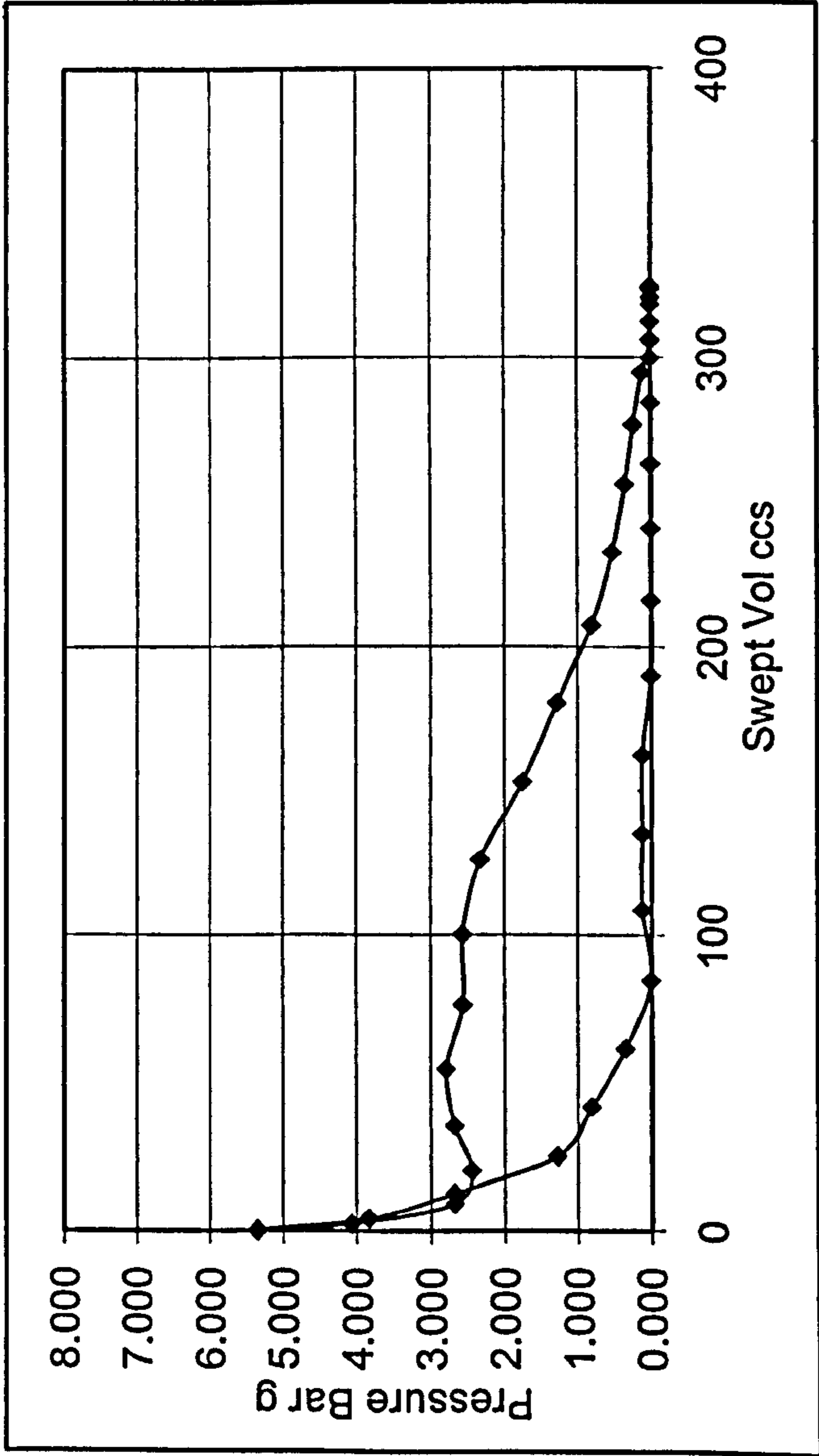
153.2512245	0.000183251	-8.630988833	3.835425384	483542.5384	13.13
180.4973732	0.000210497	-8.491949422	3.021850302	402185.0302	12.94
207.287886	0.000237288	-8.371781808	2.440725244	344072.5244	12.79
232.7827642	0.000262783	-8.269415866	2.092050209	309205.0209	12.68
256.659977	0.00028666	-8.182180614	1.743375174	274337.5174	12.56
277.1672994	0.000307167	-8.112873348	1.569037657	256903.7657	12.49
294.7151626	0.000324715	-8.057147481	1.394700139	239470.0139	12.42
306.0798397	0.00033608	-8.022641817	1.278475128	227847.5128	12.37



4.2 PV 800 RPM 29 Nm

	Crank angle	Rads	1-Cos	Stroke cm	Swept Vol cc	hight	Bar G	ccs	P	PV
0	0	0	1	0	0	46	5.346	0		
1	9.64	0.168218	0.985884685	0.043404594	2.292196618	35	4.068	2.2922	4.70711297	1.078963
2	19.28	0.336436	0.943937224	0.172393038	9.104076317	23	2.673	6.8119	3.37052534	2.295961
3	28.92	0.504654	0.875341819	0.383323905	20.24333544	21	2.441	11.1393	2.55695026	2.848253
4	38.57	0.6730465	0.781926198	0.670576942	35.41316833	23	2.673	15.1698	2.55695026	3.878851
5	48.2	0.84109	0.666650768	1.025048887	54.13283172	24	2.789	18.7197	2.73128777	5.112879
6	57.86	1.009657	0.532151153	1.438635203	75.97432509	22	2.557	21.8415	2.67317527	5.838614
7	67.5	1.177875	0.382888751	1.897617092	100.2131586	22	2.557	24.2388	2.55695026	6.197749
8	77.14	1.346093	0.222817157	2.389837242	126.2073048	20	2.325	25.9941	2.44072524	6.344457
9	86.79	1.5144855	0.056281072	2.901935703	153.2512245	15	1.743	27.0439	2.0339377	5.500565
10	96.42	1.682529	-0.111500336	3.417863534	180.4973732	11	1.278	27.2461	1.51092515	4.116689
11	106.07	1.8509215	-0.276475945	3.92516353	207.287886	7	0.814	26.7905	1.0460251	2.802355
12	115.71	2.0191395	-0.433473053	4.407929638	232.7827642	4.5	0.523	25.4949	0.66829382	1.703807
13	125.51	2.1901495	-0.580508601	4.860063947	256.659977	3	0.349	23.8772	0.43584379	1.040674
14	135	2.35575	-0.706792409	5.248386659	277.1672994	2	0.232	20.5073	0.29056253	0.595866
15	144.6	2.52327	-0.814851909	5.580669619	294.7151626	1	0.116	17.5479	0.17433752	0.305925
16	152.26	2.656937	-0.884835434	5.795868959	306.0798397	0	0.000	11.3647	0.05811251	0.066043
17	163.9	2.860055	-0.960629363	6.028935291	318.3880727	0	0.000	12.3082	0	0
18	173.57	3.0287965	-0.993645256	6.130459161	323.7495483	0	0.000	5.3615	0	0
19	183.16	3.196142	-0.998512553	6.145426101	324.5399524	0	0.000	0.7904	0	0
20	192.8	3.36436	-0.975289796	6.074016124	320.7687915	0	0.000	-3.7712	0	0
21	202.5	3.533625	-0.924134476	5.916713513	312.4616406	0	0.000	-8.3072	0	0
22	212.15	3.7020175	-0.847029362	5.679615288	299.9404834	0	0.000	-12.5212	0	0
23	221.15	3.8590675	-0.753468378	5.391915262	284.747045	0	0.000	-15.1934	0	0
24	231.43	4.0384535	-0.624065885	4.994002596	263.7332771	0	0.000	-21.0138	0	0
25	241	4.20545	-0.485503476	4.567923188	241.2320236	0	0.000	-22.5013	0	0
26	250.71	4.3748895	-0.331128675	4.093220677	216.162984	0	0.000	-25.0690	0	0
27	260.37	4.5434565	-0.168130122	3.592000125	189.6935266	0	0.000	-26.4695	0	0
28	270	4.7115	-0.00088898	3.077733614	162.5351122	1	0.116	-27.1584	0.05811251	-0.15782
29	279.56	4.878322	0.165172607	2.567094233	135.5682465	1	0.116	-26.9669	0.11622501	-0.31342
30	289.3	5.048285	0.329615248	2.061433113	108.8642827	1	0.116	-26.7040	0.11622501	-0.31037
31	298.84	5.214758	0.481503202	1.594377655	84.19908396	2	0.000	-24.6652	0.05811251	-0.14334
32	308.57	5.3845465	0.622675651	1.160272373	61.27398402	3	0.349	-22.9251	0.17433752	-0.39967
33	318.21	5.5527645	0.744893713	0.784451833	41.4269013	7	0.814	-19.8471	0.58112506	-1.15336
34	327.76	5.719412	0.845244756	0.475872377	25.13082021	11	1.278	-16.2961	1.0460251	-1.70461
35	337.4	5.88763	0.922782735	0.237443089	12.53936953	23	2.673	-12.5915	1.9758252	-2.48785
36	347.14	6.057593	0.974661789	0.077915	4.114691155	33	3.835	-8.4247	3.25430033	-2.74164
37	356.7	6.224415	0.998273523	0.005308918	0.280363974	46	5.346	-3.8343	4.59088796	-1.7603
										38.55527

**4.3 PV for 1000 RPM Zero Torque**



Indicated Power = 1280  
 Brake power = 0.0 Watts

IMEP 1.19 Bar

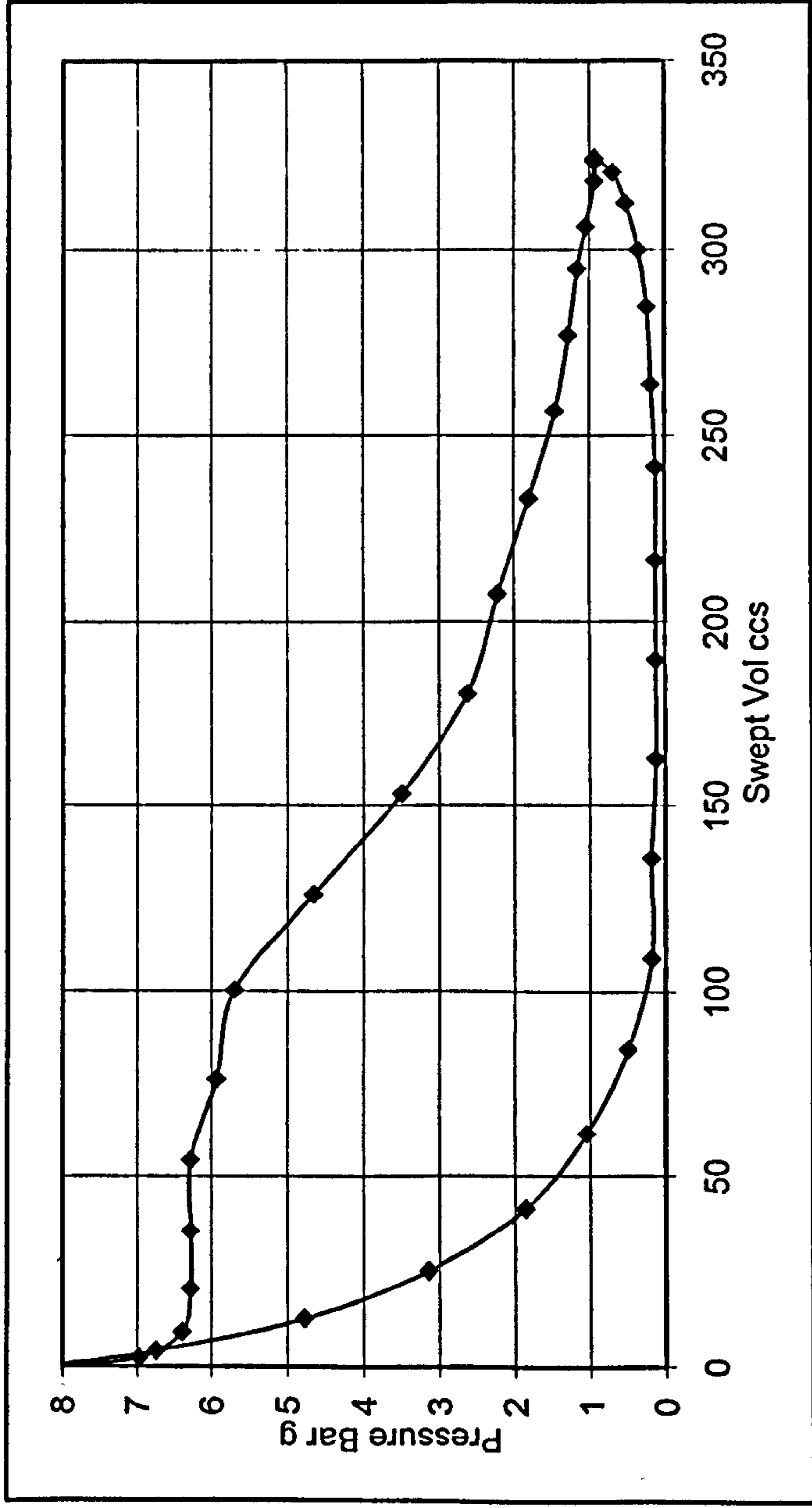
Friction power = 1280

4.3 PV for 1000 RPM Zero Torque

Crank angle	Rads	1-Cos	Stroke cm	Swept Vol cc	hight	Bar G	ccs	P	PV
0	0	1	0	0	70	8.136	0		
1	0.168218	0.985884685	0.043404594	2.292196618	60	6.974	2.2922	7.55462576	1.731669
2	0.336436	0.943937224	0.172393038	9.104076317	55	6.392	6.8119	6.68293817	4.552337
3	0.504654	0.875341819	0.383323905	20.24333544	54	6.276	11.1393	6.33426313	7.0559
4	0.6730465	0.781926198	0.670576942	35.41316833	54	6.276	15.1698	6.27615063	9.520816
5	0.84109	0.666650768	1.025048887	54.13283172	54	6.276	18.7197	6.27615063	11.74874
6	1.009657	0.532151153	1.438635203	75.97432509	51	5.927	21.8415	6.10181311	13.32727
7	1.177875	0.382888751	1.897617092	100.2131586	49	5.695	24.2388	5.81125058	14.08579
8	1.346093	0.222817157	2.389837242	126.2073048	40	4.649	25.9941	5.17201302	13.44421
9	1.5144855	0.056281072	2.901935703	153.2512245	30	3.487	27.0439	4.06787541	11.00113
10	1.682529	-0.111500336	3.417863534	180.4973732	22.5	2.615	27.2461	3.05090656	8.312545
11	1.8509215	-0.276475945	3.92516353	207.287886	19	2.208	26.7905	2.41166899	6.460985
12	2.0191395	-0.433473053	4.407929638	232.7827642	15.5	1.801	25.4949	2.00488145	5.111421
13	2.1901495	-0.580508601	4.860063947	256.659977	12.5	1.453	23.8772	1.62715016	3.885181
14	2.35575	-0.706792409	5.248386659	277.1672994	11	1.278	20.5073	1.36564389	2.80057
15	2.52327	-0.814851909	5.580669619	294.7151626	10	1.162	17.5479	1.22036262	2.141476
16	2.656937	-0.884835434	5.795868959	306.0798397	9	1.046	11.3647	1.10413761	1.254817
17	2.860055	-0.960629363	6.028935291	318.3880727	8	0.930	12.3082	0.9879126	1.215946
18	3.0287965	-0.993645256	6.130459161	323.7495483	8	0.930	5.3615	0.92980009	0.49851
19	3.196142	-0.998512553	6.145426101	324.5399524	8	0.930	0.7904	0.92980009	0.073492
20	3.36436	-0.975289796	6.074016124	320.7687915	6	0.697	-3.7712	0.81357508	-0.30681
21	3.533625	-0.924134476	5.916713513	312.4616406	4.5	0.523	-8.3072	0.61018131	-0.50689
22	3.7020175	-0.847029362	5.679615288	299.9404834	3	0.349	-12.5212	0.43584379	-0.54573
23	3.8590675	-0.753468378	5.391915262	284.747045	2	0.232	-15.1934	0.29056253	-0.44146
24	4.0384535	-0.624065885	4.994002596	263.7332771	1.5	0.174	-21.0138	0.20339377	-0.42741
25	4.20545	-0.485503476	4.567923188	241.2320236	1	0.116	-22.5013	0.14528126	-0.3269
26	4.3748895	-0.331128675	4.093220677	216.162984	1	0.116	-25.0690	0.11622501	-0.29136
27	4.5434565	-0.168130122	3.592000125	189.6935266	1	0.116	-26.4695	0.11622501	-0.30764
28	4.7115	-0.00088898	3.077733614	162.5351122	1	0.116	-27.1584	0.11622501	-0.31565
29	4.878322	0.165172607	2.567094233	135.5682465	1.5	0.174	-26.9669	0.14528126	-0.39178
30	5.048285	0.329615248	2.061433113	108.8642827	1.5	0.174	-26.7040	0.17433752	-0.46555
31	5.214758	0.481503202	1.594377655	84.19908396	5	0.500	-24.6652	0.33716876	-0.83163
32	5.3845465	0.622675651	1.160272373	61.27398402	9	1.046	-22.9251	0.77301255	-1.77214
33	5.5527645	0.744893713	0.784451833	41.4269013	16	1.860	-19.8471	1.45281265	-2.88341
34	5.719412	0.845244756	0.475872377	25.13082021	27	3.138	-16.2961	2.49883775	-4.07213
35	5.88763	0.922782735	0.237443089	12.53936953	41	4.765	-12.5915	3.9516504	-4.9757
36	6.057593	0.974661789	0.077915	4.114691155	58	6.741	-8.4247	5.75313808	-4.84683
37	6.224415	0.998273523	0.005308918	0.280363974	70	8.136	-3.8343	7.43840074	-2.85213

**4.4 PV for 1000 RPM 20 Nm Torque**

91.66166



Indicated Power = 3057  
 Brake power = 2086 Watts

IMEP 2.82 Bar

Friction power = 971 Watts

#### 4.4 PV for 1000 RPM 20 Nm Torque



7.5 Bar discharge pressure

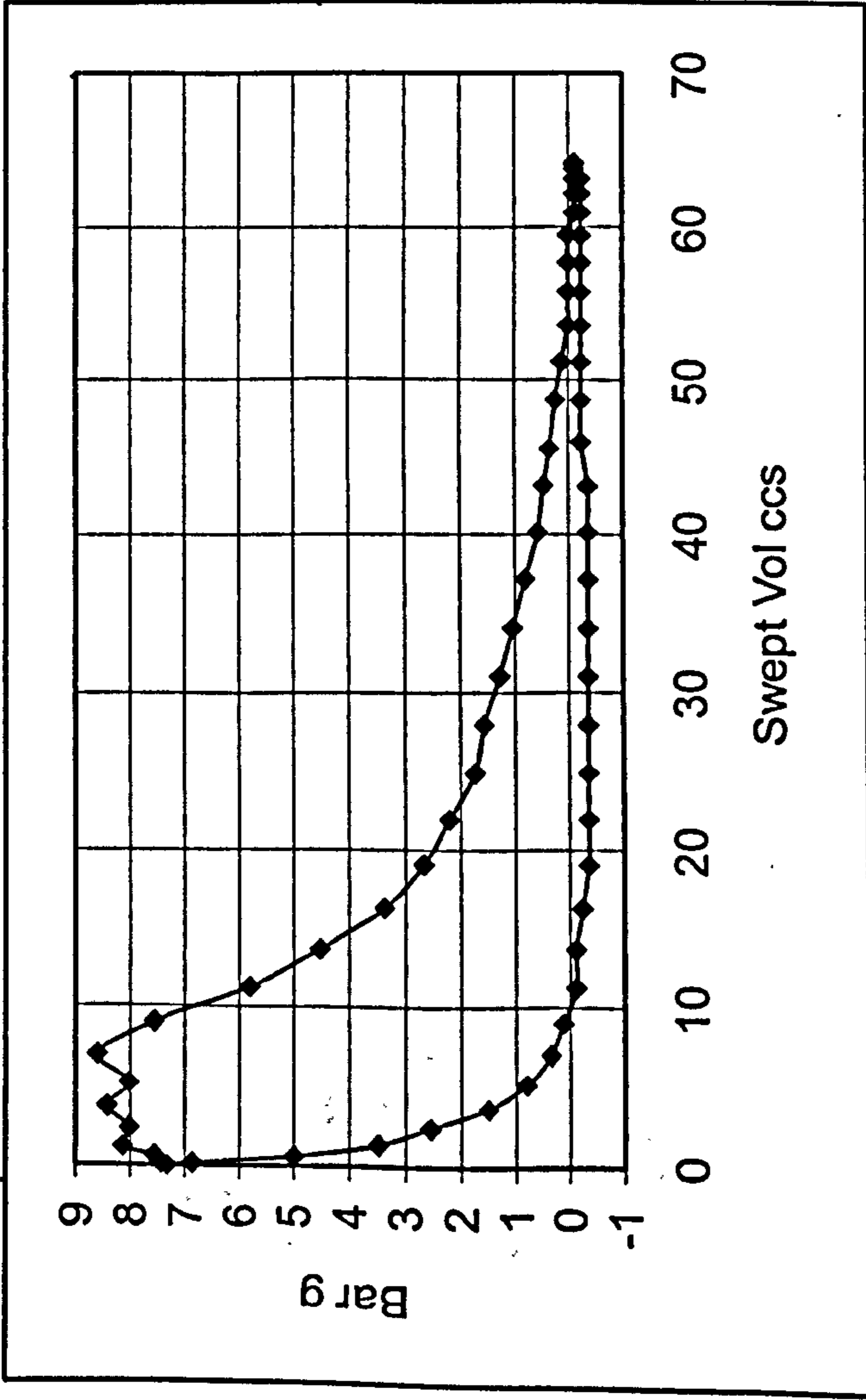
Stroke 37mm, Bore 47mm, Cv 2 ccs

Degs	1-Cos (deg)	Stroke	Swept Vol	Hight	Bar g	ccs	P ave	PV
0	1.000	0.000	0.000	63.0	7.326	0.000		
5.5	0.995	0.005	0.148	59.0	6.860	0.148	7.093	0.105
11	0.982	0.018	0.589	43.0	5.000	0.442	5.930	0.262
16.5	0.959	0.041	1.321	30.0	3.488	0.732	4.244	0.311
22	0.927	0.073	2.336	22.0	2.558	1.015	3.023	0.307
27.5	0.887	0.113	3.625	13.0	1.512	1.289	2.035	0.262
33	0.839	0.161	5.176	7.0	0.814	1.551	1.163	0.180
38.5	0.783	0.217	6.975	3.0	0.349	1.799	0.581	0.105
44	0.719	0.281	9.005	1.0	0.116	2.030	0.233	0.047
49.5	0.650	0.350	11.248	-1.0	-0.116	2.243	0.000	0.000
55	0.574	0.426	13.682	-1.0	-0.116	2.435	-0.116	-0.028
60.5	0.493	0.507	16.286	-2.0	-0.233	2.604	-0.174	-0.045
66	0.407	0.593	19.036	-3.0	-0.349	2.750	-0.291	-0.080
71.5	0.318	0.682	21.906	-3.0	-0.349	2.870	-0.349	-0.100
77	0.225	0.775	24.869	-3.0	-0.349	2.964	-0.349	-0.103
82.5	0.131	0.869	27.899	-3.0	-0.349	3.030	-0.349	-0.106
88	0.035	0.965	30.968	-3.0	-0.349	3.069	-0.349	-0.107
93.5	-0.061	1.061	34.047	-3.0	-0.349	3.079	-0.349	-0.107
99	-0.156	1.156	37.108	-3.0	-0.349	3.061	-0.349	-0.107
104.5	-0.250	1.250	40.123	-3.0	-0.349	3.015	-0.349	-0.105
110	-0.342	1.342	43.065	-3.0	-0.349	2.941	-0.349	-0.103
115.5	-0.430	1.430	45.905	-2.0	-0.233	2.840	-0.291	-0.083
121	-0.515	1.515	48.618	-2.0	-0.233	2.713	-0.233	-0.063
126.5	-0.594	1.594	51.179	-2	-0.233	2.561	-0.233	-0.060
132	-0.669	1.669	53.565	-2	-0.233	2.385	-0.233	-0.055
137.5	-0.737	1.737	55.752	-2	-0.233	2.188	-0.233	-0.051
143	-0.798	1.798	57.723	-2	-0.233	1.970	-0.233	-0.046
148.5	-0.852	1.852	59.457	-2	-0.233	1.734	-0.233	-0.040
154	-0.899	1.899	60.939	-2	-0.233	1.482	-0.233	-0.034
159.5	-0.936	1.936	62.156	-2	-0.233	1.217	-0.233	-0.028
165	-0.966	1.966	63.097	-2	-0.233	0.940	-0.233	-0.022
170.5	-0.986	1.986	63.752	-1	-0.116	0.655	-0.174	-0.011
176	-0.998	1.998	64.116	-1	-0.116	0.364	-0.116	-0.004
180	-1.000	2.000	64.195	-1	-0.116	0.079	-0.116	-0.001
184	-0.998	1.998	64.118	-1	-0.116	-0.077	-0.116	0.001
189.5	-0.986	1.986	63.758	-1	-0.116	-0.360	-0.116	0.004

Suction losses  
-1.49082 5.518973 7.009795

4.5 Portable Compressor Performance





Extra work in discharge 0.375  
 Extra work in suction 1.49  
 Total extra work 1.865  
 Ideal cycle 13.4

Compressor RPM 2850

Indicated Power Absorbed = 15.3 x 47.5

726.75 Watts

Ideal Power absorbed = 13.4 x 47.5

612.38 Watts

Cycle efficiency = 612.38/726.75

88%

Assume 90% mech efficiency on actual output

807.5 Watts

### 4.5 Portable Compressor Performance

Engine: 1500 RPM. Inlet gas 850 C. CV=0.03 xSv. Vol admitted 320ccs. Full recompression to 7.5 bar g.

Cv =3%	0.03 x Swept volume	Cycle efficiency	0.87	Mech efficiency	0.8	T in	1123
n compression	1.3	p amb Nm	101325	Bore mm	120		
n expansion	1.15	p discharge bar g	7.5	Stroke mm	100		
Discharge temp deg K	368			Vol ccs	1130		
				Cv ccs	30		

Mass flow required kg/sec  
0.0213036

Discharge Vol ccs at 368 K  
104.862

Mass flow /rev

0.0008521

Work discharge J

90.313688

Vol to compress ccs

789.9317

1123/1500 1123/1500  
CV=30ccs CV =5 ccs  
134.8 164.7

Expander  
Ideal/Cycle

Work Compression J

120.37

121.32 148.23

Work Expansion

40.33

Vol end expansion ccs

195.2941

At 90% mech efficiency  
Power delivered Watts 90% eff

3033

3705.75

Work/cycle J

170.35

Power Delivered 80%

2696

3294

Power required Watts ideal

4259

Compressor 90% eff

1989.6

1989.6

Actual power Watts 80% mech efficiency

6119.07

80% eff

2238.26

2236.26

Actual power Watts 90% mech efficiency

5439.2

Net power Watts 90% eff

1043.4

1716.15

Net Power 80% eff

457.74

1057.74

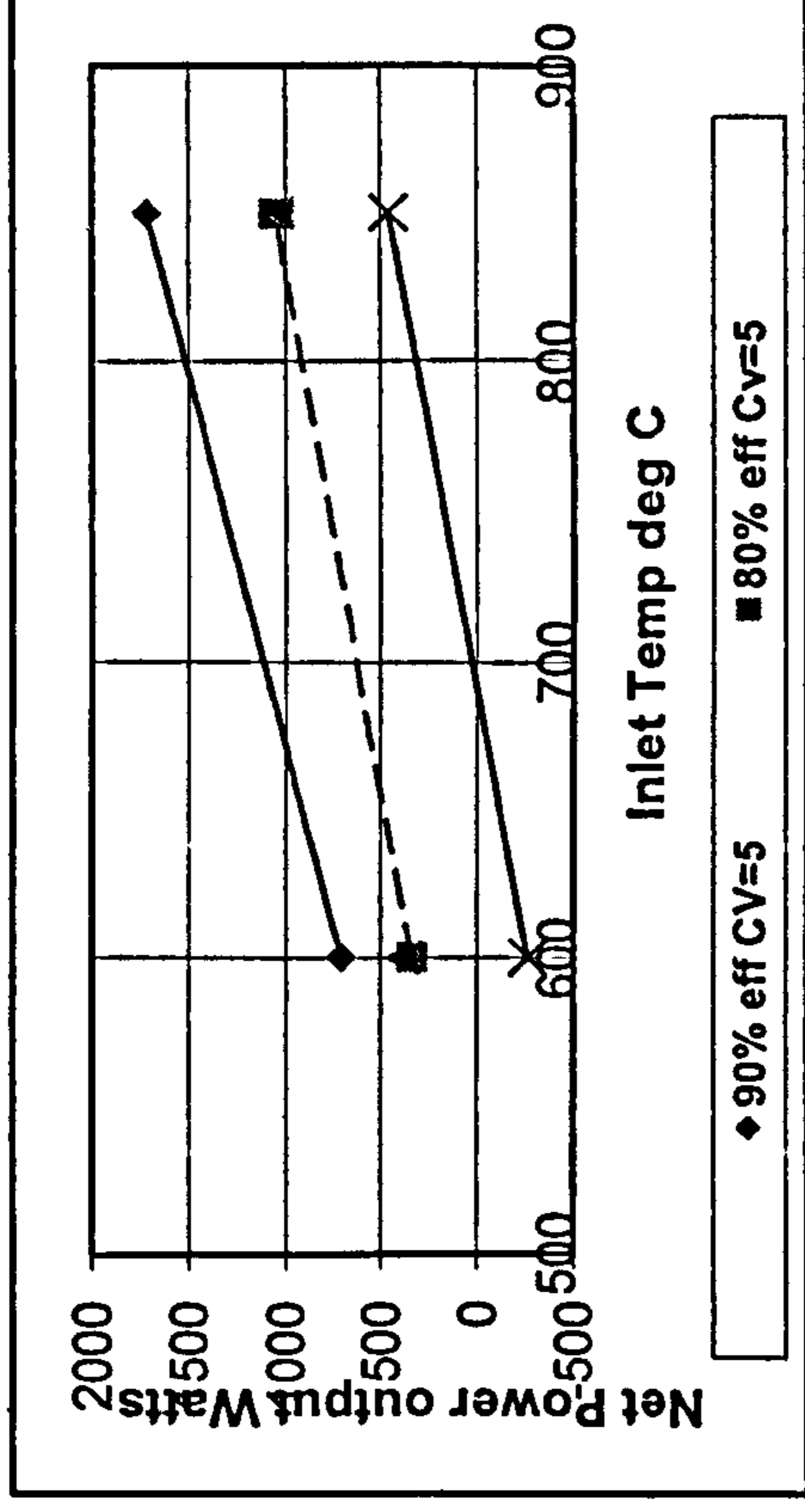
#### 4.6 Compressor Modelling

Deg c      Net work Watts  
             90% eff    80% eff    90% eff    80% eff  
             CV 5        CV 5        CV 30     CV 30

600	711	339.6	384.5	-264.4
850	1716	1057.7	1043.4	457.74

Best output Watts/cc      90% Cv=5 80% C V=5  
 Engine vol for 5kW      5.28 3.254462  
                                  946.9697 1536.352

Cyl dimensions      10.62009 12.47699  
 Bore and stroke cm



## 4.6 Compressor Modelling

873/1500 873/1500  
CV=30ccs CV=5 ccs  
131.1 161.3

117.99 131.1

2949.75 3277.5

2622 3226

2565.7 2565.7

2886.4 2886.4

384.05 711.8

-264.4 339.6

Problem	Date	Solution	Outcome
Combustion chamber flanges incorrectly designed	09/02	Remove flanges, weld new flanges, manufacture and fit new air pipework.	Engine will turn over on air but major leaks from pistons.
Major pressure losses on air. No piston rings found in the expander pistons	10/02	Remove pistons and fit standard rings. Renew sump seal.	System losses on air considerably reduced.
No gas supply	10/02	Manufacture first design of nozzle.	Erratic burning of gas and poor ignition
Cam follower bearing break and exhaust valve stems are bent. Cam is 70 deg with 6 mm lift	11/02	Manufacture new valve cam followers for all 4 valves. Renew exhaust valves and all four valve guides. Reduce lift on cams to 4 mm but at 70 deg. Manufacture new valve seats and grind in to reduce leakage losses	Erratic burning and poor ignition but no cam follower failures.
Compressor suction losses measured. Intake depression measured at 0.2 bar. Volumetric efficiency measured at 70%	11/02	Design and manufacture new compressor deliver valves using reed valve.	Volumetric efficiency improved to 80% and intake depression reduced to < 0.1 bar. Little or no improvement to ignition and burning
Poor burning and ignition	01/03	Design and manufacture new nozzle and nozzle holder with air shield. Modify spark plug holder to move spark plug further into combustion chamber and to be just inside air shield	Minor improvements to ignition and combustion

Table 4.1 RJC Technology Demonstrator Engine Development

Poor combustion and ignition	01/03 to 02/03	Experimentation with mixing tube and nozzle plate. Manufacture various tubes and nozzles and test in air	Spark need to be fed with a separate pilot jet to obtain stable ignition
Poor combustion and ignition	02/03	Manufacture and fit mixing tube and nozzle plate. Fit observation window in the combustor end plate	Stable ignition obtained and good combustion but only with additional air supplied. Temperature of 650 C obtained.
Poor air supply to combustion chamber. System will not self sustain.	03/03	Manufacture air measuring orifice and calibrate. Objective is to determine work supplied by the addition air.	System found to need 0.75 kW of air to achieve good combustion.
Insufficient air supply	04/03	Manufacture and fit new inlet cams with 80 deg and 6 mm lift	Reduction in make up air required. System pressure now reduced to 3 bar
Insufficient air supply	04/03	Manufacture and fit new inlet cams with 100 deg and new exhaust cams with 175 deg and 6 mm lift.	Reduction in make up air required due to reduced compressor work. System pressure now reduced to 2 bar. Expander inlet temperature increased to 700 deg.
System will not self sustain	05/03	Modify combustion chamber with internal tube. Secondary air supply repositioned.	Better ignition and combustion. System almost self sustains. Expander inlet temperature 700C
Major heat losses from combustion chamber reducing available energy	05/03	Lag combustion chamber and expander inlet pipework	Expander inlet temperature increased to 750 C. System self sustains but only with a rich mixture and poor combustion

**Table 4.1 RJC Technology Demonstrator Engine Development**



Poor combustion	06/03	Design and manufacture new nozzle plate. Change to propane from natural gas	Improved combustion and self sustained conditions when engine is run hotter thus reducing friction. Expander inlet temperature 750C
Poor combustion	06/03 to 07/03	Design and manufacture new combustion chamber, mixing tube, and nozzle. Combustion chamber fitted with inner tube and small number of secondary air holes. Design and manufacture new air pipework	Further improvements in combustion. Expander inlet temperature 780 C Self sustained condition with good combustion
Low expander inlet temperature	07/03	Design and modify new nozzle plate. Experimentation with number and size of nozzle holes	Expander inlet temperatures of 820 C attained.
Low expander inlet temperature	08/03	Revert to 80 deg inlet cams. Cam shaft timing adjusted to ensure correct recompression in expanders.	System pressure 4 bar. Expander inlet temperature increased to 870 C with stable ignition and clean combustion on minimum gas. RPM increased to 850.  Engine will now start on starter motor but only when hot.
Engine will only self sustain	09/03 to 10/03	Modify compressor to reduce bore from 93.650 to 82.5 mm to give a volume ratio (expanders to compressor) of 2.5 : 1	Slightly worse performance than with original piston
Engine will only self sustain	10/03 to 11/03	Determine the friction characteristics of the engine	Cold friction determined by measuring the overall work supplied by the motoring air. Power to motor the engine when cold determined as 3 kW at 750 RPM.

Table 4.1 RJC Technology Demonstrator Engine Development